Development of novel Surface Plasmon Resonance-based biosensors with purified recombinant human HER-2 and progesterone receptor produced in two different yeast species

I n a u g u r a l d i s s e r t a t i o n

zur

Erlangung des akademischen Grades eines

Doktors der Naturwissenschaften (Dr. rer. nat.)

der

Mathematisch-Naturwissenschaftlichen Fakultät

der

Ernst-Moritz-Arndt-Universität Greifswald

vorgelegt von

Alexandre Chamas

geboren am 22. April 1987

in Bordeaux, Frankreich

Greifswald, 2014

****

Dekan: Prof. Dr. Klaus Fesser.....

1. Gutachter : Prof. Dr. Rüdiger Bode.....

2. Gutachter: Prof. Dr. Raffael Schaffrath.....

Tag der Promotion: 27/03/2015.....

Table of contents

Summary

The following work is describing the development of two innovative biosensors for the detection of biologically relevant molecules in the field of ecology and medical diagnostics. Biosensors have the particularity to possess a biological partner which recognizes the target molecule and a physical detection method responsible for the transformation of this biological interaction into measurable information. In the present case, both biosensors are designed following the same strategy and use a recombinant produced human receptor as biological partner and the surface plasmon resonance (SPR) technique to transform the biological interaction in quantitative information.

The progesterone biosensor is aimed to detect and quantify substances with affinity to the human progesterone receptor. The recent discoveries that some chemicals present in low quantities in the ecosystem called endocrine disrupting chemicals (EDCs) have a negative impact on the aquatic life fitness raised concerns about the effects of these same molecules to the human health. In order to assess the effects of these EDCs, the use of classical analytical detection methods like high performance liquid chromatography (HPLC) or gas chromatography (GC) is not sufficient as these techniques only quantify a defined molecule without giving information about its biological activity. By integrating a recombinant human progesterone receptor, the progesterone biosensor can determine the biological activity of an unknown molecule or of a mixture of molecules in a real sample. In this work, two different yeasts – one methylotrophic (*Hansenula polymorpha*) and one non-methylotrophic (*Arxula adeninivorans*) - were selected as host for the recombinant protein production and their performances were compared. Different purification strategies were assayed and the binding activity of the purified progesterone receptor was then confirmed by enzyme like receptor assay (ELRA) and SPR. This led to the design of a first version of the biosensor with the immobilization of a progesterone-BSA ligand to the surface of a SPR chip and the use of a progesterone receptor mixed with the target molecule as sample. This competitive assay format was successfully utilized with a commercial progesterone-BSA ligand as target molecule and the next step will be the adaptation of this biosensor for real samples measurements.

The HER-2 biosensor was developed as an answer for one of the most critical issue in the field of breast cancer diagnostics. In approximately 30 % of cancer cases, the transmembrane protein HER-2 can be found in large amount at the surface of the carcinoma cells and these cases are known to be particularly aggressive. Based on the amount of HER-2 protein at the surface of the cells, the pathologists established a scale with four levels to adapt the treatment to each patient. Although effective therapies have been developed to treat the HER-2 positive breast cancer, one of the major challenges remains the classification of breast sample in this scale as the only accepted determination methods are immunohistochemistry (IHC) and fluorescent *in situ* hybridization (FISH) which are only qualitative. In this work, a biosensor has been designed to quantify the amount of the HER-2 protein in a crude cell extract from a breast cancer tissue sample. To achieve this, the strategy is to utilize an antibody specifically targeted against the HER-2 protein and bound to a SPR chip. As the development of this biosensor necessitated the use of large amount of purified HER-2 protein, it was decided to produce recombinant full-length HER-2 in two different yeasts and to

purify it by chromatography. This recombinant protein production required particular attention due to the membrane localization of HER-2. The structural integrity of the recombinant protein was confirmed by Western Blot and ELISA and different antibodies were bound to SPR chips in order to detect the HER-2 protein. After finding the conditions giving an optimal SPR signal, a protocol was developed to extract native HER-2 from breast tissue sample and the biosensor was assayed with this crude cell extract.

Zusammenfassung

Die folgende Arbeit beschreibt die Entwicklung von zwei innovativen Biosensoren für die Detektion von biologisch relevanten Molekülen im Bereich der Ökologie und der medizinischen Diagnostik. Beide Biosensoren sind mit biologischen Komponenten zur Erkennung eines Zielmoleküls und einen Transducer, der die Wechselwirkung zwischen biologischer Komponente und Zielmolekül mittels physikalischer Detektionsmethode in ein messbares Signal umwandeln kann, ausgerüstet. Als biologische Komponenten enthalten sie ein rekombinantes humanes Protein, während als Detektionsmethode die Surface Plasmon Resonanz (SPR) Technik angewandt wird.

Ziel des ersten Biosensors, den Progesteron-Biosensor, ist die Erkennung und Quantifizierung von Substanzen mit Affinitäten zum humanen Progesteron-Rezeptor. Umfangreiche Studien haben bisher gezeigt, dass zahlreiche Chemikalien als sog. endokrine Disruptoren einen negativen Einfluss auf die Umwelt bzw. auf die menschliche Gesundheit haben, da sie eine hohe Affinität zum entsprechenden Hormon-Rezeptor aufweisen. Um den Einfluss dieser endokrinen Disruptoren einzuschätzen, ist die Verwendung von klassischen analytischen Detektionsmethoden wie der Hochleistungsflüssigkeitschromatographie (HPLC) oder Gaschromatographie (GC) nicht ausreichend, da diese Techniken nur bekannte Substanzen messen, ohne Informationen über deren biologische Aktivität zu erhalten. Durch erstmalige Nutzung eines rekombinant humanen Progesteron-Rezeptors als Biokomponente kann der Progesteron-Assay die biologische Aktivität einer unbekannten Substanz bzw. einer Mischung aus verschiedenen Substanzen in einer Realprobe bestimmen. Im Rahmen dieser Arbeit wurden zwei verschiedene Hefearten - Hansenula polymorpha (eine methylotrophe Hefe) und Arxula adeninivorans (eine dimorphe Hefe) - als Wirtsorganismen für die Synthese des rekombinanten humanen Progesteron-Rezeptors ausgewählt und ihre Leistungsfähigkeit bezüglich maximaler Rezeptor-Akkumulation verglichen. Zusätzlich wurde die Reinigungsprozedur des rekombinanten Rezeptors optimiert und dessen spezifische Affinität gegenüber Progesteron per Rezeptorassay (ELRA) und SPR ermittelt. Abschließend konnte ein erster Biosensor mit Progesteron-BSA Ligand funktionalisierten SPR-Chips und einem Mix aus Progesteron-Rezeptor und Zielmolekül als Messprobe etabliert werden.

Der zweite auf HER-2 basierende Biosensor wurde als Tool für die Brustkrebsdiagnostik entwickelt. So weisen etwa 30 % aller Brustkrebs-Patienten eine Überexpression des HER-2-Gens auf, dessen Genprodukt als Transmembranprotein in hohen Konzentrationen an der Zell-Oberfläche akkumuliert wird. Diese Fälle sind eine besonders aggressive Art des Brustkrebses. Basierend auf der Konzentration des HER-2-Proteins an der Zelloberfläche wird in der Pathologie zur Diagnostik dieses Typs von Brustkrebs eine vier Scores umfassende Skala als Entscheidungshilfe für die individuelle Behandlung eines jeden Patienten genutzt. Obwohl bereits heute wirksame Therapien zur erfolgreichen Behandlung von HER-2 positiven Brustkrebs verfügbar sind, bleibt die Klassifizierung der Brustkrebs-Gewebeprobe mit Hilfe dieser Skala eine Herausforderung. Zurzeit sind Immunohistochemie (IHC) und Fluorescence in situ Hybridization (FISH) die einzigen akzeptierten Entscheidungsmethoden. Aus diesem Grund wurde im Rahmen dieser Dissertationsarbeit ein Biosensor designt, mit dem sich die Konzentration an HER-2-Proteinen in Brustkrebs-Gewebeproben

detektieren lässt. Dazu wurde ein SPR-Chip mit einem Anti-HER-2-Antikörper funktionalisiert. Da hierzu gereinigtes HER-2 Protein als Kontrolle benötigt wurde, wurde dieses Proteine als rekombinantes Protein in vollständiger Länge in zwei verschiedenen Hefen synthetisiert und per chromatographischen Verfahren gereinigt. Eine wesentliche Herausforderung dieser Prozedur war die Solubilisierung der membran-lokalisierten HER-2-Proteine. Die strukturelle Vollständigkeit des rekombinanten Proteins wurde per Western-Blot und ELISA bestätigt und mit Anti-HER2-Antikörpern funktionalisierten SPR-Chips deren Funktionstüchtigkeit detektiert. Nach Optimierung der SPR-Methode wurde ein Protokoll zur Extraktion von nativem HER-2 aus Brustgewebeproben erstellt und diese Zellextrakte in Kombination mit den HER-2 Kontrollproteinen für erste Biosensortests eingesetzt.

Abbreviations

Short name	Full name
% v/v	volume percent
% w/v	mass percent
°C	degree Celsius
A	Ampere
bp	base pair
DBD	DNA binding domain
dcw	dry cell weight
ddH_2O	double distilled H_2O
DNA	deoxyribonucleic acid
EDC	endocrine disrupting chemical
ELISA	enzyme linked immunosorbant assay
ELRA	enzyme like receptor assay
FDA	Food and Drug Administration
FFPE	freshly frozen paraffin embedded
FISH	fluorescence in situ hybridization
g	centrifugal force
h	hour
hPR	human progesterone receptor
IHC	immunohistochemistry
kDa	kilo Dalton
l	liter
LBD	ligand binding domain
M	molar
min	minute
OD	optical density
PCR	polymerase chain reaction
pH	potential hydrogen
RTK	receptor tyrosine kinase
s	Second
SDS-PAA	SDS polyacrylamide
SOC	synthetic oral contraceptive
SPR	surface plasmon resonance
V	Volt

1 Introduction

In the last years, the awareness of the scientific community and the general population about the need of efficient sensing strategies was constantly growing. Measuring concentrations or molecule quantities of the simplest gas to the most complicated protein is the purpose of several studies as it appears to be one of the key information for the progress in ecology and medical science. By analyzing rivers, atmosphere or body fluids composition for example and by linking molecule quantities to physiological disorders or environmental observations, these researches allowed the discovery of several compounds with negative impact on the ecosystem or on the human health. These results were in some cases used by governmental organizations to establish strict recommendations relative to the production, utilization or treatment of these compounds and the impact of such decisions were generally described as positive. Still, many compounds stay hardly detectable or their impact could not have been linked to a specific biological target yet. That's why the design of new detection systems or the amelioration of the existing ones remains very important. In order to detect natural or artificial compounds, the use of biosensors is constantly growing. A biosensor has the particularity to use a biological partner, which can be strictly identical or derived from a natural occurring molecule produced by a living organism or an entire organism and is able to recognize a target analyte. The second part of a biosensor is the transducer which should transform this biological interaction into physically detectable information. This information can be transported in several states (light, current, heat…) to a detector who will transform, amplify or process this information in order to give a numerical value. This study will describe the development of two biosensors aimed to detect compounds binding to the progesterone receptor (called the "progesterone biosensor") and a membrane receptor related to breast cancer (called the "HER-2 biosensor"). They are both using the Surface Plasmon Resonance (SPR) as detection method. Because the two biosensors focus on different research fields and use different biological partners, this introduction will therefore treat each of them separately (in the section 1.1 for the progesterone biosensor and 1.2 for the HER-2 biosensor). But as the host organisms for recombinant receptor production or the detection method of both of them are identical, these aspects will be treated in the same subsets (respectively 1.3 and 1.4). Finally the principle of each biosensor will be clearly exposed in the two last subsets.

1.1 The progesterone biosensor

1.1.1 Compounds with progesterone activity

The endocrine system is composed of glands designed to control and regulate metabolism, growth, sexual functions and reproduction [1]. The reproduction control for example is made possible by the secretion of five different classes of cholesterol derived molecules called steroids: progestogens, estrogens, androgens, mineralocorticoids and glucocorticoids [2, 3]. Even though our knowledge of the endocrine system is mainly based on human observations, it is known that all vertebrates and a high number of arthropods and crustaceans also share an equivalent system [4, 5]. Progestogens, also often named progestagens, are known to be the precursors of all other steroids and can

therefore be produced by several glands both in male and female specimens [6]. One important member of this steroid class is the progesterone (pregn-4-ene-3,20-dione), and is mainly synthesized in the ovary (corpus luteum) and in the placenta of female mammals as its principal role is to maintain the pregnancy and to regulate the ovarian system [7]. In male, the production of progesterone is considerably lower and restricted to the adrenal glands [8]. Beside naturally produced progestogens, synthetic progestogens called progestins were synthesized in the last decades [9]. They are also referred as SOCs for Synthetic Oral Contraceptives as their main role is the control of the female contraception [10]. Released in the 1960s, these molecules continue to be a popular method for contraception with an estimated yearly usage of 1723 kg/year in United Kingdom for example (to compare with the 706kg/year of estrogens and androgens) and their consummation is thought to increase as more women across the world have now access to these molecules. These SOCs mainly derive from the progestogen molecular structure and have all a relative affinity to the progesterone receptor. The chemical formulas of some of the members of this progestin family together with progestogens are to see in the Table 1-1, with mifepristone and medroxyprogesterone being the more common. They are all based on a pregnane skeleton composed by 21 carbon atoms and four rings with a highly conserved ketone function at the position 3 and a variable functionalization on position 17. Beside the SOCs, a few compounds are known to also have a binding affinity to the progesterone receptor in a similar way that xenoestrogens binds to the estrogen receptor. Vonier et al. [11] described a binding affinity of the insecticides endosulfan and kepone and of the herbicide alachlor to the progesterone receptor of the American alligator. More recently, large screening for progesterone receptor binding were conducted with industrial chemicals, phytoestrogens and pesticides, showing that many compounds known as xenoestrogens possess higher affinity for the progesterone receptor than for the estrogen receptor [12, 13].

Table 1-1. Chemical formula of some progestogens and progestins. All graphical representations are from the Chemspider database (www.chemspider.com/chemical structure).

Class	Compound	Formula
progestogens	progesterone	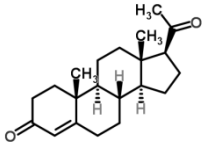
	17-αhydroxyprogesterone	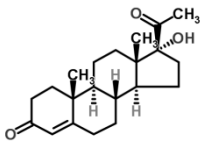

	3,20-pregnanedione	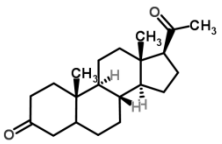
	11-deoxycorticosterone	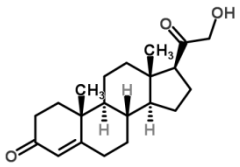
progestins	medroxyprogesterone	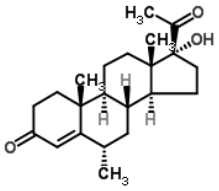
	mifepristone	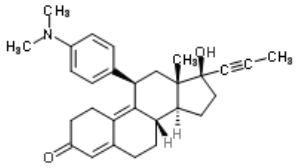
	norgestrel	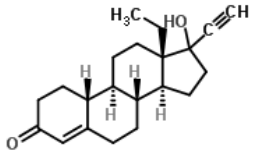
	levonorgestrel	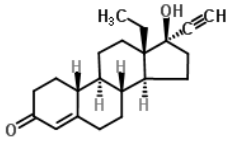

1.1.2 The human progesterone receptor

The human progesterone receptor (hPR) is with the estrogen receptor or the androgen receptor one member of the nuclear hormone superfamily of transcriptional activators [14, 15] and its coding gene is located on the chromosome 11 [16, 17]. Even though one sequence corresponding to the progesterone receptor can be found, the gene is expressed as two main isoforms called PR-B and PR-A due to alternative promoter utilization [18-21]. These two proteins can be found in the cytoplasm and the nucleus of the progesterone target tissues with different ratios [22]. More recently, other isoforms of the progesterone receptor were described but their role seems to be minor for steroid binding activity [23-26]. For example the isoform called PR-M was found in the mitochondrion and is described as an actor of the cellular respiration [27]. Other isoforms like PR-C can only be found during pregnancy [28] and in fetal cells [29]. Isoform PR-B was chosen as the canonical sequence as it corresponds to the full-length receptor whereas PR-A lacks 164 amino acids on the N-terminus of the protein. Both isoforms are known to be essential in steroid binding system as mice lacking both protein were presenting abnormalities relative to sexual functions and organism development whereas mice lacking only the isoform PR-A didn't display all these symptoms [20, 30]. The modular structure of both PR-B and PR-A is shown in the Figure 1-1.

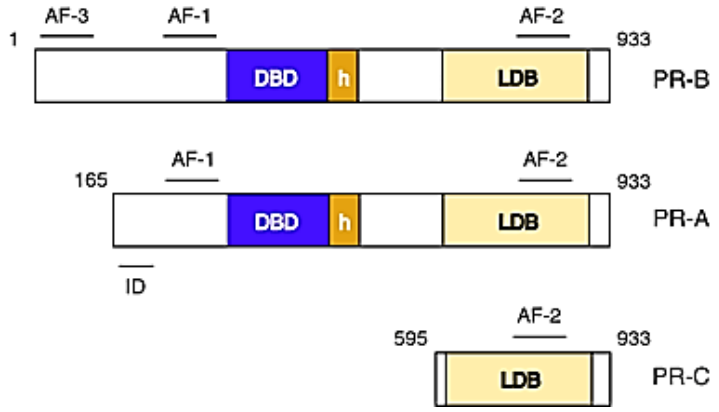

Figure 1-1. Overview of the three main human progesterone receptor isoforms structure. DBD: DNA binding domain, h: hinge region, LDB: ligand binding domain, the numbers indicate the positions of amino acids, AF-1,-2 and -3 are transcription activation domains [19].

It consists mainly of one C-terminal steroid binding region called ligand binding domain (LBD), one central DNA-binding region (DBD) and one proline-rich poorly characterized N-region. This N-region is thought to possess a nuclear localization signal responsible for the translocation of the protein from cytoplasm to the nucleus upon binding of the ligand [15]. The DBD harbors two C4-type zinc finger regions carrying four cysteine and characteristic for nuclear receptors. Many DNA-regions are described as targets of the DBD region and it is interesting to note that some of them are strictly selective for PR-A or PR-B [31]. Most of the activated regions are involved in mammary gland development, cell membrane signaling, metabolism, transcription, cell growth and apoptosis, and nucleic acid and protein processing [30, 32]. This diversity of targets explains why progesterone receptor isoforms are very often involved in cancer development as an overexpression or a

malfunction of these proteins can lead to a deregulation of one of the most important metabolic pathways. The general mechanism of target gene transcription regulation is highly similar to the one of other steroid receptors [33, 34]. This involves the binding of the receptor to the hormone (here progesterone) via the LBD in the cytoplasm, a conformational change followed by the association of the receptor with a multiprotein sequestering complex composed of heat shock protein and immunophilins, a translocation in the nucleus, the dissociation of the multiprotein complex, a dimerization of the progesterone receptor and finally, the binding of the DBD to the target gene [35]. This mechanism is also presented in Figure 1-2. Beside this ligand mediated pathway, it exists for the progesterone receptor a second pathway called ligand-independent signaling causing progesterone activation without binding of the hormone [36].

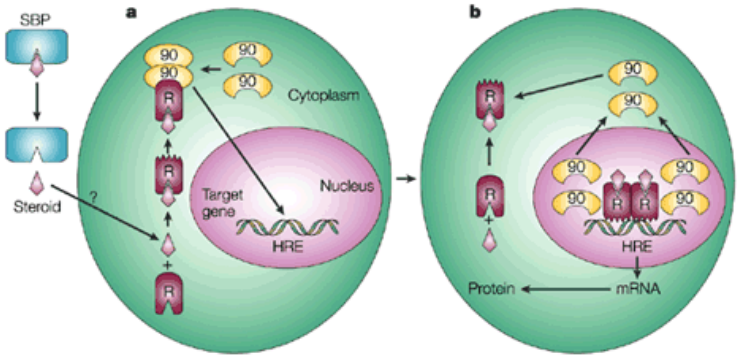

Figure 1-2. Activation of steroid receptor by their ligand. (A) The steroid (progesterone) is released from its circulating steroid-binding protein (SBP) and is transported into the cytoplasm of the target cell by passive diffusion or active transport. When bound to the non-ligand-bound receptor (R) it induces a conformational change that allows it to bind the Hsp90 dimer (90), which acts as its chaperone. The nuclear localization signal of the receptor allows the R–Hsp90 complex to translocate into the nucleus. (B): Once in the nucleus, the ligand–receptor complex dissociates from Hsp90 and itself dimerizes. The removal of Hsp90 unmasks the DNA-binding site of the receptor, which allows it to interact with the hormone response element (HRE) in the target gene promoter to activate transcription [35].

1.1.3 Effect of compounds with progesterone activity on the environment

More and more evidences are pointing the negative impact of endocrine disrupting chemicals (EDCs) for the environment and most of their members like parabens or bisphenol A are nowadays familiar to the general population [37-40]. These molecules are defined as followed by the European commission: “An endocrine disruptor is an exogenous substance or mixture that alters function(s) of the endocrine system and consequently causes adverse health effects in an intact organism, or its progeny, or (sub)populations”. Altering the function of the endocrine system means that these chemicals can interfere at the level of steroid receptors, mainly the estrogen, androgen and progesterone receptors [41]. Among them, the effect of estrogen receptor [42-44] or androgen receptor [45] binding substances have been the most studied and their concentrations are now strictly controlled thanks to several detection systems. In comparison, effect of compounds with progesterone activity remained for a long time obscure even though recent researches made

progress. Recently, progestins have been classified as possibly carcinogenic by the Agency for Research on Cancer (IARC) based on carcinogenicity in experimental animals and inadequate evidence of carcinogenicity in human [46]. Another concern about these molecules comes from their effect on the wildlife. Because progestins have generally an androgenic activity, it is supposed that they could also present risks for the aquatic life [47]. One precise example for this risk was described by the study of Pietsch et al. [48], which demonstrated that medroxyprogesterone could influence the innate immunity of fish, thus altering their behavior and threatening their survival. More recently Paulos et al. [49] demonstrated a decrease in fish fecundity after exposure to norethindrone and Zeilinger et al. [50] pointed the inhibition of fecundation caused by levonorgestrel and drospirenone. The accumulating evidences that exposure to progestins could have adverse effects in water ecosystem make necessary the development of more sensing strategies to detect it. Besides progestins, the fact that other EDCs thought to be binding to the estrogen receptor showed high affinity to the progesterone receptor [12] pushes the scientific community to accelerate the development of sensing systems targeted to progesterone receptor binding substances.

1.1.4 Progestins and other EDCs detection methods

Detection methods made a lot of progress in the last years and followed different directions in order to obtain the best sensitivity, specificity, low cost and rapidity.

- Analytical methods

Because most of the EDCs and the progestins in particular are present at very low levels in the environment, a suited detection method should quantify them at the µg/l or ng/l level. That's why analytical methods are often preferred. Among them Ultra Performance Liquid Chromatography (UPLC), High Performance Liquid Chromatography (HPLC) or Liquid Chromatography (LC) coupled with Mass Spectrometry (MS) or MS/MS were used for the detection of almost all progestins like levonorgestrel, medroxyprogesterone or mifepristone with detection limit in the ng/l range [51-56]. The use of Gas Chromatography (GC) also coupled with MS [57, 58], ELISA (for Enzyme Linked ImmunoSorbant Assay) [59, 60] and LDTD (Laser Diode Thermal Desorption) [61, 62] coupled with MS are also described in the literature. These methods were used to detect molecules in several matrixes like tap water, river water, wastewater, aquatic products, river sediment and soil with a recovery oscillating from 55 % in soil to 100 % in most of the studies. It is to note than even if urine or meat sample have been already successfully tested with GC-MS for natural estrogens, androgens or EDCs [63, 64], none of the recently published articles make mention of them for progestins or progestogens. The most popular method for quantification stays the LC with its improvement HPLC and UPLC. It is known to give low limit of quantification and limit of detection and doesn't require derivatization of sample prior measurement as for the GC-MS or GC-MS/MS methods. LDTD is a relatively new detection method using a diode to volatilize and ionize an analyte without the need of a LC step, making the experiment time of about 15s [65]. ELISA was used only in the case of levonorgestrel and was for the moment not applied to any other SOCs.

- The biosensors

Like for the analytical detection methods, many *in vivo* and *in vitro* biosensors have so far focused on estrogen-related compounds [66-69]. *In vitro* biosensors are mainly consisting in competitive ligand binding assays, cell proliferation assays and recombinant receptor/reporter assays. The last category is one of the most developed classes of biosensors and contains for example the cell-based assays like the YES-assay (using *S. cerevisiae* as organism) or the A-YES assay (using *A. adeninivorans* as organism). Among the few biosensors dedicated to progesterone detection, a majority of them are utilized for milk sample as it is of a great interest in food processing industry. It has been indeed demonstrated that monitoring the progesterone concentration of cow milk can be helpful in order to control their health and to detect estrus, which inform about their reproductive status [70]. Detection in a range comprised between 3-30 ng/ml is generally considered as sufficient and development of biosensors based on electrochemical detection [71, 72], surface plasmon resonance detection [73], lateral flow assay [74] and total internal reflectance fluorescence (TIRF) [75] have been reported. Most of them are using anti-progesterone antibodies as biological partners thus making them able to detect progesterone at very low levels in a competitive format assay. The main drawback of all these described biosensors remains that they were designed to detect only the progesterone molecule. A compound with progesterone activity like progestin or other progestogens will be impossible to detect with these described methods. One explanation for the absence of such biosensors may lay in the relatively low offer on recombinant progesterone receptor available. Development of broad range assay for estrogenic activity screening made indeed great advance because recombinant estrogen receptor or estrogen receptor LBD have been successfully expressed in various organisms and integrated in *in vivo* or *in vitro* biosensors [76-79]. Recombinant progesterone receptor has also been reported as full-length protein produced in insect cells [80, 81] as well as ligand binding domain expressed in *E. coli* [81, 82]. Unfortunately, the difficulties in its purification concerning the total protein or the fact that the LBD could not have the same binding properties as the complete receptor made the integration of these proteins in a biosensor so far challenging. That's why producing a purified full-length human progesterone receptor can greatly accelerate the development of a biosensor for progestogens and progestins detection.

1.2 The HER-2 biosensor

1.2.1 Breast cancer

Breast cancer stays one of the highest causes of death by cancer worldwide and the most common cancer in women. According to the last official data available published on the website of the GLOBOCAN project, more than 1.5 million new cases of breast cancer were diagnosed worldwide in 2012 [83]. There are slightly more cases diagnosed in less developed regions than in more developed regions but the mortality rate is much higher in the less developed regions with almost 37 % to compare with the 25 % mortality rate in more developed regions. This is a sign that available therapy against breast cancer made significant breakthrough as the more developed regions have a better access to these therapies. Breast cancer cannot be seen as a homogeneous disease as it

shows various morphological appearances, molecular features and behaviors. That's why pathologists made a great effort in order to establish different classes of breast cancer and so adapt the therapy to each patient. The four main classification determinants are the lymph node status, the tumor size, the gene expressed and the histological grade [84]. Lymph nodes are small organs part of the lymphatic system and are key elements in the propagation of cancer. The more carcinoma cells are present in the lymph node and the more risks have the patients to suffer from metastatic cancer, thus lowering its survival prognosis [85]. Tumor size is one of the first classification method historically developed and do inform the pathologist on the stage at which the cancer might be by measuring the tumor in centimeters or millimeters [86]. Recent researches tend to reduce the use of tumor size as classification method as small tumors showed in some cases more aggressiveness than bigger ones [87, 88]. Genomic assays called molecular profiling tests are a relatively new set of DNA arrays which aim to detect the presence or absence of particular genes in the tumor cells [89-92]. Thanks to the last advances in oncological research, it is now known that cancer formation involves the mutation or deletion of different type of genes called oncogenes and that each cancer has its own genomic history. Some of these genes are more often affected than the others and companies now offer the possibility to test their status in order to adapt the treatment of the patient. The most used tests are currently Oncotype DX® (Genomic Health, Inc., Redwood City, USA) and MammaPrint® (Agendia BV, Amsterdam, Netherlands). One of the best-established classification methods stays the histological grade determination called the Scarff-Bloom-Richardson grading system with the Nottingham (Elston-Ellis) modification [93-95]. Abbreviated in NGS for Nottingham Grading System, this is the grading system recommended by almost all professional pathologist organizations (World Health Organization [WHO], American Joint Committee on Cancer [AJCC], European Union [EU] and the Royal College of Pathologists (UK RCPath) [96, 97]). By looking at tumor tissue differentiation, the pathologists grouped all tumors in 3 grades with two stages for each grade. Most important morphological features for helping this determination are tubule or gland formation, nuclear pleomorphism and mitotic count [93, 96]. Beside these four main classification determinants, the expression of particular protein in cancer cells has been found to be good prediction markers of cancer aggressiveness and progression. The role of hormonal receptors expression was indeed discovered in the eighties and is now integrated in the recommendations of the American Society of Clinical Oncology (ASCO) [98]. Positive cancers for estrogen or progesterone receptors gene expression are known to respond positively to hormonal therapy involving the use of selective estrogen-receptor response modulators (like Tamoxifen) [99], aromatase inhibitors [100], estrogen-receptor down-regulators [101] or luteinizing hormone-releasing agents [102]. In case of the cancer doesn't show any expression of hormonal receptor, the presence of another receptor have been intensively studied in the last years, the HER-2 protein.

1.2.2 HER-2 and the EGFR family

In the eighties, three different research groups discovered the presence of one particular gene responsible for the production of a 185 000 Dalton protein associated with tumor formation [103-105]. They called these genes respectively *neu*, *HER2* and *c-erbB-2* and some years later, following researches demonstrated that these three genes were in fact one [106] and were coding for a 138

kDa protein. The apparent molecular mass of 185 kDa in SDS-PAA gel electrophoresis is generally attributed to glycolisation events or incomplete SDS binding [107]. The scientific community decided then to use *ERBB2* as recommended gene name and receptor tyrosine-protein kinase erbB-2 as recommended protein name [108]. Despite these recommendations, this receptor is often named HER2, HER-2, HER-2/neu or c-erb B2 and no real consensus about its name has been for made so far. In the following work, the receptor will be called HER-2 as it is one of the most used terminologies. HER-2 is a member of the epidermal growth factor receptor (EGFR) family which also include three other members: EGFR (also named HER-1 or erbB1), HER-3 (erbB3) and HER-4 (erbB4) [109, 110]. EGFR family is itself member of the supra family of the receptor tyrosine kinases (RTKs) known to be involved in several metabolic pathways related with cell proliferation, differentiation, adhesion, survival and migration [111, 112]. All HER proteins possess a similar structure composed of one extracellular domain harboring a ligand binding region, a transmembrane fragment and an intracellular region with a tyrosine kinase activity [113]. Exceptions of this rule are HER-2 which doesn't possess a ligand binding domain and HER-3 which show no tyrosine kinase activity [114]. Ligands of these receptors are multiple but selective for HER receptors. For example epidermal growth factor (EGF) can only bind to HER-1, epiregulin (EREG) is interacting only with HER-1 and HER-4 and neuregulin 1 (NRG1) shows solely affinity for HER-3 and HER-4 [115, 116]. Upon binding to the ligand, a common dimerization process occurs for each receptor either in a homodimer or in a heterodimer way [117]. Even though HER-2 is considered as an orphan receptor, it is the favorite partner for heterodimerization in the EGFR family [118]. This dimerization is the key factor for activating the kinase activity of the receptor intracellular part and therefore the starting point of the kinase cascade and the trigger of all downstream pathways [119]. After that, the ligand-receptor interaction is broken and dimerized receptors are then inactivated [120].

1.2.3 HER-2 in breast cancer: signification and consequences

Once this 185 kDa HER-2 was discovered, several *in vivo* and *in vitro* studies highlighted the association between the presence of this protein and the development of tumors [121-123]. High level of the receptor on the surface of carcinoma cells is observed in 10 to 34 % of all breast cancer [124] and 88 % of recently published researches could establish a correlation between prognosis and HER-2 status [125]. Nowadays, HER-2 is considered as one of the most important predictive and prognostic marker for tumor aggressiveness and patient survival [109]. In response to these scientific findings, the American society of clinical oncology (ASCO), which is the reference organization worldwide for pathologists, recommends the testing of every newly diagnosed case of breast cancer for the overexpression of HER-2 or the amplification of the related gene [126]. This testing allows patients with HER-2 type breast cancer to receive a specific therapy consisting generally of monoclonal antibody targeting the extracellular part of the receptor (Trastuzumab (Herceptin®, Roche)) [127-129], tyrosine kinase inhibitor (Lapatinib (Tyverb®, GSK)) [130] or a combination of both [131]. The biological background of the involvement of HER-2 during cancer development is slowly becoming uncovered and is likely to be related with the dimerization processes of EGFR. Recent studies showed that heterodimerization after binding to a ligand allows amplification and diversification of signal response and that each particular association is the part of

a complex network [116]. Overexpression of HER-2 may break this network balance and lead to the dominant formation of HER-2/HER-2 homodimers without any ligand binding thus activating the downstream pathways in an uncontrolled way [132]. This hypothesis is strengthened by the fact that HER-2 is known to have the most efficient tyrosine kinase domain [133]. As these downstream pathways concern cell proliferation, survival or differentiation, the negative effect of this loss of control can be explaining the formation of cancer cells. Although HER-2 has been historically linked with breast cancer, new evidences of its implication in colon [134], bladder [135], ovarian [136], endometrial [137], lung [138], uterine cervix [139], head and neck [140], esophageal [141] and gastric carcinomas [142] have been revealed.

1.2.4 HER-2 testing in breast cancer

In order to detect the presence of the HER-2 protein or the amplification of the responsible gene, only two methods are recommended by the Federal Drug Administration (FDA) for diagnosis purpose [143].

- Immunohistochemistry (IHC)

This observation technique is generally the first test performed once a breast cancer has been detected. A small part of the tumor is surgically removed during a biopsy and either frozen or embedded in paraffin in order to fix the tissue. A monoclonal or polyclonal antibody directed against the HER-2 protein is then allowed to search for its antigen in the fixed tissue and a colorimetric detection of the antibody reveals this binding to the pathologist. According to the staining, the pathologist can class the tumor specimen in a 4-graded scale going from 0 to 3+ [144, 145]. The signification of level of this scale and how the pathologist should determine it is given in the algorithm in Figure 1-3 published by the American society of clinical oncology.

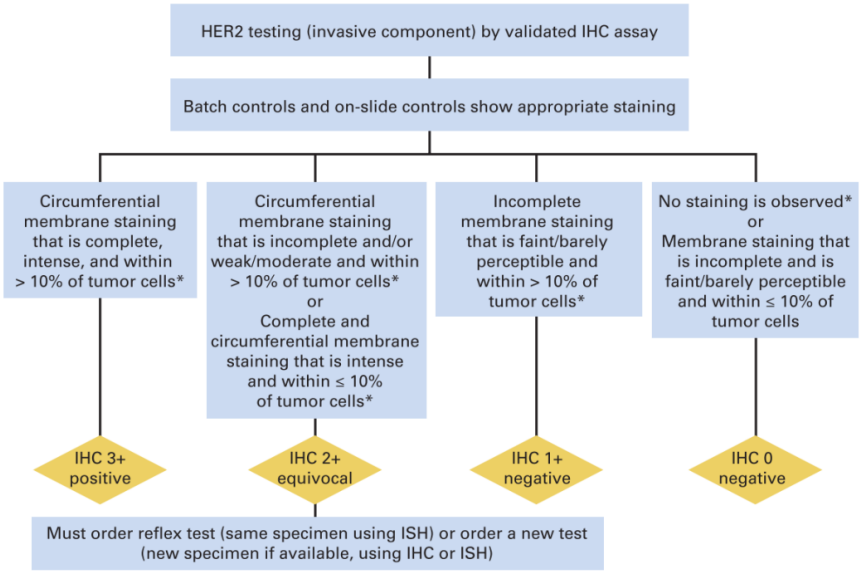

Figure 1-3. Algorithm for evaluation of HER-2 level by immunohistochemistry. (*)Readily appreciated using a low-power objective and observed within a homogeneous and contiguous invasive cell population [146].

Only two tests for immunohistochemistry are currently FDA-approved [147, 148] and the qualitative information that these tests give makes the need of a quantitative alternative desirable [149, 150].

- Fluorescence In Situ Hybridization (FISH)

FISH detection method is more labor-intensive, complex and expensive than the IHC but also proven more reliability, sensitivity and reproducibility [151]. Starting from the same material, FISH will look for gene amplification instead of protein presence at the membrane by using a fluorescent probe targeted against the *HER-2* gene. In a similar way as for IHC, the pathologist can then observe hybridization images and classify the tumor sample according to an algorithm presented in Figure 1-4.

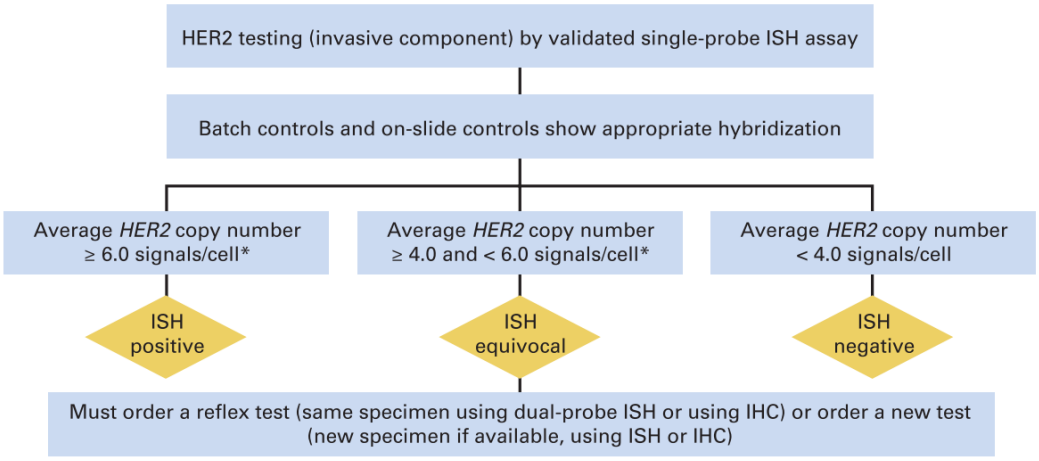

Figure 1-4. Algorithm for evaluation of *HER-2* expression by in-situ hybridization. (*)Observed in a homogeneous and contiguous population [146].

One of the remaining problems of this detection method stays the qualitative information given which is the cause of important inter-laboratory discrepancy [151-154]. Polysomy of the chromosome 17, which is relatively frequent in breast carcinomas, is also the source of false positive in FISH analysis [155], thus necessitating the use of dual color FISH and so increasing the complexity of the assay.

Even though these two techniques are the gold standard of HER-2 testing, alternatives are needed in order to ameliorate it. One of the most important pitfalls of both tests remains the presence of intratumoral heterogeneity which can lead to dramatic change in the results dependent on the biopsy localization. Other concerns are raised due to the low concordance between IHC and FISH for the intermediate grades like 1+ or 2+ which necessitate to perform both tests thus increasing the costs and the duration of the testing.

1.2.5 New HER-2 testing strategies

To face this need of new HER-2 testing methods, the scientific community explored different strategies in the last years.

- CISH / SISH / BDISH

Chromogenic In Situ Hybridization (CISH) [156, 157], Silver In Situ Hybridization (SISH) [158, 159] and Brightfield Double In Situ Hybridization (BDISH) [160] can all be considered as improvement of the FISH technology as they all use similar tissue and a similar technique to assess gene amplification in breast carcinoma. The differences between them lay in the visualization method based on enzymatic reaction at the probe instead of fluorescence emission. These In Situ Hybridization techniques have the great advantage to be less costly than FISH as a simple brightfield microscope is needed and the tested samples remain stained for a long period without fading. Moreover, concordance between FISH and CISH for example has been shown to be superior to 99 % for both positive and negative results [157].

- PCR

With the development and amelioration of the polymerase chain reaction (PCR) called RT-QPCR (Taqman-based Reverse Transcription Quantitative PCR), the scientific community can now detect very low levels of mRNA in a wide range of tissues in a very reproducible way and this method has been therefore employed for the detection of *HER-2* mRNA [161, 162]. The quantitative aspect of the technique is a major advantage in comparison to IHC or FISH because no human subjective decision has to be made if the protocol was scrupulously followed. Additionally, this method allows multiple screening of one particular sample for other cancer-related receptors like the estrogen receptor (ER) or the progesterone receptor [162]. The main drawback remains its affection by dilutional artifacts made possible by the heterogeneity of the tissue. Breast cancer often shows a discontinuous morphology with normal healthy cells surrounded by carcinoma cells and, as the RT-QPCR will only need few cells for the test, the risk to miss the problematic cells is high and will lead to a false negative result. IHC and FISH lower this risk because the pathologist can look at different position on the tissue morphology under microscope.

- ELISA

A proteolysis product of HER-2 called HER-2 ECD or p105 can be found in circulating blood and is believed to be an interesting tool for cancer diagnosis and monitoring. As blood samples are much easier to handle than fixed tissue, development of ELISA techniques for detection of HER-2 ECD gained a rising interest [163]. Until now, no direct correlation could have been made between HER-2 ECD concentration in blood tissue and presence of HER-2 at the surface of cancer cells [164] but an increase in HER-2 ECD concentration in blood has been linked to the formation of particularly aggressive metastatic cancer [165]. Commercially ELISA tests detecting HER-2 full receptor are also available (PathScan® Total HER2/ErbB2 Sandwich ELISA Kit, Cell Signaling Technology®) or the Her2 (Total) Human ELISA kit ("NOVEX®", Thermo Fisher Scientific) but their performances and benefits are unclear and none of these tests are recommended for diagnosis as they are mostly used to detect HER-2 protein extracted from artificial cell lines and not the one present in breast tissue.

- Other methods

Detection of either HER-2 or its extracellular cleavage product HER-2 ECD is also the goal of studies using Western blot [166], Dot Blot [167], piezoelectric microcantilevers (PEMS) [168] or surface

plasmon resonance (SPR) [169] but none of these techniques could reach the high standards of a FDA approved detection method for diagnosis purpose. It is to note that all these quantitative methods are lacking the presence of a purified standard in high quantity and are only relying on cellular lysate preparation of human breast cancer cells.

1.3 Yeast as hosts for recombinant protein production

Recombinant protein production is now a well-established market for the bio-pharmaceutical industry with a value of 87 billion USD in 2009. Preferred hosts for recombinant protein production are higher eukaryotes with 50 % of the market, prokaryotic hosts with 20 % of the market and yeasts with 30 % of the market [170]. As most of the recombinant proteins are originating from eukaryotic organism, the use of an eukaryotic host is often preferred against prokaryotic host as the latter generally doesn't offer the possibility to produce correctly folded and glycosylated proteins [171, 172]. Yeast cells in particular have the advantage to be considered as easier to handle than mammalian or insect cells. Among all yeast species discovered until now, nearly 100 % of all commercial recombinant proteins were produced in the baker yeast *Saccharomyces cerevisiae* [170]. To explain this, the historical importance of this particular yeast as main fermentative actor of beer and bread together with its intensively studied metabolism are often proposed. No yeast genome have been more analyzed and modified, thus making it a designated candidate for any recombinant protein production. Now that the genome of many other types of yeast becomes undercover, other candidates have been selected in order to produce recombinant proteins. They are often classified in conventional and non-conventional yeasts or Crabtree positive and Crabtree negative yeasts but these classifications tend to vanish as they are just separating *Saccharomyces cerevisiae* from all other yeasts [170]. Nowadays and in regard to recombinant protein production, the most appropriate separation should be made between methylotrophic yeasts which can use single carbon compound like methanol as carbon source and non-methylotrophic yeasts which cannot use these substrates. Both types of yeast show different expression capacities and should therefore be tested for recombinant protein production. That's why the following work will use the non-methylotrophic yeast *Arxula adeninivorans* and the methylotrophic yeast *Hansenula polymorpha* for production of recombinant human receptors.

1.3.1 *Arxula adeninivorans*

Arxula adeninivorans (syn. *Blastobotrys adeninivorans*) is a non-methylotrophic yeast which has been investigated in detail for more than 20 years [173]. This dimorphic, haploid and non-pathogenic organism proved in several occasion its ability to produce a wide range of enzymes like feed additive phytic acid phosphatase [174], tannase [175], lipase [176], adenine deaminase [177], xanthine oxidoreductase [178], urate oxidase [179] as well as therapeutics like interleukin-6 [180] and other proteins like human serum albumin [181]. Additionally, *A. adeninivorans* is the main component of the A-YES assay (A-YES®_AQUA 1.1, New Diagnostics GmbH), a yeast-based assay for the detection of estrogenic compounds, in where its genome was modified in order to produce recombinant human estrogen receptor [76, 77]. All these protein productions are made possible by the development of a patented expression system platform called Xplor®2, based on an *E. coli-A.*

adeninivorans hybrid plasmid [182-184]. The yeast part of the vector possesses two *A. adeninivorans* derived ribosomal fragments called d25S-rDNA1 and d25S-rDNA2 separated by a multi-cloning site allowing the introduction of up to five different modules for selection or expression. *E. coli* part consists of replication origin and selection marker for cloning steps and is removed before the transformation of the yeast with the linearized vector. An overview of the Xplor2 plasmid can be observed in Figure 1-5.

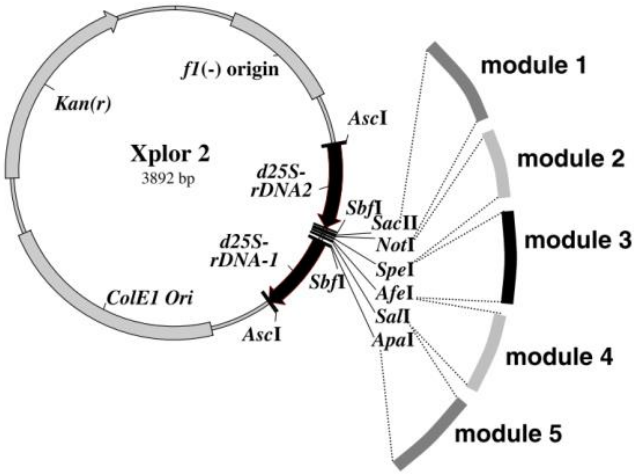

Figure 1-5. Overview of the Xplor2 yeast rDNA integration plasmid with *E. coli* part for cloning steps, two rDNA sequence for targeted integration in yeast genome and a multicloning site allowing insertion of up to five modules for selection and expression.

Linearization of the Xplor2 vector can be performed by two different enzymes: *Asc*I and *Sda*I. Restriction with *Asc*I will produce a vector containing the two rDNA sequences and this will lead to the targeted integration of the desired gene in *A. adeninivorans* rDNA cluster. Such product is called YRC for Yeast rDNA Integrative Cassette. Restriction with *Sbf*I will remove these two sequences and therefore allow random integration of the gene in *A. adeninivorans* genome. Such fragment is called YIC for Yeast Integrative Cassette.

Selection for positive transformants is based on complementation of auxotrophic *A. adeninivorans* G1212 mutants which are unable to grow on medium without tryptophane because they lack the phosphoribosyl anthranilate isomerase (Atrp1p), an enzyme essential for tryptophane synthesis. The selection module therefore consists in the mutated *ATRP1m* gene under the control of the *ALEU2* promoter. In this particular configuration, the vector is called Xplor2.2 [185]. Expression module consists in the constitutive *A. adeninivorans* derived *TEF1* promoter, the desired gene ORF with or without His-tag encoding sequences and the *S. cerevisiae* derived *PHO5* terminator. An overview of a typical YRC used in the following work can be seen in Figure 1-6.

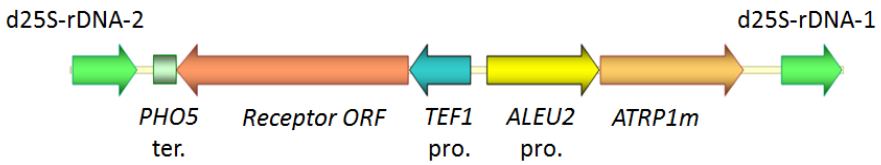

Figure 1-6. Physical map of YRC102-receptor for recombinant receptor production.

Transformation in auxotrophic *Arxula adeninivorans* mutants G1212 is followed by a stabilization procedure because of the presence of mitotic unstable transformants. This step is performed by passaging the yeasts in selective (without tryptophane) and non-selective (with tryptophane) media. After this step, transformants have been shown to be stable for several generations [186].

1.3.2 *Hansenula polymorpha*

Hansenula polymorpha (syn. *Hansenula angusta*, *Pichia angusta*) is one of the two most cultivated methylotrophic yeasts for recombinant protein production together with *Pichia pastoris* [187, 188]. Its major feature is the presence of one MOX (methanol oxidase) enzyme which allows this yeast to use methanol as carbon source by oxidizing it in formaldehyde which can then enter both the cytosolic dissimilatory pathway and the assimilatory pathway [187, 189]. Interesting for recombinant protein production is that this MOX enzyme as well as the formate dehydrogenase (FMD) and the dihydroyacetone synthase (DAS) are only produced in presence of methanol, thus enabling the use of the genes responsible for their production as inducible promoters [190, 191]. Additionally, the integration of a *Hansenula* Autonomous Replication Sequence (*HARS*) in expression vector shows remarkable mitotic stability and allows transformation without prior linearization of the vector [192-194]. Auxotrophic mutants can also be constructed and one of the most used mutants, the RB11 strain, presents an incapacity to grow without addition of uracil. It is because one of its essential genes for uracil synthesis has been knocked-out [195]. So the uracil-related *Saccharomyces cerevisiae* derived orotidine 5'-phosphate decarboxylase gene (*URA3*) can be used as selection marker [194, 196]. These findings led to the construction of the pFPMT121 vector for production of recombinant protein described in Figure 1-7.

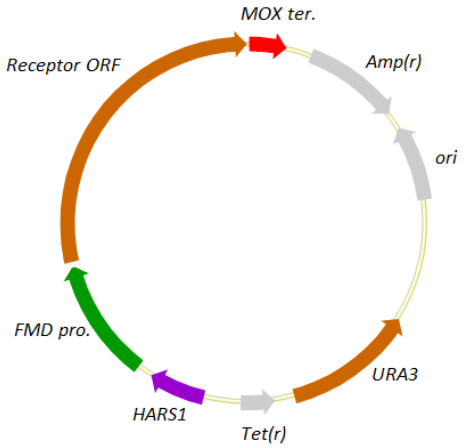

Figure 1-7. Genetic map of the pFPMT121 expression vector for production of recombinant human receptor. Ampicillin resistance gene (*Amp*), tetracycline resistance gene (*Tet*) as well as *E. coli* replication origin (*ori*) are necessary for cloning step and are not removed before yeast transformation.

For this study, it was decided to use *FMD* as methanol-induced promoter as it shows a very high activity in *Hansenula polymorpha* strain RB11 and the *MOX* terminator as it is until now the only successful terminator. No direct comparison between *FMD* and *MOX* promoters was so far performed but indirect comparisons give a small advantage for the *FMD* promoter in terms protein production [197]. It should also be mentioned that if *FMD* is described as a methanol-induced promoter, new studies are reporting higher recombinant protein yield with the use of glycerol as carbon source [198, 199]. This could mean that the derepression of the *FMD* promoter when glucose is not present in the culture may be more important than the induction via methanol.

1.4 Surface Plasmon Resonance: theory and applications

1.4.1 SPR theory

Surface Plasmon Resonance (SPR) is a binding interaction determination method based on an optical phenomenon discovered in the beginning of the twentieth century [200]. To observe this phenomenon, a polarized light beam should hit a thin metal layer in total internal reflection (TIR) conditions. It is known for centuries that when a light propagates with an angle a in a dense medium with a refractive index n2 and meet another less dense medium with refractive index n1, the angle b at which the light will propagate in the second medium will be different from a. This situation is described in the first part of the Figure 1-8. It was also observed that passed a critical angle Θ, no propagation of the light in the less dense medium will be observed, thus leading of the TIR conditions observed in last part of the Figure 1-8 when the angle a is superior to Θ.

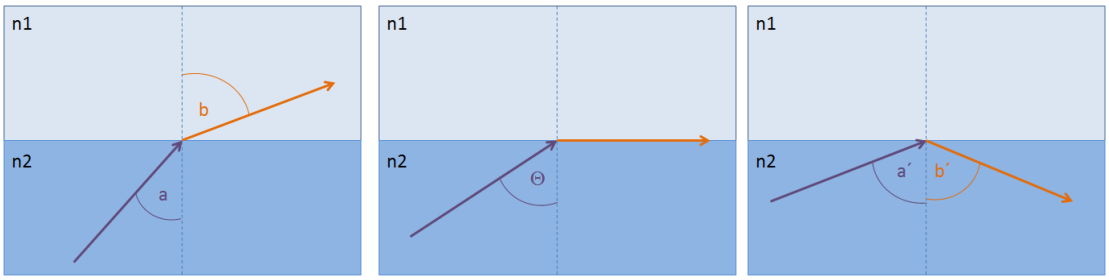

Figure 1-8. Scheme of the total internal reflection conditions.

If a thin layer of metal is positioned at the interface between the two media and if TIR conditions are met, then it will be observed that for one unique incident angle, the reflected light beam will show a decreased intensity in comparison to the incident light. This occurs because the electrons composing the external band of the metal have the possibility to absorb the energy of the incoming photons and convert themselves into entities called surface plasmon. The absorbed energy will then lead to the absence of photons in the reflected light materialized as a decreased light intensity. This energy transfer from the photon to the surface plasmon is called surface plasmon resonance and occurs only when the photon is hitting the metal with a particular angle [201, 202]. The value of this angle is itself dependent on two main parameters: the nature of the metal and the refractive index of both media at the interface. The metal at the interface should possess conduction band electrons capable of resonating with the incoming light at a suitable wavelength. Metals satisfying this condition are silver, gold, copper, aluminum, sodium and indium [203]. Because gold is known to be very stable relating to oxide or sulfide formation in comparison to silver, less reactive than sodium, less expensive than indium and possesses a narrower SPR response than aluminum and copper, it is the most used metal for SPR experiments. The refractive indexes of both media are dependent on the composition of the media and the temperature. As the medium where the light is propagating is generally glass, it can be considered that no significant change in temperature or composition occurs during the experiment. The upper medium is generally consisting of a chamber filled with liquid solution and its refractive index can be modified by its composition or temperature. As most of the SPR platforms possess a temperature regulating system, the only changing parameter determining the position of the resonance angle stay the composition of the medium on nearby region of the gold surface.

By immobilizing one partner involved in a molecular interaction (antibody-antigen, receptor-ligand, DNA-DNA) on the gold surface, the refractive index of the medium in the near proximity of the interface is slightly modified and this lead to a change of position of the resonance angle (angle α in Figure 1-9). Because this resonance angle position can be modified by any change in the upper medium refractive index until up to 300 nm, a binding of the second interaction partner to the immobilized one will modify the refractive index of the medium near to the gold surface, thus leading to a change in the position of the resonance angle from α to β [204]. This all process is again described in Figure 1-9.

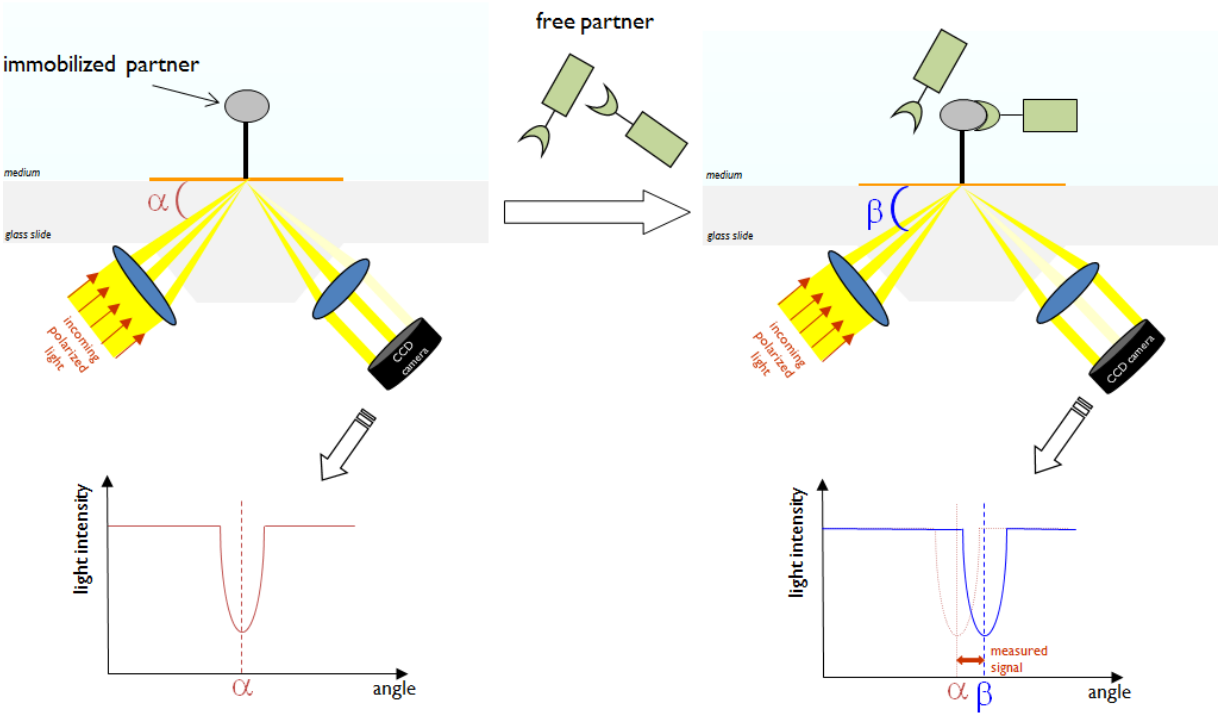

Figure 1-9. Schematic description of an SPR experiment. Angles α and β refers to the angles mentioned in the text of the section 1.4.1.

It has been demonstrated that the change of the resonance angle position is correlated with the number of molecules attached to the metal surface and this correlation follows a linear shape in the case of most protein-protein interactions [205, 206]. This ensures that this method is quantitative.

1.4.2 SPR method in biosensors: some examples

The SPR market is constantly growing and the number of manuscripts describing sensors using the SPR technology is increasing in an exponential way. Nowadays, one SPR device, the Biacore (GE Healthcare, Little Chalfont, UK), is used most of the time but other companies like Bio-Rad, Texas Instruments or IBIS Technologies are also developing their own SPR-based sensors. In the following work, all SPR-experiments will be performed by using a device developed conjointly by the IOF Fraunhofer Institute Jena and the IWS Fraunhofer Institute Dresden. If the method used for resonance angle determination is following exactly the same theory as explained in the precedent section, the novelty of this device and its recent commercialization are the reasons why only few research publications can be found using it [207, 208]. Moreover, the device possesses some particular features which will be examined in detail in the Material and Methods section 3.10.1.

Among all sensors using the SPR technology and reviewed in the work of Homola et al. [209], particular attention should be given to biosensors as their number is constantly increasing. From the first description of a biospecific interaction in 1983 [210], SPR technique has been used for the determination of human glycoprotein binding kinetics with monoclonal antibodies [211], for the examination of antibacterial synthetic peptides structure –function relationship [212] or for testing

of a library in order to determine binding affinity of a T-4 monoclonal antibody Fab fragment for thyroxine analogs [213]. SPR biosensors have been also developed to be used in medical diagnosis as they can monitor the concentration of pathogenic antigens in blood sample or measure directly the quantity of viruses in several fluids [214-216].

2 Aims of the thesis

The following work will follow the development of two novel biosensors aimed to detect compounds with progesterone activity and to quantitatively determine the amount of HER-2 protein in breast carcinoma cells. If their field of application is completely different, both biosensors are sharing the same SPR-detection method and the biological components will be produced in the same yeast species.

2.1 The progesterone receptor biosensor

The key component of a SPR-based progesterone biosensor will be the production of a recombinant human progesterone receptor. In the following study, its production in two different yeasts, the methylotrophic *Hansenula polymorpha* and the non-methylotrophic *Arxula adeninivorans*, will be considered. Starting from yeast optimized genetic sequence of this human receptor, all necessary cloning steps will be performed in order to build functional vectors for protein production in both organisms with the integration of His-tag at the N-terminus, at the C-terminus and without His-tag integration. All these cloning steps will be performed in the prokaryote *E. coli*. After transformation of both yeasts species, expression of the human progesterone receptor would have to be confirmed by Western blot using different progesterone-targeted antibodies. In order to have a better control on the recombinant protein production and maximize it, some medium tests will be performed as well as batch cultivation in bioreactor. In a next step, protein purification strategies will be designed by using His-tag affinity columns, anion exchange chromatography and CHT hydroxyapatite chromatography. Once a sufficient amount of purified human progesterone receptor will be produced, functional studies will be conducted in order to confirm that the recombinant protein can bind progesterone, its favorite ligand. This will be performed by an own designed ELRA test (Enzyme Like Receptor Assay) which is well-established for estrogen receptor binding studies. Finally, experiments to test the suitability of a SPR-based biosensor for the detection of compounds with progesterone activity will be performed. For this, different immobilization strategies and SPR-experiments will be designed and tested as no protocol for this particular device and application type are available so far.

2.2 The HER-2 biosensor

For the development of an HER-2 SPR-based biosensor, the recombinant production of human HER-2 protein in yeast will be one of the major challenges. Gene of this protein will also be cloned in different plasmids with or without His-tag encoding sequence for transformation in *Arxula adeninivorans* and *Hansenula polymorpha*. Production of this receptor will be observed by Western blot and its localization in yeast will be determined. These steps are necessary for this protein as its transmembrane domain and high molecular mass can interfere with normal production of the recombinant protein. Once the production of HER-2 in yeast will be confirmed, solubilization of the protein as well as its purification will be considered. In parallel, batch cultivation in bioreactor should also be performed in order to monitor and maximize the recombinant protein production.

With a sufficient amount of purified HER-2, ELISA will be performed in order to test if the recombinant protein is suitable for immunodetection. This will ensure that the conformation of the protein is not damaged and can be recognized by an antibody. If this step is successful, SPR experiment will then be performed but as no recommended protocol has been yet proposed for this particular device, several immobilization strategies and experiment designs will have to be envisaged. These steps will lead to the establishment of the protocol for SPR-detection of recombinant HER-2 protein. Finally, real breast cancer samples from the Institute of Pathology from Dresden will be tested by the biosensor in order to test its suitability. As no standard protocol for HER-2 extraction from paraffin embedded tissue exists, its determination will first have to be performed by using different strategies and buffer formulations to then allow SPR quantitation.

3 Material and methods

3.1 Chemicals - kits - software - equipment

3.1.1 Chemicals

The following table shows an overview of used common chemicals with their manufacturers.

Table 3-1. Used chemicals.

Commercial name or chemical formula	Manufacturer	Location
1,4-dithiothreitol (DTT)	Roth	Karlsruhe, Germany
3-(*N*-morpholino)ethanesulfonic acid (MES)	Serva	Heidelberg, Germany
3-mercaptoethanol	Sigma-Aldrich	Saint Louis, USA
3,3´-dithiobis[sulfosuccinimidylpropionate] (DTSSP)	Pierce-Thermo-Fisher Scientific	Rockford, USA
3,3',5,5'-tetramethylbenzidine (TMB)	Sigma-Aldrich	Saint Louis, USA
acetic acid	Roth	Karlsruhe, Germany
acrylamide solution Rotiphorese®	Roth	Karlsruhe, Germany
agarose	Sigma-Aldrich	Saint Louis, USA
ammonium persulfate (APS)	Merck	Darmstadt, Germany
antipain dihydrochlorid	Sigma-Aldrich	Saint Louis, USA
bicine	Roth	Karlsruhe, Germany
biotin	Sigma-Aldrich	Saint Louis, USA
boric acid	Roth	Karlsruhe, Germany
bromophenol blue	Sigma-Aldrich	Saint Louis, USA
bovine serum albumin (BSA)	Sigma-Aldrich	Saint Louis, USA
$Ca(NO_3)_2$	Roth	Karlsruhe, Germany
$CaCl_2$ x $2H_2O$	Riedel-de Haen-Sigma-Aldrich	Saint Louis, USA
carrier DNA	Sigma-Aldrich	Saint Louis, USA
CHAPS	Sigma-Aldrich	Saint Louis, USA
citric acid	Roth	Karlsruhe, Germany
cobalt (II) chloride	Fluka	Buchs, Switzerland
complete Freund's adjuvant	Sigma-Aldrich	Saint Louis, USA
$CuSO_4$ x 4 H_2O	Riedel de Haen	Saint Louis, USA
DEAE Sephadex A-25	Pharmacia	Uppsala, Sweden
decyl-β-D-maltoside (Dmal)	Fluka	Buchs, Switzerland
digitonin	Sigma-Aldrich	Saint Louis, USA
dimethylsulfoxide (DMSO)	Riedel de Haen	Saint Louis, USA
dithiobis(C3-NTA)	Dojindo	Kunamoto, Japan
D-pantothenic acid hemicalcium salt	Sigma-Aldrich	Saint Louis, USA
ethanol	Roth	Karlsruhe, Germany
ethidium bromide	Merck	Darmstadt, Germany
ethylene glycol	Roth	Karlsruhe, Germany

ethylenediaminetetraacetic acid (EDTA)	Roth	Karlsruhe, Germany
$FeCl_3$ x $6H_2O$	Serva	Heidelberg, Germany
formaldehyde (28%, v/v)	Roth	Karlsruhe, Germany
glucose	Roth	Karlsruhe, Germany
glycerol	Roth	Karlsruhe, Germany
glycine	Sigma-Aldrich	Saint Louis, USA
4-(2-hydroxyethyl)-1-piperazineethanesulfonic acid (HEPES)	Roth	Karlsruhe, Germany
imidazole	Sigma-Aldrich	Saint Louis, USA
inositol	Sigma-Aldrich	Saint Louis, USA
isopropanol	Roth	Karlsruhe, Germany
isopropyl β-D-1-thiogalactopyranoside (IPTG)	AppliChem	Darmstadt, Germany
K_2HPO_4	Roth	Karlsruhe, Germany
KCl	Sigma-Aldrich	Saint Louis, USA
KH_2PO_4	Roth	Karlsruhe, Germany
KI	Sigma-Aldrich	Saint Louis, USA
leupeptin hydrochloride	Sigma-Aldrich	Saint Louis, USA
lysing enzyme from *Trichoderma harzianum*	Sigma-Aldrich	Saint Louis, USA
Macro-Prep® Ceramic hydroxyapatite	Bio-Rad	Munich, Germany
methanol	Roth	Karlsruhe, Germany
methyl-6-O-(N-heptylcarbamoyl)-α-D-glucopyranosid (Hecameg)	Sigma-Aldrich	Saint Louis, USA
$MgCl_2$ x $6H_2O$	Roth	Karlsruhe, Germany
$MgSO_4$ x $7H_2O$	Roth	Karlsruhe, Germany
$MnCl_2$ x $4H_2O$	Roth	Karlsruhe, Germany
$MnSO_4$ x $4H_2O$	Roth	Karlsruhe, Germany
N,N-dimethyldodecylamine N-oxide (LDAO)	Sigma-Aldrich	Saint Louis, USA
Na_2MoO_4	Ferak	Berlin, Germany
NaCl	Roth	Karlsruhe, Germany
$NaNO_3$	Roth	Karlsruhe, Germany
NaOH	Roth	Karlsruhe, Germany
$NH_4H_2PO_4$	VEB Laborchemie	Apolda, Germany
NH_4OH	Sigma-Aldrich	Saint Louis, USA
nickel (II) chloride hexahydrate	Roth	Karlsruhe, Germany
nickel (II) sulfate hexahydrate	Fluka	Buchs. Switzerland
nicotinic acid	Serva	Heidelberg, Germany
n-octane	Sigma-Aldrich	Saint Louis, USA
n-octyl-β-D-glucoside (OG)	Sigma-Aldrich	Saint Louis, USA
nonfat dry milk	Roth	Karlsruhe, Germany
o(3-(aminoethyl)polyethylene glycol (HO-PEG-NH_2)	Sigma-Aldrich	Saint Louis, USA
octylphenoxypolyethoxyethanol (nonidet P40)	Roche Diagnostics GmbH	Mannheim, Germany

pepstatin A	Sigma-Aldrich	Saint Louis, USA
phenol/chloroform/isoamylalcohol solution 25:24:1	Sigma-Aldrich	Saint Louis, USA
phenylmethylsulfonyl fluoride (PMSF)	Serva	Heidelberg, Germany
phosphoric acid	Roth	Karlsruhe, Germany
piperazine-N,N′-bis(3-ethanesulfonic acid) (PIPES)	Roth	Karlsruhe, Germany
progesterone 3-(O-carboxymethyl)oxime:BSA-fluorescein isothiocyanate conjugate (progesterone-BSA)	Sigma-Aldrich	Saint Louis, USA
protein A	Amersham-GE Healthcare	Munich, Germany
protein G	Pierce-Thermo-Fisher Scientific	Rockford, USA
pyridoxine-HCl	Serva	Heidelberg, Germany
sodium acetate	Roth	Karlsruhe, Germany
sodium dodecyl sulfate (SDS)	Roth	Karlsruhe, Germany
sorbitol	Sigma-Aldrich	Saint Louis, USA
sulphuric acid	Roth	Karlsruhe, Germany
tetramethylethylenediamine (TEMED)	Riedel de Haen	Saint Louis, USA
thiamine dichloride	Merck	Darmstadt, Germany
trichloroacetic acid (TCA)	Fluka	Buchs, Switzerland
tris(hydroxymethyl)aminomethane (Tris)	Roth	Karlsruhe, Germany
triton X-100	Boehringer	Mannheim, Germany
tryptone	Sigma-Aldrich	Saint Louis, USA
tryptophane	Sigma-Aldrich	Saint Louis, USA
tween-20	AppliChem	Darmstadt, Germany
xylene	Sigma-Aldrich	Saint Louis, USA
yeast extract	Sigma-Aldrich	Saint Louis, USA
$ZnSO_4$ x $7H_2O$	Riedel de Haen	Saint Louis, USA

3.1.2 Kits and enzymes

All restriction enzymes and their respective buffers were form Thermo-Scientific (Rockford, USA). In Table 3-2, the used kits and other specific enzymes are presented.

Table 3-2. Used kits and enzymes.

Commercial kit or enzyme	Manufacturer	Location
BCIP/NBT tablets	Roche diagnostics GmbH	Mannheim, Germany
Bio-Rad protein assay	Bio-Rad	Munich, Germany
Calf intestinal alkaline phosphatase (CIAP)	Promega	Madison, USA
DreamTaq Polymerase	Thermo-scientific	Rockford, USA
Glucose assay kit	Roche diagnostics GmbH	Mannheim, Germany

Instantblue™ total protein staining	Expedeon	Harston, UK
Nucleo Spin Gel & PCR Clean-Up	Macherey-Nagel	Düren, Germany
PD10 columns	GE-Healthcare	Munich, Germany
Plasmid Midi Kit	Qiagen	Limburg, Netherlands
Protino® Ni-TED/IDA	Macherey-Nagel	Düren, Germany
Spin Miniprep Kit	Qiagen	Limburg, Netherlands
T4 DNA ligase	Thermo-scientific	Rockford, USA
TOPO®-TA cloning kit	Thermo-Scientific	Rockford, USA

3.1.3 Software

The following table shows the used software.

Table 3-3. List of the used software.

Software	Company	Location
Biostat®-A*plus* Fermentor system	Sartorius Stedim Systems GmbH	Melsungen, Germany
Codoncode Aligner	CodonCode Corporation	Centerville, USA
Endnote	Thomson Reuters	Philadelphia, USA
Magellan™	Tecan	Männedorf, Switzerland
Microsoft Excel 2013	Microsoft corporation	Redmond, USA
SigmaPlot 11.0	Systat Software Inc	San Jose, USA
Vector NTI®	Thermo-Scientific	Rockford, USA

3.1.4 Equipment

The following table shows the used equipment.

Table 3-4. List of the used equipment.

Equipment	Company	Location
analytical balance	Sartorius AG	Goettingen, Germany
BluMarine™ 200 electrophoresis	Serva Electrophoresis GmbH	Heidelberg, Germany
DNA Speed-vac DNA 100	Thermo-Scientific	Karlsruhe, Germany
Econo chromatography system	Bio-Rad	Munich, Germany
Fresco 17 centrifuge	Eppendorf	Hamburg, Germany
gel image system	Intas Science Imaging Instruments GmbH	Goettingen. Germany
Gel-drier Model 583	Bio-Rad	Munich, Germany
Lyophilisator Loc-3-M	Martin Christ Gefriertrocknungsanlage GmbH	Osterode am Harz, Germany
Mastercycler Gradient	Eppendorf	Hamburg, Germany
Maxisorp Immunowell plate	NUNC™	Roskilde, Denmark

Miniprotean electrophoresis and Western blot equipment	Bio-Rad	Munich, Germany
Minitron/Multitron shaking systems	Infors	Bottmingen, Switzerland
Mixer Mill M200	Retsch	Haan, Germany
Nanodrop 2000c spectrophotometer	PEQLAB Biotechnologie GmbH	Erlangen, Germany
Optima TL ultracentrifuge	Beckman Coulter Inc	Brea, USA
Polydimethylsiloxane (PDMS) flow cell	IWS Fraunhofer Institute Dresden	Dresden, Germany
R810.R centrifuge	Eppendorf	Hamburg, Germany
RC 6 centrifuge	Sorvall-Thermo Scientific	Rockford, USA
SPR chips	Capitalis Technology GmbH	Berlin, Germany
SPR device	Capitalis Technology GmbH	Berlin, Germany
SPR pumping system	MLE	Dresden, Germany
SPR vacuum pump ME 4 NT	Vacuubrand GmbH + CO KG	Wetheim, Germany
Sunrise reader	Tecan Trading AG	Zürich, Switzerland
Thermomixer 5436	Eppendorf	Hamburg, Germany
Ultrasound device	Schütt Labortechnik	Goettingen, Germany
Univessel 1L	Sartorius Stedim Biotech GmbH	Goettingen, Germany
Vibrofix VF1 vortexer	Janke & Kunkel, IKA Labortechnik	Staufen, Germany
Vivaspin 2 (30 kDa)	Sartorius Stedim GmbH	Goettingen, Germany
Water bath	Schütt Labortechnik	Goettingen, Germany

3.2 Strains - Vectors - Primers - Antibodies

3.2.1 Strains

Table 3-5. Used strains.

Strain	genotype	origin	reference
***E. coli* xl1 blue**	*recA1 endA1 gyrA96 thi-1 hsdR17 supE44 relA1 lac* [*F' proAB lacI^{q}ZΔM15* Tn*10* (Tet^r)]	Agilent Technologies, USA	[217]
***E. coli* BL21**	B F- *dcm ompT hsdS*(r_B-m_B-) gal [malB$^+$]$_{K-12}$(λ^S)	Agilent Technologies, USA	[218]
***Arxula adeninivorans* G1212**	[*aleu2 atrp1::ALEU2*]	Gatersleben, Germany	[184]
***Hansenula polymorpha* RB11**	*ura3-1*	Gatersleben, Germany	[195]

3.2.2 Primers

The underlined parts represent enzyme restriction site.

Table 3-6. Cloning primers.

Cloning primer name	Sequence
Pra-1-sense	GTTTGGAATTCATATGGGGCCACCGCCCCCGCTGCCGCCGCCGCGAG
Pra-1-antisense	GTAATAGGATCCCTACTGCGGCAGGCCCTCCTTGAGCAC
Pra-2-sense	GTCAGGAATTCATATGAAGGAAGATTCCCGCTTCTCAGCGC
Pra-2-antisense	AGATTCGGATCCCTAATAGAGAGGGTACGCGTCGTCCTTG
HER2a-sense	AGTCTAGAATTCATATGTATGTGAACCAGCCAGATGTTCGG
HER2a-antisense	ACATGCGGATCCCTATTTGAAGGTGCTGGGTGGAGCC
PROG-HT1	GAATTCATGACTGAGCTGAAG
PROG-HT2	GGATCCCTAGTGGTGGTGATGATGGTGCTTCTTGTGGAACAGCAGAG
HER2-HT1	GAATTCATGGAGCTGGCTGC
HER2-HT2	GGATCCCTAGTGGTGGTGATGATGGTGGACAGGGACGTCCAGTCC
HER-2-HT3	ATCGAGGTCGGCACTCAGAG
HER-2-HT4	GGATCCCTAGTGGTGGTGATGATGGTGGACAGGGACGTCCAGTCCCAAGTACTCG
Nter-HER2-P1	GAATTCATGCACCATCATCACCACCACGAGCTGGCTGCTCTGTGCCGATGGGGACT
Nter-HER2-P2	GGATCCCTAGACAGGGACGT
Prog-Nhis-P1	GAATTCATGCACCATCATCACCACCACACTGAGCTGAAGGCTAAGGGACCT
Prog-NHis-P2	GGATCCCTACTTCTTGTG

Table 3-7. Sequencing primers.

Sequencing primer name	Sequence
Tef-seq	TCCTTGTCAACTCACACCG
PHO5-seq	TCTCAATAGACTGGCGTTG
Her2neu-seq	CCTGAGTACGTCACTCCTCA
Prog-seq	TAAGCTGCTGGACAACCTGC

3.2.3 Vectors

Table 3-8. Used vectors.

Vector	Resistance gene	Reference/manufacturer
pBS-Amp^r-TEF1-PHO5	Amp^r	[182]
pB25S-Kan^r-ALEU3-ATRP1m-AS	Kan^r	[182]
pCR4®-Amp^r-Kan^r-TOPO	Amp^r, Kan^r	Invitrogen, Carlsbad, USA
pFPMT$_{121}$-HARS1-URA3	Amp^r, Tet^r	[195]
pET-16b	Amp^r	EMD Millipore, Darmstadt, Germany

pMK-RQ-ERbB2	Kan^r	Invitrogen, Carlsbad, USA
pMK-RQ-PR	Kan^r	Invitrogen, Carlsbad, USA

3.2.4 Antibodies

Table 3-9. Commercial antibodies used.

Reference name	Antigen	Clonality	Host	Manufacturer/Location
MA514842 Progesterone Receptor B (R.809.9)	Progesterone receptor isoform B	monoclonal	rabbit	Fisher Scientific GmbH, Schwerte-Geisecke, Germany
MA515050 HER2/ErbB2 (K.929.9)	HER-2	monoclonal	rabbit	Pierce Biotechnology, Rockford, USA
S3731 Anti Rabbit IgG (Fc) AP conjugate	Rabbit IgG (Fc)	polyclonal	goat	Promega. Madison, USA
A048529-2 Anti-c-erbB-2 oncoprotein	HER-2	polyclonal	rabbit	DAKO, Glostrup, Denmark
A8275 Anti-Rabbit IgG (Whole molecule) peroxidase conjugate	Rabbit IgG	polyclonal	goat	Sigma-Aldrich, Saint Louis, USA
Anti-HIS pAb	Polyhistine sequence	polyclonal	rabbit	Micromol GmbH, Karlsruhe, Germany

3.3 Molecular biological methods

3.3.1 Buffers

The following table shows the composition of some general buffers. Other specific buffers are described in their respective section.

Table 3-10. Composition of some routinely used buffers.

Buffer	Component	Quantity for 1 l buffer	Final concentration
Potassium phosphate buffer (20 mM, pH=7.5)	K_2HPO_4	2.73 g	15.7 mM
	KH_2PO_4	0.571 g	4.2 nM
Potassium phosphate buffer (20 mM, pH=6.8)	K_2HPO_4	1.41 g	8.1 mM
	KH_2PO_4	1.61 g	11.8 mM
Phosphate buffer saline (PBS)	Na_2HPO_4	7.65 g	4.3 mM
	KH_2PO_4	1.905 g	1.4 mM
	KCl	2.013 g	2.7 mM

	NaCl	8.006 g	0.137 M
Phosphate buffer saline with tween (PBS-t)	Na_2HPO_4	7.65 g	4.3 mM
	KH_2PO_4	1.905 g	1.4 mM
	KCl	2.013 g	2.7 mM
	NaCl	8.006 g	0.137 M
	Tween-20 (10 % stock solution)	0.5 g	0.05 % w/v

3.3.2 Human genomic DNA extraction

DNA samples from four different persons were extracted and then were pooled together to ensure sample anonymization. For this, the subject was rinsing his mouth with 20 ml of sterile H_20 for at least 15 s and then spiting the sample into a clean 50 ml tube. After a centrifugation at 15,000 g for 10 min, the pellet was resuspended in 500 µl extraction buffer (20 mM Tris-HCl, pH= 7.8) and transferred into a new tube. After addition of a 1:1:1 solution of phenol/chloroform/isoamylalcohol, the tube was inverted 5 times and centrifuged again at 17,900 g for 3 min. The upper phase was transferred in a new tube with a new solution of phenol/chloroform/isoamylalcohol. Then, after a centrifugation for 3 min at 17,900 g, the upper phase was transferred in a new tube and a 3M solution of sodium acetate (CH_3COONa) was added. The DNA was then precipitated by addition of isopropanol and incubation for 10 min at -20 °C. This solution was then centrifuged for 30 min at 17,900 g at 4°C and the supernatant was discarded. After a final wash with 70 % ethanol, the DNA was resuspended in ddH_2O. The concentration of the obtained DNA was measured via Nanodrop to be 15.7 ng/µl. This amount of DNA was sufficient to perform the subsequent steps.

3.3.3 Polymerase chain reaction

All the polymerase chain reactions (PCR) were performed with DreamTaq DNA polymerase as well as the DreamTaq polymerase buffer following the manufacture recommendations. An example of PCR program used can be seen on the Table 3-11. Depending on the length of the target fragment or the nature of the primers, the elongation time, the annealing temperature or the number of cycles were adjusted to obtain the maximum yield. A gradient PCR was for this purpose systemically performed.

Table 3-11. Overview of a typical PCR program.

Step	Number of cycles	Temperature	Time
Initial denaturation	1	94 °C	2 min
Denaturation	30	94 °C	30 s
Hybridization		55 °C	30 s
Elongation		72 °C	1 min
Final elongation	1	72 °C	5 min

3.3.4 DNA electrophoresis

An agarose/TBE solution (0.8-2.0 %, w/v-depending on the DNA-fragment length) was poured into a Bio-Rad casting device until solidification and then placed in a Bio-Rad electrophorese chamber with

TBE as running buffer. To allow visualization of the DNA under UV light, 1 % ethidium bromide was mixed within the gel solution. DNA sample was then mixed with load dye (6X DNA Loading Dye, Thermo-Scientific) at a 6:1 ratio and loaded on the gel. For DNA length estimation, DNA ladder (GeneRuler 1Kb DNA Ladder, Thermo-Scientific) was used. Electrophoresis was performed at 90 V and the ethidium bromide complexed DNA fragment was observed by a gel image system.

Table 3-12. Composition of the TBE buffer.

Buffer	Component	Quantity for 1 l buffer	Final concentration
TBE buffer	Tris	12.1 g	0.1 M
	EDTA	0.74	2.5 mM
	Boric acid	5.6 g	0.09 M

3.3.5 Enzyme restriction

All restrictions with one or two enzymes were performed according to the manufacturer at 37 °C for at least one hour. When three enzymes must be used, first a double restriction was performed, then the digested DNA was precipitated and the third restriction was performed.

3.3.6 DNA precipitation without phenol

Depending on the starting quantity of DNA, the following protocol was adapted to give the highest yield. For a 20 µl restriction solution, 5 µl of a 3M sodium acetate solution at pH=5.2 was first added, followed by 110 µl cold ethanol (96 %, -20 °C). After incubation at -20 °C for 10 min and centrifugation at 4 °C for 10 min, the supernatant was carefully removed and the precipitated DNA was resuspended in 1 ml ethanol/water solution (70%, v/v). Then, centrifugation at 4 °C for 3 min and 17,900 g was performed and the resulting pellet was resuspended in 1 ml ethanol (96 %). Finally, the tube was again centrifuged for 3 min at 4°C and 17,900 g and the air-dried pellet was then used as start material for the second restriction.

3.3.7 Dephosphorylation

To avoid recircularization of the vector after restriction, dephosphorylation was performed by adding 1 µl of calf intestinal alkaline phosphatase (CIAP, 1U/µl) at the end of the restriction and incubating this mix for 30 min at 37 °C. A final incubation at 65 °C for 15 min was then performed to inactivate the enzyme.

3.3.8 DNA ligation

Before each ligation reaction, 5 µl of the insert and 5 µl of the desired opened vector were loaded on an agarose gel for electrophorese and the relative quantity of DNA of each of them was estimated. Depending on the size of each DNA fragment, the ratio insert/vector was oscillating between 1:1 and 6:1. First, both fragments were incubated for 10 min at 50 °C and then T4-DNA ligase (5 U/µl) and T4-DNA ligase buffer were added in the tube followed by incubation for 20 min at 23 °C.

3.3.9 DNA extraction from agarose gel

Isolation and purification of DNA from agarose gel was performed by using the Nucleo Spin PCR & Gel Clean-up kit following manufacturer recommendations. For this experiment, a special set of comb allowing wide holes was used in the casted agarose gels.

3.3.10 Cloning with TOPO vector

Cloning of PCR product in a pCR4-TOPO vector was performed by using kit following manufacturer recommendations. For each reaction, the optional addition of 3' A-overhangs post-amplification was performed. For this, the gel-purified DNA fragment was incubated for 10 min at 72 °C with DreamTaq polymerase buffer, dATP and 0.5 unit of DreamTaq polymerase.

3.3.11 Mini preparation

To control the introduction of the correct plasmid into *E. coli* cells, mini preparation with solutions from the Spin Miniprep kit was performed. In a typical experiment, a transformed bacterial colony was cultivated in 2 ml LB medium supplemented with the appropriate antibiotic for at least 12 h at 37 °C under vigorous shaking. After pelleting the cells by centrifugation for 3 min at 17,900 g, 200 µl of cold buffer P1 (supplemented with RNase A to a final concentration of 20 µg/ml) was added and the resulting solution was vortexed. Then, 200 µl of the P2 buffer was added, the tube was inverted 6 times and lysis of the cells was allowed to occur for 3 min at 23°C. Subsequently, 200 µl of cold P3 buffer was added and the tube was inverted 12 times to allow complete precipitation of proteins and chromosomal DNA. After a 20 min centrifugation at 4°C, 500 µl of the plasmid-DNA rich supernatant was transferred in a new tube and the DNA was allowed to precipitate for 2 min by addition of 350 µl isopropanol (96 %). The tube was then centrifuged for 25 min at 17,900 g and 4°C and the precipitated DNA was resuspended in ethanol/H_2O solution (70 %, v/v). After a final centrifugation at 4 °C and 17,900 g for 3 min, the supernatant was discarded and the DNA pellet was allowed to dry until complete ethanol evaporation. Resuspension of the pellet was then performed in 50 µl dd$H_2$0 and depending on the minipreparation efficiency, 1 to 2 µl of DNA (approximately 1µg) was used for subsequent enzyme restriction.

3.3.12 Midi preparation

To obtain large amount of purified vectors, midi preparation was performed according to the Plasmid Midi kit following manufacturer recommendations. For this, a bacterial colony already tested via mini preparation and grown in 50 ml LB medium supplemented with the appropriate antibiotic was used as starting material. From this 50 ml, 2 ml were used to produce a glycerol stock of the colony and the rest was used for the midi preparation. At the end of the protocol, a control restriction was always performed with a 1:10 dilution of the resulting DNA as starting material.

3.3.13 Production of chemically competent XL1 blue or BL21 *E. coli* cells

A colony of *E. coli* XL1 blue or BL21 was cultivated for 10 h at 37 °C under vigorous shaking in 25 ml SOB medium (first pre-culture) and then diluted in 250 ml SOB medium for overnight cultivation at 18 °C under mild shaking (second pre-culture). This culture was then diluted in SOB medium to reach an OD_{620nm} value of 0.55. After the culture cooled down for 15 min in ice, the cells were centrifuged for 10 min at 3,000 g and 4°C and then resuspended in 50 ml cold INOUE buffer. After a centrifugation for 10 min at 3,000 g and 4°C, the pelleted cells were resuspended in 20 ml cold INOUE buffer supplemented with 1.5 ml DMSO. After sufficient mixing, the cells were incubated on ice for 10 min and then divided in 50 µl aliquots. For long-term storage these aliquots were frozen in liquid nitrogen and placed at – 80 °C.

Table 3-13. Buffer composition for chemically competent cells preparation.

Buffer	Component	Quantity for 1 l buffer	Final concentration
INOUE buffer	$MnCl_2$ x $4H_2O$	10.88 g	55 mM
	$CaCl_2$ x $2H_2O$	2.2 g	15 mM
	KCl	18.65 g	0.25 M
	0.5 M PIPES solution (pH=6.7)	20 ml	10 mM
	Sterile-filtered and stored at 4°C		
SOB buffer	Tryptone	20 g	2 % (w/v)
	Yeast extract	5 g	0.5 % (w/v)
	NaCl	0.5 g	8.5 mM
	KCl	0.15 g	2 mM
	$MgCl_2$ x $6H_2O$	2.03 g	10 mM
	$MgSO_4$ x $7H_2O$	2.47 g	10 mM
	Adjusted to pH=7.0 with NaOH, autoclaved and stored at 4°C		

3.3.14 Transformation of chemically competent *E. coli* cells

The transformation of XL1 blue or BL21 *E. coli* cells was performed on the basis of the modified protocol from Hanahan et al. [219]. In a typical experiment, 1 µl of ligation reaction (approximately 100 ng of plasmid DNA) was mixed with 50 µl of competent cells and incubated for 30 min in ice. Then, the tube was immerged for 90 s at 42 °C in a water bath and incubated in ice again for at least 5 min. After this so-called “heat shock”, 800 µl of sterile SOC medium (SOB medium + 20 mM glucose) was added to the cells and the whole reaction mix was incubated for 30 min at 37°C under shaking. Finally the transformed cells were transferred on agar culture plate supplemented with the appropriate antibiotic and then spread all over the surface with help of a sterile loop. Incubation of the plates occurred overnight at 37 °C.

3.3.15 Cultivation of *E. coli* cells

The cells were cultivated in LB broth medium supplemented with whether ampicillin at a 50 mg/l concentration or kanamycin at a 100 mg/l. Cultivation was performed under vigorous shaking at 37 °C.

Table 3-14. Preparation of *E. coli* media.

Medium	Quantity for 1 l buffer	Manufacturer
LB medium	20 g	Sigma-Aldrich
LB medium with agar	35 g	Sigma-Aldrich

3.3.16 Production of yeast competent cells (*A. adeninivorans* and *H. polymorpha*)

A colony of *A. adeninivorans* G1212 or *H. polymorpha* RB11 was isolated and cultivated in 10 ml yeast total medium (YPD) supplemented with 50 µg/ml tryptophane overnight either at 30 °C (*A. adeninivorans*) or 37 °C (*H. polymorpha*). This first pre-culture was then diluted with a 1:10 factor in 10 ml YPD supplemented with 50 µg/ml tryptophane for overnight incubation at the correct temperature. Then in order to obtain a main culture start OD_{600nm} of 0.5, a volume of this second preculture was transferred in 100 ml YPD supplemented with 20 µg/ml tryptophane. This culture was allowed to grow at the optimal temperature until OD_{600nm} reach 1.5. After that, the culture was centrifuged (5min/5,000 g/4°C) and the pelleted cells were resuspended in 50 ml cold sorbitol based buffer. After a second centrifugation at 4°C for 5 min at 5,000 g, the cells were resuspended in 2 ml sorbitol based buffer, aliquoted in tubes, frozen with help of liquid nitrogen and finally stored at -80°C.

3.3.17 Transformation of *A. adeninivorans* and *H. polymorpha* cells

Transformation of yeast cells is based on the work of Dohmen et al. [220] modified by Steinborn et al. [184]. Transformation of *A. adeninivorans* and *H. polymorpha* competent cells was slightly different because the vector should be linearized in the case of the first cited yeast. This was performed by enzyme restriction using *Asc*I to obtain YRC (yeast rDNA integrative expression cassette) or *Sda*I to obtain YIC (yeast integrative expression cassette). 20 µl carrier DNA was first denatured for 5 min at 100°C and then added to 200 µl still frozen competent cells together with 2 µl of the desired vector. After a 5 min incubation at 37 °C under vigorous shaking, 1.4 ml PEG-bicine solution was added and the tube was inverted several times. Then, one hour incubation at 30 °C without shaking was performed and the cells were then pelleted by a 5 min centrifugation at 23°C and 5,000 g. The supernatant was discarded and the cells were resuspended in 1.4 ml NaCl-bicine solution. After centrifugation (5 min/5,000 g/23 °C), the cells were resuspended in 500 µl NaCl-bicine solution and spread on a YPD agar plate with a sterile loop. Incubation of the plate occurred at 30 °C for *A. adeninivorans* and 37 °C for *H. polymorpha*.

Table 3-15. Composition of buffers for production and transformation of yeast competent cells.

Buffer	Component	Quantity for 1 l buffer	Final concentration
sorbitol based buffer	sorbitol	182.17 g	1 M
	bicine	1.63 g	10 mM
	ethylene glycol	30 ml	3 % (v/v)
	DMSO	50 ml	5 % (v/v)
	autoclaved and stored at 4°C		
PEG-bicine solution	PEG-1000	400 ml	40 % (v/v)
	bicine	32.63 g	0.2 M

	adjusted to pH=8.35 with NaOH, autoclaved and stored at 4°C		
NaCl-bicine solution	NaCl	8.77 g	0.15 M
	bicine	1.63 g	10 mM
	adjusted to pH=8.35 with NaOH, autoclaved and stored at 4°C		

3.3.18 Cultivation media for *A. adeninivorans* and *H. polymorpha*

All media were autoclaved before the introduction of the C-source and the vitamin mix.

Table 3-16. Composition of the yeast cultivation media.

Cultivation medium	Component	Quantity for 1 l buffer	Final concentration
Yeast extract-peptone-dextrose medium (YPD)	YPD-broth (Fluka)	50 g	
Yeast minimal medium with ammonium and glucose (YMM-ammonium-glucose)	$(NH_4)H_2PO_4$	5 g	43 mM
	KH_2PO_4	6.75 g	50 mM
	K_2HPO_4	1.75 g	10 mM
	$MgSO_4$ x 7 H_2O	1 g	8 mM
	minerals mix	1 ml	0.1 % v/v
	$FeCl_3$ x $6H_2O$ (2 g/l stock solution)	1 ml	0.012 mM
	$Ca(NO_3)_2$ (20 g/l stock solution)	1 ml	0.12 mM
	glucose (20 % w/v stock solution)	100 ml	2 % w/v
	vitamin mix	10 ml	1 % v/v
Yeast minimal medium with nitrate and glucose (YMM-nitrate-glucose)	$NaNO_3$	3.7 g	43 mM
	KH_2PO_4	6.75 g	50 mM
	K_2HPO_4	1.75 g	10 mM
	$MgSO_4$ x 7 H_2O	1 g	8 mM
	minerals mix	1 ml	0.1 % v/v
	$FeCl_3$ x $6H_2O$ (2 g/l stock solution)	1 ml	0.012 mM
	$Ca(NO_3)_2$ (20 g/l stock solution)	1 ml	0.12 mM
	glucose (20 % w/v stock solution)	100 mL	2 % w/v
	vitamin mix	10 ml	1 % v/v
Yeast minimal medium with nitrate and glycerol (YMM-nitrate-glycerol)	$NaNO_3$	3.7 g	43 mM
	KH_2PO_4	6.75 g	50 mM
	K_2HPO_4	1.75 g	10 mM
	$MgSO_4$ x 7 H_2O	1 g	8 mM
	minerals mix	1 ml	0.1 % v/v
	$FeCl_3$ x $6H_2O$ (2 g/l stock solution)	1 ml	0.012 mM
	$Ca(NO_3)_2$ (20 g/l stock solution)	1 ml	0.12 mM

	glycerol	20 mL	2 % v/v
	vitamin mix	10 ml	1 % v/v
Yeast minimal medium with nitrate and methanol (YMM-nitrate-methanol)	$NaNO_3$	3.7 g	43 mM
	KH_2PO_4	6.75 g	50 mM
	K_2HPO_4	1.75 g	10 mM
	$MgSO_4$ x 7 H_2O	1 g	8 mM
	minerals mix	1 ml	0.1 % v/v
	$FeCl_3$ x $6H_2O$ (2 g/l stock solution)	1 ml	0.012 mM
	$Ca(NO_3)_2$ (20 g/l stock solution)	1 ml	0.12 mM
	methanol	20 mL	2 % v/v
	vitamin mix	10 ml	1 % v/v
Minerals mix	H_3BO_4	500 mg	6.4 mM
	$CuSO_4$ x 4 H_2O	100 mg	0.63 mM
	KI	100 mg	0.6 mM
	$MnSO_4$ x 4 H_2O	400 mg	2.65 mM
	$ZnSO_4$ x 7 H_2O	400 mg	2.48 mM
	Na_2MoO_4	200 mg	0.97 mM
	$CoCl_2$	100 mg	0.77 mM
Vitamin mix	thiamine dichloride	400 mg	1.19 mM
	inositol	4 g	22.2 mM
	nicotinic acid	100 mg	0.81 mM
	pantothenic acid	400 mg	1.53 mM
	pyridoxine	400 mg	2.36 mM
	biotin	4 mg	0.016 mM

3.3.19 Determination of glucose concentration in the medium

In order to determine the glucose concentration of a medium, a culture sample was taken and centrifuged at 17,900 g for 10 min. After that, the supernatant was used as sample for the glucose concentration determination kit (Glucose assay kit) following manufacturer recommendations.

3.3.20 Stabilization of *A. adeninivorans* and *H. polymorpha* transformants

Stable yeast transformants were obtained after passaging on selective and non-selective media according to the protocol described by Klabunde et al. [186]. First, the transformed yeasts were transferred in fresh media consisting in YMM-nitrate-glucose every 48 h for a total of seven times. Then, the yeast were allowed to grow in YPD for 24 h and transferred in fresh YPD for 24 h cultivation. Finally, a last cultivation step in YMM-nitrate-glucose was performed. At the end of the stabilization process, 500 µL of the culture was mixed with 500 µL glycerol to obtain a stock solution which was stocked by -80 °C.

3.3.21 Screening of *E. coli* cell transformants

After transformation of competent BL21 cells with the desired vector, a colony was picked and cultivated for recombinant protein expression. For this, a preculture in LB medium supplemented with the correct antibiotic was incubated overnight at 37 °C under shaking and then divided in two main cultures of 50 ml LB with a start OD_{600nm} of 0.5. After a 30 min incubation at 37 °C, 0.5 mM IPTG was added in one of the culture and both were then cultivated for 3 h at 37 °C. Finally 1 ml of each culture was centrifuged and the pelleted cells were chemically lysed to extract the proteins. For this 100 µl of P1 buffer and 100 µl of P2 buffer from Quiagen mini preparation kit were used. The proteins were then prepared for SDS-PAA electrophoresis.

3.3.22 Screening of yeast transformants

The transformants were cultivated for 48 h in 750 µl YMM-nitrate-glucose at 30 °C under vigorous shaking. 400 µl culture was harvested (5,000 g, 5 min), and the pellet was washed with phosphate buffer saline (PBS). Cells were disrupted in lysis buffer by silica beads using a Mixer Mill MM400 for 3 min at a frequency of 30 s^{-1} and at 4 °C. After removal of cell debris (centrifugation at 5,500 g for 20 min) the lysate was kept on ice.

3.3.23 Cultivation of yeast transformants

As every strain has its own best cultivation conditions, the protocol is slightly different for each one. An overview of all the parameters can be seen in the Table 3-17.

Table 3-17. Cultivation plan for the different yeast strains.

Strain	G1212-YRC-negative	G1212-YRC-HER-2	G1212-PR	RB11-pFPMT121-HER-2	RB11-pFPMT121-PR
Cultivation temperature	30°C	30°C	30°C	37°C	37°C
Step 1	48 h in YMM-nitrate-glucose	48 h in YMM-nitrate-glucose	48 h in YMM-nitrate-glucose	24 h in YMM-nitrate-glucose	24 h in YMM-nitrate-glucose
Step 2				48 h in YMM-nitrate-glycerol	48 h in YMM-nitrate-glycerol
Step 3				48 h in YMM-nitrate-methanol	48 h in YMM-nitrate-methanol
Shaking	170 rpm	170 rpm	170 rpm	180 rpm	180 rpm

3.3.24 Measurement of culture OD_{600nm}

For calculating the optical density, a sample of the culture with a volume inferior to 1 % of the total volume was taken and introduced in a 2 ml disposable plastic cuvette. This cuvette was placed in a Nanodrop device for absorbance measurement at 600 nm.

3.3.25 Determination of dry cell weight (dcw)

A sample for the culture was taken and disposed in weighted aluminum receptacle. Then the receptacle was allowed to dry in an oven at 100 °C and the weight was recorded every 4 h. When no change in weight could be detected, the weight of the dried cell material was determined. For calibration, the cell culture was diluted several times and these dilutions were submitted to the same procedure. It allowed the creation of a calibration curve for direct determination of the dcw for a given OD_{600nm}.

3.3.26 Preparation of BL21 cell lysate

One colony was cultivated overnight in 20 ml LB medium supplemented with the correct antibiotic at 30°C. Then this preculture was transferred in 200 ml LB medium supplemented with the correct antiobiotic and allowed to grow at 30 °C until OD_{600nm} reach 0.7. After that 0.5 mM IPTG was added to the culture and the cells were cultivated overnight at 30 °C under shaking. The next day, the culture was centrifuged (10 min/5,000 g/4°C) and the pellet was washed with 100 ml PBS. After a second centrifugation (10 min/5,000 g/4°C), the pellet was resuspended in 30 ml of the desired binding buffer and the cells were disrupted by ultrasonic waves for 2 times 5 min at 4°C. Then the suspension was centrifuged for 10 min at 5,000 g and 4°C and the supernatant was kept for protein purification.

3.3.27 Preparation of yeast cell lysate

In a typical, a 200 ml culture was grown is the appropriate medium for the desired cultivation time. The cells were then centrifuged for 15 min at 5,500 g and the pellet was washed with 100 ml PBS. After a new centrifugation (5,500 g, 15 min) the pelleted yeast were resuspended in 10 ml of the lysis buffer. Then, a mixing mill device was used to break the cells and release the proteins. For HER-2, this step was followed by one hour incubation at 4 °C under mild shaking to allow solubilization of the membrane protein. The lysate was then centrifuged at 4°C for 20 min at 15,000 g and the supernatant was transferred in a new tube.

Table 3-18. Composition of buffer for yeast cell lysate.

Buffer	Components	Quantity for 1 l	Final concentration
Yeast cells lysis buffer: 20 mM sodium phosphate, pH=7.6	Na_2HPO_4 (1M stock solution)	16.9 ml	16.9 mM
	NaH_2PO_4(1M stock solution)	3.10 ml	3.10 mM
	PMSF (1 M stock solution in ethanol)	1 ml	0.001 M

3.3.28 Determination of total protein concentration

Total protein concentration was determined by using Bio-Rad Protein assay following manufacturer recommendations. This assay was performed both in cuvette and in micro titter plate format.

3.3.29 Concentration of proteins

For protein concentration, up to 3 ml sample was introduced in a Vivaspin 2 tube with a cutoff of 30,000 kDa. The tube was then centrifuged at 4,000 g for 20 min at 20°C in a swing bucket rotor. This led to a final volume of approximately 150 µL.

3.3.30 SDS-PAA gel preparation

All polyacrylamide gels were prepared with SDS to assure denaturing conditions. For complete receptors, the separation gel contained 7 % of acrylamide whereas it was containing 15 % acrylamide in the case of small antigen expression. The quantity of gel solutions given in Table 3-19 is sufficient for the casting of 4 gels. Preparation of the gels was performed with Bio-Rad Miniprotean equipment following manufacturer recommendations.

Table 3-19. Composition of solution for SDS-PAA gel preparation.

Solution	Compound	Quantity
SDS PAA stacking gel (5 %)	ddH_20	4.8 ml
	Rotiphorese® acrylamide (37.5 : 1, v/v)	1 ml
	Tris (1.0 M, pH = 6.8)	0.5 ml
	SDS (10 %, w/v)	80 µl
	APS (10 %, w/v)	80 µl
	TEMED 20 %, v/v	80 µl
SDS PAA separation gel (7 %)	ddH_20	9 ml
	Rotiphorese® acrylamide (37.5 : 1, v/v)	3.5 ml
	Tris (1.0 M, pH = 8.8)	7.5 ml
	SDS (10 %, w/v)	200 µl
	APS (10 %, w/v)	200 µl
	TEMED (20 %, v/v)	200 µl
SDS PAA separation gel (15 %)	ddH_20	5 ml
	Rotiphorese® acrylamide (37.5 : 1, v/v)	7.5 ml
	Tris (1.0 M, pH = 8.8)	7.5 ml
	SDS (10 %, w/v)	200 µl
	APS (10 %, w/v)	200 µl
	TEMED (20 %, v/v)	200 µl

3.3.31 Sample preparation for SDS-PAA gel electrophoresis

For SDS-PAA gel electrophoresis, all samples were mixed with SDS loading buffer at a 4:1 ratio and incubated at 70 °C for 15 min. Then 25 µl of each sample were loaded on a SDS-PAA gel and electrophoresed in electrophoresis buffer at 60 V for the first 60 min and 100 V for the next 2 h.

3.3.32 Gel staining for total protein content

For total protein staining the Coomassie staining was systemically used. The gel was immersed in 10 ml Instantblue™ solution for 40 min and then washed in 20 ml ddH_2O for 60 min. After staining of the gel, it was dried and fixed on Whatman paper by the use of a Bio-Rad Gel-drier and then scanned.

3.3.33 Western blot analysis

Western blot analysis was performed by transferring the gel to a PVDF (polyvinylidene fluoride) membrane (Immobilon®-P Membrane; EMD Millipore Corporation, Billerica, USA) in Western blot transfer buffer for 12 h at 100 mA. This operation was performed in a Bio-Rad tank chamber.

Table 3-20. Buffer composition for SDS-PAA electrophoresis and Western blot.

Buffer	Component	Quantity for 1 l buffer	Final concentration
Electrophoresis buffer	Tris	3.03 g	25 mM
	glycine	15.0 g	0.2 M
	SDS	1 g	0.1 % (w/v)
	pH was set to 8.3 with fuming HCl, autoclaved and stored at 4 °C		
Western blot transfer buffer	Tris	0.303 g	2.5 mM
	glycine	1.44 g	20 mM
	methanol	20 ml	2 % (v/v)
	SDS	100 mg	0.01 % (w/v)
	pH was set to 8.3 with fuming HCl, autoclaved and stored at 4 °C		
SDS loading buffer	Tris	12 g	100 mM
	SDS	40 g ml	4 % (w/v)
	glycerol	200 ml	20 % (v/v)
	bromophenol blue	200 mg	0.02 % (w/v)
	ß-mercaptoethanol	100 ml	10 % (v/v)
	pH was set to 6.8 with fuming HCl and stored at -20 °C		

3.3.34 Protein-antibody hybridization

After washing of the membrane twice with PBS for 10 min, the membrane was first blocked with 1 % non-fat dry milk for one hour under shaking at 23°C. Then the membrane was washed twice for 5 min with PBS-tween, one time with PBS for 5 min and then incubated for 60 min at 23 °C under shaking with the appropriate first antibody (specific antibody). After that, the membrane was washed with PBS-tween (twice for 5 min) and PBS (one time for 5 min) and then incubated with a second antibody (detection antibody) for one hour at 23 °C. Finally, the membrane was washed four times with PBS-tween and the bound antibodies were chromogenically detected with BCIP/NBT tablet. The stained membrane was then scanned.

3.4 Solubilization of membrane protein

The solubilization test is based on the work of White et al. [221] with some modifications. In a 1 l shaking flask, a 60 ml culture of *A. adeninivorans* G1212/YRC102-6H-HER-2 was grown in YMM-nitrate-glucose for 48 h at 30 °C, 180 rpm agitation until the culture reached an OD_{600nm} of approximately 1.5. Cells were then harvested by centrifugation (10 min at 8,000 g) and resuspended in 850 µl lysis buffer. The cells were then disrupted using silica beads in a Mixer Mill MM400. Lysed samples were then centrifuged at 11,500 g, 4 °C for 25 min. The supernatant was transferred to a new tube and protein concentration was assessed using the Bio-Rad Protein Assay to be 22 mg/ml.

Nine solubilization solutions were prepared. The first (the control solution) consisted of solubilization buffer with the remaining eight solutions supplemented with the following detergents (all concentrations are w/v): 1% n-octyl-β-D-glucoside (OG), 1% 3-[(3-cholamidopropyl)dimethylammonio]-1-propanesulfonate hydrate (CHAPS), 1% methyl-6-O-(N-heptylcarbamoyl)-α-D-glucopyranosid (HECAMEG), 1% N,N-dimethyldodecylamine N-oxide (LDAO), 1% decyl-β-D-maltoside (Dmal), octylphenoxypolyethoxyethanol (Nonidet P40) ,1 % Digitonin and 1% Triton X-100 (TX-100). 20 µl of lysate (440 µg of total protein) was added to 2 ml of the solubilization solution and gently agitated at 4 °C for 60 min. After this the samples were centrifuged in a Beckman TLA-100.3 rotor at 70,000 g for 60 min. 500 µl of supernatant was kept on ice for further analysis and the rest of the supernatant was carefully removed by aspiration. The pellet was subsequently resuspended in 100 µl PBS. All samples (supernatant and resuspended pellets) were then prepared for SDS-PAA gel electrophoresis and the presence of the HER-2 protein was determined by Western blot analysis.

Table 3-21. Composition of solubilization buffer.

Buffer	Components	Quantity for 1 l	Final concentration
Lysis buffer for solubilization	Tris	6.057 g	50 mM
	EDTA	0.29 g	1 mM
	NaCl	58.44 g	1 M
	PMSF (1 M stock solution in ethanol)	1 ml	1 mM

3.5 Batch cultivation

Batch cultivations were conducted in a 1.5 L stirred-tank reactor (Univessel 1L) and the monitoring of cultivation parameters was performed using a Biostat®-A*plus* Fermentor system. The stirrer speed was adjusted to maintain 40 % oxygen saturation in the culture medium and the pH was maintained automatically at 6.0 by the addition of an HCl solution (0.1 M). A 60 ml preculture of the desired yeast strain was used as inoculum and the final volume was always 660 ml. Dry cell weight (dcw), glucose concentration, total protein content determination and SDS-PAA gel electrophoresis were performed from 2 ml samples of culture taken at the beginning of the experiment and subsequently at different time points of the cultivation. For each sample, 1 ml was used for OD_{600nm} measurement

with a Nanodrop 2000c spectrophotometer to calculate the dry cell weight (dcw). A calibration curve was constructed by diluting a culture sample in different volumes of YMM-nitrate-glucose. The culture was in the exponential phase to avoid the presence of a large number of dead cells. The OD_{600nm} of these dilutions was first measured and then an identical volume of these dilutions was dried at 100 °C until no further change in mass was observed. Plotting the OD_{600nm} as a function of the mass of the dilutions resulted a linear relationship yielding the equation: $OD_{600nm} = a \times dcw + b$. Thus by measuring the OD_{600nm}, the dcw could be determined.

The rest of the sample was centrifuged at 6,000 x g for 20 min and the supernatant was used for determination of the glucose concentration using a D-glucose kit as per the user manual instructions. The pellet was resuspended in extraction buffer and lysed. The lysate was analysed using the Bio-Rad Protein Assay for quantification of the total protein and 5 µg of the protein solution was loaded onto a SDS-PAA gel for Western Blot analysis.

3.6 Protein purifications

3.6.1 Purification by immobilized metal affinity chromatography (His-tag affinity)

Two different metals (cobalt and nickel) as chelators and three different immobilized resin chemistries (TED, NTA and IDA) were assayed. For the nickel-NTA purification, 10 ml of this cell lysate was mixed with 5 ml of binding buffer and 4 ml of nickel-activated agarose solution (giving a column bed volume of approximately 2 ml) and this solution was gently shaked for 2 h at 4°C. After that the slurry was introduced in a polypropylene column with a polyethylene frit and the resin was settled by gravity. The first flow-through was conserved and reloaded on the column. Then the resin was washed with 10 ml binding buffer (wash 1) and 10 ml wash buffer (wash 2). Finally the agarose bound proteins were eluted with three times 2.5 ml elution buffer (elution 1, elution 2 and elution 3). For cobalt-based purification, the agarose resin was activated with Co^{2+} ions instead of Ni^{2+} ions. For TED and IDA purification, the prepacked columns and buffers from Macherey Nagel Kit were used following the manufacturer recommendations.

Table 3-22. Buffer composition for His-tag purification.

Buffer	Component	Quantity for 1 l buffer	Final concentration
Binding buffer	NaCl	29.22 g	0.5 M
	Tris	2.43 g	20 mM
	imidazole	0.34 g	5 mM
Wash buffer	NaCl	29.22 g	0.5 M
	Tris	2.43 g	20 mM
	imidazole	4.08 g	60 mM
Elution buffer	NaCl	29.22 g	0.5 M
	Tris	2.43 g	20 mM
	imidazole	68.08 g	1 M
all buffers were adjusted to pH=7.9 with fuming HCl, autoclaved and stored at 4°C			

3.6.2 Desalting of samples

To remove high salt concentrations from elution fractions (mainly imidazole), a PD10 desalting column based on Sephadex™ G-25 Medium was used following manufacturer recommendations. Elution was performed in PBS.

3.6.3 Ion exchange chromatography

The Econo system from Bio-Rad and a DEAE Sephadex A-25 resin were used for anion exchange chromatography. 10 g of a DEAE 23 SH-cellulose resin was resuspended in 500 ml HCl (0.5 M), sonicated for 2 min then allowed to settle for 30 min and then the supernatant was discarded. After several washes with ddH_20 to neutralize the pH, the resin was resuspended in 500 ml NaOH (0.5 M), sonicated for 2 min and again allowed to settle for 30 min. After several washes with ddH_20 to neutralize the pH, the activated resin was resuspended in start buffer and poured into a column. The column was then equilibrated with several bed volumes of buffer and the cell lysate was loaded on the column. After that, potassium phosphate buffer was applied at a flow rate of 0.8 ml/min for 30 min and then the elution could start with increasing concentrations of KCl. For this, a gradient based on two potassium phosphate buffer solutions containing respectively 0 M KCl (start buffer) and 0.5 M KCl (elution buffer) was applied to the column. The presence of proteins eluted after the column was detected with help of a 280 nm spectrometric sensor and each elution fraction volume was set to be approximately 2 ml. After this gradient, solution B was applied to the column for 100 min to elute all proteins and all the fractions were tested with Western blot.

Table 3-23. Buffer composition for anion exchange chromatography.

Buffer	Components	Quantity for 1 l	Final concentration
Start buffer	Tris	6.057 g	50 mM
	pH was adjusted to 8.0 with fuming HCl		
Elution buffer	Tris	6.057 g	50 mM
	KCl	37.27 g	0.5 M
	pH was adjusted to 8.0 with fuming HCl		

3.6.4 CHT™ ceramic hydroxyapatite chromatography

The Econo system from Bio-Rad was also used for this protein purification. For this, 40 g of dry ceramic hydroxyapatite powder were poured in 70 ml of degased start buffer and allowed to settle for one hour. This gave a final bed volume of 60 ml. Then, 5 column volumes of start buffer were added to the column and the column was inserted in the Econo-chromatography apparatus. The sample consisted of yeast cell lysate prepared as in the section 3.6.3 with the difference that hydroxyapatite lysis buffer was used instead of the lysis buffer described there. A 200 ml culture was lysed in 8 ml buffer which give a final sample volume of approximately 10 ml. The sample was added to the column and start buffer was applied for 30 min at a flow rate of 0.8 ml/min. Elution was then started with increasing concentrations of phosphate in the buffer. For this, a gradient based on two potassium phosphate buffer solutions containing respectively 5 mM phosphate (solution A) and 400 mM phosphate (solution B) was applied to the column. The presence of proteins eluted after the column was detected with help of a 280 nm spectrometric sensor and each elution fraction volume

was set to be approximately 2 ml. After this gradient, solution B was applied to the column for 100 min to elute all proteins and all the fractions were tested with Western blot.

Table 3-24. Buffers composition for hydroxyapatite purification.

Buffer	Components	Quantity for 1 l	Final concentration
Start buffer: 5mM sodium phosphate, pH=6.8	Na_2HPO_4 (1M stock solution)	2.3 ml	2.3 mM
	NaH_2PO_4(1M stock solution)	2.7 ml	2.7 mM
Lysis buffer	Na_2HPO_4 (1M stock solution)	4.6 ml	4.6 mM
	NaH_2PO_4(1M stock solution)	5.4 ml	5.4 mM
	PMSF (1 M stock solution in ethanol)	1 ml	1 mM
Solution A	Na_2HPO_4 (1M stock solution)	4.6 ml	4.6 mM
	NaH_2PO_4(1M stock solution)	5.4 ml	5.4 mM
Solution B	Na_2HPO_4 (1M stock solution)	184 ml	184 mM
	NaH_2PO_4(1M stock solution)	216 ml	216 mM

3.7 Differential centrifugation of *A. adeninivorans* protoplasts

3.7.1 Production of *A. adeninivorans* protoplasts

A first pre-culture of the desired yeast was grown for 12 h at 30 °C in 2 ml YPD and then transferred in a 50 ml culture of YPD. The cells were cultivated at 30 °C until the OD_{600nm} reached 1.5, then pelleted by centrifugation (5 min, 5,500 g, 23°C), resupended in 0.9 % NaCl (w/v) and centrifuged again at 5,500 g for 5 min. After that the pelleted cells were resuspended in 50 ml VBM solution supplemented with 1% 3-mercaptoethanol (w/v) and incubated at 23 °C for 10 min. After centrifugation (5 min, 5,500 g, 23 °C), the pellet was washed with 1 M sorbitol and then centrifuged again (5min, 5,500 g, 23 °C). In the next step, the cells were resuspended in 10 ml PP-solution and the suspension was incubated for 2 h at 37 °C under gentle shaking to allow breaking of the cell wall. The quality of the protoplasts was controlled by microscopic observation under white light.

3.7.2 Differential centrifugation

First the protoplasts were washed twice with 1M sorbitol by successive resuspensions and centrifugations (5min, 3,000 g, 23°C). Then, in order to break the cytoplasmic membrane, the pellet was resuspended in 400 µl enzyme mix and 3.2 ml of cold Tris-HCl (10 mM, pH=7.5) was added carefully to the solution. After this step, a first centrifugation at 4°C and 1,000 g was performed. The supernatant (S1) was transferred in a new centrifuge tube and the pellet (P1) was stored at 4°C. The supernatant (S1) was then centrifuged again at 4°C and 13,000 g, giving a supernatant (S2) and a pellet (P2). (S2) was then centrifuged at 4°C and 30,000 g, thus leading to the supernatant (S3) and the pellet (P3). Finally, (S4) and (P4) were obtained after a new centrifugation at 4°C and 100,000 g. All these steps are summarized in Figure 3-1. All supernatants (S1, S2, S3 and S4) were kept at 4°C whereas all pellets (P1, P2, P3 and P4) were precipitated using trichloroacetic acid (TCA) and resupended in 300 µl PBS.

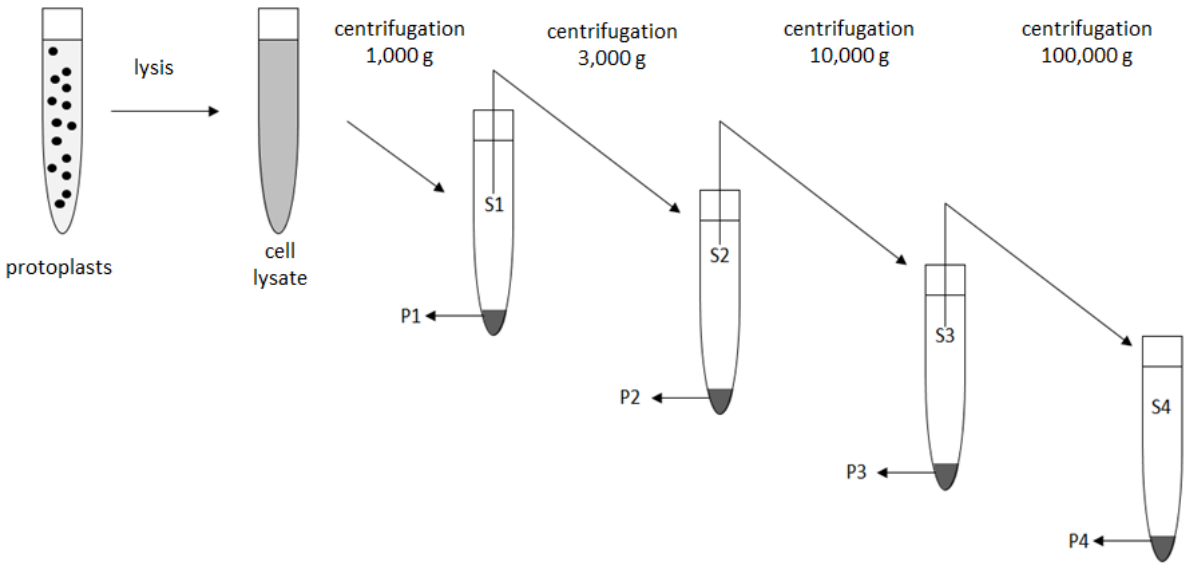

Figure 3-1. Overview of the differential centrifugation procedure.

3.7.3 Precipitation of proteins by trichloroacetic acid (TCA)

50 µl of 100 % trichloroacetic acid (w/v) was added to 500 µl protein suspension and this solution was incubated for 10 min at 4°C to allow protein precipitation. Then, a centrifugation for 10 min at 5,000 g and 4 °C was performed and the pellet washed with a 4:1 (v/v) ethanol/ether solution. Finally the pellet was dried and the proteins were resuspended in PBS.

Table 3-25. Solutions composition for differential centrifugation.

Solution	Component	Quantity for 1 l buffer	Final concentration
VBM solution	Tris	1.21 g	10 mM
	EDTA	1.46 g	5 mM
	Adjusted to pH=9.0 with fuming HCl, autoclaved and stored at 4°C		
PP solution	sorbitol	182.17 g	1 M
	lysing enzyme from *Trichoderma harzianum*	10 g	100 mg/10ml
Enzyme mix	sorbitol	327.91 g	1,8 M
	MES	0.976 g	5 mM
	KCl	74.5 mg	1 mM
	EDTA	0.15 g	0.5 mM
	PMSF	0.174 g	1 mM
	DTT	0.154	1 mM
	antipain	5 mg	5 µg/ml
	leupeptid	0.5 mg	0.5 µg/ml
	pepstatin	0.7 mg	0.7 µg/ml

3.8 Enzyme linked immunosorbant assay (ELISA)

For the ELISA test, 200 µl of recombinant HER-2 purified protein was immobilized in triplicate on a Maxisorp Immunowell plate for 16 h at 4 °C. The coated wells were then washed three times with PBS-tween and blocked for 60 min at room temperature with the appropriate blocking solution and then washed a further three times with PBS-tween. The first antibody diluted in PBS-tween was added and incubated for 60 min at room temperature. After three more washes with PBS-tween, the second antibody possessing a horseradish peroxidase was added and incubated for 60 min at room temperature. After a final washing step (six times with PBS-tween) colorimetric detection was performed by adding 100 µL of the substrate solution. After blocking the reaction with 1 M phosphoric acid, the absorbance at 450 nm was measured using a Sunrise reader and the results analyzed by SigmaPlot 11.0, statistical analysis and graphics display.

3.9 Enzyme linked receptor assay (ELRA)

For the ELRA test, 200 µl of progesterone-BSA at the desired concentration was immobilized in triplicate on a Maxisorp Immunowell plate for 16 h at 4 °C. The coated wells were then washed three times with PBS-tween and blocked for 60 min at room temperature with PBS-tween containing 5 mg/ml BSA and then washed a further three times with PBS-tween. The first antibody consisting in a 1:1000 dilution of the anti-progesterone receptor B (R.809.9) in PBS-tween was added and incubated for 60 min at room temperature. After three more washes with PBS-tween, the second antibody consisting in the anti-rabbit IgG (Whole molecule) peroxidase conjugate at a 1:1000 dilution was added and incubated for 60 min at room temperature. After a final washing step (six times with PBS-tween) colorimetric detection was performed by adding 100 µL of the substrate solution. After blocking the reaction with 1 M phosphoric acid, the absorbance at 450 nm was measured using a Sunrise reader and the results analyzed by SigmaPlot 11.0 to allow statistical analysis and graphics display.

Table 3-26. Substrate solution composition for ELISA and ELRA.

Solution	Component	Quantity for 1 l buffer	Final concentration
TMB substrate solution	TMB	0.116 g	0.5 mM
	sodium acetate	8.25 g	0.1 M
	H_2O_2 (30 % v/v stock solution)	1 ml	0.03 % (v/v)
	pH adjusted to 6.0 by addition of citric acid		

3.10 Surface plasmon resonance experiments

3.10.1 Surface Plasmon Resonance Platform

All SPR experiments were performed by using the SPR device developed by the Fraunhofer Institut für Werkstoff- und Strahltechnik (IWS) and commercialized by Capitalis Technology GmbH. It uses a collimated light at a constant wavelength of 810 nm from a near-infrared light emitting diode (LED)

to irradiate a sensor chip consisting of a bare gold surface on a plastic support. The chip itself was maintained in contact with the flow cell with help of a vacuum pump. This flow cell is made of PDMS material and possesses one 50 µm wide path to allow flowing of the sample. To ensure a temperature control of the chip surface during experiments, an external water bath was used and a pumping system was cooling or heating the flow cell. In the Figure 3-2, the different parts of the platform can be observed as they are installed in the laboratory. A closer look at the chip and its PDMS flow cell can be seen in the Figure 3-3. To inject a sample, a pump was used which allows several different flow rates.

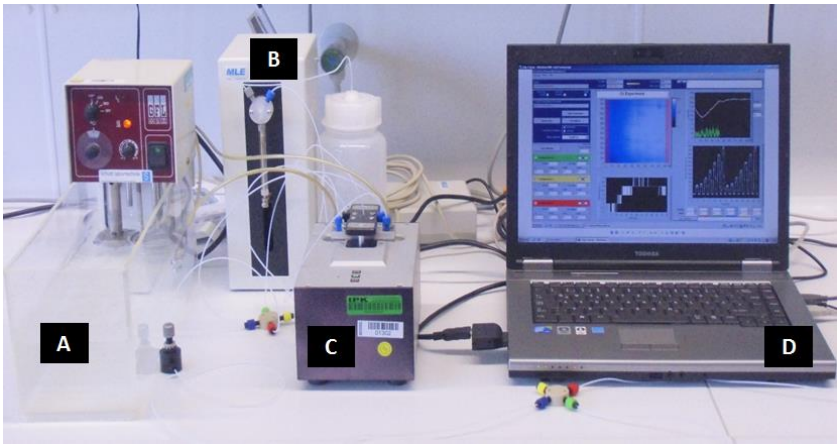

Figure 3-2. General overview of the SPR platform. (A) Water bath, (B) syringe pump, (C) SPR optical device with flow cell, (D) computer with SPR5 software.

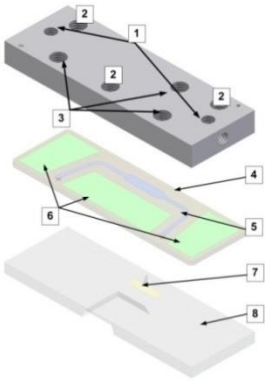

Figure 3-3. Overview of the temperature controlled flow cell: (1) Connections to temperature control, (2) connections to vacuum, (3) connections to sample, (4) PDMS flow-cell, (5) flow path, (6) vacuum chambers, (7) gold surface, (8) plastic support of the chip.

3.10.2 SPR device settings

The SPR device was controlled by the software SPR5 and its interface is shown in Figure 3-4. This software calculates the value of the resonance angle for 117 positions of the gold surface by interpreting the CCD camera intensity values. The part 1 of the Figure 3-4 shows a representation of the entire gold surface with a 90° clockwise inclination where a dark blue pixel represents a low value of reflected light intensity and a light blue pixel a high value of reflected light intensity. The

part 2 takes a closer look to one of the 117 positions (marked with a red horizontal line in the part 1) and represents with a white curve the signal with numerical values instead of colored pixels. The tested angles are on the x-axis and the light intensities are on the y-axis. An algorithm will produce a fit of this curve and determine the position of the minimum of this curve. In green is represented the difference between the original intensity value and the fit values. The position of the minimum (marked with the dashed red line in part 2) is then plotted in part 3 as a function of time. The software allows also observation of the optical device temperature in arbitrary units (part 4), setting of the CCD camera (button 5) and selection of the Working Mode (button 6). The Test Mode allows direct visualization of the chip surface and determination of the resonance angle without any recording whereas the Experiment Mode will perform the same calculations and save in a .txt file the position of the resonance angle for every 117 positions of the gold chip and for every time unit. This time unit will depend on the chosen exposure time. The software offers the choice between four different algorithms for determination of the resonance angle value: polynomial of the second order, polynomial of the third order, analytical (complex algorithm with five parameters) and centroid (center of mass calculation). All experiments were performed with the resource consuming analytical algorithm as it is giving the best fit. The CCD camera parameters contain also two important parameters: the gain and the exposure time. Increasing the exposure time will increase the numerical values of the reflected light intensity as more light can reach the CCD camera. This will create a sharpening of the curve for low intensity values near the resonance angle position. The drawback will be that by increasing the exposure time, rapid changes in the angle position will not be detected, thus negatively affecting the shape of the curve plotting the resonance angle as a function of time. Increasing the gain multiplies the intensity value by a constant factor. This leads to a good determination of resonance angle even at very small exposure time but also to loss of precision as noise signal will also be amplified. As every buffer and every chip preparation will cause different effects, the exposure time and gain settings were adapted for every experiment to obtain a good compromise between precision and time-dependency of the signal.

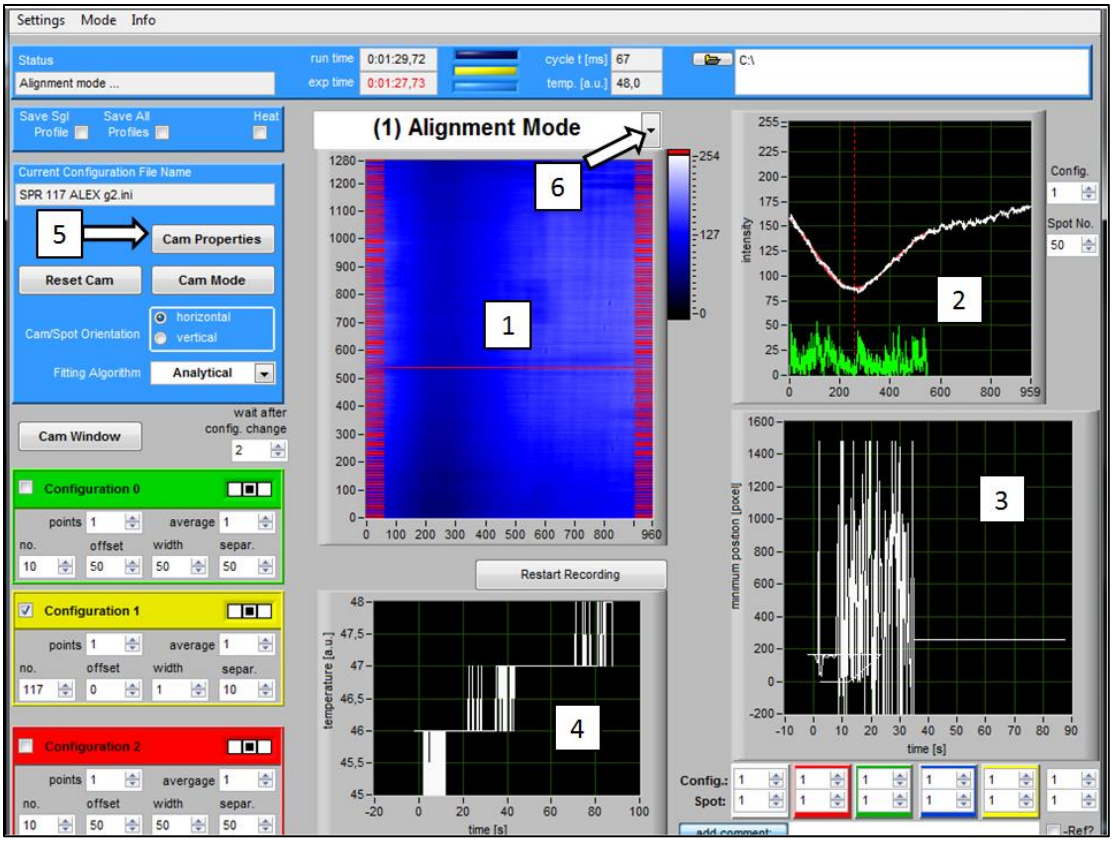

Figure 3-4. Overview of the software interface.

3.10.3 Cleaning of the gold surface

The bare gold chip was first cleaned by using 10 drops of fuming sulphuric acid for 10 s and then washed with ddH_2O. After drying of the surface with nitrogen flow, 70 µl of the freshly made 'piranha solution' (H_2O: NH_4OH: 30 % H_2O_2 / 5:1:1 (v/v)) was added to the chip for 2 min, thus allowing neutralization of the surface. Then, the chip was washed with running buffer and dried again with nitrogen flow.

3.10.4 Immobilization of protein with 17-channel flow cell

For immobilization of proteins by His-tag, the 17-channel flow cell presented in Figure 3-5 was used. This device consists of one metal part and one PDMS part possessing 17 paths thus allowing separate immobilization of 17 positions of the chip. After cleaning, a chip was put in contact with 17-channel flow cell and screwed tightly. Then a solution of dithiobis(C3-NTA) was added in the desired channel and incubated for one hour at 23 °C. The channel was then washed with 100 µl run buffer with the help of two pipettes in the two holes of the flow cell. After this step, the chip was released from the flow cell, the surface was washed again with run buffer and 100 µl of block solution was added for 4 h at 23°C. Finally, the chip was washed with run buffer and the chip was then mounted in the SPR device.

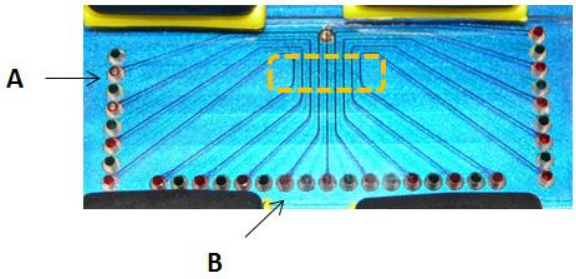

Figure 3-5. Overview of the 17-channel flow cell with the theoretical position of the gold surface in shaded orange. For the need of the picture, one half of the channels were artificially colored in black. (A) shows the entry of the channel number 7 and (B) shows its exit.

3.10.5 Immobilization through hydrophobic interaction

The immobilization of antibodies, ligand or other proteins on the gold surface was not always performed with the 17-channel flow cell but also with a micropipette directly on the surface. For this, two “hydrophobic barriers” were added to the chip in order to separate the surface in three different parts. This barrier consisting of water-insoluble marker showing no affinity for water based solutions and allowing clear separation of droplets. After cleaning, a chip was separated in three different surfaces with hydrophobic barriers and two different probes were applied to the two outer surface. The central surface was always serving as control surface. After incubation, the whole surface was washed with run buffer, dried with flow nitrogen and finally blocked with block solution for 4 h at 23°C. After a last cleaning with running buffer and drying of the chip, it was mounted on the SPR device and ready for experiments.

3.10.6 SPR experiment general protocol

A functionalized chip was placed under the PDMS flow cell and vacuum was applied in the vacuum chambers to maintain them tight. The water bath was switched on to allow constant temperature of the flow cell and the PDMS flow cell was then mounted and tightly fixed on the SPR device. The SPR5 software was opened and switched to Test Mode. Running buffer was then flowed on the chip until no change in the position of the resonance angle for the 117 positions and no change in the optical device temperature could be detected. Even though the PDMS flow cell has its own temperature control system, heating of the optical device could interfere with the obtained results. When these values were stable, the software was switched to Experiment Mode, 500 µl of run buffer was flowed on the chip and then the sample was applied. For this, a tube was inserted in the sample and 100 µl of sample was aspired by the pump placed after the chip at desired flow rate. So the sample could entirely cover the gold surface. After this, 50 cycles of aspiration and pressure was applied to allow repetitive passing of the sample on the chip. These cycles are performed to ensure the binding reaction reaches its equilibrium as technical limitations of the pump don’t allow too slow flow rates. Once the sample was applied, it was expulsed in the original tube and 500 µl of run buffer was then flowed on the chip.

3.10.7 Vocabulary conventions for SPR experiments

All the SPR experiments conducted in these work are focusing on antibody-protein interactions, ligand-protein interactions and protein-ligand interactions. As convention and to ease the comprehension of the results, the word “probe” will always refers to the relevant molecule (protein or chemical) immobilized on the chip, “linker” will be the molecule (protein or chemical) immobilized first to allow immobilization of the probe and “sample” will be the molecule (protein or chemical) the experiment proposes to detect and which will flow on the chip. When an interaction will be studied (for example “antibody-protein interaction)”, the first partner cited (in this example “antibody”) will always describe the probe and the second will always describe the sample (here “protein”).

3.10.8 General description of SPR results: graphical display

With the SPR device developed by the Fraunhofer Institut, the operator has access to the resonance angle position calculated for 117 positions of the gold chip. These angle positions are calculated every 55 ms and compiled in a text document. Once the experiment performed, this test document is converted in a excel file in which calculations can be carried out. For the graphical display and the creation of fit curves, the data processed in the excel file are subsequently opened with SigmaPlot software. In order to present these results, the raw data will always be shown as sensogram and chip profile. The sensogram is the graphical representation of the position of the resonance angle (called pixel) for one position of the gold chip with the time as x-axis. For convenience, the position of this angle is set to 0 at the beginning of the experiment. A binding experiment will typically present a sensogram containing an exponential growth (association), a plateau (equilibrium) and an exponential decrease (dissociation) of the resonance angle position. A chip profile is the representation of the bound analyte to the surface for all positions of the chip. For this the position of the resonance angle at the equilibrium will be presented for every of the 117 observed positions of the gold surface. As parts of the chip are covered with hydrophobic barrier and will therefore show inconsistent values, the chip profile will mostly concern not all 117 positions but selected interesting parts of the chip. In all experiments, a control surface is always present to ensure comparisons between chips and therefore the sensogram presented will always be a normalized one in which the values of the control surface are subtracted from the values of the desired position (unless told otherwise).

3.10.9 SPR experiments: most used conditions

For each application the nature of the blocking solution, the length of the incubation step, the nature of the linker, the nature of the probe, the nature of the sample, the temperature of the flow cell and the composition of the buffer are the key parameters and have been therefore optimized. These optimization steps will not be presented in the results section as it will have unnecessary increase this part. In total, two buffers will be shown: the HEPES buffer for receptor-ligand interactions and the PBS-t buffer for antibody-antigen interactions. The temperature of the PDMS flow cell was 25 °C for all experiments and the blocking solution A was used for receptor-ligand

interaction whereas blocking solution B was used for antibody antigen interactions. The nature of the linker will be indicated during the presentation of the related experiment in the results section.

Table 3-27. Buffer composition for SPR experiments.

SPR run buffers	Component	Quantity for 1L buffer	Final concentration
HEPES Buffer	HEPES	2.383 g	10 mM
	NaCl	5.844 g	0.1 M
	tween-20 (10 % w/v stock solution)	0.2 mg	0.02 % (v/v)
	EDTA	14.6 g	50 mM
	Adjusted to pH=6.9 with fuming HCl, autoclaved and degased		

Table 3-28. Blocking solutions composition for SPR experiments.

SPR block solutions	Blocking agent	Dissolving agent	Final concentration
Block A	BSA	PBS	5 % (w/v)
Block B	BSA	PBS	2.5 % (w/v)
	HO-PEG-NH_2	PBS	100 mM

Table 3-29. Linkers used for SPR-experiments.

Linkers	Dissolving agent	Final concentration	Application
Protein A	PBS	1 mg/ml	antibody-protein
Protein G	PBS	0.1 mg/ml	antibody-protein
DTSSP	H_2O	5 mM	antibody-protein
dithiobis(C3-NTA)	H_2O	1mM	receptor-ligand

3.11 Protein extraction from breast tissue

3.11.1 Breast cancer tissue samples

Real probes consisted of breast tissue embedded in paraffin and cut in 10 µm slice. For each sample 3 of these 10 µm slices were present in one tube. From a total number of 20 samples, 10 were described as “negative”, two were described as “1+” and 8 were described as “positive”. These determinations of HER-2 status were performed in the Institute of Pathology of the Carus University in Dresden by immunohistochemistry and FISH. For our common use, all samples were renamed from “yeast 1” to “yeast 20” and kept at 4°C until use. The descriptions of the samples are summarized in the Table 3-30.

Table 3-30. Description of the tissue samples.

Sample name	Pathology institute internal number	Tissue	HER-2-status
Yeast 1	08/4287-1G	breast	negative
Yeast 2	08/5284-1H	breast	negative
Yeast 3	08/13827-1G	breast	positive
Yeast 4	08/15241 G	breast	positive
Yeast 5	08/21424-1G	breast	1+
Yeast 6	08/31869-1G	breast	positive
Yeast 7	08/34022 K	breast	positive
Yeast 8	08/36541 G	breast	positive
Yeast 9	08/37657-1E	breast	negative
Yeast 10	09/898-1G	breast	1+
Yeast 11	08/170-1G	breast	negative
Yeast 12	08/3101-1E	breast	negative
Yeast 13	08/3932 2	breast	positive
Yeast 14	08/4071-1C	breast	negative
Yeast 15	08/4194 E	breast	positive
Yeast 16	08/5284-1C	breast	negative
Yeast 17	08/6360-1G	breast	positive
Yeast 18	08/6714-1G	breast	negative
Yeast 19	08/7281 G	breast	negative
Yeast 20	08/7804-3G	breast	negative

3.11.2 Paraffin removal with xylene

This protocol is derived from the protocol used for DNA extraction in pathology institute in Dresden. It consisted of an incubation of the tissue slices at 60 °C for 2 h followed by the addition of 1 ml xylene and incubation at 45 °C for 15 min. After that the tube was centrifuged at 17,900 g and 23°C for 10 min and the pellet was resuspended in 1 ml xylene and incubated again for 15 min at 45°C. After a second centrifugation (17,900 g, 23°C, 10 min) the pellet was resuspended in 1 ml 96 % ethanol, vortexed for 1 min and then centrifuged (17,900 g, 23°C, 10 min). This step was repeated a second time and the pellet was finally dried in speed-vac.

3.11.3 Paraffin removal with n-octane

The tissue slices were incubated for 16 h at 60 °C and then 1 ml n-octane was added to bind to the paraffin. After a 10 s vortexing, 75 µl of methanol were added to protect the tissue and the tube was vortexed again for 10 s. After a centrifugation at 23°C and 17,900 g for 1 min, the supernatant was discarded and the pellet was dried under fume hood.

3.11.4 Antigen Retrieval (AR) method

This protocol is derived from the work of Shi et al. [222]. After removal of the paraffin, 50 µL of extraction buffer with 2 % SDS was added to the sample and heated for 20 min at 100 °C in heat

block. After that, the sample was incubated for 2 h at 60 °C and the lysate was used for further operations or stored at-20 °C.

Table 3-31. Composition of the AR extraction buffer.

Buffer	Component	Quantity for 1L buffer	Final concentration
AR extraction buffer	Tris	2.42 g	20 mM
	SDS	20 g	2 % (w/v)
	Adjusted to pH=7 with fuming HCl		

3.12 Production of antibodies

Antibodies were produced in 3 rabbits type New Zealand White for each receptor by the Phytoantibodies group of the IPK-Gatersleben. A total of 1 mg antigen (*E. coli* produced fragment of the receptor) was injected in three different immunizations together with 1 mg Complete Freund's Adjuvant (CFA) to stimulate an immune response. These three different injections were performed at day 1, day 30 and day 37. After 42 days, a sample of blood was taken and the presence of antibodies against the receptor was confirmed by Western blot. If it was the case, the rabbits were then euthanized and the serum was aliquoted, frozen with liquid nitrogen and stored at -80°C without any purification.

4 Results

4.1 Antibodies production

As many experiments will require the utilization of antibodies (Western blot, ELISA, SPR), the production of polyclonal antibodies was performed. As neither the complete progesterone receptor nor the complete HER-2 would be suitable for rabbit immunization, it was decided to clone a small fragment of each receptor in a vector and then perform the expression of this polypeptide in *E. coli*. As template for the cloning, human DNA extracted from mouthwash was used and the desired fragment was amplified via PCR. For both receptors special care was taken to the exact position of the genes in the human chromosomes as the presence of introns could impede the correct amplification of the desired DNA fragment. For this, the online-available database from NCBI (www.ncbi.nlm.nih.gov/gene/) was used and a region of 300 base pairs (100 amino acids) in the exon 8 of the human chromosome 11 was chosen for the progesterone receptor whereas 300 base pairs in the exon 31 of the human chromosome 17 were selected for the HER-2 protein. The length of 100 amino acids was chosen to obtain a fragment small enough to be easily expressed in a bacterial system but long enough to ensure a good specificity of the future antibody. Both fragments are named HER-2 antigen and PR antigen. As mentioned in the material and methods (section 3.3.2), the DNA template used for the PCR consisted of human genomic DNA as progesterone receptor and HER-2 are two natural occurring receptors in *Homo sapiens* and it was important to pool genomic DNA from different subjects for ethical aspects. As both receptors are located on somatic chromosomes, female and male genomic DNAs were mixed. Genomic DNA extraction from human is now widely documented from a lot of different tissues and both high yield and high purity can be achieved. For this particular case, simplicity and feasibility were the most important parameters so extraction from mouth tissue was chosen. To overcome the low yield and weak purity of this DNA extraction method, it was decided to perform a double PCR where the first PCR use genomic DNA as template and the second one use the product of the first PCR as template. Primers used for these two PCR also inserted *Nde*I and *Bam*HI restriction sites at both ends of the fragment which allows integration in the cloning site of the commercial pET16b vector by ligation. This vector possesses all needed components for bacterial recombinant protein production as well as a coding sequence for 10 histidine amino acids in the nearby region of the cloning site. This allows the attachment of a decahistidine tag at the N-terminus of the polypeptide which will be important for purification process.

E. coli cells from the strain BL21 were then chosen for their outstanding properties in bacterial heterologous protein production. To determine the adequate concentration of IPTG necessary to induce a high yield of recombinant protein, cultures were inoculated with different quantity of inducer and the best results were achieved with 0.5 mM IPTG. After culture and cell disruption as described in the Material and Methods, the protein-rich lysate was purified by His-tag affinity chromatography and the recombinant antigens were eluted with imidazole containing buffer. After desalting, the purified proteins could be lyophilized and stored at 4°C. The performance of the purification steps can be seen in the Figure 4-1 for the HER-2 antigen (A) and the PR antigen (B).

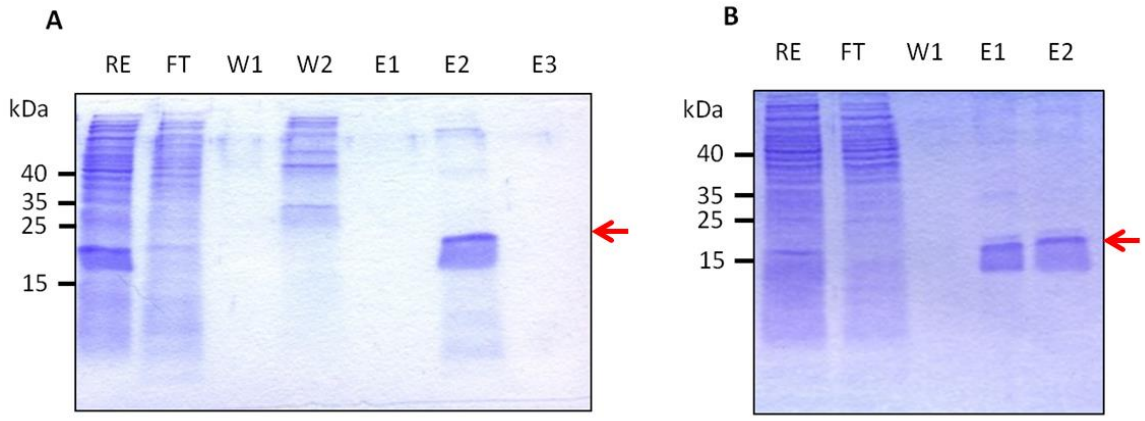

Figure 4-1. Coomassie staining of 12 % SDS-PAA gel after affinity protein purification of the HER-2 antigen (A) and the PR antigen (B).RE = raw extract, FT = flow-through, W = wash fraction, E = elution fraction, kDa = kilo Dalton. The red arrow represents the position of the antigen for both cases.

Both Coomassie stainings show a clear and large band in the elution fractions at approximately 15 kDa for HER-2 antigen and 18 kDa for PR antigen. These values are in agreement with the predicted molecular mass of these proteins (calculated with Vector NTI molecular mass calculator) which are respectively 13.45 kDa and 14.17 kDa.

These purified polypeptides were then injected in rabbits in order to obtain an immunogenic response. Serums collected after 42 days were tested for presence of antibody against either the HER-2 or the PR antigen. For this, SDS-PAA gel electrophoreses with increasing quantities of antigens were performed, the gels were transferred to a PVDF membrane for Western blot analysis with a dilution of rabbit serum as detection antibody. The results of this experiment can be seen in the Figure 4-2. The bands visible at approximately 15 kDa and 18 kDa confirm the presence of anti-HER-2 and anti-PR antibodies in the serum of rabbits. The detection limit of both antibodies is less than 10 ng polypeptide.

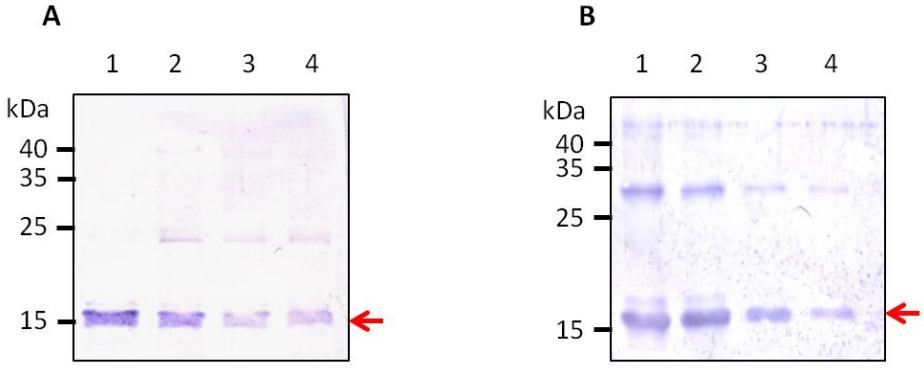

Figure 4-2. Western blot detection of HER-2 antigen (A) and PR antigen (B). Detection antibody was a 1:5000 dilution of rabbit serum immunized with HER-2 antigen (A) or PR antigen (B).1 : 100 ng antigen, 2 : 50 ng antigen, 3 : 25 ng antigen, 4 : 10 ng antigen. The red arrow represents the position of the antigen for both cases.

4.2 Cloning and expression screening of *HER-2* and *hPR* genes in *A. adeninivorans* and *H. polymorpha*

4.2.1 Cloning of *HER-2* and *hPR* genes in *A. adeninivorans*

For production of recombinant proteins in *A. adeninivorans*, the well-established Xplor®2 platform was used. It consists of a donor plasmid Xplor2.2 possessing a yeast part with a selection marker module (*ALEU2* promoter - *ATRP1m* gene – *ATRP1* terminator), an expression module (*TEF1* promoter – multicloning site – *PHO5* terminator), two rDNA sequences and an *E. coli* part with antibiotic resistance gene and origin of replication. The bacterial part allowed the cloning of the gene of interest in the vector and was removed before the transformation of the auxotrophic mutant *A. adeninivorans* G1212. In this mutant, the *ATRP1* gene was deleted and therefore the yeast cannot synthetize its own tryptophane [182]. Both the HER-2 and the progesterone receptor ORFs were provided by Life Technology with optimized codons for expression in *A. adeninovorans* and already inserted in a pMK vector. To allow future purification of the receptors, it was decided to insert a hexahistidine polypeptide at one extremity of each of them. As it was impossible to predict if this insertion will interfere with the protein production or the protein stability in the yeast cell, the His-tag was either inserted at the N-terminus or at the C-terminus. As positive control, a plasmid was also constructed with the gene ORF whitout adding the sequence coding for additionnal histidines. For His-tag coding sequence integration, special primer pairs in which one of them contains the sequence coding for 6 histidines were designed and PCR was performed. Even if this unusually long primer (around 30 bases) was not completely matching the template sequence, the PCR yield was sufficient to clone this product in a pCR4-TOPO vector. This vector was then sent to an external laboratory for sequencing in order to confirm that the polyhistidine sequence was inserted at the correct position and whithout any mutation. Complete sequencing of the vector was not performed due to the extreme length of the ORFs. The gene of interest was subsequently cloned in a pBS-TEF-PHO5-EBN to add the strong constitutive *TEF1* promoter and the *Saccharomyces* derived *PHO5* terminator. Finally, expression cassette was cloned in a Xplor2.2 vector to allow insertion in the yeast genome via yeast rDNA integration (YRC). For this, the *E. coli* part of the vector was removed by *Asc*I enzymatic restriction and the mutant G1212 was transformed by the linearized vector. An overview of all constructed final expression cassettes for *A. adeninivorans* protein production can be seen in Figure 4-3.

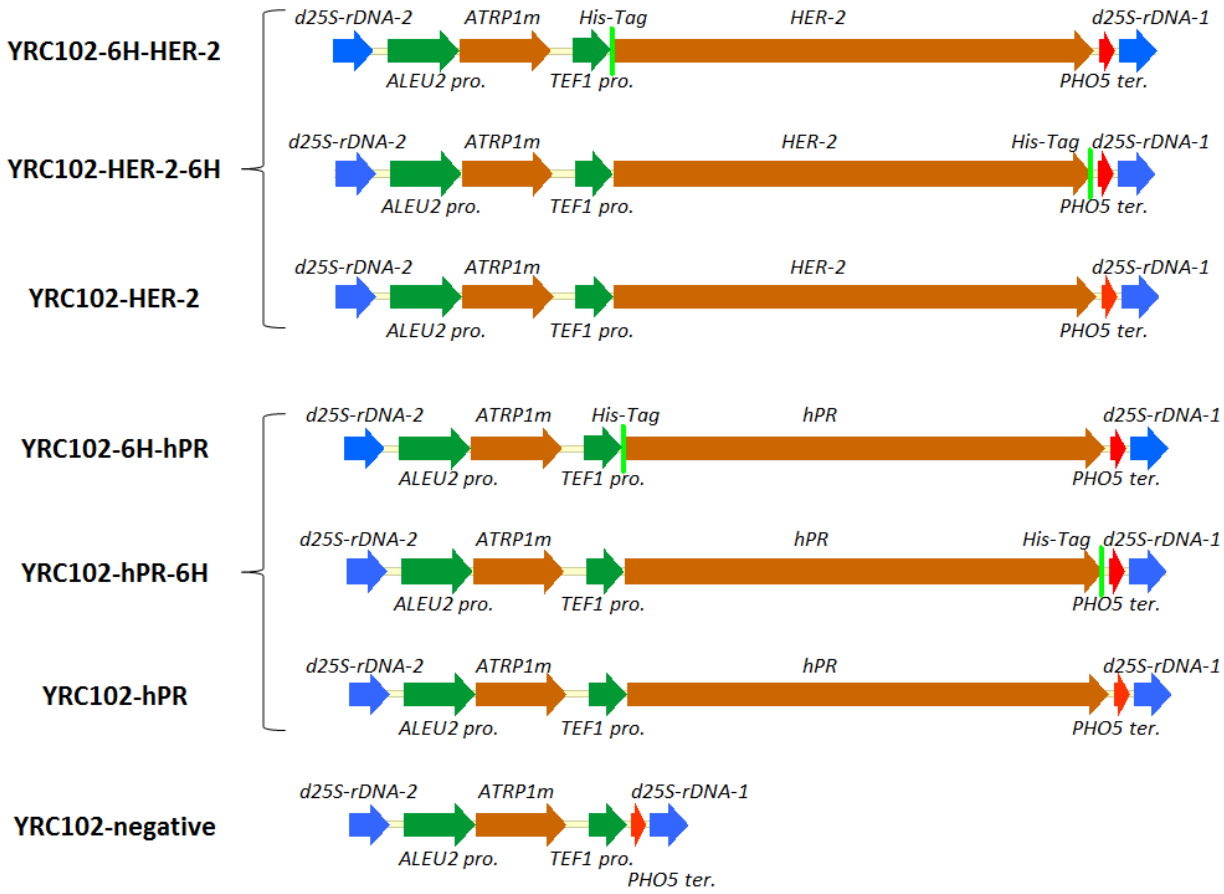

Figure 4-3. Name and expression module map of all the used YRCs. Orange represents gene ORFs, dark green represents promoter regions, red represents terminator regions, light green represents His-tag sequence and blue represents rDNA sequences.

4.2.2 Cloning of *HER-2* and *hPR* genes in *H. polymorpha*

The methylotrophic yeast *H. polymorpha* is known for its recombinant protein production efficiency and, among all available vectors, the pFPMT121 integration/expression plasmid was chosen. In this work, the utilized pFPMT121 plasmid was carrying the inducible *FMD* promoter, the *MOX* terminator, the autonomously replicating sequence *HARS1* as well as the *S. cerevisiae* derived *URA3* gene for orotidine 5'-phosphate decarboxylase production (an enzyme required for uracil production). As for *A. adeninivorans* transformation, both the *HER-2* and the *progesterone receptor* genes were inserted in the vector with polyhistidine encoding sequence at the 3´- or at the 5´-ends. For this, the ORFs were directly taken from the pCR4-TOPO vectors already described in the precedent section. *H. polymorpha* RB11, an uracil-auxotrophic mutant in which the orotidine-5'-phosphate carboxylase gene was deleted, was transformed with the constructed vectors. Contrary to the transformation in *A. adeninivorans*, no linearization of the vector is necessary before the transformation in *H. polymorpha*. An overview of the four constructed vectors with their respective names can be seen in Figure 4-4.

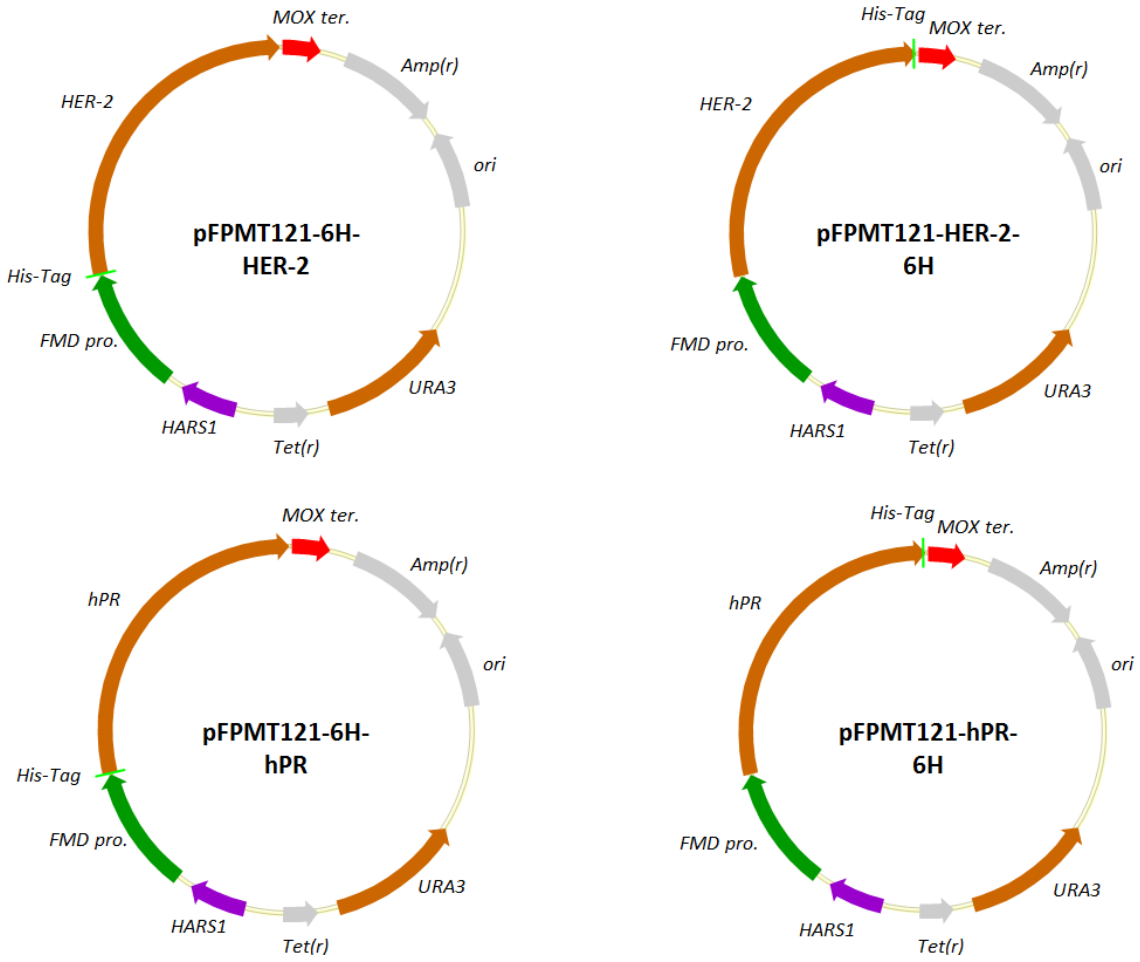

Figure 4-4. Plasmid maps of the four constructed pFPMT121 vectors. Orange represents gene ORFs, dark green represents promoter regions, red represents terminator regions, light green represents His-tag encoding sequence, violet represents eukaryotic autonomous replication sequence and grey represents prokaryotic regions.

4.2.3 Screening of *A. adeninivorans* transformants for HER-2 production

Each transformation of *A. adeninivorans* G1212 cells with respectively YRC102-HER-2, YRC102-6H-HER-2 and YRC102-HER-2-6H gave more than 50 colonies as well as the transformation with YRC102-negative. 48 colonies of each transformation were submitted to stabilization process in order to ensure a stable integration of the foreign gene in the yeast genome. In order to see if these transformants were producing the recombinant HER-2 protein, Western blot technique with two different detection antibodies was performed. For this, each transformant was grown on yeast extract-peptone-dextrose medium (YPD), the cells were lysed and the total protein content was loaded on two different SDS-PAA gels. After that, hybridization was performed for each membrane either with the polyclonal anti-HER-2 antibody from rabbit serum or from a commercial polyclonal anti-HER-2 antibody (A048529-2 Anti-c-erbB-2 oncoprotein). The protein staining pattern of each transformant was then compared with the pattern of the negative control G1212/YRC102. For a clear presentation of the results, only one Western blot concerning a restricted number of transformants from one transformation event and hybridized with one detection antibody will be

shown. The results for seven yeast colonies transformed with YRC102-HER-2 are presented in Figure 4-5.A. Compared to the negative control, three transformants are exhibiting an extra protein band at a molecular mass of approximately 185 kDa which is the apparent molecular mass of the HER-2 protein. The Western blot also shows bands of strong intensity for smaller molecular masses but they are probably signs of unspecific antibody hybridization as they are occurring in every transformant and in the negative control. Figure 4-5.B presents the Western blot results for G1212/YRC102-HER-2-6H. In this case, five transformants are showing a band at 185 kDa except for the negative control and the intensity of this band is varying among colonies. For the transformation with YRC102-6H-HER-2, hybridization with commercial antibody during the Western blot is presented (Figure 4-5.C) and the membrane shows also a high intensity band above 170 kDa in all transformants except for the negative control. It is to note that, with this particular antibody, less unspecific signal can be observed as the negative control doesn't show any band. These results prove that *A. adeninivorans* transformants have the capacity to produce the recombinant human HER-2 and the absence of high intensity band at lower molecular mass with the commercial antibody indicates that the protein doesn't appear to be highly degraded. For all three receptors (with C-terminus His-tag, N-Terminus His-tag and without His-tag), one of the transformants showing the highest band intensity after hybridization with the commercial antibody and with the anti-HER-2-rich rabbit serum was further selected for the next experiments.

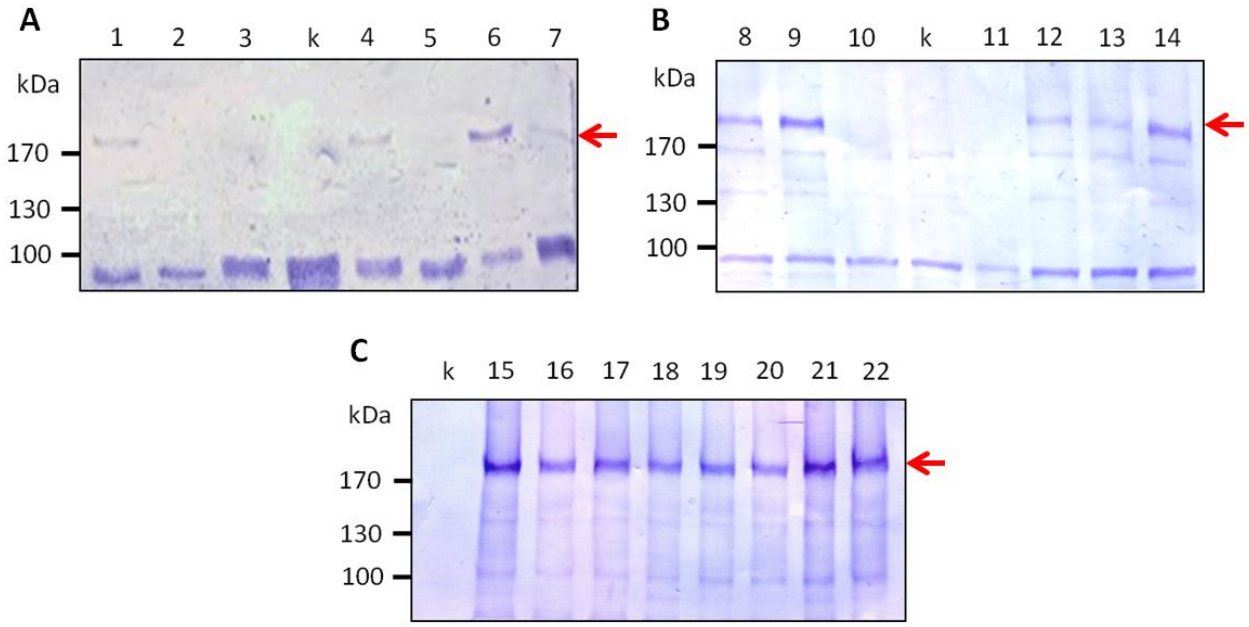

Figure 4-5. Western blot analysis of *A. adeninivorans* transformed from YRC102-HER-2 (A), YRC102-HER-2-6H (B) and YRC102-6H-HER-2 (C). (A) and (B) were obtained by using anti-HER-2 from rabbit serum as detection antibody, (C) by using the commercial anti-HER-2. k: negative control G1212/YRC102, 1-7: G1212/YRC102-HER-2 transformants n°1 to 7, 8-14: G1212/YRC102-HER-2-6H transformants n°1 to 7, 15-22: G1212/YRC102-6H-HER-2 transformants n°1 to 8. The red arrow represents the position of the HER-2 protein.

4.2.4 Screening of *A. adeninivorans* transformants for progesterone receptor production

The same experiments as in the precedent section were performed with *A. adeninivorans* transformed with YRC102-hPR, YRC102-6H-hPR and YRC102-hPR-6H. For each transformation event, the raw extract of all 48 stabilzed transformants was loaded on a SDS-PAA gel for electrophoresis and then Western blot was performed with anti-progesterone receptor from rabbit serum and commercial anti-progesterone receptor isoform B antibody (MA514842 Progesterone Receptor B (R.809.9)) on two different membranes. Some of the Western blot results can be seen in the Figure 4-6 where parts A, B and C present the results for respectively G1212/YRC102-hPR, G1212/YRC102-hPR-6H and G1212/YRC102-6H-hPR. In all three transformation events, a protein with a molecular mass of approximately 125 kDa can be detected in some transformants but never in the control strain G1212/YRC102. This band is present if the Western blot was hybridized with the anti-progesterone receptor from rabbit serum (Figure 4-6.A and B) or with the commercial antibody R.809.9 (Figure 4-6C). In the case of G1212/YRC102-hPR (Figure 4-6.A), only a few transformants are showing a low intensity band. As for the HER-2 producing yeasts, one transformant for each of the three receptor variants showing the highest band intensity in Western blot with the commercial antibody and with the serum-derived antibody was selected for further experiments.

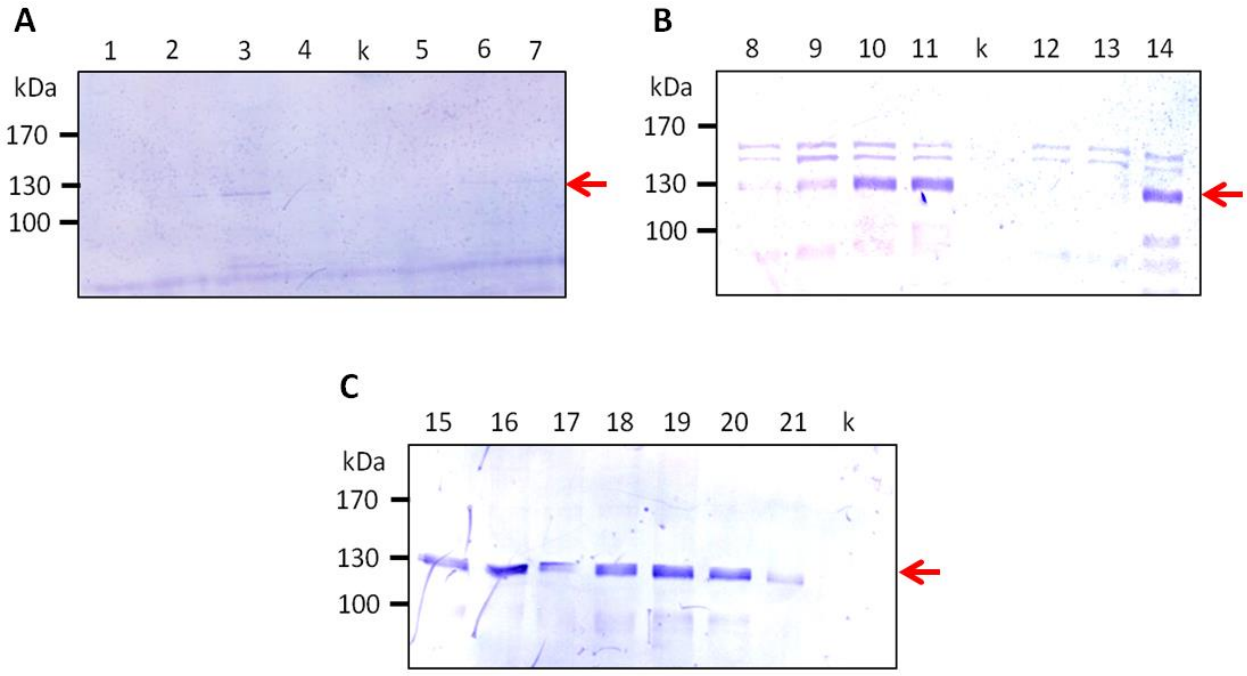

Figure 4-6. Western blot analysis of *A. adenini*vorans transformed with YRC102-hPR (A), YRC102-hPR-6H (B) and YRC102-6H-hPR (C). (A) and (B) were obtained by using anti-PR antibody from rabbit serum as detection antibody, (C) by using the commercial anti-PR antibody. k: negative control G1212/YRC102, 1-7: G1212/YRC102-hPR transformants n°1 to 7, 8-14: G1212/YRC102-hPR-6H transformants n°1 to 7, 15-21: G1212/YRC102-6H-hPR transformants n°1 to 8. The red arrow represents the position of the progesterone receptor isoform B.

4.2.5 Screening of *H. polymorpha* transformants for HER-2 production

In the case of *H. polymorpha*, 48 transformants were also stabilized after transformation with pFPMT121-6H-HER-2 and pFPMT121-HER-2-6H. These transformants were grown first on YPD for one day, then in YMM-nitrate-glycerol for 18 h and finally on YMM-nitrate-methanol for one day. All cultivation steps were performed at 37 °C under vigorous shaking. Lysate of the cells were then loaded on a SDS-PAA gel for electrophoresis and Western blot was performed with the commercial anti-HER-2 antibody as detection antibody. The results of these Western blots for some transformants after transformation with pFPMT121-HER-2-6H and pFPMT121-6H-HER-2 can be seen respectively in Figure 4-7.A and B. As no RB11 was transformed with a pFPMT121 vector containing no ORF for gene expression, the negative control of this experiment was RB11 strain transformed with pFPMT121-6H-hPR. For all transformants resulting from the transformation with pFPMT121-6H-HER-2, a band at 185 kDa can be detected but not in the case of the control strain. For transformation with pFPMT121-HER-2-6H, only five transformants from the 48 stabilized show a band at this molecular mass. One of them is present in Figure 4-7.A. Taken together, these results indicates that *H. polymorpha* is also able to produce recombinant HER-2. One transformant from each transformation (either with pFPMT121-6H-HER-2 or pFPMT121-HER-2-6H) was selected for further experiments.

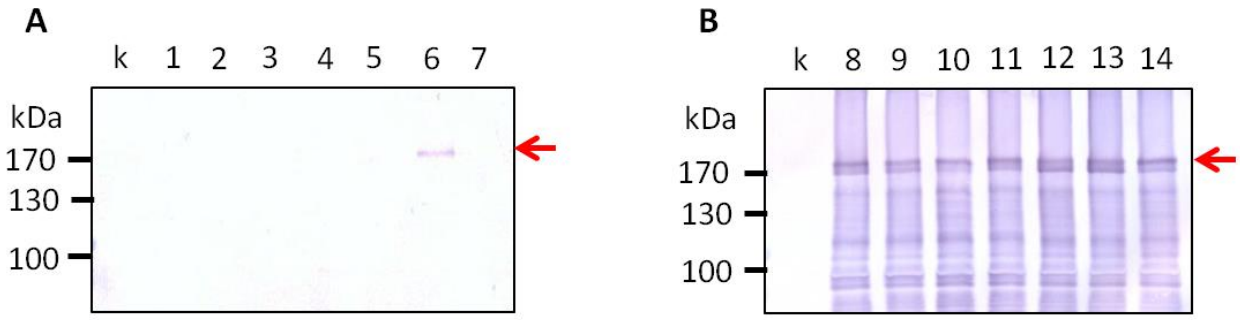

Figure 4-7. Western blot analysis of *H. polymorpha* transformed with pFPMT121-HER-2-6H (A) and pFPMT121-6H-HER-2 (B). (A) and (B) were obtained by using the commercial anti-HER-2 antibody as detection antibody. k: negative control RB11/pFPMT121-6H-hPR, 1-7: RB11/pFPMT121-HER-2-6H transformants n°1 to 7, 8-14: RB11/pFPMT121-6H-HER-2 transformants n°1 to 7. The red arrow represents the position of the HER-2 protein.

4.2.6 Screening of *H. polymorpha* transformants for progesterone receptor production

Transformants resulting from the transformation of RB11 cells with pFPMT121-6H-hPR and pFPMT121-hPR-6H were also tested via Western blot in order to determine if *H. polymorpha* can produce the human progesterone receptor. For this, exactly the same procedure as for the above section was performed with the difference that commercial anti-progesterone receptor antibody was used for detection. Results of the Western blot for some transformants are to see in the Figure 4-8.A for transformation with pFPMT121-hPR-6H and Figure 4-8.B for the transformation with pFPMT121-6H-hPR. A band at 125 kDa corresponding to the human progesterone receptor isoform B is present in all transformants transferred to this membrane except for transformant n°4 in Figure 4-8.B and this band is not to see in the negative control. In this case, the negative control consisted

in RB11 strain transformed with pFPMT121-6H-HER-2. For the next experiments, also one transformant producing the receptor with a His-tag at the N-terminus and one transformant producing the receptor with a C-terminal His-tag were selected.

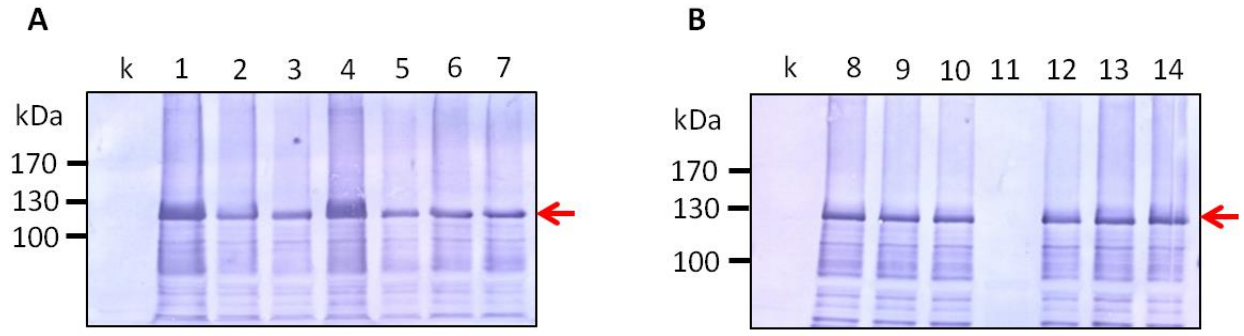

Figure 4-8. Western blot analysis of *H. polymorpha* transformed with pFPMT121-hPR-6H (A) and pFPMT121-6H-hPR (B). (A) and (B) were obtained by using the commercial anti-progesterone receptor antibody as detection antibody. k: negative control RB11/pFPMT121-6H-HER-2, 1-7: RB11/pFPMT121-hPR-6H transformants n°1 to 7, 8-14: RB11/pFPMT121-6H-hPR transformants n°1 to 7. The red arrow represents the position of the progesterone receptor isoform B.

4.3 Medium screening for *A. adeninivorans* transformants

In order to optimize the production of recombinant protein in *A. adeninivorans*, the composition of the culture medium was modified. This yeast species is known to grow in several medium and can use different nitrogen sources. In this case, YPD, yeast minimal medium with nitrate as nitrogen source (YMM-nitrate-glucose) and yeast minimal medium with ammonium as nitrogen source (YMM-ammonium-glucose) were tested. For the first medium (YPD), dextrose is the carbon source and for both YMM media, glucose is the carbon source. This medium screening was not performed for all receptors in all possible configurations (with His-tag at the N-terminus, C-terminus or without His-tag) but only for the G1212/YRC102-HER-2-6H transformant and G1212/YRC102-hPR-6H transformant. Then the assumption was made that the presence or the position of the His-tag will have a little influence on the results and the findings were extended to the other variants. To perform this experiment, the tested colonies were grown for 48 h in one of the three media, the cells were harvested, lysed and all protein lysates were diluted to the same concentration to be loaded on a SDS-PAA gel. The detection was performed by Western blot with anti-HER-2 or anti-hPR antibodies from rabbit-serum. The results of this Western blot are presented in the Figure 4-9.A for G1212/YRC102-HER-2-6H. It shows that cells grown for 48 h in YMM-nitrate-glucose show a highest intensity band corresponding to the receptor HER-2 than cells grown in YPD. Additionally, it can be seen that cells grown in YMM-ammonium-glucose show no band at all. In the case of G1212/YRC102-6H-hPR, the Western blot analysis presented in Figure 4-9.B shows a band corresponding to the progesterone receptor isoform B for all treatments with YPD producing the highest intensity band.

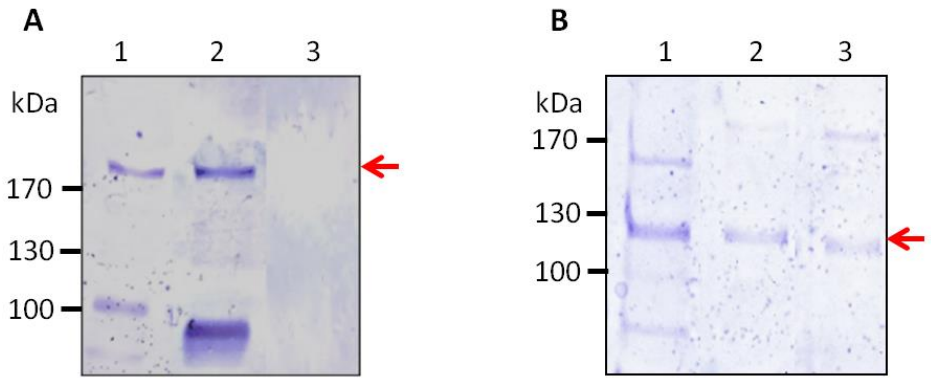

Figure 4-9. Western blot analysis G1212/YRC102-HER-2-6H (A) and G1212/YRC102-hPR-6H (B) cultivated on different media. (A) and (B) were obtained by using respectively the serum-based anti-HER-2 and anti-PR as detection antibodies. (1) cultivation in YPD, (2) cultivation in YMM-nitrate-glucose, (3) cultivation in YMM-ammonium-glucose. The red arrow represents the position of the HER-2 protein (A) and the position of the progesterone receptor isoform B (B).

4.4 Localization of HER-2 in *A. adeninivorans* via differential centrifugation

Because HER-2 contains one transmembrane domain, this protein is generally localized in the plasma membrane of the human cell. Due to the differences between the composition of yeast and mammalian membranes, an experiment was designed in order to know where the recombinant HER-2 is localized in *A. adeninivorans*. The differential centrifugation was chosen for this purpose as it can selectively separate membrane fractions, organelles and cytoplasm. Unfortunately, no specific marker antibodies are available for *A. adeninivorans* and those targeted to other yeasts (like *S. cervisiae* for example) didn't show any reactivity with *A. adeninivorans* proteins. That's why only one antibody directed against HER-2 was used in this study. After removal of the cell wall by enzymatic lysis, the protoplasts underwent several centrifugation steps described in the Material and Methods section 3.7. The composition of each pellet is to find in Table 4-1 which was constructed by analogy with the *S. cerevisiae* results.

Table 4-1. Overview on pelleted elements of yeast protoplasts for different centrifugal forces. Data are originated from *S. cerevisiae* experiments and adapted to *A. adeninivorans*.

Centrifugation force	Pelleted elements
1,000 g	unbroken cells, nuclei
13,000 g	peroxisome, mitochondrion
30,000 g	membrane vesicle, organelles
100,000 g	ER, Golgi apparatus

The pellets and final supernatant of both G1212/YRC102-6H-HER-2 and G1212/YRC102 were loaded on SDS-PAA gels for Western blot analysis and Coomassie staining. Results of this experiment can be observed in the Figure 4-10. The Coomassie staining (A) shows similar protein pattern between the negative control and the G1212/YRC102-6H-HER-2 strain and the Western blot (B) shows the presence of a 185 kDa band corresponding to HER-2 in the pellet 1, 2 and 3. The presence of a band

slightly under 170 kDa can be also detected in the pellet 2 as well as some bands of lower molecular masses which are presumably degradation products. No band at all can be seen in the pellet 4 and in the final supernatant of the G1212/YRC102-6H-HER-2 transformant as well as in all fractions of the control strain. These results indicate that HER-2 is mainly present in the membrane fraction of the *A. adeninivorans* cells.

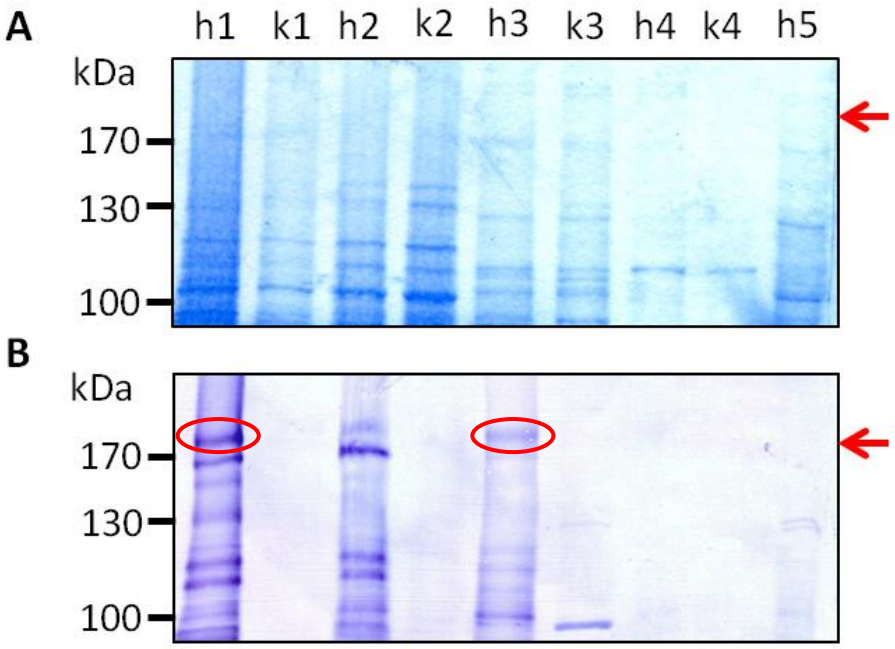

Figure 4-10. Coomassie staining (A) and Western blot analysis (B) of the differential centrifugation samples. 1: pellet after 1,000g centrifugation, 2: pellet after 13,000g centrifugation, 3: pellet after 30,000g, 4: pellet after 100,000g centrifugation, 5: final supernatant. k refers to the results of the negative strain G1212/YRC102, h refers to the results of the strain G1212/YRC102-6H-HER-2. Western blot was performed with commercial anti-HER-2 antibody. The red arrow represents the position of the HER-2 protein in Coomassie staining and a red circle is showing the position of HER-2 in Western-Blot.

4.5 Solubilization of HER-2

Because the HER-2 protein contains one transmembrane domain and is found in the membrane fraction of *A. adeninivorans*, the solubilization of this protein was examined in detail. For this, a broad range of commonly used detergents was tested. To ensure the solubilization effectiveness, the detergents were always added at a concentration above the critical micelle concentration (cmc) and generally the ratio of lysate:detergent solution was approximately 1:15. Assessment of detergent solubilization effectiveness was performed by Western blot as it has the capacity to report the protein size and the presence of any degradation products, which appear as additional bands at lower molecular masses. Western blotting of the solubilized proteins (Figure 4-11.A) shows a very faint band at the expected molecular mass of the HER-2 protein (approximately 185 kDa) for the control lysate (i.e. without detergent) and for the two samples treated with the non-ionic detergents Dmal and OG which indicates that both of these detergents are not effective for

solubilization of the protein. A faint band can be observed for treatment with Hecameg, NP 40 and Digitonin indicating a partial solubilization of the membrane protein with these detergents. The most intensive bands were observed for the Triton X-100 treatment and for the two zwitterionic detergents LDAO and CHAPS. It is probable that the band occurring at 100 kDa in all lanes may be due to degradation of the receptor. This may mean that low intensity of this band in the LDAO treatment is a sign of a protective effect of this detergent. However the visible distortion of the 185 kDa band will be problematic for future Western blot analysis. The opposite hypothesis could be inferred from observation of the results of the Triton X-100 treatment due to the appearance of an intense 100 kDa band. These findings are supported by Western blotting of resuspended pellets (Figure 4-11.B) where a very faint band for the treatment with LDAO is present, meaning that a large amount of the receptor is in the solubilized fraction and not in membrane fraction. This contrasts with the large band observed for the control. Although the result is quite clear for LDAO, the poor quality of the Western blotting due to the nature of the sample make further interpretation relative to band intensity impossible. Proteins from resuspended pellets generally migrate with difficulty during electrophoresis and Western blotting often shows smearing bands. From this experiment, the conclusion can be made that CHAPS shows the best compromise between effective solubilization and protection for degradation effects.

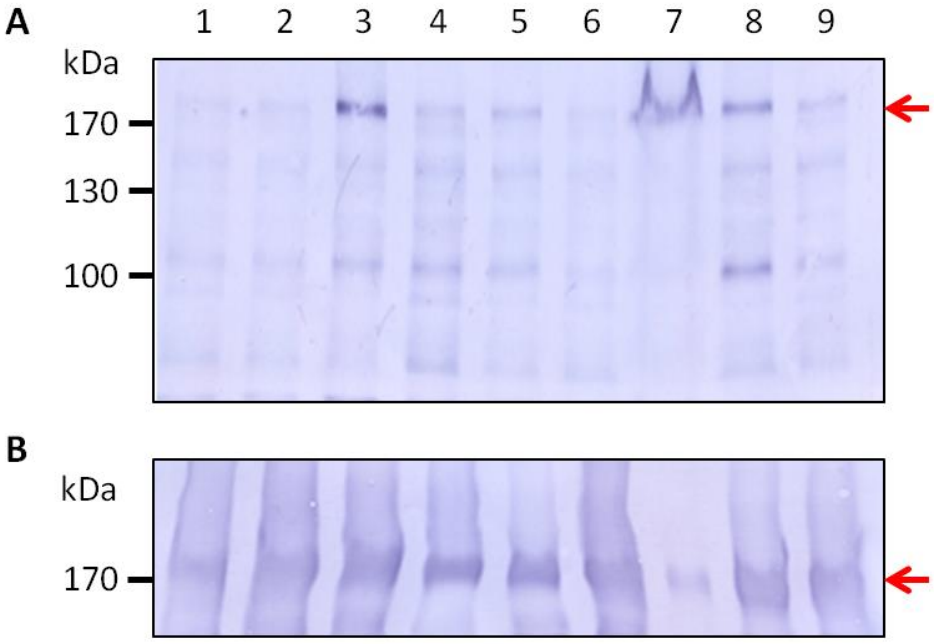

Figure 4-11. Western blot analysis of the lysate (A) and the resuspended pellets (B) of the strain G1212/YRC102-6H-HER-2-after solubilization with 8 different detergents. 1: no detergent, 2: solution with octyl-glucoside, 3: solution with CHAPS, 4: solution with Nonidet P-40, 5: solution with Hecameg, 6: solution with D-maltoside, 7: solution with LDAO, 8: solution with Triton X-100, 9: solution with Digitonin. Western blot was performed with commercial anti-HER-2 antibody. The red arrow represents the position of the HER-2 protein.

4.6 Batch cultivation

To increase the yield of protein production and to have better control over the cultivation parameters, four transformed yeasts were cultivated in batch mode in a bioreactor. It consisted of the two *A. adeninivorans* strains G1212/YRC102-6H-HER-2 and G1212/YRC102-6H-hPR as well as the two *H. polymorpha* strains RB11/pFPMT121-6H-HER-2 and RB11/pFPMT121-6H-hPR. In all cases, culture pH was maintained at 6.0 with HCl solution and the cultivation temperature was 30 °C for *A. adeninivorans* and 37 °C for *H. polymorpha* strains. To avoid a limiting effect of oxygen on the yeast growth, the influent air and the stirrer speed were automatically controlled to maintain a concentration of dissolved oxygen in the medium of 40 % saturation. Because the high density of yeast at the end of the exponential growth phase required more oxygen than was available from the atmosphere, pure compressed oxygen was used during the final h of the experiment.

4.6.1 Batch cultivation of *A. adeninivorans* G1212/YRC102-6H-HER-2

To monitor the cultivation phases and determine the optimal period for HER-2 production, samples were taken at regular intervals and the glucose content of the medium as well as the dry cell weight per liter culture (which will be written as dcw) of yeasts were measured. Results of these measurements can be seen on Figure 4-12. After a lag phase of approximately 8 h characterized by low glucose consumption and a limited increase in dcw, the cells then enter typical exponential growth. After about 22 h, almost all glucose was consumed and the dcw then decreased slowly which is corresponding to the stationary phase and the beginning of the death phase. The specific growth rate was also calculated from the dcw measurements. For this, some values were plotted again in a semi-logarithmic scale and the parameters of the linear fit curve were determined. This representation can be observed in Figure 4-12.B. It gives a specific growth rate value of 0.0558 ± 0.0013 h^{-1}.

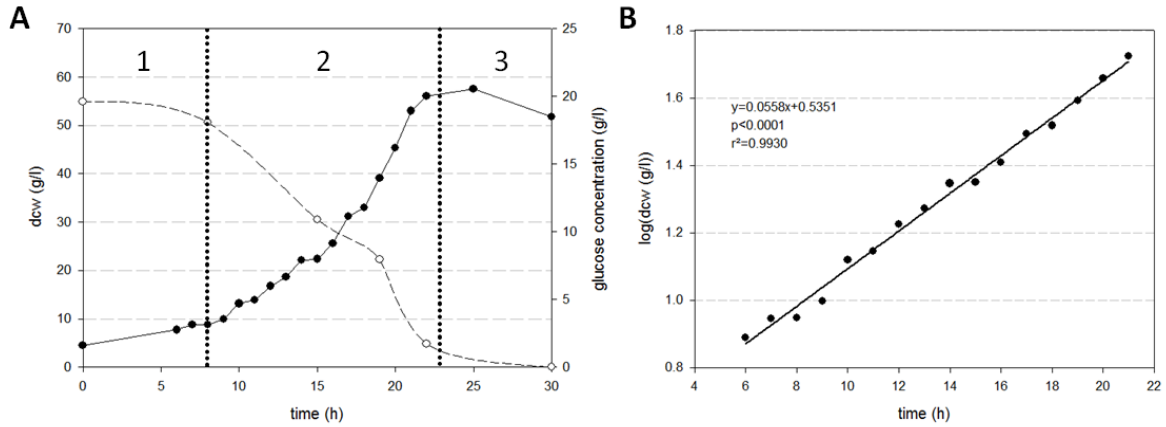

Figure 4-12. Determination of the growth phases of *A. adeninivorans* G1212/YRC102-6H-HER-2. (A) Evolution of the dcw (black dots and straight black line) and the glucose concentration (white dots and dashed black line) with the time. The two vertical dotted lines mark the separation between lag phase (1), exponential phase (2) and stationary/death phase (3). (B) Evolution of the dry cell weight logarithm (black dots) with the time. Linear shaped fit curve (in black) was calculated by Sigmaplot, parameters of the fit are given on the diagram.

In order to find the optimal period of HER-2 production, the total protein concentration for all samples was measured by Bio-Rad protein assay and an equal quantity of proteins was loaded on a SDS-PAA gel to perform Coomassie staining and Western blot analysis. The results of these experiments can be seen in Figure 4-13. In a first diagram (Figure 4-13.A) both the dcw and the total protein concentration are plotted together. It shows that the total protein content increases in a similar pattern as the dcw even though some protein production peaks can be suspected to appear at t=9 h, t=12 h and t=16 h. Maximum in total protein production is also reached at t=24 h and start to decline after that. In the Coomassie staining (Figure 4-13.B) the same pattern cannot be observed as an equal quantity of protein (4 µg) was loaded on the SDS-PAA gel so all lane looks quite similar except for the lanes 1 to 5 where no bands can be detected. This is because not enough proteins were present in these samples in order to reach the 4 µg of total proteins. The two last lanes also seem to contain less proteins but it can be due to the fact that protein degradation may be important at the end of the cultivation. This will lead to many small molecular mass peptides which give a signal by protein concentration determination but are non-visible in the selected portion of the gel. The Western blot analysis (C) shows a start in the production of HER-2 at t=12 h and a continuous production until t= 20 h after what the signal tends to be decreasing. It is also to note the visible presence of degradation production starting at t=16 h which is increasing until the end of the experiment.

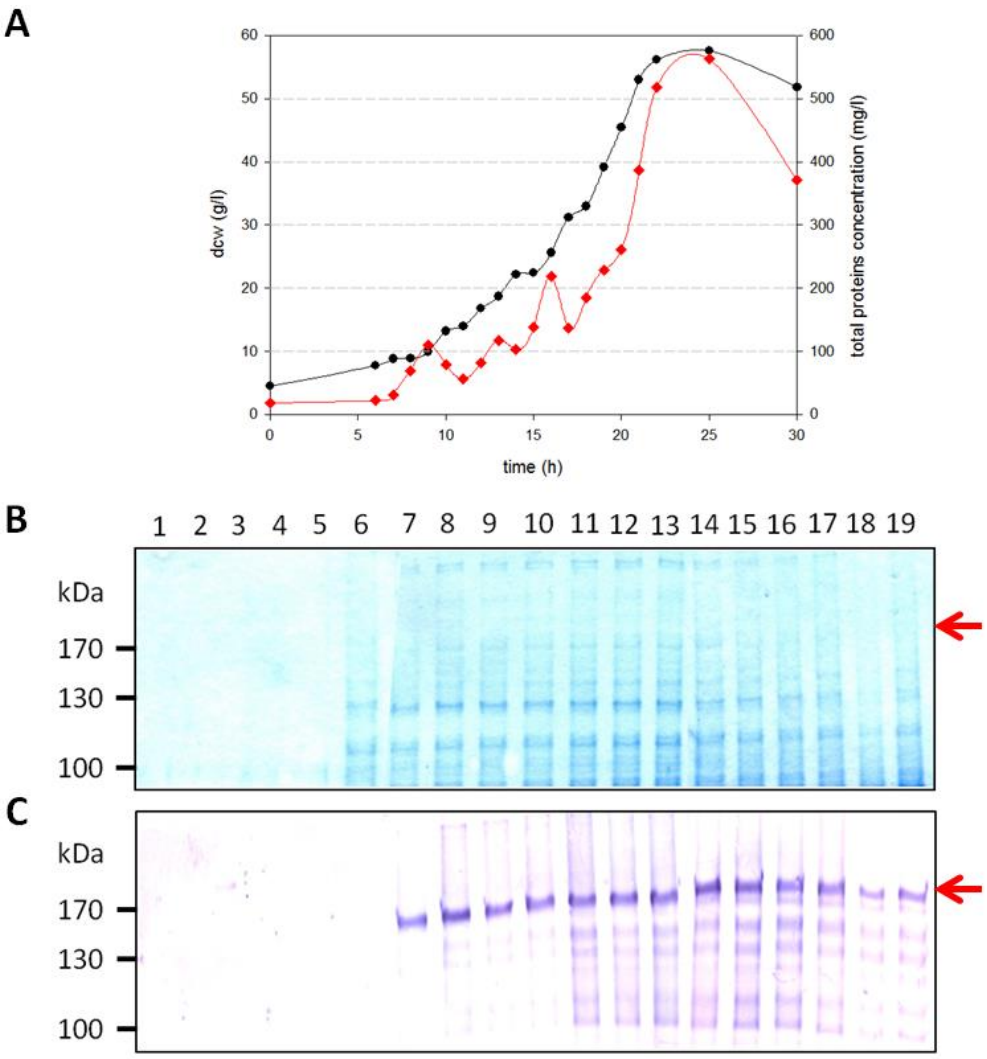

Figure 4-13. Evolution of the total protein production and the HER-2 production during batch fermentation of *A. adeninivorans* G1212/YRC102-6H-HER-2. (A): Evolution of the dcw (black dots and line) and the total protein concentration (red diamonds and line) with the time. (B) and (C): Respectively Coomassie staining and Western blot analysis of culture samples after 6 (1), 7 (2), 8 (3), 9 (4), 10 (5), 11 (6), 12 (7), 13 (8), 14 (9), 15 (10), 16 (11), 17 (12), 18 (13), 19 (14), 20 (15), 21 (16), 22 (17), 25 (18) and 30 h (19). The red arrow represents the position of the HER-2 protein.

4.6.2 Batch cultivation of *A. adeninivorans* G1212/YRC102-6H-hPR

The same experiment as in last section has been performed with *A. adeninivorans* transformed to produce the human progesterone receptor with His-tag at the N-terminus. Figure 4-14.A presents the dcw results during the whole experiment together with the glucose concentration of the medium at selected time points. It is interesting to note that, in comparison to the results obtained for the same yeast transformed to produce HER-2, the exponential phase starts earlier (after about 5 h culture) and the stationary phase is reached between 15 and 20 h. Unfortunately, the fact that no sample was taken between t=14h and t=20h makes it difficult to known more precisely when the exponential phase really end. As a concentration of about 5 g/l glucose is still present in the medium

at t=14 h, it is sure that the stationary phase will only begin after this time point. As for the precedent section, the specific growth rate was also calculated based on the logarithmic values of the dcw (visible in Figure 4-14.B) and gives a value of 0.1850 ± 0.0088 h^{-1}.This value is higher than the value obtained with HER-2 and confirms that *A. adeninivorans* transformed to produce human progesterone receptor has a faster growth than the same yeast transformed to produce HER-2.

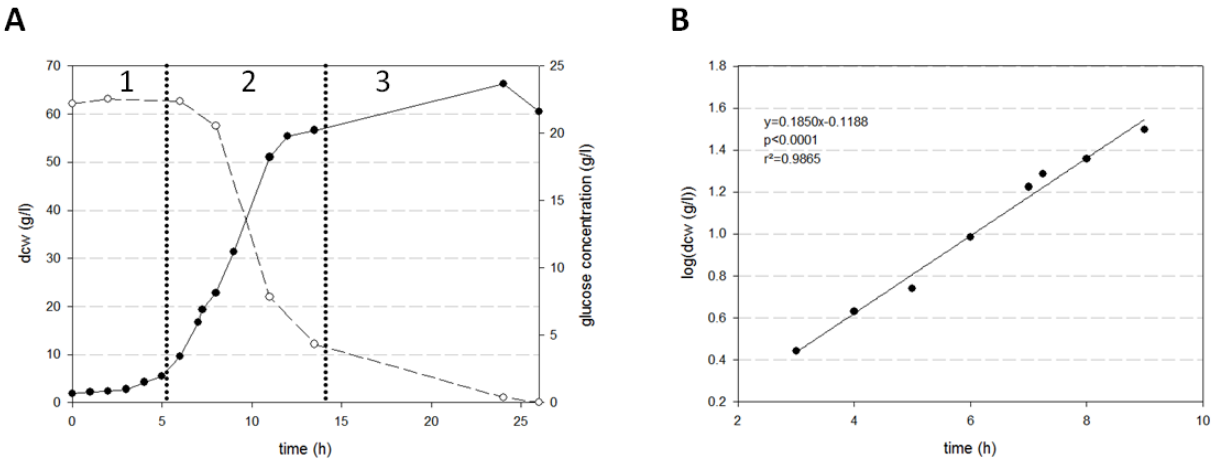

Figure 4-14. Determination of the growth phases of G1212/YRC102-6H-hPR. (A) Evolution of the dcw (black dots and straight black line) and the glucose concentration (white dots and dashed black line) with the time. The two vertical dotted lines mark the separation between lag phase (1), exponential phase (2) and stationary/death phase (3). (B) Evolution of the dry cell weight logarithm (black dots) with the time. Linear shaped fit curve (in black) was calculated by Sigmaplot, parameters of the fit are given on the diagram.

The total protein concentration was calculated by Bio-Rad protein assay and plotted in a diagram in Figure 4-15.A together with the dcw. This diagram shows a similar behavior of both curves except at the very beginning of the experiment where the protein production starts to increase already after 2 h whereas the dcw stays flat until 4 h. Another interesting result is the relatively low total protein concentration obtained for all samples if they are compared to the results obtained in the precedent section. No concentration above 200 mg/l can be seen when the progesterone receptor is produced whereas values over 500 mg/l were observed in the case of the HER-2 production. The Coomassie staining and Western blot analysis of some culture samples are presented respectively in Figure 4-15.B and Figure 4-15.C and show also differences in comparison to the precedent section. The two first lanes of the Coomassie staining show very faint bands and it is due to the very low concentration on total proteins at the beginning of the experiment. Then, at t=3 h, 4 µg of total proteins could be loaded on all lanes. The Western blot show a strong production of the progesterone receptor at t=3 h, almost no production until t= 9 h and again a strong production of the recombinant protein until t= 12h. After that, the production is slowly decreasing until the end of the experiment. It is interesting to note that the production of receptor at t= 3 h show less degradation products than the lanes for later times and may correspond to the small increase in total protein production which has been seen in Figure 4-15.A.

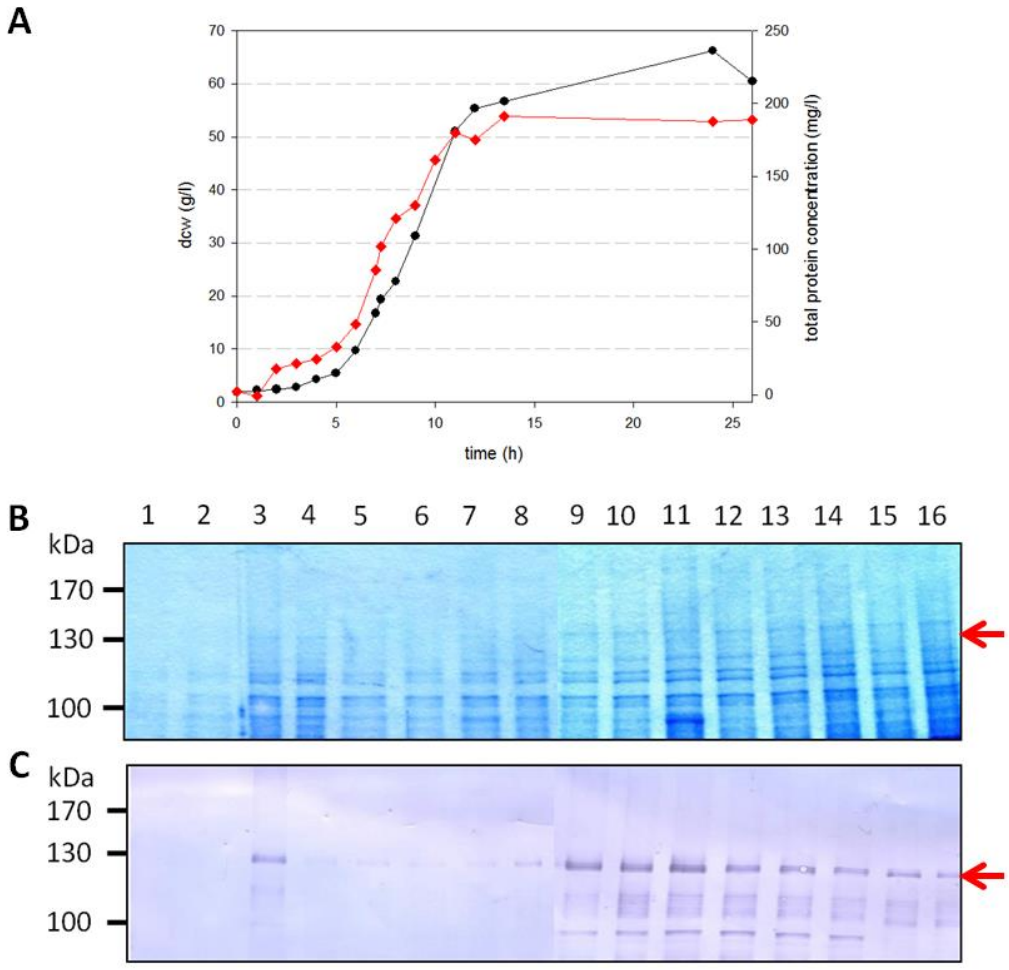

Figure 4-15. Evolution of the total protein production and the hPR production during batch fermentation of G1212/YRC102-6H-hPR. (A) Evolution of the dcw (black dots and line) and the total protein concentration (red diamonds and line) with the time. (B) and (C): Respectively Coomassie staining and Western blot analysis of culture samples after 1 (1), 2 (2), 3 (3), 4 (4), 5 (5), 6 (6), 7 (7), 8 (8), 9 (9), 10 (10), 11 (11), 12 (12), 13 (13), 14 (14), 23 (15) and 26 h (16). The red arrow represents the position of the progesterone receptor isoform B.

4.6.3 Batch cultivation for *H. polymorpha* RB11-pFPMT121-6H-HER-2

Batch cultivation of *H. polymorpha* was also performed with the strain RB11/pFPMT121-6H-HER-2 in a final volume of 660 ml culture. Because the production of the recombinant protein is controlled by the *FMD* promoter, a different cultivation process than for *A. adeninivorans* was adopted. It involved the shift of culture medium from YPD to YMM-nitrate-glycerol after 24 h in order to derepress the *FMD* promoter and then, a second shift in YMM-nitrate-methanol after 48 h (time since begin of the experiment = 72 h). The yeasts were allowed to grow in this final medium for 90 h (total duration of the experiment = 162 h). In order to observe the culture comportment of RB11/pFPMT121-6H-HER-2, culture samples were taken at regular intervals and dcw was calculated. The results of the most representative time points are presented in the histogram in Figure 4-16. Green bars represent the dcw value for a sample taken when YPD was the culture medium and blue and red bars represents the values when respectively glycerol and methanol were present in the

medium. Cell density is increasing during the first 24 h of the culture but significant growth is not visible until 22 h and the dcw reaches 18 g/l. After the first medium shift, the growth is slowed and then increases again to reach its maximum (approximately 45 g/l) after 65 h. No significant increase can be then observed in the dcw until the end of the experiment, this meaning that the culture reached its maximum cell density before the shift in minimal medium with methanol and so before the introduction of the promoter inducer. Another interesting point is that the dry culture weight for this *H. polymorpha* has a maximum at approximately 50 g/l, which is lower than the *A. adeninivorans* strain which could reach 65 g/l.

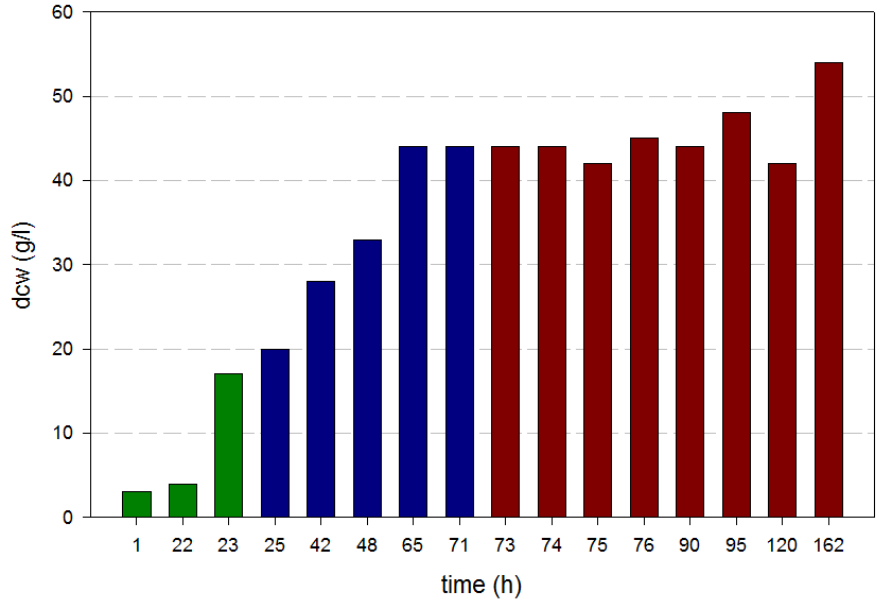

Figure 4-16. Evolution of the dcw of *H. polymorpha* RB11/pFPMT121-6H-HER-2 during batch cultivation. Green bars: cultivation in YPD, blue bars: cultivation in YMM-nitrate-glycerol, red bars: cultivation in YMM-nitrate-methanol.

Additional small culture samples were taken during the cultivation and were also submitted to gel electrophorese. Both the total protein content and the presence of HER-2 were visualized by Coomassie staining (Figure 4-17.A) and Western blot analysis (Figure 4-17.B). Contrary to the procedure for *A. adeninivorans* cultivation study, no normalization of the total protein quantities was performed, thus meaning that the same volume of protein extract was loaded on the gels. Only one sample from the first part of the cultivation in YPD was included in the Western blot analysis as flask cultivation already showed that no recombinant protein was produced during this phase. The Coomassie staining shows a slow increase of protein bands intensity until approximately 24 h after the shift in YMM-nitrate-glycerol which is consistent with the dcw measurements. The Western blot analysis shows HER-2 production already one hour after the shift in YMM-nitrate-glycerol with a production peak between 2 h and 8 h. After that, the band intensity is slowly decreasing until the second shift in YMM-nitrate-methanol. Then, production of HER-2 seems to stay constant in the first hours in this new medium and after 18 h, another band under 185 kDa seems to be the most produced protein. It is also to note the presence of degradation bands after 6 h in the medium with

glycerol, bands which are absent after the shift in the YMM-nitrate-methanol and bands which appear again strongly after 100 h.

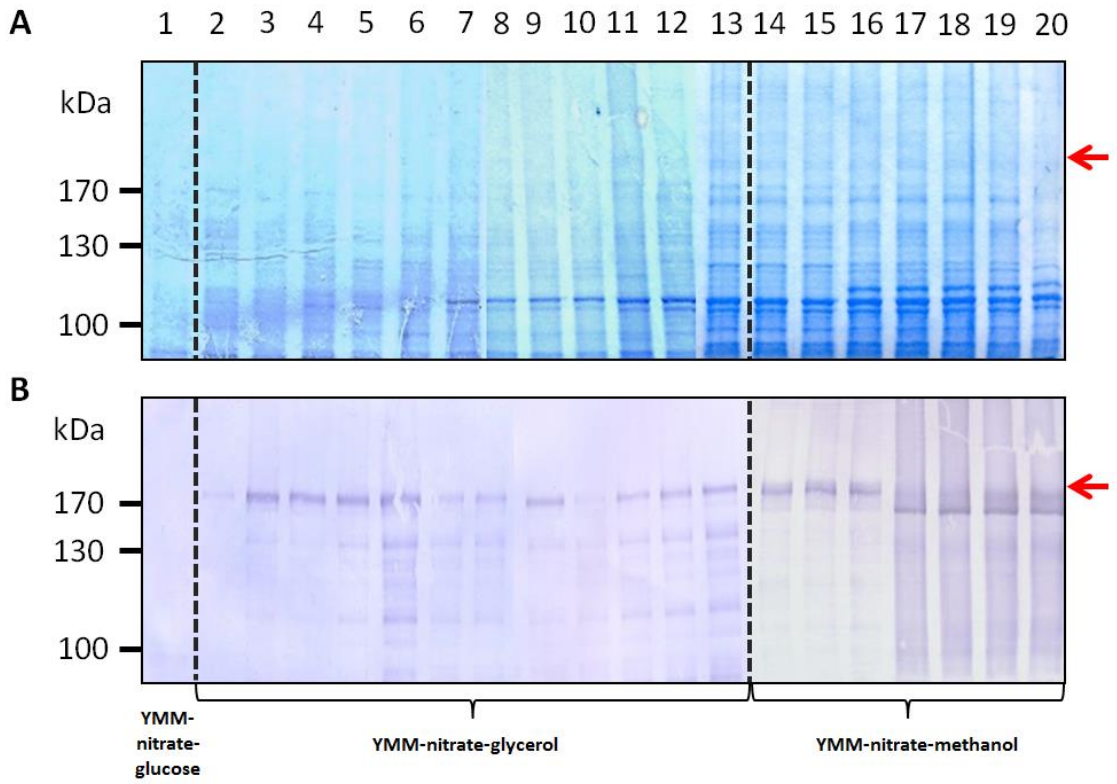

Figure 4-17. Coomassie staining (A) and Western blot analysis (B) of culture samples from *H. polymorpha* RB11/pFPMT121-6H-HER-2 batch cultivation taken after 23 (1), 25 (2), 26 (3), 28 (4), 30 (5), 32 (6), 34 (7), 48 (8), 50 (9), 52 (10), 54 (11), 58 (12), 71 (13), 73 (14), 74 (15), 75 (16), 99 (17), 101 (18), 103 (19) and 162 h (20). The red arrow represents the position of the HER-2 protein. The medium utilized for the culture is annotated under the figure.

4.6.4 Batch cultivation of *H. polymorpha* RB11/pFPMT121-6H-hPR

The same cultivation process was performed for the *H. polymorpha* strain producing the human progesterone receptor with His-tag at the N-terminus. The diagram in Figure 4-18 presents the values of the dcw for some representative time points of the cultivation and the colors of the bars represent the same conditions as for the precedent section. As for the results with HER-2 production in *H. polymorpha*, dcw reaches approximately 20 g/l in the first phase of the cultivation with YPD as medium but with the difference that this value is reached earlier in the present case. After the first shift (cultivation in YMM-nitrate-glycerol), a slow decrease in the dcw can be observed and the growth increases again to reach its maximum after 48 h. After the second shift of medium (cultivation in YMM-nitrate-methanol), no significant change can be seen and the dry weight per liter culture stays at values in the range of 30 g/l. This value for RB11/pFPMT121-6H-hPR is lower than the maximal dcw obtained with G1212/YRC102-6H-hPR and RB11/pFPMT121-6H-HER-2.

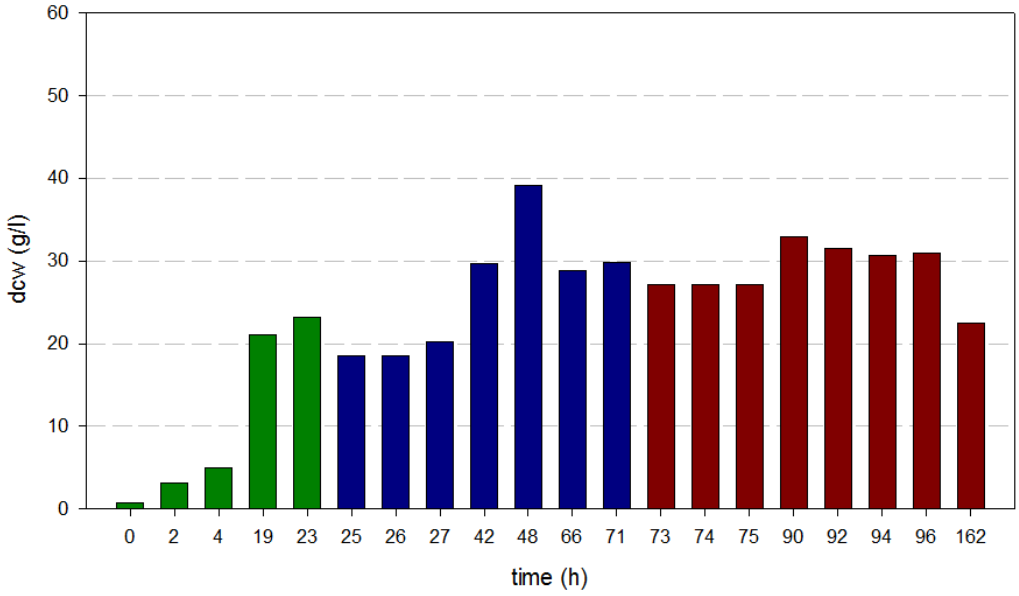

Figure 4-18. Evolution of the dcw of RB11/pFPMT121-6H-hPR during batch cultivation. Green bars: cultivation in YPD, blue bars: cultivation in YMM-nitrate-glycerol, red bars: cultivation in YMM-nitrate-methanol.

As for the precedent section, the cell extract of some samples was loaded in SDS-PAA gels and submitted to Coomassie staining (Figure 4-19.A) as well as Western blot analysis (Figure 4-19.B). The total protein staining shows a slow increase in band intensity until 24 h in YMM-nitrate-glycerol after which no change regarding the bands intensities can be observed. The Western blot presents one band representing the isoform B of the human progesterone receptor after 3 h in YMM-nitrate-glycerol and the intensity of this band increases then in the next hours. The apparition of several other stained bands at lower molecular mass is also increasing after 42 h and these bands stay intense after the shift in YMM-nitrate-methanol.

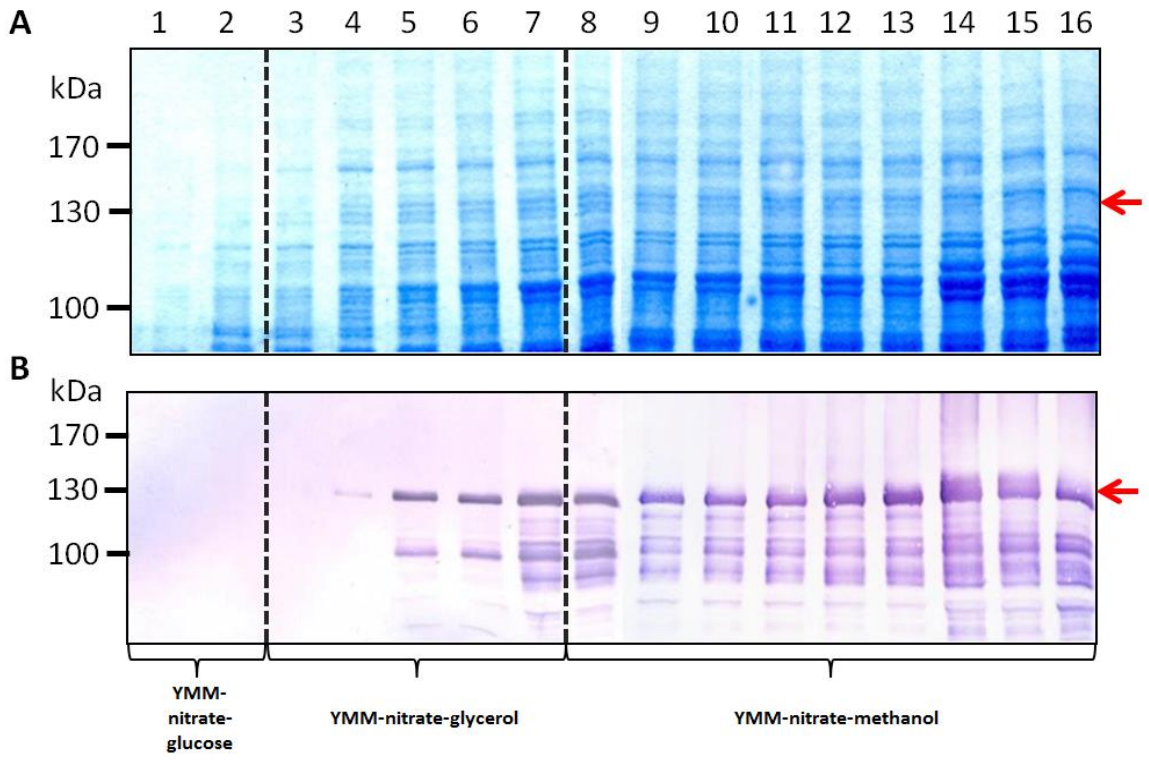

Figure 4-19. Coomassie staining (A) and Western blot analysis (B) of culture samples from *H. polymorpha* RB11/pFPMT121-6H-hPR batch cultivation taken after 1 (1), 23 (2), 25 (3), 27 (4), 42 (5), 48 (6), 66 (7), 72 (8), 73 (9), 74 (10), 75 (11), 76 (12), 99 (13), 101 (14), 127 (15) and 162 h (16). The red arrow represents the position of the progesterone receptor isoform B. The medium utilized for the culture is annotated under the figure.

4.7 Purification of the recombinant receptors

In the following sections, the purification of both the HER-2 and the progesterone receptor will be observed in detail. Although the cultivation in batch mode with temperature and oxygen flow control gives a higher yield of recombinant protein, it was decided to perform the culture of the different yeasts involved in shaking flasks with a culture volume of 200 ml. The main advantage was that flasks cultures allowed performing purifications in parallel, which was impossible for bioreactor cultivation as only one controlling station was available during this work.

4.7.1 Purification of HER-2 from *A. adeninivorans* with His-tag affinity chromatography

The main objective of this part is to find the best method in order to obtain a pure fraction of HER-2 by using the His-tag in affinity chromatography purification. For this, the main strategy was to use different resin chemistries and metal ions to perform the chelation of the histidine amino acids. The nature of the chemical groups attached to the agarose beads have a strong effect on the binding capacity of the column so three different chemical groups with three different selectivity have been assayed: nitrilotriacetic acid (NTA), tris(carboxymethyl)ethylene diamine (TED) and iminodiacetic acid (IDA). It is possible that the position of the His-tag (N-terminal or C-terminal) will have an effect on the purification process but only the receptor with His-tag at the N-terminus was tested for this

purification as this particular variant showed higher recombinant protein production in the screening step both for *A. adeninivorans* and *H. polymorpha* transformants. To assess the effectiveness of the purification, the Coomassie staining and the Western blot are important as they give precious insight relating to the purity of the elution fraction and the quantity of obtained protein. Additionally, the total protein concentration of the first elution fraction E1 determined by Bio-Rad Protein assay is also a good indication in order to compare the different treatments. All these elements are presented in Figure 4-20. The purification with TED as chelating group (Figure 4-20.A) shows the lowest concentration of protein in elution fraction 1 and a restricted number of bands by Coomassie staining. A band appears in the Western blot, which also indicates that the receptor HER-2 was successfully purified and present in the few bands seen by Coomassie staining. Additionally, the intense band observed in flow-through and wash fractions show that a high proportion of the protein is not binding to the column. Part B shows the purification with IDA-chemistry as chelating group on the resin. There, the highest concentration of the elution fraction was measured and it is confirmed by the Coomassie staining where several bands can be observed in this particular fraction. The Western blot shows the presence of a high intensity band corresponding to the HER-2 in the elution fraction. Purification with NTA (Figure 4-20.C) seems to be intermediary between the TED and the IDA chemistries. These results indicate that the His-tagged HER-2 can be purified by IMAC and that the choice of resin chemistry will allow to tend either to more purity or to more yield. Calculation of yield of receptor pro liter culture is made difficult by the presence of other bands in the elution fraction Coomassie staining. The percentage of HER-2 in this fraction oscillates between 0.1 % for the IDA results and 5 % for the TED column, thus giving a yield of purified receptor between 1 µg HER-2 pro liter culture (IDA) and 60 µg pro liter culture (TED).

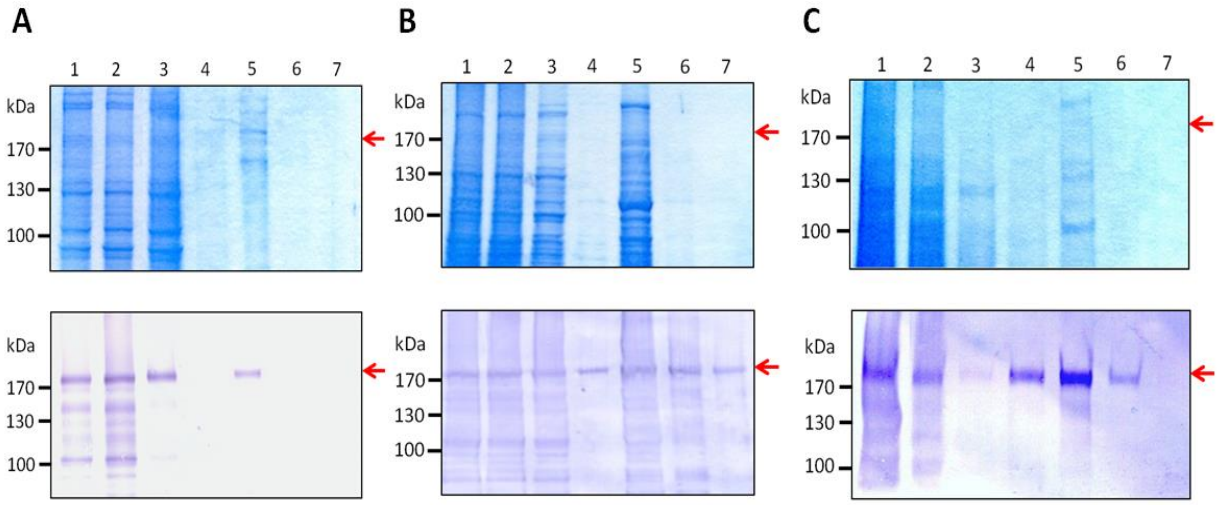

Figure 4-20. Coomassie staining (top) and Western blot analysis (bottom) of the purification process with TED resin (A), IDA resin (B) and NTA resin (C) of *A. adeninivorans* G1212/YRC102-6H-HER-2. 1: raw extract, 2: flow-through, 3: wash fraction 1, 4: wash fraction 2, 5: elution fraction 1, 6: elution fraction 2, 7: elution fraction 3. The red arrow represents the position of the HER-2 protein. Concentration of elution fractions: A5=80 µg/ml, B5=425 µg/ml, C5=126 µg/ml.

4.7.2 Purification of HER-2 from *H. polymorpha* with His-tag affinity chromatography

The same experiments were performed with the HER-2 protein with His-tag at the N-terminus produced in *H. polymorpha*. The results are presented in the same form as for the precedent section in the Figure 4-21. In this case also, the purification was successful with the three resin chemistries tested but the intensities of the bands in the elution fractions are clearly lower than for the protein produced in *A. adeninivorans*. The Coomassie staining is also showing weak bands in the elution fractions and low total protein concentrations. As no clear band is visible in the Coomassie staining corresponding to the HER-2 protein, it is impossible to determine the percentage of receptor in the elution fraction and therefore the yield of purified protein pro liter culture.

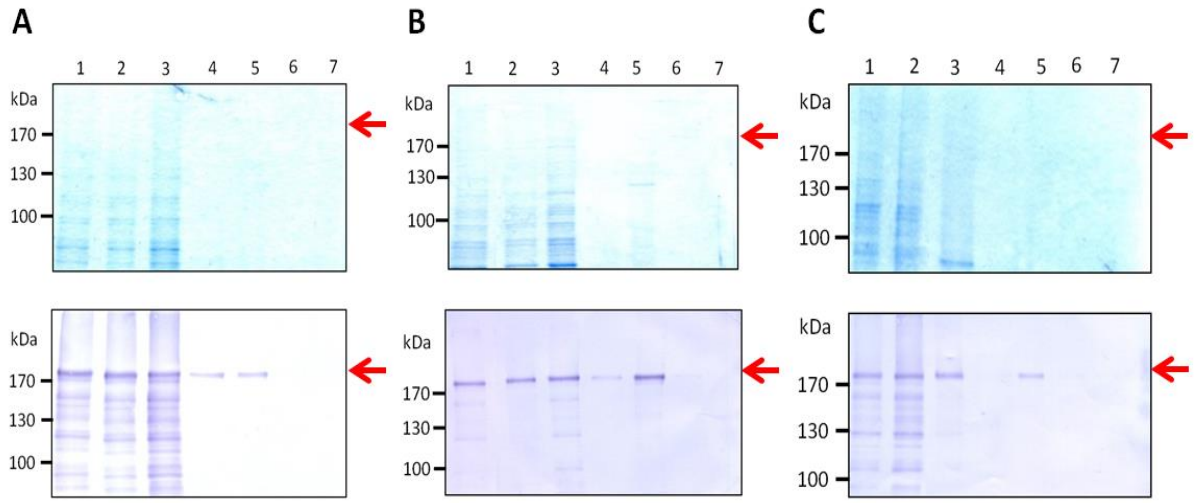

Figure 4-21. Coomassie staining (top) and Western blot analysis (bottom) of the purification process with TED resin (A), IDA resin (B) and NTA resin (C) of *H polymorpha* RB11/pFPMT121-6H-HER-2. 1: raw extract, 2: flow-through, 3: wash fraction 1, 4: wash fraction 2, 5: elution fraction 1, 6: elution fraction 2, 7: elution fraction 3. The red arrow represents the position of HER-2. Concentration of elution fractions: A5=22 µg/ml, B5=91 µg/ml, C5=45 µg/ml.

4.7.3 Purification of the progesterone receptor from *A. adeninivorans* with His-tag affinity chromatography

The purification of the progesterone receptor by His-tag affinity chromatography was also studied but with the difference that both configurations (His-tag at the N- or C-terminus) were tested. The reason for this is that receptor-ligand experiments will be performed with the progesterone receptor and its ligand binding domain is localized at the C-terminus. That means that the presence of the His-tag at this particular end could have a great impact on its functionality. So the receptor showing the highest purification effectiveness can also be nonfunctional, that's why both of them should be involved in purification experiments. For simplification, only the purification performed with resin carrying TED groups are shown in the Figure 4-22 and Figure 4-23. Purification with IDA and NTA chemistries were also performed but didn't improve the effectiveness of the purification (data not shown). Figure 4-22 presents the results of affinity purification with the Coomassie staining (top) and the Western blot analysis (bottom) of the fractions from *A. adeninivorans*

G1212/YRC102-hPR-6H (A) and G1212/YRC102-6H-hPR (B). In both Western blots, a band at 120 kDa corresponding to the isoform B of the human progesterone receptor can be detected in the elution fraction 1, showing that the purification was successful. The Coomassie staining shows also that the purity of the elution fraction is clearly non-optimal as several other proteins co-elute with the progesterone receptor. This is strengthened by the fact that a strong band can be seen in the Western blot in the flow-through fractions, meaning a competition for binding to the resin between the tagged protein and other proteins. The other intense bands appearing at lower molecular masses for the purification of the progesterone receptor with His-tag at the N-terminus may also indicates a decreased stability and therefore a degradation of this particular protein during the chromatography. By considering that the progesterone receptor isoform B represents 1 % of the total protein content in the elution fraction, the yield of purified protein can be calculated to be in 20.85 µg pro liter culture the case of G1212/YRC102-hPR-6H and 26.4 µg pro liter culture in the case of G1212/YRC102-6H-hPR.

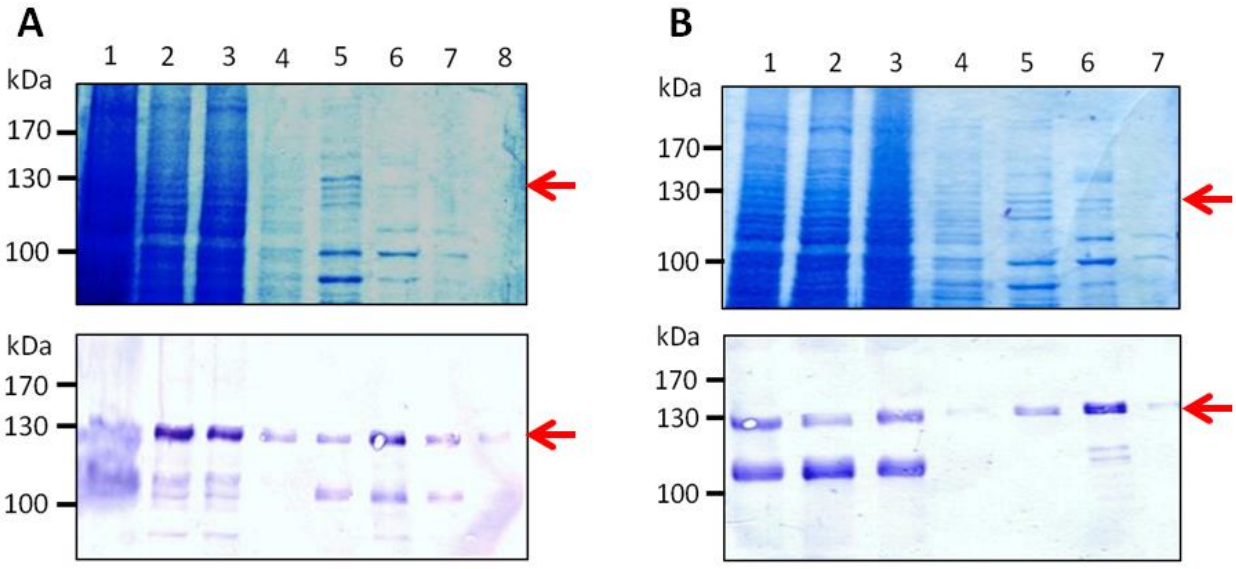

Figure 4-22. Coomassie staining (top) and Western blot analysis (bottom) of the purification process with TED resin of the strains *A. adeninivorans* G1212/YRC102-hPR-6H (A) and G1212/YRC102-6H-hPR (B). 1: raw extract, 2: flow-through, 3: flow-through 2, 4: wash fraction 1, 5: wash fraction 2, 6: elution fraction 1, 7: elution fraction 2, 8: elution fraction 3. The red arrow represents the position of the progesterone receptor isoform B. Concentration of elution fractions: A6=139 µg/ml, B6=176 µg/ml.

4.7.4 Purification of the progesterone receptor from *H. polymorpha* with His-tag affinity chromatography

His-tag purification results of the *H. polymorpha* transformants are presented in the Figure 4-23.A (RB11/pFPMT121-hPR-6H) and the Figure 4-23.B (RB11/pFPMT121-6H-hPR). Both first elution fractions show a band in the Western blot corresponding to the progesterone receptor isoform B but this band is not clearly to see in the Coomassie staining. For the receptor with C-terminal His-tag, it is to note that the raw extract shows a low total protein content which is in agreement with the results obtained in the screening section. The band in elution fraction is more intense than the

band in the raw extract, thus indicating a strong enrichment effect. For the N-terminal His-tag receptor, other proteins are co-eluted in the first elution fraction, making the observation in the Coomassie staining difficult. As for the section 4.7.2, the fact that no clear band can be attributed to the progesterone receptor in the Coomassie staining of the elution fraction makes impossible to determine the percentage of receptor and so to calculate a yield of purified receptor pro liter culture in the case of RB11/pFPMT121-hPR-6H. In the case of RB11/pFPMT121-6H-hPR, considering that 1% of the total proteins is the progesterone receptor, the yield can be calculated to be 12.75 µg pro liter culture.

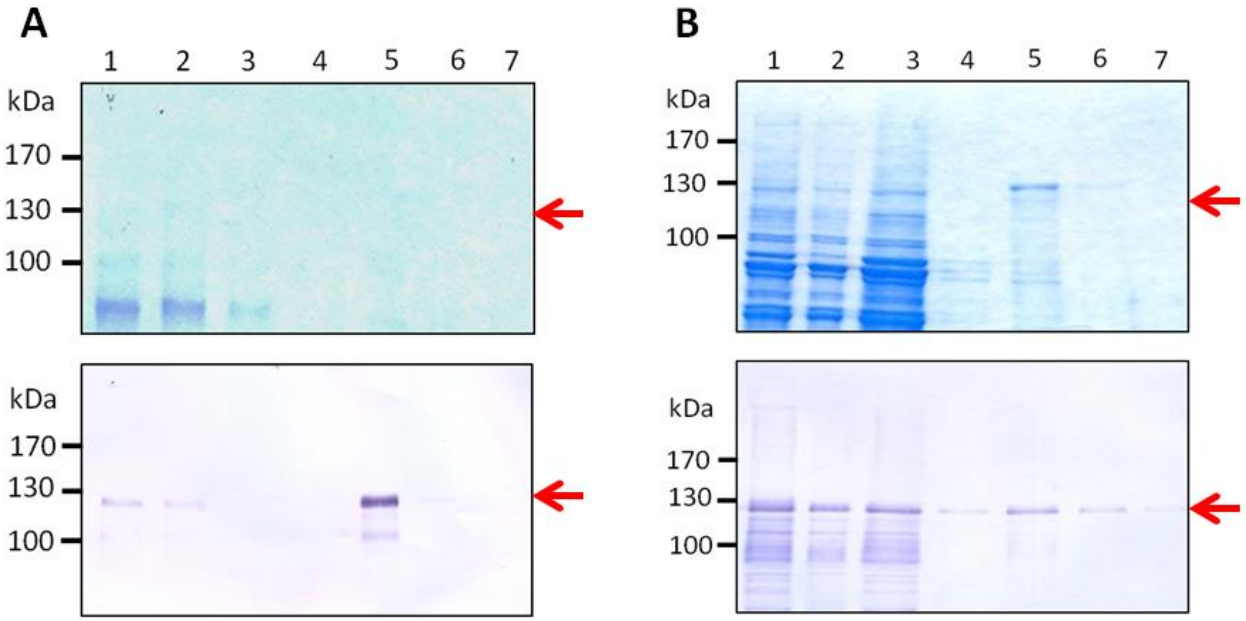

Figure 4-23. Coomassie staining (top) and Western blot analysis (bottom) of the purification process with TED resin of the strains *H. polymorpha* RB11/pFPMT121-hPR-6H (A) and RB11/pFPMT121-6H-hPR (B). 1: raw extract, 2: flow-through, 3: wash fraction 1, 4: wash fraction 2, 5: elution fraction 1, 6: elution fraction 2, 7: elution fraction 3. The red arrow represents the position of the progesterone receptor isoform B. Concentration of elution fractions: A5=27 µg/ml, B5=85 µg/ml.

4.7.5 Purification of HER-2 with anion exchange chromatography

Another option for protein purification is the use of anion exchange chromatography. Like for His-tag affinity chromatography purification, several possibilities based on specific chemistries of the column material are available. For this work, the weak anion exchanger diethylaminoethyl cellulose (DEAE) was selected as it is known to be successful for a broad range of proteins. The elution was performed with a gradient of increasing NaCl concentration as the Cl^- anions will compete with the negatively charged amino acids of the receptor for the binding to the positively charged diethylaminoethanol groups. This chromatography is generally used as a first step of a multistep purification and lead generally to an acceptable but not optimal separation of the proteins. For this experiment, only the *A. adeninivorans* strain producing the HER-2 protein with His-tag at the N-terminus was used as it shown the best production of recombinant protein during the screening

step. To check in which elution fractions HER-2 was present, a great number of them were loaded on a SDS-PAA gel for Western blot analysis. The membrane from this experiment can be seen in Figure 4-24. A band at 185 kDa can be seen in the lane corresponding to the raw extract but only degradation bands can be observed in the elution fractions 1 to 22. As no clear band corresponding to HER-2 could be detected, no further purification of these elution fractions was performed.

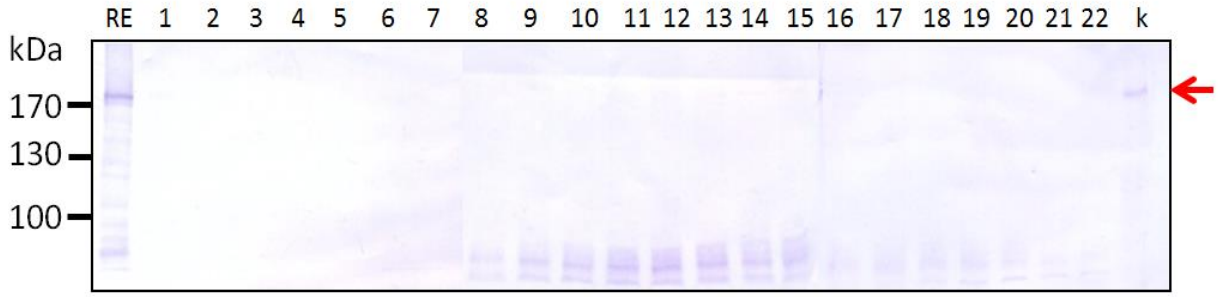

Figure 4-24. Western blot analysis of the purification process of *A. adeninivorans* G1212/YRC102-6H-HER-2 by DEAE anion exchange chromatography.RE: raw extract, 1-22: elution fractions, k: positive control. The red arrow represents the position of the HER-2 protein.

4.7.6 Purification of hPR with anion exchange chromatography

As for the HER-2, anion exchange chromatography using diethylaminoethyl (DEAE) resin was performed with the recombinant human progesterone receptor. Due to the good results obtained with the His-tag purification, it was decided to perform this anion exchange chromatography only with the receptor expressed in *H. polymorpha* with His-tag at the N-terminus. After the chromatography procedure, different elution fractions were loaded on a SDS-PAA gel for Western blot analysis and the results can be seen in Figure 4-25. If a band corresponding to the isoform B of the progesterone receptor can be detected for the raw extract before loading the sample on the column, no other band can be seen in the elution fractions.

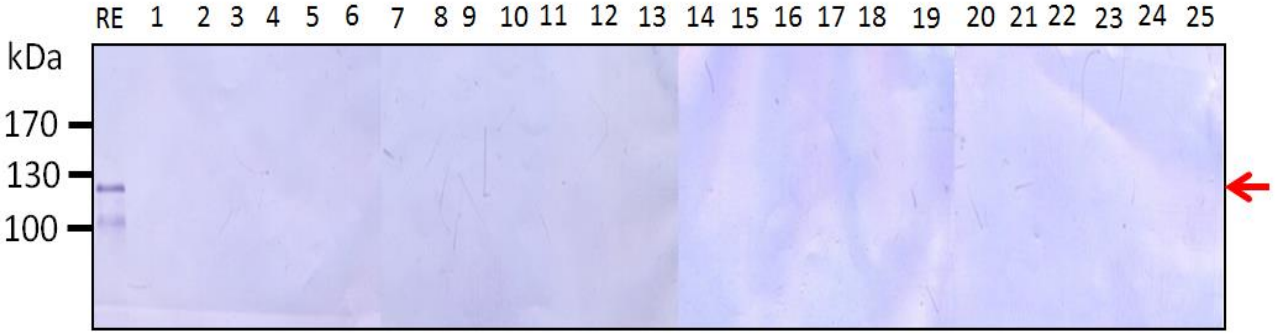

Figure 4-25. Western blot analysis of the purification process of RB11/pFPMT121-6H-hPR by DEAE anion exchange chromatography. RE: raw extract, 1-25: elution fractions. The red arrow represents the position of the progesterone receptor isoform B.

4.7.7 Purification of HER-2 with CHT™ ceramic hydroxyapatite column

MACRO-PREP™ ceramic hydroxyapatite based purification was also performed with the N-His-tagged HER-2 expressed in *H. polymorpha*. The chromatography material consists of a particular form of calcium phosphate ($Ca_5(PO_4)_3OH)_2$ called hydroxyapatite which possess Ca^{2+} sites (called C-sites) and PO_4^- sites (called P-sites) in a repetitive construction. These two sites will bind proteins as the C-sites can be involved in metal affinity interactions with the carboxyl groups of amino acids and P-sites can be involved in ionic interactions with amine groups of amino acids. Elution of the bound proteins was performed by applying an increasing gradient of phosphate concentration, as the phosphate will act as a competitor for the binding to the C-sites of the column and will also bind to the amine sites of the proteins, thus destroying the ionic interaction between the column and the proteins. The results of this chromatography can be observed in the Figure 4-26 where some elution fractions were loaded on SDS-PAA gel and analyzed by Western blot. If a band corresponding to HER-2 can be observed in the raw extract before applying it to the column, no elution fraction is showing any band at 185 kDa. Only for some elution fraction, degradation product signals can be observed but also with a low intensity. These results indicate that hydroxyapatite seems not to be a suitable purification procedure for the recombinant HER-2 protein.

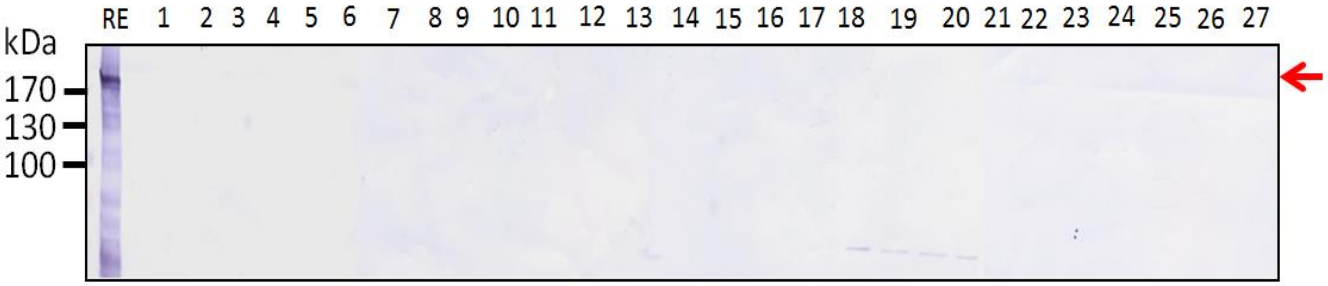

Figure 4-26. Western blot analysis of the purification of H. polymorpha RB11/pFPMT121-6H-HER-2 by MACRO-PREP™ ceramic hydroxyapatite chromatography. RE: raw extract, 1-27: elution fractions. The red arrow represents the position of the HER-2 protein.

4.7.8 Two steps purification of hPR with CHT™ ceramic hydroxyapatite and His-tag affinity chromatography

MACRO-PREP™ ceramic hydroxyapatite based purification was also performed with the N-His-tagged progesterone receptor produced in *H. polymorpha* as a first step of a two-step purification. The results of this chromatography can be observed in the Figure 4-27 where some elution fractions were loaded on SDS-PAA gel and then Coomassie staining (A) and Western blot analysis (B) were performed. The total protein staining indicates a good separation even though the presence of some high intensity bands in a lot of fractions is the sign of a relatively poor selectivity and specificity. The Western blot staining shows bands corresponding to the progesterone receptor (120 kDa) in the elution fractions 17 to 19. Unfortunately, these bands are faint in comparison to the band present in the raw extract and it is due to the dilution of the elution fractions. Rapidly after the drying of the membrane, the intensity of these faint bands decreased and that is the reason why they are hard to distinguish in this scan.

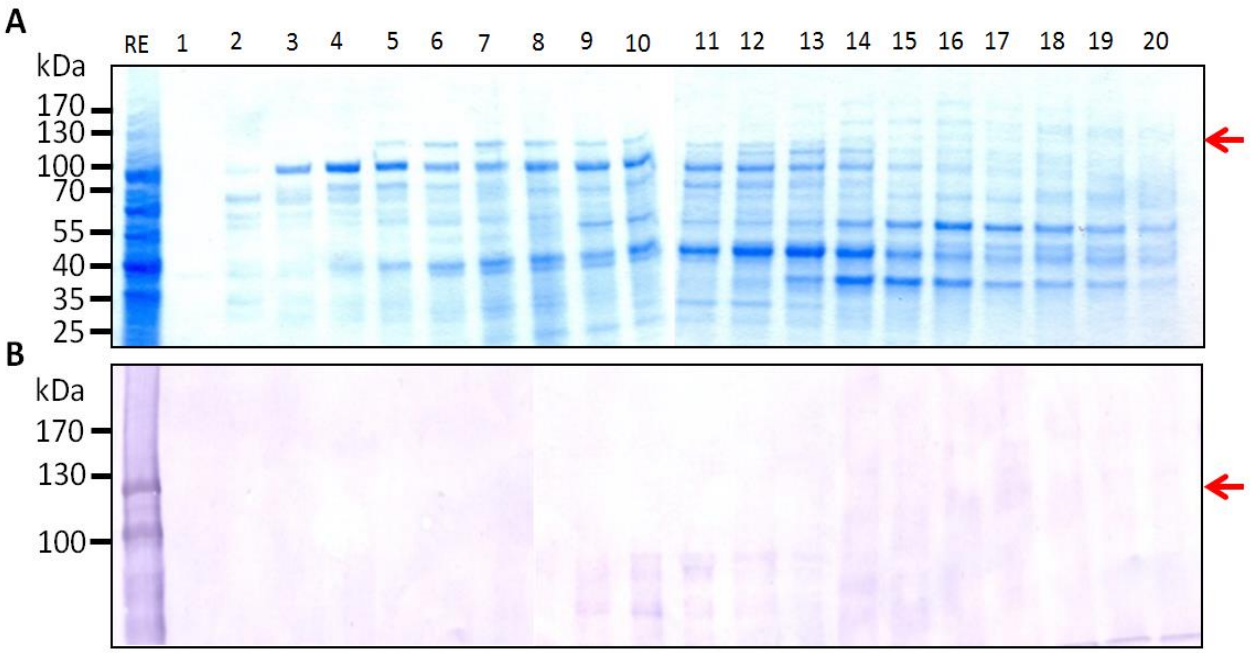

Figure 4-27. Coomassie staining (A) and Western blot (B) analysis of the purification process of *H. polymorpha* RB11/pFPMT121-6H-hPR by MACRO-PREP™ ceramic hydroxyapatite chromatography. RE: raw extract, 1-20: elution fractions. The red arrow represents the position of the progesterone receptor isoform B.

The second step of the purification process is the His-tag based affinity purification. For this the elution 17 to 19 from the first purification were pooled together, concentrated to a final volume of 1.5 ml and then loaded on a TED column. The results of this second purification can be seen in the Figure 4-28 as Coomassie staining (A) and Western blot analysis (B). A band corresponding to the progesterone receptor can be detected both in the Coomassie staining and in the Western blot and the elution fraction doesn't show high intensity extra band. By the two-step purification, a higher purity could be achieved (approximately 60 %) with give a final yield of protein 10.94 µg for a starting culture of 200 ml, this mean approximately 50 µg per liter culture.

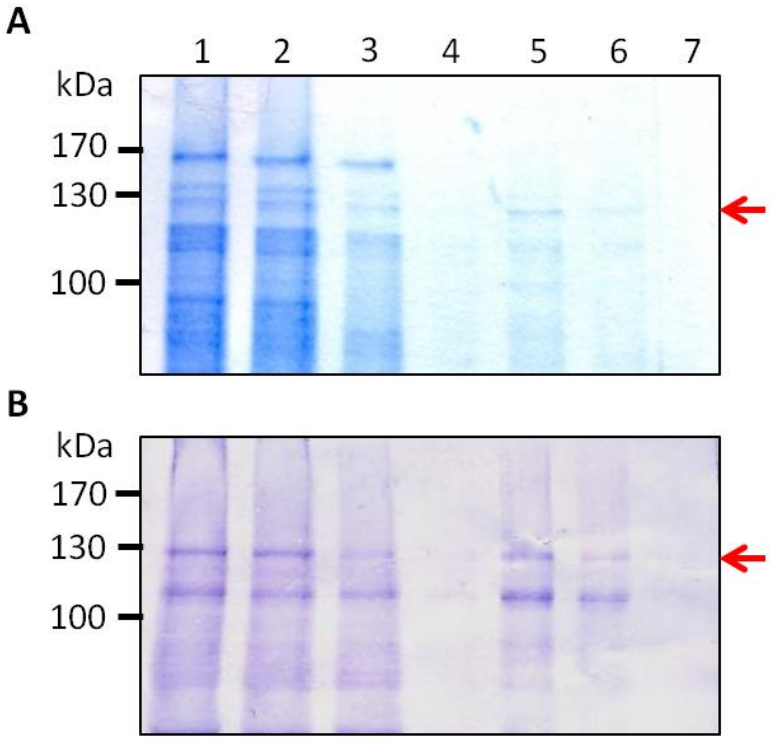

Figure 4-28. Coomassie staining (A) and Western blot analysis (B) of the purification process with TED resin of the strains *H. polymorpha* RB11/pFPMT121-6H-hPR. 1: raw extract, 2: flow-through, 3: wash fraction 1, 4: wash fraction 2, 5: elution fraction 1, 6: elution fraction 2, 7: elution fraction 3. The red arrow represents the position of the progesterone receptor isoform B. Concentration of elution fraction: 5=76 µg/ml.

4.8 Progesterone receptor-ligand interactions

4.8.1 Receptor-ligand interaction theory

An interaction between two molecules can follow different theoretical models and these models allow the determination of interesting binding parameters. In this study the model considered will always be the commonly used Langmuir model in a 1:1 configuration, meaning that one ligand molecule interacts with one analyte molecule following second order kinetics. As this work doesn't plan to redemonstrate the equations already proposed to describe this model and available in numerous publications [223, 224], the utilized equations, conventions and approximations will be only mentioned in this Results part and discussions about the pertinence and validity of the model will be treated in the Discussion part. It can already be stated that for the following calculations, the effect of mass transport or the possibility of one analyte molecule to bind several times will be neglected. In the considered model, the interaction between a receptor R and a ligand L forming the complex RL can be described by the relation:

$$R + L \underset{kd}{\overset{ka}{\rightleftarrows}} RL$$

The association constant of this reaction is called ka and the dissociation constant is called kd. By taking as convention that square brackets are used to indicate molar concentrations, the equilibrium dissociation constant called K_D can be defined as:

$$K_D = \frac{[R][L]}{[RL]} = \frac{kd}{ka}$$

In both binding assay presented in this work, the experiments will give access to either a SPR signal or an absorbance signal which are only appearing when RL is formed and which are proportionally correlated with the concentration [RL]. For the following equation [RL] can then be replaced by S, the signal obtained and the Equation 1 can be obtained:

Equation 1

$$K_D = \frac{[R][L]}{S} = \frac{kd}{ka}$$

Additionally, the conservation law imposes that if $[L]_t$ is the concentration of ligand at the time t and $[L]_{tot}$ the total concentration of ligand, then the Equation 2 can be obtained:

Equation 2

$$[L]_t = [L]_{tot} - [RL]_t = [L]_{tot} - S_t$$

A receptor-ligand binding interaction can be described by three distinct phases: the association, the equilibrium and the dissociation phase. The SPR technique shows the evolution of resonance angle (i.e. S_t) during the whole time of the experiment. This will allow the calculation of parameters ka and kd and the observation of the association binding curve. During the association phase, the derivation of Equation 1 with the utilization of Equation 2 will give Equation 3 with the assumptions that the concentration of receptor [R] stays constant during the experiment and that if all available ligand is forming the complex RL then $[L]_{tot}$ is equivalent to S_{max}, the maximum signal.

Equation 3

$$S_t = \frac{S_{max} * [L]}{K_D + [L]} * \left[1 - e^{-(ka*[L]+kd)t}\right]$$

During the dissociation phase, the derivation of the same Equation 1 with the assumptions that the concentration of ligand [L] tends to 0 gives the following equation:

Equation 4

$$S_t = S_0 * e^{-kdt}$$

where S_0 represents the signal at the beginning of the dissociation.

At the equilibrium, the association rate is equal to the dissociation rate and the Equation 3 becomes Equation 5 as the exponential factor tends to 0:

Equation 5

$$Seq = \frac{S_{max} * [L]}{K_D + [L]}$$

The linearization of Equation 5 gives Equation 6:

Equation 6

$$\frac{Seq}{[L]} = \frac{Smax}{K_D} - \frac{Seq}{K_D}$$

which allows the drawing of the Scatchard plot, an interesting way to observe if a reaction follows the normal binding interaction model.

4.8.2 Competitive assay theory

By analogy with the calculations made in enzymology, the ligand-receptor interactions also consider the presence of inhibitors called in this case competitors. A competitor will also bind to the same receptor following the reaction:

$$[I] + [R] \rightleftarrows [IR]$$

with the affinity constant:

$$K_i = \frac{[I][R]}{[IR]}$$

So by considering that $K_D \neq K_i$, by taking all signals at the equilibrium and by introducing IC_{50}, the concentration of I giving $S_t = \frac{S_{max}}{2}$, the Equation 7 can be obtained:

Equation 7

$$S_i = \frac{IC_{50}}{1 + \frac{[I]}{K_D}}$$

4.8.3 Enzyme Linked Receptor Assay (ELRA) for progesterone

To test whether or not the purified progesterone receptor is able to bind progesterone, an ELRA approach was selected. For this, the ligand progesterone-BSA is immobilized on micro titter plates functionalized with the high binding affinity Maxisorp surface. This ligand consists in one BSA protein conjugated with 5 to 10 molecules progesterone and 2 to 5 molecules fluorescein isothiocyanate (FITC). Then, remaining free positions of the well are blocked with BSA at high concentration and a solution containing the progesterone receptor is then allowed to bind for one hour. After that, an antibody directed against the progesterone receptor and produced in rabbit is incubated, followed by a second antibody directed against rabbit IgG carrying a horseradish peroxidase. This enzyme can then oxidize the 3,3',5,5'-tetramethylbenzidine (uncolored) in an intense blue colored compound which can be detected at 450 nm after amplification of the signal by addition of concentrate acid. The principle of this assay is summarized in Figure 4-29.

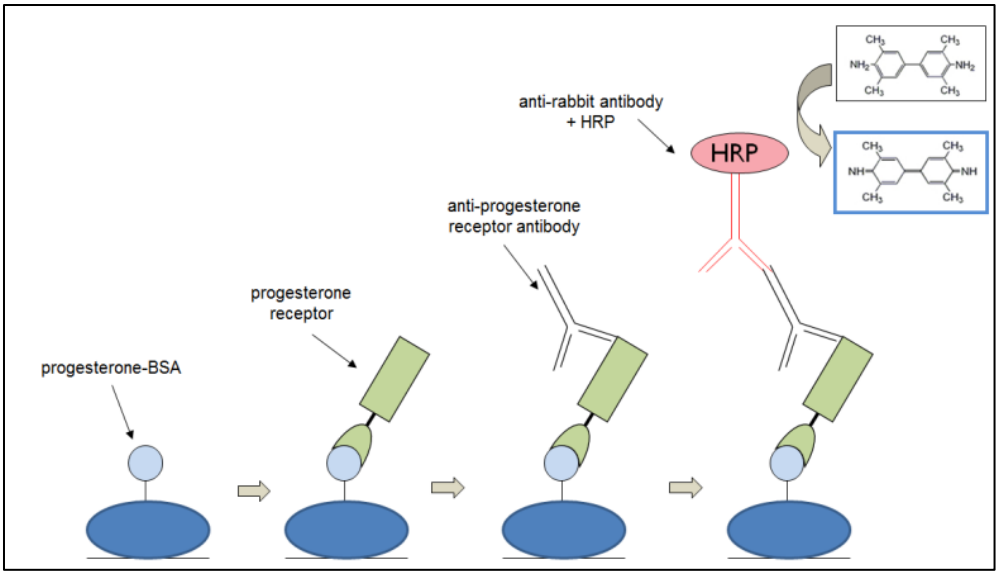

Figure 4-29. Description of the ELRA for progesterone binding. HRP: horseradish peroxidase.

In a first experiment, the selectivity and specificity of the assay were tested. For this, a control protein with no affinity to progesterone (here HER-2) was used and several control conditions were included. The progesterone receptor used in this experiment was the purified receptor from *H. polymorpha* with His-Tag at the N-terminus. The different immobilization procedures are described in the Table 4-2 and the resulting signal can be observed in Figure 4-30.

Table 4-2. Overview of all the tested ELRA combinations.

Experiment name	1st. step	2nd step	3rd step	4th step	5th step
A		progesterone receptor (10 µg/ml)	BSA	anti-progesterone receptor	anti-rabbit with peroxidase
B		BSA	progesterone receptor (10 µg/ml)	anti-progesterone receptor	anti-rabbit with peroxidase
C		ligand	BSA	anti-progesterone receptor	anti-rabbit with peroxidase
D	ligand	BSA	HER-2 (10 µg/ml)	anti-HER-2	anti-rabbit with peroxidase
E	ligand	BSA	progesterone receptor (10 µg/ml)	anti-progesterone receptor	anti-rabbit with peroxidase
F			BSA	anti-progesterone receptor	anti-rabbit with peroxidase

The procedure A serves as positive control to know if the anti-progesterone receptor antibody is able to work in micro-titter plate format. The high absorbance signal obtained in comparison with the signal of the negative controls confirms that this is the case. The procedures B and F were performed in order to see if the blocking with BSA toward respectively protein and antibodies is effective. The values at approximately 0.08 for both cases indicate that neither the protein nor the antibodies can bind to the well once the blocking step was performed. The procedure E is the strategy used in order to perform an ELRA and show a higher signal than the negative control without reaching the values of the positive control (procedure A). The procedure C was tested in order to see if the antibodies can bind directly to the ligand. The low signal obtained demonstrates that this is not the case Finally, the procedure D was conducted in order to test the specificity of the ligand-protein reaction. In this case, the signal comparable to the negative controls indicates that another protein than the progesterone receptor cannot bind to the ligand. All together, these results suggest that ELRA may be suitable for determination of progesterone receptor binding capacities. As the purified progesterone receptor with N-terminal His-tag produced in *H. polymorpha* showed successful results, it was used for all the following ELRA experiments.

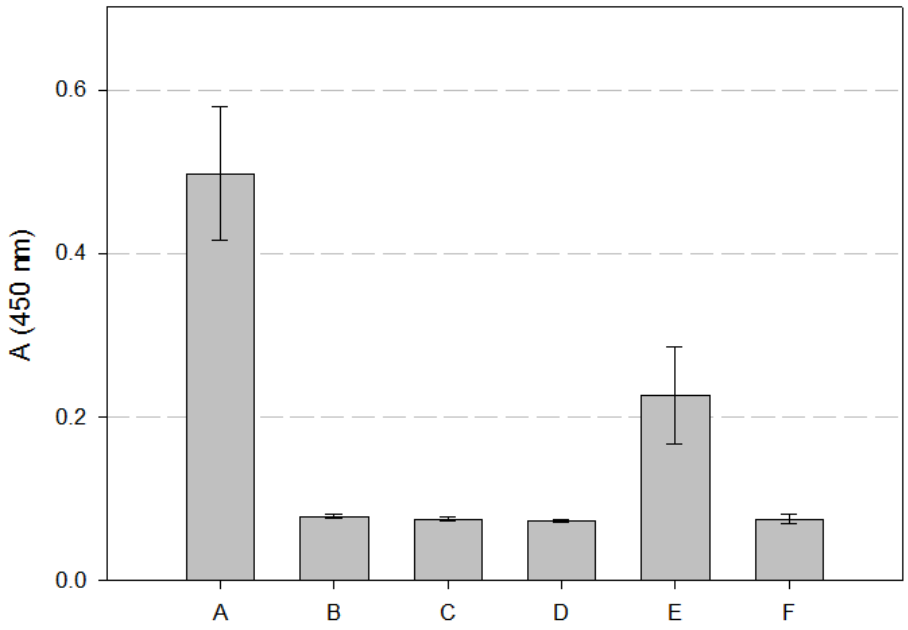

Figure 4-30. Absorbance at 450 nm for the experiments described in table 4-2. The letters A, B, C, D, E and F correspond to the experiment names described in Table 4-2. All experiments were performed in triplicate and error bars represent the standard deviation.

4.8.4 ELRA: response to different progesterone receptor concentrations

In order to find the range of progesterone receptor concentrations susceptible to give an absorbance signal, a plate was prepared where a unique concentration of ligand (progesterone-BSA) was immobilized (0.1 mg/ml). After the blocking step with 5 % BSA, three different protein concentrations were allowed to bind to the ligand as well as one blank solution containing only PBS. The results of this experiment are presented in Figure 4-31 and show a raise in absorbance signal

with increasing concentrations of progesterone receptor. The protein concentrations refer to the concentrations of elution fraction containing the progesterone receptor and not to the receptor only as the purity of the elution fraction was batch-dependent. According to these results, a protein concentration of about 10 µg/ml is sufficient to produce a significant absorbance signal.

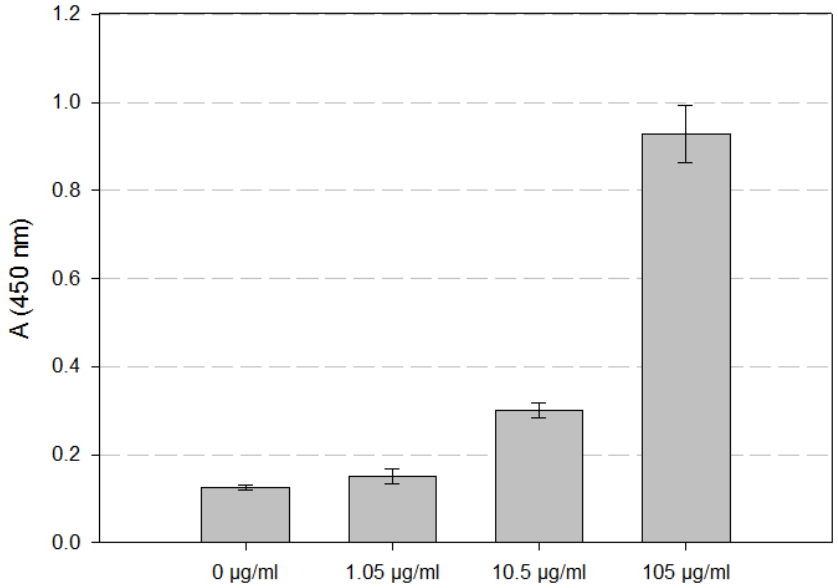

Figure 4-31. Absorbance at 450 nm for different concentrations of purified progesterone receptor when 0.1 mg/ml progesterone-BSA is immobilized. All experiments were performed in triplicate and error bars represent the standard deviation.

4.8.5 ELRA: receptor-ligand saturation assay

Different concentrations of ligand were immobilized on micro-titer plates and the same concentration of elution fraction containing the progesterone receptor (20 µg/ml) was applied to each of them in order to obtain the K_D of the binding reaction. The equations already presented in section 4.8.1 and in particular Equation 3 can be applied in the case of ELRA as the absorbance value represents the equilibrium signal. The same experiment was performed with different concentrations of BSA instead of progesterone-BSA to confirm that the progesterone receptor is binding to the progesterone part of the ligand and not to the BSA itself. The absorbance values for each concentration can be observed in Figure 4-32.A. They show an increase in the absorbance signal only when the concentration of immobilized ligand increases but not in the case of increasing concentrations of BSA. In the Figure 4-32.B, the same values are plotted in a logarithmic scale together with a fit curve following a hyperbolic shape with two parameters corresponding to Equation 3. The values of S_{max} and K_D with their respective standard deviations as well as the value of r^2 are presented under the diagram. Additionally, the Scatchard plot corresponding to Equation 6 was also drawn in Figure 4-32.C.

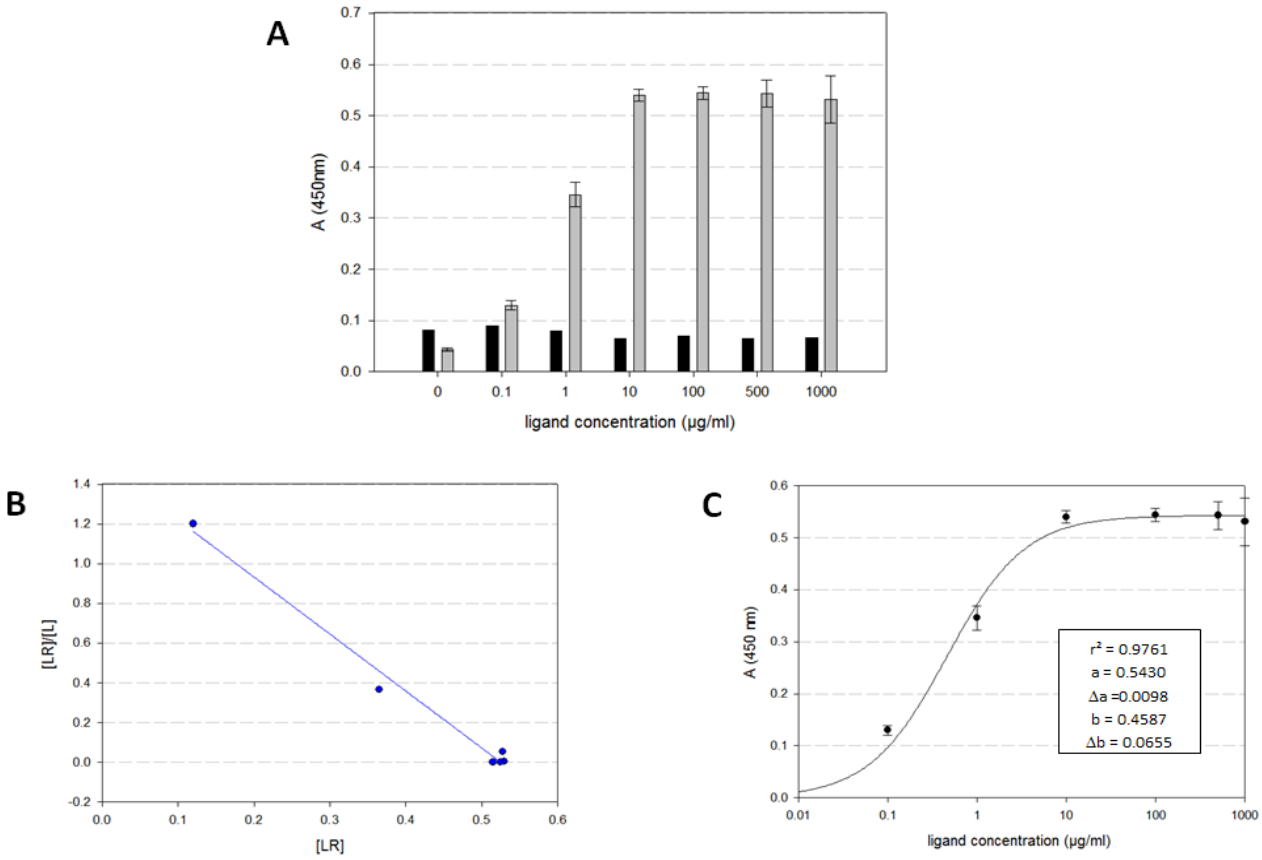

Figure 4-32. (A) Absorbance at 450 nm for different concentrations of immobilized progesterone-BSA (grey bars) and BSA (black bars). (B) Scatchard plot of the interaction (blue dots) with a linear shaped fit curve (blue line) following a y=1.5059-2.869 x and with r^2=0.9866. (C): Evolution of the absorbance at 450 nm with the concentration of ligand in semi-logarithmic scale (black dots) with fit curve following a $y = \frac{ax}{b+x}$ shape. Value of parameters a and b with their respective standard error Δa and Δb as well as the r^2 value are in the diagram.

It is to note that the Scatchard plot shows a linear fit with a satisfying correlation factor thus indicating a good acceptance between the chosen model and the obtained data. The hyperbolic fit curve gives a value for the K_D of 0.4587 ± 0.0655 mg/l which can then be calculated to be 6.28 nM with a molecular mass of the ligand of 73014.28 g/mol.

4.8.6 ELRA: competition assay with free progesterone-BSA

The final aim of an ELRA based test for progesterone detection will be to introduce a sample containing compounds with progesterone activity with the progesterone receptor to observe a decrease in the absorbance signal. This was tested in this experiment way by introducing progesterone-BSA as free ligand together with the progesterone receptor. There will then be a competition for the binding to the progesterone receptor between immobilized ligand and free ligand. As the goal of this experiment is only to prove that this competition is possible, only a few concentrations of ligand were tested and no competition parameters were determined. The results of this experiment are presented in Figure 4-33.

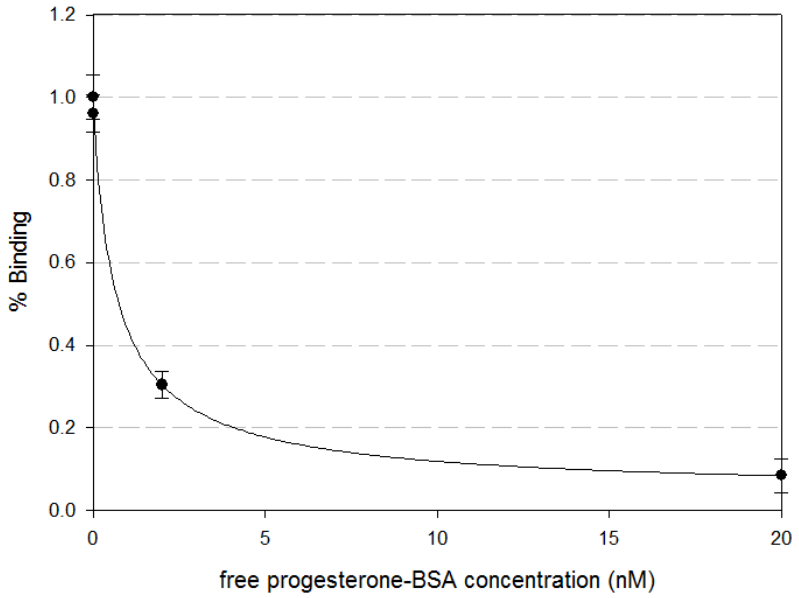

Figure 4-33. Evolution of the percentage of binding of the elution fraction containing the progesterone receptor (40 µg/ml) with increasing concentration of free progesterone-BSA (black dots). Fit curve based on four-parameter logistic function is represented only for informative display as the number of points (4) is insufficient for non-linear regression.

4.8.7 SPR experiments with progesterone receptor: general aspects

As the results concerning receptor/ligand interaction with SPR will always be presented as sensograms or chip profiles and as this vocabulary can be obscure, two special sections in the Material and Methods part called: “Vocabulary conventions for SPR experiments” (section 3.10.7) and “General description of SPR results: graphical display” (section 3.10.8) should be read before starting the reading of the following results.

One powerful advantage of the SPR detection method is the theoretical possibility to have access to the kinetic constants to all biomolecular interactions. Among them the association constant (ka), the dissociation constant (kd) and the equilibrium constant (K_D) can be determined directly on a SPR sensogram with the help of a mathematical algorithm. Unfortunately these algorithms are always specific for a special SPR device and relatively complex as more than one binding model must be at disposition to reflect the diversity of all binding interactions. During the time of this work, attempts have been made by an external partner to insert these mathematical tools to the SPR system developed by the Fraunhofer Institute but without success. Because of that, the following work will not give an estimation of the kinetic parameters for every binding experiment as it would have been too much time-consuming but only for some representative examples.

4.8.8 SPR experiments with progesterone receptor: immobilization of progesterone receptor to the SPR chip

The receptor was bound to the gold surface with the help of a dialkyl disulfide linker in six different channels of the 17-channels flow cell described in the Material and Methods. This linker possesses a symmetric chemical structure with sulfur-sulfur bond in the center, two alkyl chains and three carboxyl groups at both ends. It can form a self-assembled monolayer (SAM) on the bare gold because the sulfur bond can break and make a covalent bond with a gold atom, thus presenting the carboxyl groups for subsequent binding. By the addition of nickel sulfate solution, a nickel ion (Ni^{2+}) can make a chelate complex with the coordinate bonds of the three carboxyl groups. As nickel ions can be involved in a six bonds chelate complex, this interaction let three free places for the His-tagged progesterone receptor to bind to the linker. In the following experiment, the purified receptor from *H. polymorpha* RB11/pFPMT121-6H-hPR was chosen. To ensure the specificity of this interaction, the same procedure was performed with another protein possessing a His-tag but which have no known affinity to progesterone and with one protein without His-tag. For this, the purified HER-2 produced in *A. adeninivorans* G1212/YRC102-6H-HER-2 and the commercially available BSA protein were respectively chosen. The concentrations of the elution fraction containing the progesterone receptor, the HER-2 and the BSA were all similar and equal to 600 µg/ml. The results of this experiment consisting in the chip profiles and the sensograms at the mentioned position are presented in the Figure 4-34. As already explained in the Material and Methods section, the sensograms are obtained by subtracting the values of a position outside the functionalized areas to the values at the desired position, thus removing the unspecific bindings. The SPR profiles from both receptors show a high signal between 100 and 120 for the progesterone receptor and between 70 and 80 for the control receptor only in the six used channels. This indicates that the linker is functional and that both proteins can attach to it with their His-tag. For the BSA no significant signal can be detected in any of the chip position. The sensograms confirm these results as a rise in SPR value following a typical exponential rise to the maximum shape can be observed once the both His-tagged proteins are injected. The equilibrium is reached after 20 minutes and the injection of buffer did not lead to dissociation of the protein, thus showing a very strong association.

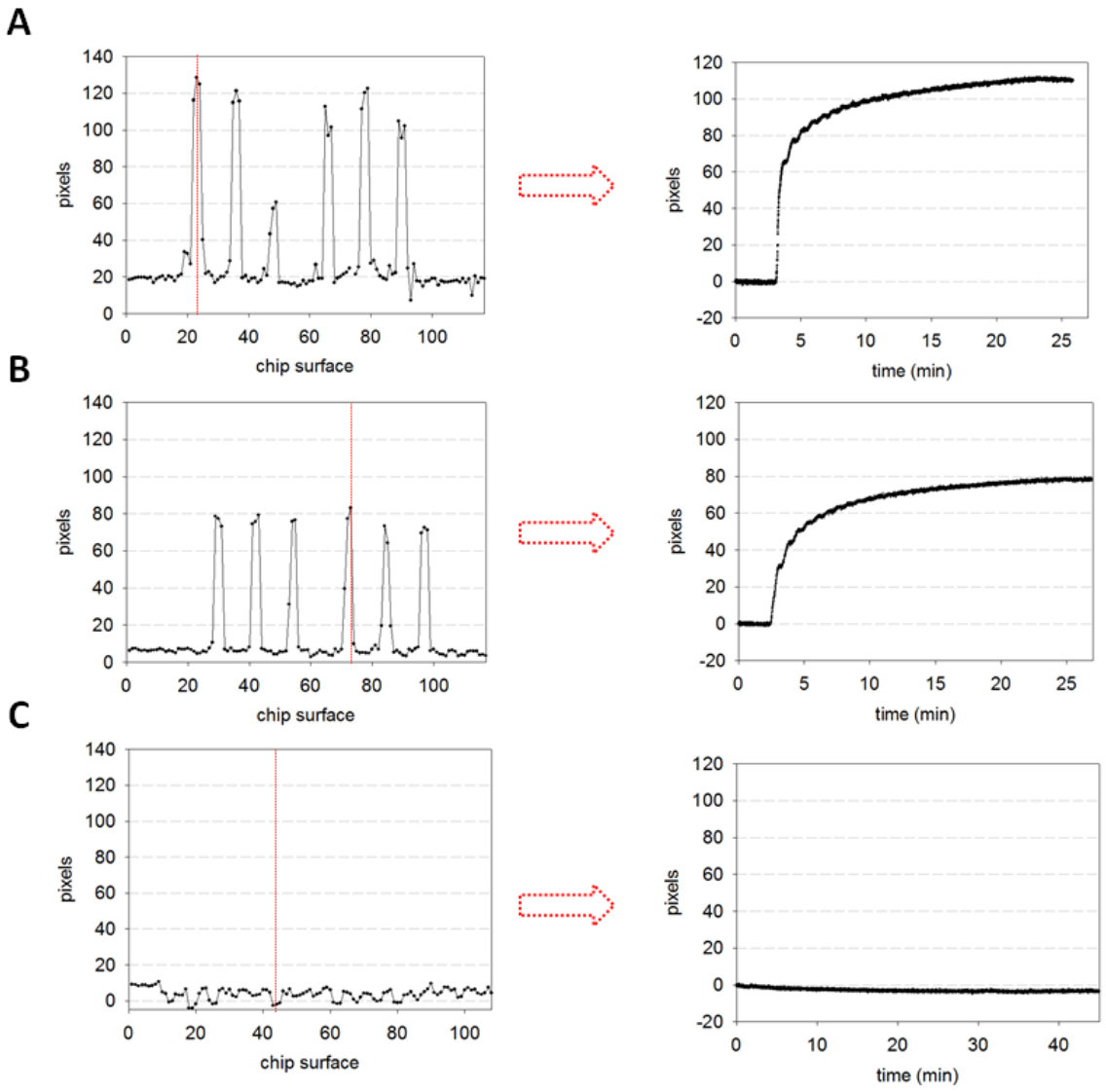

Figure 4-34. Chip profile (left) and sensogram for one functionalized position (right) after injection of purified progesterone receptor (A), purified HER-2 (B) and BSA (C). The dotted red line on the surface profile indicates the position where the sensogram was recorded.

4.8.9 Binding of progesterone-BSA to the immobilized progesterone receptor

As mentioned in the introduction, the SPR technique allows the detection of binding through refractive index change in the medium thus meaning that the analyte should be heavy enough to have a significant impact on this index. That's the reason why the analyte used for this experiment was the progesterone-BSA conjugate and not the progesterone alone. The Figure 4-35 shows the results of the binding experiment from the progesterone-BSA to the progesterone receptor and HER-2 immobilized to the chip in the precedent section. These immobilizations were observed in the Figure 4-34. In case of the HER-2, no change in the resonance angle could be detected for any position of the chip and especially at the position where the protein was immobilized, meaning that no ligand was binding to the receptor. This finding is strengthened by the sensogram showing no

significant increase in the SPR signal when the anlayte is injected. For the progesterone receptor, six peaks can be detected in the chip profile at exactly the same positions as where the receptor was immobilized. The signal values oscillate between 20 and 25 pixels and the sensogram of the position 23 show a binding curve following exponential rise to the maximum. As for the receptor, no dissociation can be detected when the buffer was injected. The kinetic constants of the receptor-ligand interaction were not calculated from this experiment because it was impossible to know precisely the concentration of bound receptor on the surface of the chip and because the 17-channel flow cell causes too high variations in the signal value between the different channels.

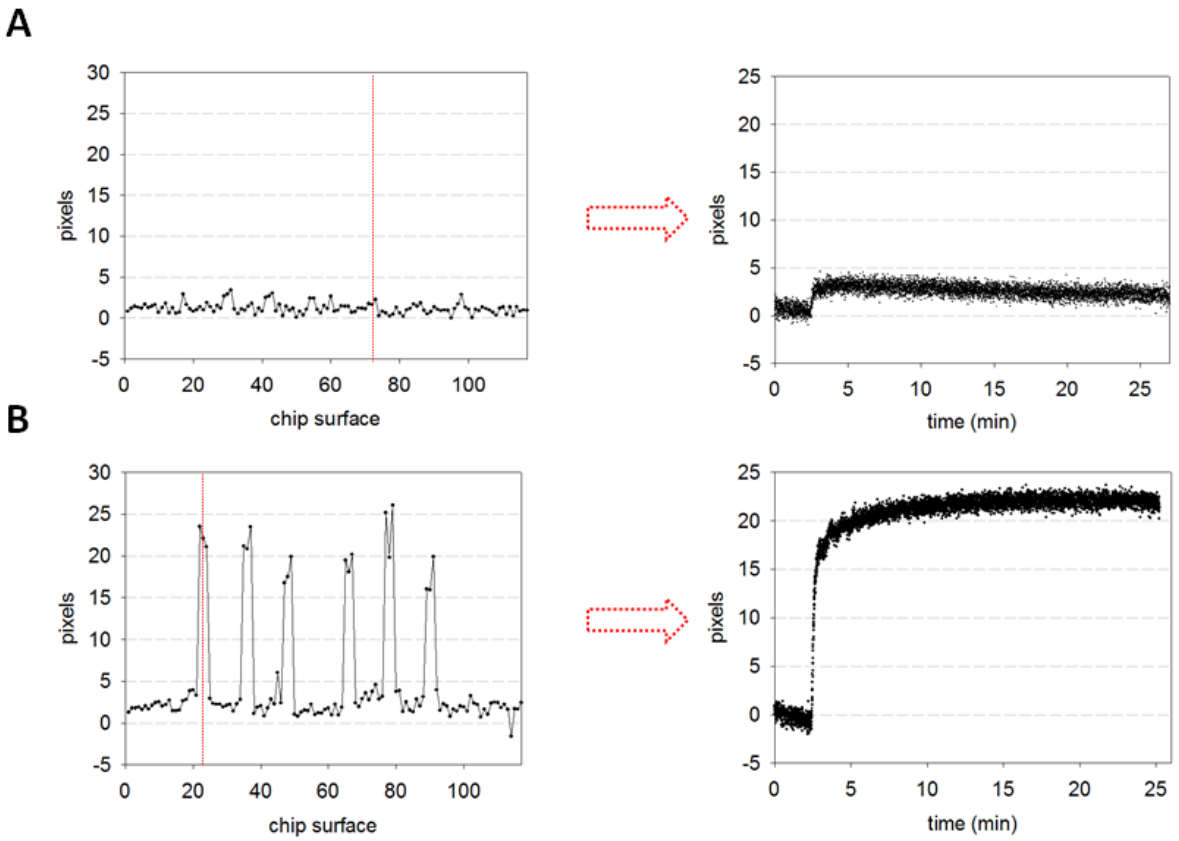

Figure 4-35. Chip profile (left) and sensogram for one functionalized position (right) after injection of 0.1 mg/ml progesterone-BSA to the immobilized HER-2 (A) and to the immobilized progesterone receptor (B). The dotted red line on the surface profile indicates the position where the sensogram was recorded.

4.8.10 Influence of the His-tag position for the binding of progesterone-BSA

The progesterone receptor has been successfully produced in *H. polymorpha* with a His-tag either at the N or at the C-terminus. Because this particular modification could have an impact on the binding capacity of the protein, an experiment was conducted to verify it. After blocking, an elution fraction containing the N-tagged progesterone receptor and an elution containing the C-tagged at the same concentration (40 µg/ml) were used as analyte for two different chips. After this first binding step, the progesterone-BSA at a concentration of 0.1 mg/ml was allowed to flow over both chips and the

sensogram was recorded. The results are presented in the Figure 4-36. The dark blue line represents the sensogram obtained after binding of the receptor to the linker. As it has been expected, the signal reaches in both cases approximately the same value of 25. It is to note that the experiment time was longer for the N-tagged receptor (40 min) as for the C-tagged receptor (15 min). It is because two different flow rates (respectively 5 µl/s and 3µl/s) were used for these two experiments but this has no impact on the signal value, only on the shape of the curve. From these sensograms and as both receptors have the same molecular masses, it can be stated that an equal quantity of receptors was immobilized to the linker. The light blue line on both graphs represents the sensograms obtained after the binding of the ligand progesterone-BSA. It is to note that a rise in the signal value after injection of the analyte can be seen only in the case where the progesterone receptor with His-tag at the N-terminus was immobilized. In the case of the receptor with C-terminal His-tag, no change in the signal value could be observed. These results indicate that the His-tag position has a great impact on the binding capacity of the progesterone receptor when the receptor is immobilized to the chip. Binding assays should be performed with the receptor with the His-tag at the N-terminus.

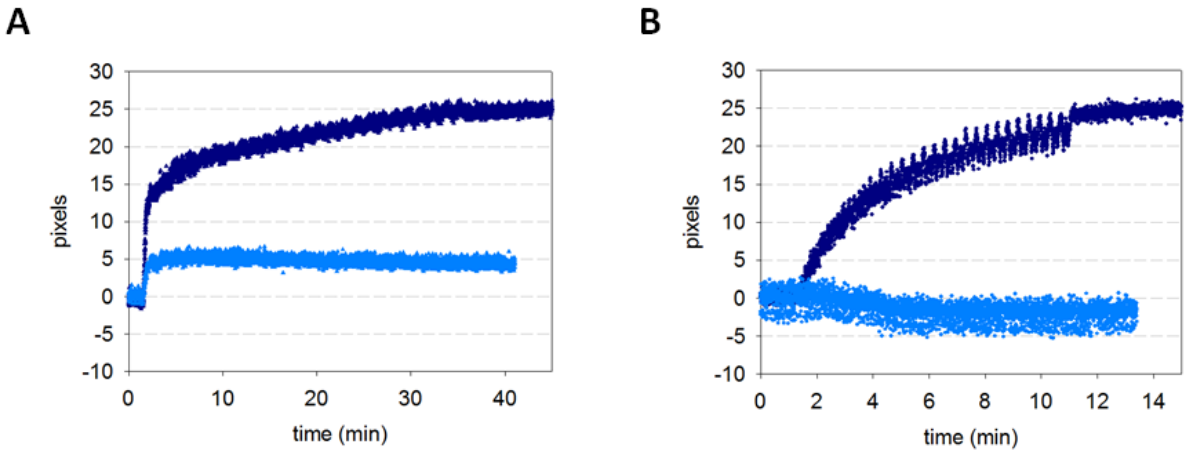

Figure 4-36. Impact of His-tag position on the binding capacities of the receptor. Sensograms of receptor binding (dark blue) and progesterone-BSA binding (light blue) in the case where the N-tagged progesterone (A) or the C-tagged progesterone receptor (B) is immobilized.

4.8.11 Binding of progesterone receptor to the immobilized ligand

In order to have access to the kinetic parameters of this interaction, a strategy where the ligand is immobilized was preferred as the concentration of progesterone-BSA can be precisely determined whereas the concentration of progesterone receptor is highly dependent of the purity of the elution fraction. For this, a simple hydrophobic absorption of ligand to the gold surface was performed and the binding of progesterone receptor to this ligand was recorded. The sensograms obtained for two different ligand concentrations (0.1 mg/ml and 1 mg/ml) and the elution fraction containing the progesterone receptor at a concentration of 38 µg/ml can be seen in the Figure 4-37.A. The green line represents the binding of the receptor to the surface immobilized with 1 mg/ml ligand, the blue

line with 0.1 mg/ml and the red line represent the binding to the control surface (1 µg/ml BSA). The highest binding occurs when the highest concentration of ligand is immobilized and the signal reaches approximately 30. In the case of 0.1 mg/ml ligand, the sensogram still shows a binding curve and reaches 19 whereas the control surface shows a weak binding and the signal doesn't exceed 5, meaning that the unspecific binding remains low. In the Figure 4-37.B, the final signal value for at least 15 positions of each surface was plotted in a histogram and the standard deviation was calculated, showing a clear statistical difference between the three surfaces.

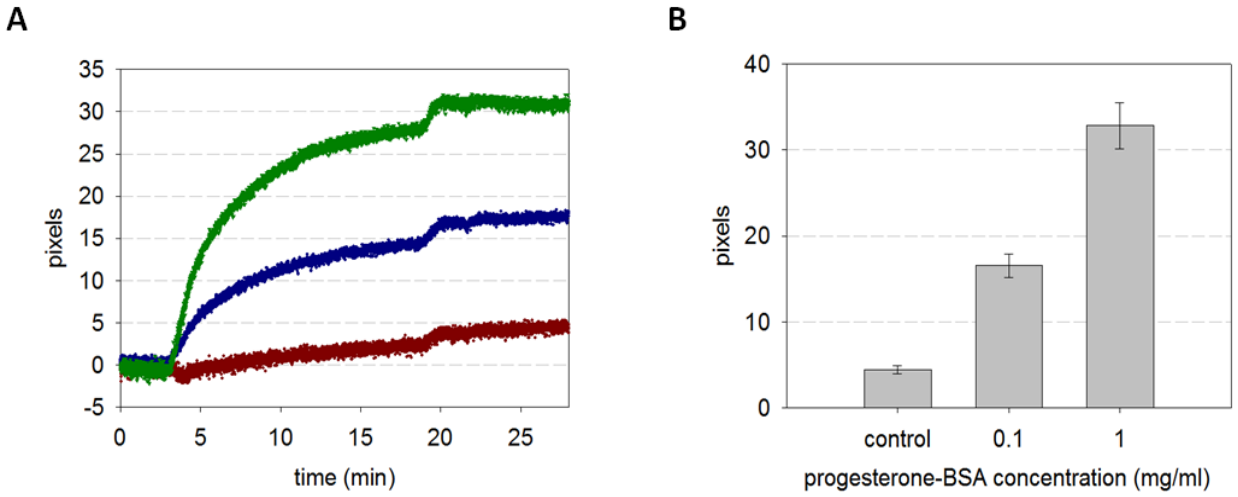

Figure 4-37. (A) Sensograms of receptor binding to 1 mg/ml immobilized progesterone-BSA (green). 0.1mg/ml immobilized progesterone-BSA (blue) and control surface without progesterone-BSA immobilization (red). (B) Histogram showing the equilibrium signal values for 15 positions of the three surfaces. Error bars represent the standard deviation for at least 10 positions of the chip.

In order to ensure the specificity of this interaction, another protein was tested with a chip identically immobilized as for the precedent experiment. In the Figure 4-38, the sensogram corresponding to the binding of an alcohol dehydrogenase produced in yeast (in red) can be observed together with the sensogram of the progesterone receptor (in blue) for comparison. The concentration of both elution fractions were identical (70 µg/ml) but it is to note that the alcohol dehydrogenase possesses a higher purity degree. To simplify the figure, the sensograms of the control surface were subtracted from the sensogram of the functionalized surfaces. A clear binding signal can be observed when the analyte is the progesterone receptor whereas the signal barely reaches 5 when the analyte is the alcohol dehydrogenase. This means that the binding of progesterone receptor to progesterone-BSA is specific.

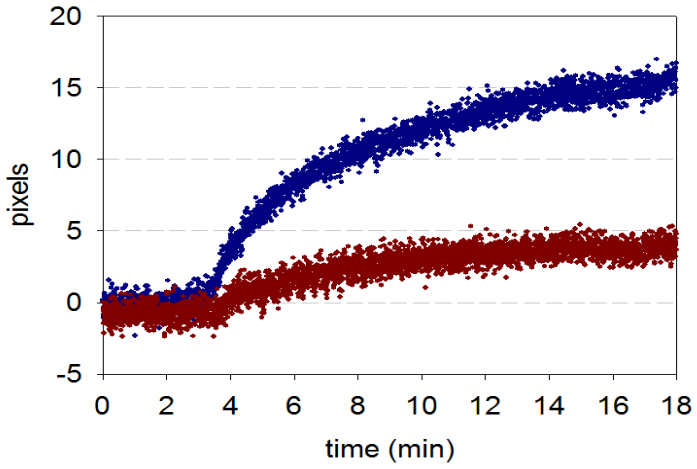

Figure 4-38. Sensogram showing the binding of progesterone receptor (blue) and alcohol dehydrogenase (red) to the immobilized progesterone-BSA (0.1 mg/ml).

4.8.12 Determination of progesterone receptor/ligand binding parameters

- **kd and ka**

As already mentioned, all the parameter determinations were made without the help of any integrated software. For this, at least three different experiments with three different protein batches were used to ensure reproducibility of the measurements. It is to note that even though the association phase can generally be observed in all sensograms, the dissociation phase remains most of the time flat and doesn't follow an exponential decay. That's why no constant determination can be made from the dissociation phase. In the Figure 4-39 are presented three sensograms from three association phases of progesterone receptor to immobilized progesterone-BSA. The concentration of immobilized ligand was always 1 mg/ml for the three experiments and the nature of the analyte was always slightly different as the elution fractions came from different purification experiments. On the sensograms is also always presented as a red line a fit curve following an exponential rise to the maximum with two parameters. As it was explained in the section 4.8.1, the signal is following during the association phase the Equation 3 which can be simplified in $S(t) = a * [1 - e^{-bt}]$ where a = $\frac{Smax*[L]}{K_D+[L]}$ and b = $ka * [L] + kd$. So by plotting a nonlinear regression of the signal following this particular shape, the two parameters a and b can be obtained. For each fit, the value of r^2, a, b and the standard error for both of them are indicated on their respective curves.

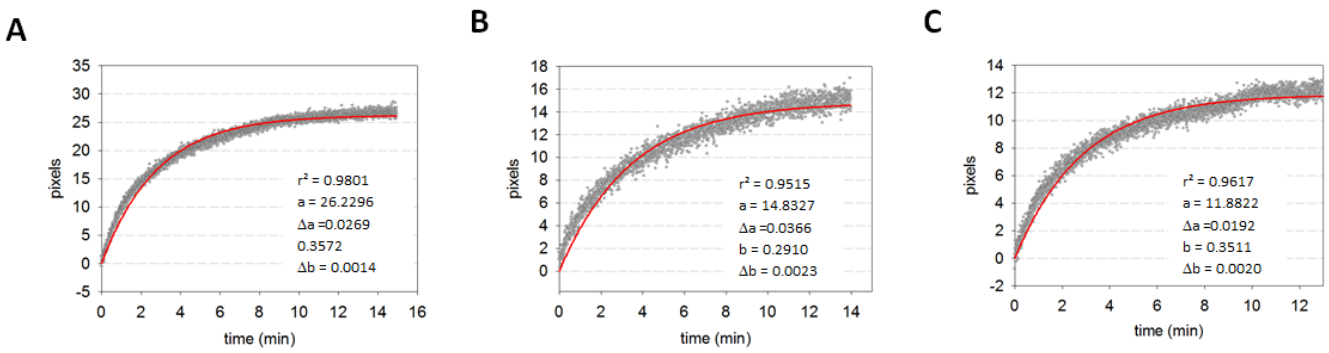

Figure 4-39. Sensograms of the association phase for three different progesterone receptor purification batches (A, B and C). In red is plotted the fit curve calculated by Sigmaplot software. Parameters and r^2 are near their respective curves.

For the three experiments with progesterone receptor from different purifications, it is to see that the r^2 are superior to 0.95 but inferior to 0.99 which is not a sign of very good correlation but is still acceptable. The values of parameter a are different for the three curves because a depends on R_{max} which is highly dependent on the progesterone receptor concentration. On the other hand, the values of b are similar for the three experiments and the average is 0.333. As the molecular mass of the ligand is 73014.28 g/mol, the concentration of immobilized ligand can then be calculated to be 1.370×10^{-5} M (1 mg/ml) and as the unit of ka and kd are using seconds, the following relation can be obtained: $ka * (1.370 \times 10^{-5}) + kd = 0.0055$.

- **K_D**

For the determination of the K_D, another set of experiments was designed. Eight different concentrations of ligand were immobilized on four different SPR chips and the same concentration of the same elution fraction of progesterone receptor was allowed to bind. Each chip consisted of two surfaces with two different concentrations of ligand and a control surface for subtraction of non-specific binding to the chip. The experiment was performed until the equilibrium was reached and the signals were recorded during the whole experiment time. The sensograms for these eight concentrations are compiled in the Figure 4-40.

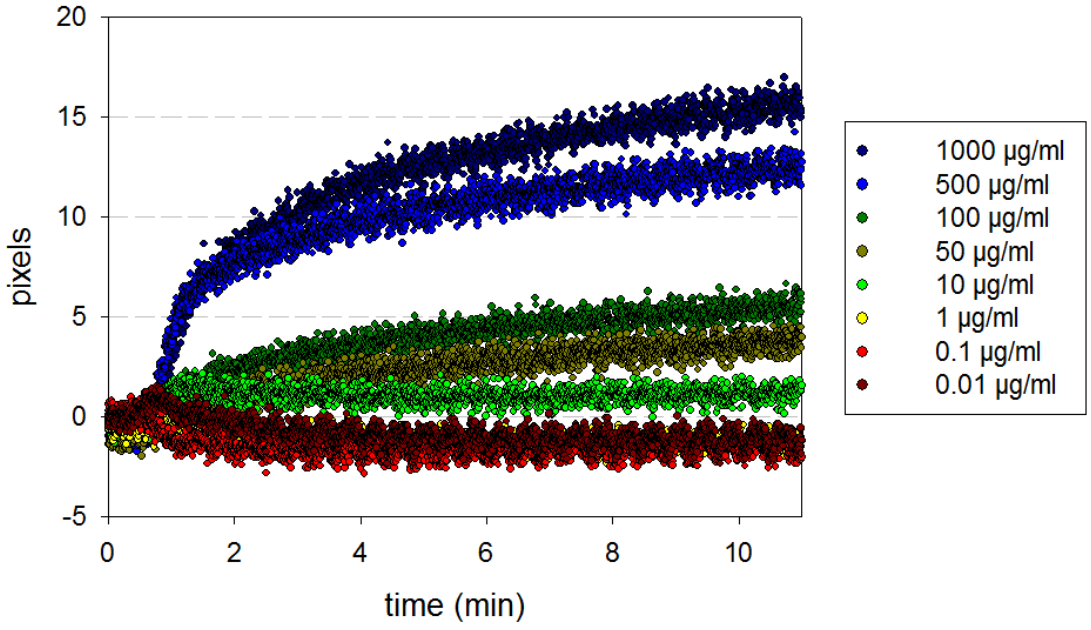

Figure 4-40. Compiled sensograms for the binding of progesterone receptor on different concentrations of immobilized progesterone-BSA (indicated in the right box in µg/ml).

They show a clear increase in the binding signal after injection of the analyte and higher signal when a higher concentration of receptor is used. Additionally, it is to note that the signal values for low concentrations of immobilized ligand are negative thus indicating that another effect is occurring.

The signals at the equilibrium for each concentration were isolated and plotted in Figure 4-41.A. Because the presence of negative values for low concentrations will disturb future analyses, a constant was added to all values. According to the Equation 5, the signal values should follow a relation described by the function $Seq = \frac{a*[L]}{b+[L]}$ where a = S_{max} and b = K_D called single rectangular hyperbola. A non-linear regression of these data following this shape can be observed in the diagram from Figure 4-41.A as a red dashed line and the parameters of this fit are visible in the middle column of the. Even though the fit curve is converging, the correlation factor r^2 under 0.95 and the visual observation that the fit curve doesn't follow the data points are signs that the equation 5 cannot be used in this case. Additionally, the shape of the Scatchard plot presented in Figure 4-41.B shows an upward concave curve instead of an expected straight line. All together, these results indicate that the binding of receptor to the ligand is not following the equation 5 and that other parameters should be included. The particular shape of the Scatchard plot may be the sign of a strong non-specific binding occurring between the ligand and other proteins or molecules present in the elution fraction. It was indeed already mentioned, that binding experiment were performed with partially purified progesterone receptor. Generally, non-specific binding can be integrated in the ligand binding model by replacing the Equation 5 by Equation 8 with non-specific binding parameters K_D' and S_{max}':

Equation 8

$$Seq = \frac{S_{max} * [L]}{K_D + [L]} + \frac{S'_{max} * [L]}{K'_D + [L]}$$

A non-linear regression following a shape $Seq = \frac{a*[L]}{b+[L]} + \frac{c*[L]}{d+[L]}$ was then performed with the same data from Figure 4-41.A and the resulting fit curve is presented on the diagram as a black straight line. The correlation factor and the parameters with their respective standard deviation are present in the right side of the Table 4-3. With a value of 0.9845, r^2 is more satisfying with this non-linear regression and the visualization of the curve on the diagram show that almost all points are reached by the fit curve. Additionally, the parameters indicate the presence of two different K_D: one low (b) probably describing the high affinity interaction between the receptor and its ligand and one high K_D (d) probably describing the low affinity non-specific binding. If b represents the receptor-ligand K_D, that means that K_D=4.9026 ± 2.1143 µg/ml= 67.14 nM. It was already calculated that ka * (1.370×10^{-5}) + kd = 0.0055 and K_D = kd/ka, so by dividing this last relation by ka, it gives: ka = 0.399×10^{3} $M^{-1}s^{-1}$. Finally it gives kd = 3.37×10^{-4} s^{-1}.

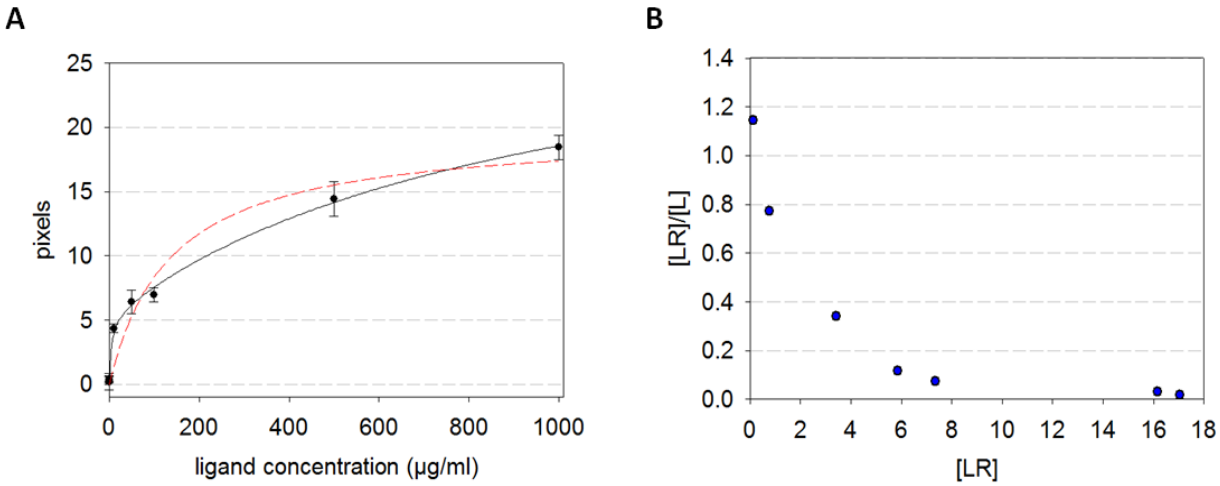

Figure 4-41. (A) SPR signals at the equilibrium for different concentrations of progesterone-BSA (black dots) with single rectangular hyperbola fit (dashed red line) and double rectangular hyperbola fit (straight black line). (B) Scatchard plot of the receptor-ligand interaction (blue dots).

Table 4-3 Value of r^2 and of the fit parameters with their respective standard errors for the two curves drawn in Figure 4-41.B

Parameter	Single rectangular hyperbola	Double rectangular hyperbola
r^2	0.9440	0.9845
a	19.7785	5.3976
Δa	0.9019	0.6732
b	136.8943	4.9026
Δb	21.2668	2.1143
c		26.2392
Δc		4.6077
d		988.1917
Δd		386.9965

4.9 Enzyme Linked ImmunoSorbent Assay (ELISA) with HER-2 protein

4.9.1 ELISA: primary antibody screen

There are several antibodies available commercially which are raised against the HER-2 protein. Unfortunately, some of them are non-suitable for ELISA test because the capacity of antibodies to recognize the target protein in micro-titter plate format is highly susceptible and unpredictable. In the screening and purification sections, two antibodies were intensively used: a polyclonal antibody present in serum of immunized rabbit and a commercial polyclonal antibody (anti-c-erbB-2 oncoprotein). A first experiment was conducted in order to determine if both are suitable for ELISA and if it is the case, which of them show the most interesting reactivity. They were both raised in rabbit so the secondary antibody carrying the horseradish peroxidase will be the same for both primary antibodies and its dilution was set to 1:2000 for this experiment. Different quantities of purified HER-2, HER-2 antigen and negative control were immobilized in micro-titter plate functionalized with the Maxisorp surface and three different dilutions of each first antibody were applied. The HER-2 antigen already mentioned in section 4.1 is the polypeptide used to obtain the serum-based antibody and consist of a small region of HER-2. The negative control consists of an elution fraction of the *A. adeninivorans* G1212/YRC102 strain after His-tag purification. The results of this screen can be seen in Figure 4-42. Each histogram presents the results for one antibody dilution with the serum-based antibody on the top and the commercial polyclonal antibody in the bottom of the figure. The red, orange and green columns represent the absorbance signals for respectively the antigen, the negative control and the purified HER-2.

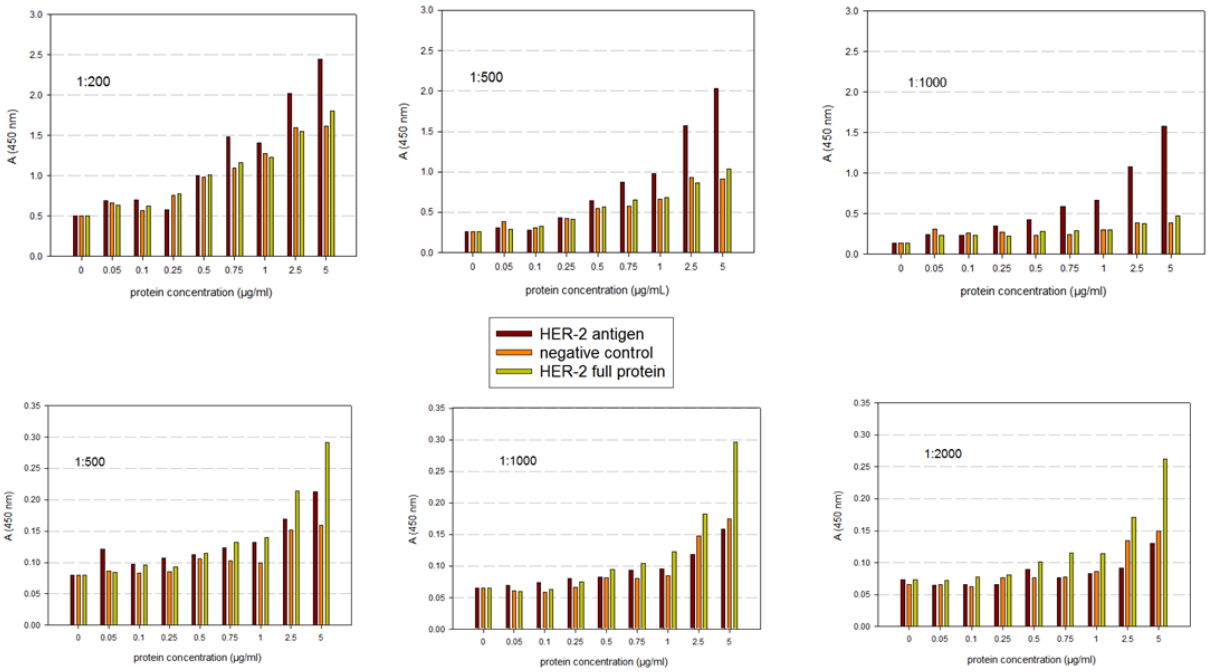

Figure 4-42. Absorbance at 450 nm for different concentrations of HER-2 antigen (red), negative control (orange) and HER-2 (green) with polyclonal antibody from rabbit serum (top) and commercial polyclonal antibody anti-c-erbB-2 oncoprotein (bottom) at different dilutions (indicated on the respective diagram) as primary antibody.

In the case of polyclonal serum-based antibody, the highest signals come with the lowest dilution of antibody and where the antigen was immobilized. This was predictable as the antibodies were obtained after rabbit immunization with this particular peptide. But for all protein concentrations or antibody dilutions, no significant difference can be observed between the signal of the negative control and the purified HER-2. This means that this antibody is not specific enough to be used in an ELISA format. In the case of the commercial antibody, it is to note that for a protein concentration of 5µg/ml, purified HER-2 shows for all antibody dilutions the highest signal. Maximum signal stays relatively low in comparison to serum antibody and doesn't increase with increasing antibody concentration after the 1:1000 dilution whereas the signal of the negative control and of the antigen are at the lowest for the 1:2000 and 1:1000 dilutions. With this experiment, it was concluded that only the commercial antibody is suitable as primary antibody for ELISA test.

4.9.2 ELISA: Secondary antibody optimization

For the first step of ELISA optimization, different dilutions of the second antibody carrying the horseradish peroxidase and directed against rabbit IgG were assayed. Different concentrations of HER-2 and negative control were immobilized in micro-titter plate and primary monoclonal antibody at a 1:1000 dilution was used. As for the precedent experiment, the negative control corresponds to an elution fraction of the *A. adeninivorans* G1212/YRC102 strain after His-tag purification. The results are displayed in Figure 4-43 with blue, green and red curves corresponding respectively to

the 1:1000, 1:2000 and 1:5000 secondary antibody dilutions. All straight lines represent the signal for the purified receptor and dashed lines represent the signals for the negative control.

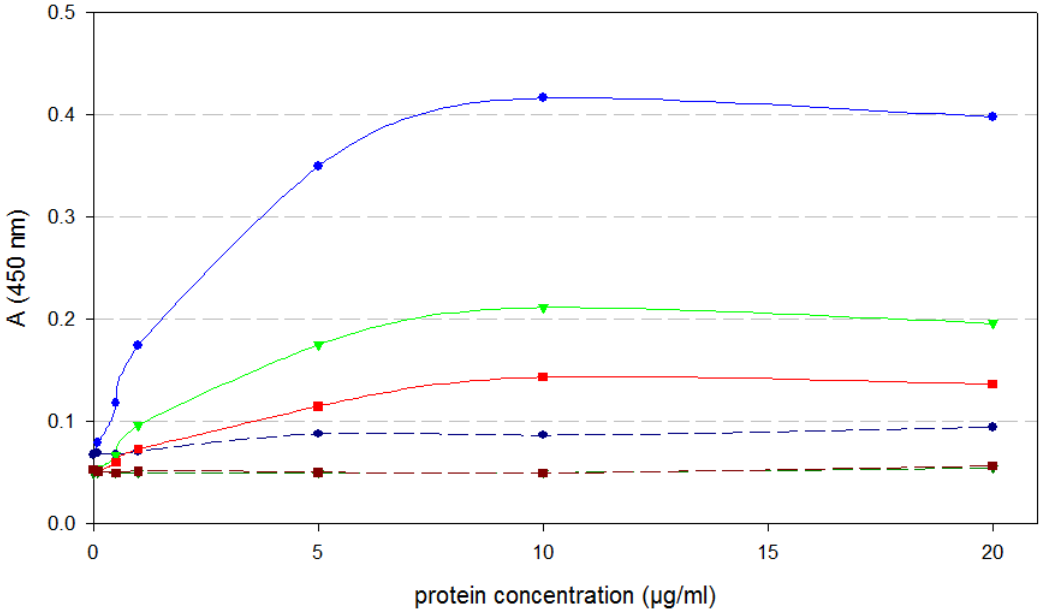

Figure 4-43. Absorbance at 450 nm for different concentrations of HER-2 (straight lines) and negative control (dashed lines) after usage of secondary antibody at 1:1000 (blue), 1:2000 (green) and 1:5000 (red) dilutions.

This diagram shows an increase in signal for each concentration when the antibody dilution is decreasing. The effect is more significant for the purified receptor as the signals corresponding to the negative control only increase when the dilution passes from 1:2000 to 1:1000. According to these results, it was decided to adopt a secondary antibody dilution of 1:1000 in the future experiments as it shows the highest signal for the purified HER-2. This dilution also causes an important signal for the negative control but the difference between specific and non-specific signal is larger (almost 0.3 units of absorbance) than for the other dilutions.

4.9.3 ELISA: Optimization of the blocking solution

The nature or the concentration of the blocking solution can have a great impact on the ELISA sensitivity. A good blocking solution should not reduce the specific signal and prevent non-specific binding of the antibody directly to the wells. Historically, the two mainly used blocking agents are non-fat dry milk and BSA and were therefore selected for this optimization step. For this experiment several protein concentrations of the negative control (elution fraction of G1212/YRC102) and the purified HER-2 were immobilized and different blocking solution were applied in a second step. Finally, the same primary and secondary antibody concentrations were added to the well in order to ensure the same treatment for all different blockings. The results are presented in Figure 4-44 where each diagram presents the absorbance signal for different protein concentrations for one particular blocking solution. The red column represents the wells where the negative control was immobilized and the orange represents the purified HER-2.

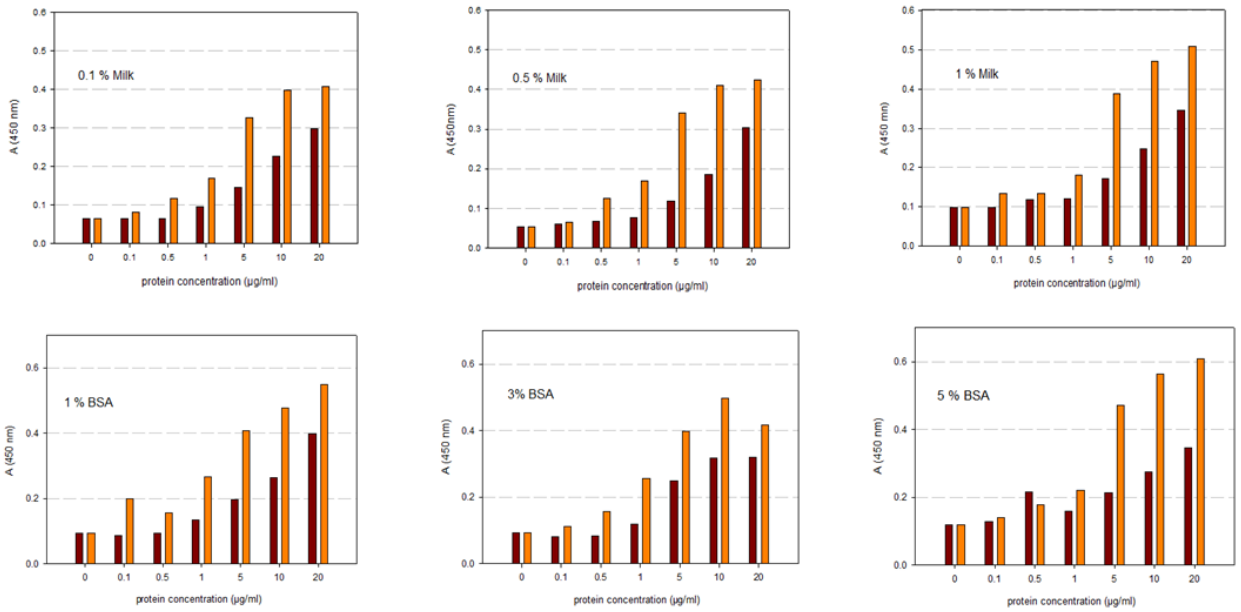

Figure 4-44. Absorbance at 450 nm for different concentration of negative control (red) and HER-2 (orange) after blocking with milk (top) or BSA (bottom). Blocking solution concentrations are indicated on their respective diagram.

Concerning the results when milk was used as blocking agent, it is surprising to see that high concentration show higher specific and non-specific binding for all concentrations of immobilized proteins. This can be explained firstly by the fact that the antibodies itself can interact with the blocking agent and therefore increase the signal when no proteins are immobilized. A second explanation could be that the milk has a stabilizing effect at high concentration of immobilized proteins. The immobilized proteins possess indeed a complex structure made of helixes and sheets which can interact via weak interactions with other parts of the protein or the surface of the well, thus hiding some epitopes from the antibody. By occupying all left places of the well when its concentration is very high, the blocking agent can destroy these weak interactions between the immobilized protein and the well and this can lead to higher binding possibility for the antibody. Taking in account these two effects, the 1 % milk concentration seems to be the best suited for this ELISA as it increase the signal value for HER-2 of about 0.1 units and increase the non-specific binding (when no protein is immobilized or when the negative control is immobilized) of about 0.05 units in comparison to the two other solutions. In the case of BSA as blocking agent, the same observations as for the milk use can be made. When 5 % BSA is used, higher signals can be measured as when lower concentrations of BSA are used. Also at high concentrations of HER-2 or negative control the signal are at the highest when 5 % BSA is used and this can also be explained by the an increased stability of protein. As for the milk, these results indicates that a higher concentration of blocking agent leads to a higher non-specific binding at low concentrations of proteins but also to a higher specific binding at high protein concentrations. Even if the first effect is non-desirable, it has a weaker impact on the final result than the second as the signal amplitude (between no protein immobilized and the highest concentration of immobilized protein) is the highest when 5% BSA is utilized.

In order to decide which of the two blocking agents, milk or BSA, should be used, the precedent results where plotted together in a single graphic in Figure 4-45. The blue triangles represent the experiment where BSA was used and the red dots where milk was used. Straight and dashed lines represent respectively the purified HER-2 and the negative control signals. The purified receptor shows a higher signal for all concentrations tested when BSA was used whereas the negative control signal is very similar for both treatments. When no protein is immobilized (protein concentration= 0 µg/ml), the signals are also all very similar. These results indicate that 5% BSA seems to be the most appropriate tested blocking solutions for this particular assay.

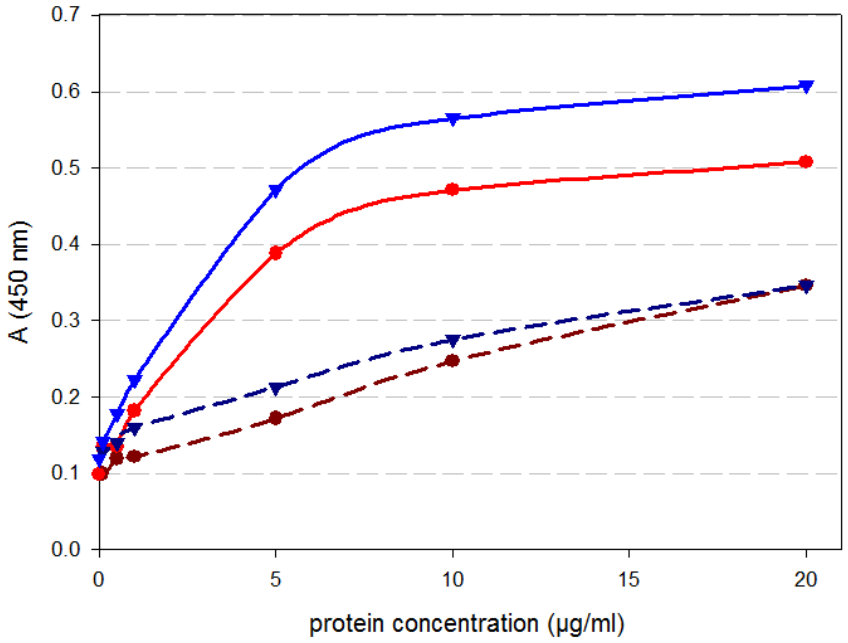

Figure 4-45. Absorbance at 450 nm for different concentrations of negative control (dashed lines) and HER-2 (straight lines) after blocking with 1 % milk (red) or 5% BSA (blue).

4.9.4 Influence of CHAPS in ELISA test

Because HER-2 is a membrane protein, a solubilization strategy involving the utilization of CHAPS as detergent was performed in the section 4.5. ELISA is known to be susceptible to a large number of interfering chemicals particularly in the case of direct ELISA where the protein is directly coated on the micro-titter plate well. For this reason the effect of CHAPS on ELISA performance should be tested. For this, two different batches of HER-2 producing *A. adeninivorans* G1212/YRC102-6H-HER-2 were cultivated and the recombinant protein was purified via His-tag either with or without CHAPS in the buffer. After imidazole removal via gel filtration, the elution fractions were recovered in PBS with or without CHAPS. The same procedure was performed with two batches of negative *A. adeninivorans* G1212/YRC102 strains in order to obtain consistent negative controls. These two fractions were coated on micro-titter plates and ELISA test was performed. The results of this experiment can be observed in Figure 4-46 where Western blot analysis of the four purification procedures can be seen. The positive control consists of a purified HER-2 obtained in a precedent purification without CHAPS and serves as reference band. They show a band at 185 kDa only in the

case when *A. adeninivorans* G1212/YRC102-6H-HER-2 was cultivated. It is difficult to assess by Western blot which of the purification led to a higher yield of HER-2 but as the positive control was the same for four Western blots, it can be supposed that the elution fraction with CHAPS contains more receptor as its band is stronger than the band of the positive control whereas it's the inverse situation when no CHAPS was included in the buffers.

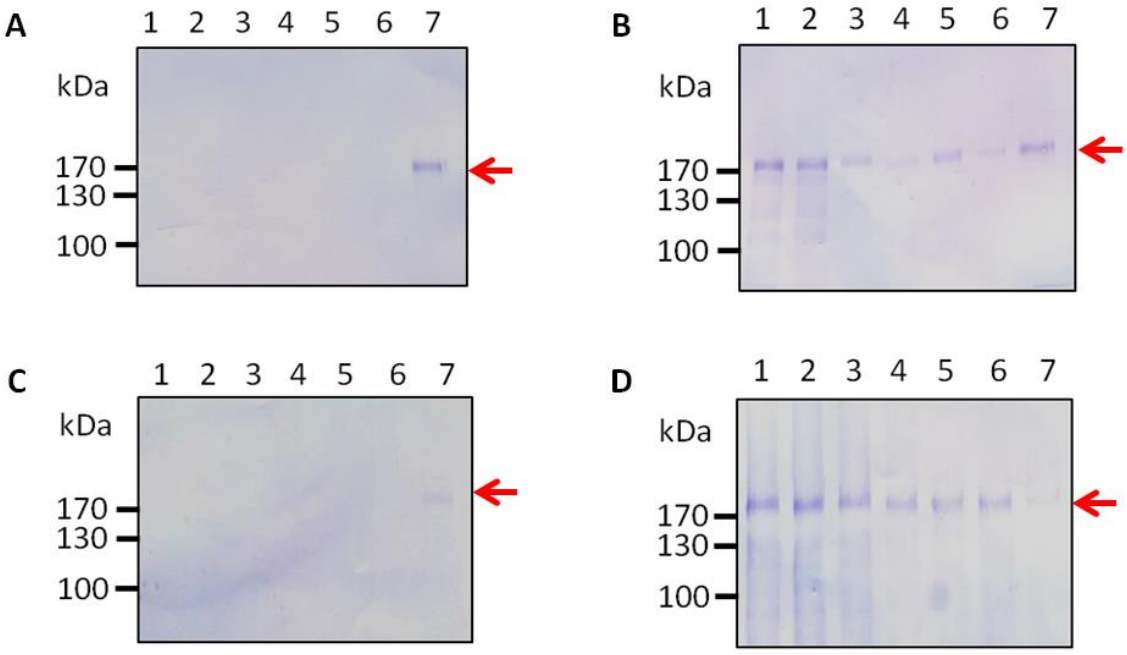

Figure 4-46. Western blot analysis of the purification process for A. adeninivorans G1212/YRC102 (A and C) and G1212/YRC102-6H-HER-2 (B and D) with no detergent (A and B) and with CHAPS (C and D). 1: raw extract, 2: flow-through, 3: wash fraction 1, 4: wash fraction 2, 5: elution fraction 1, 6: elution fraction 2, 7: positive control. The red arrow represents the position of HER-2.

The results obtained after the ELISA test and presented in Figure 4-47 show an increasing signal with increasing protein concentration only when the receptor purified without detergent was coated in the wells of the micro-titter plate. The presence of 1% CHAPS in the buffer seems to prevent any binding of the receptor thus leading to a signal similar to the negative control.

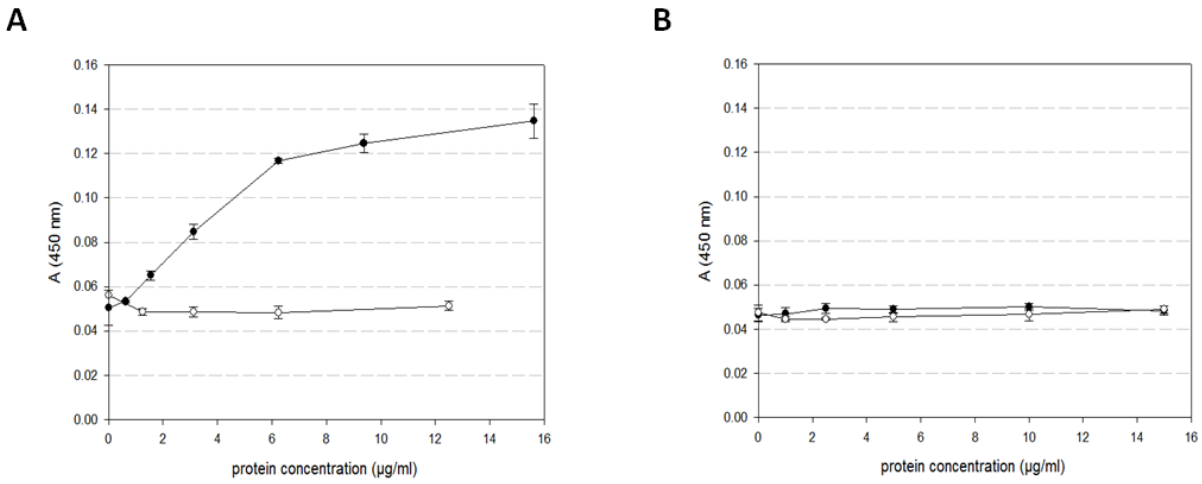

Figure 4-47. Absorbance at 450 nm for different concentrations of elution fraction of the negative control A. adeninivorans G1212/YRC102 (white dots) and purified HER-2 from A. adeninivorans G1212/YRC102-6H-HER-2 (black dots) after purification without CHAPS (A) and with CHAPS (B).

4.10 HER-2 detection by Surface Plasmon Resonance (SPR)

4.10.1 Binding of antibody-rich rabbit serum to immobilized HER-2

To test whether the rabbit serum containing polyclonal antibody directed against HER-2 could be used in a SPR-biosensor, it was first decided to immobilize the receptor and use the antibody as analyte. For this, the chip was functionalized with dithiobis-NTA in four different channels and nickel sulfate solution was used for chelating the carboxyl groups. After that, an elution fraction containing the affinity purified HER-2 from G1212/YRC102-6H-HER-2 was allowed to bind on the chip and the SPR signal was recorded. The chip profile of this protein immobilization can be seen in Figure 4-48. The four channels are identifiable with SPR signals reaching 40 whereas the background signal stays approximately by 15. It is to note that one channel only reach 27, but the fact that the three other present very similar values indicates that this particular low signal is probably due to a problem for this channel only.

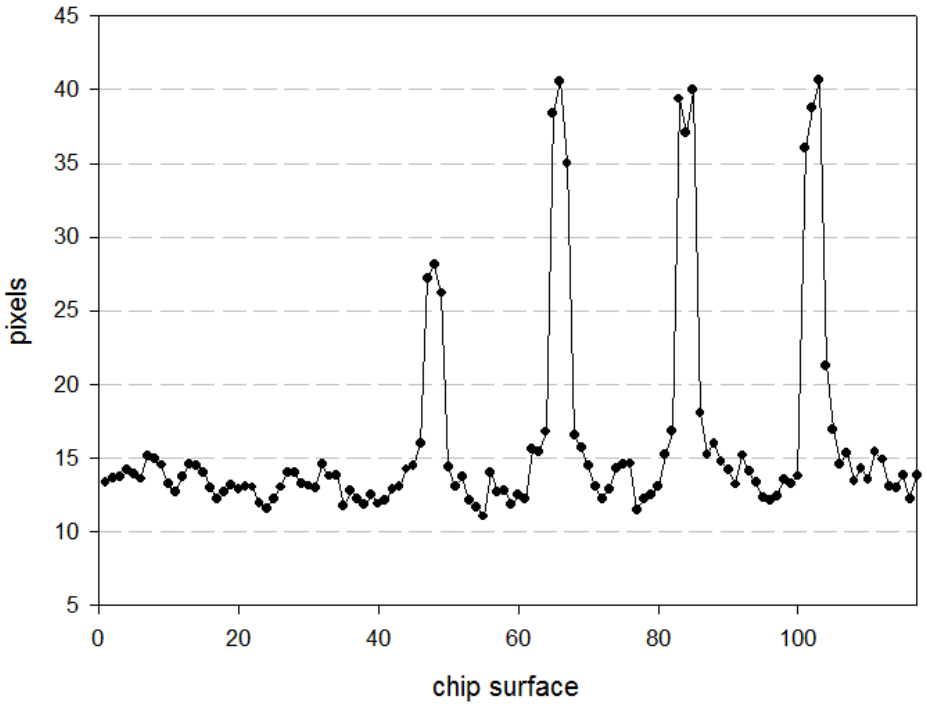

Figure 4-48. Chip profile after immobilization of HER-2 on four functionalized channels of the chip. The chip was first immobilized with dithiobis-NTA at positions 43, 62, 81 and 103.

After immobilization of HER-2 to the gold chip, three increasing antibody concentrations were applied sequentially. The sensograms resulting from this experiment can be observed in Figure 4-49.B and shows an increase of the signal only after the injection of the 1:100 dilution of polyclonal antibody. This result is confirmed by the SPR profile presented in Figure 4-49.A where all three dilutions are plotted on the same chip profile. For the 1:10000 dilution, the signal stays near to 0 for all positions of the chip. After the 1:1000 dilution, the background signal reaches 5 and no significant increase of SPR signal in the protein immobilized channels can be seen even though a small signal can be supposed at the positions 102 and 82. In the case of the 1: 100 dilution, a background signal of approximately 17 can be observed and a raise of signal reaching 30 occurs in the four positions where HER-2 is present. As it was noted that the channel at position 42 showed a smaller protein immobilization signal as the other three, the same observation can be made for this experiment because the first peak only reach a signal value of 25. These results and observations indicate that HER-2 can be detected with the rabbit serum containing anti-HER-2 antibodies.

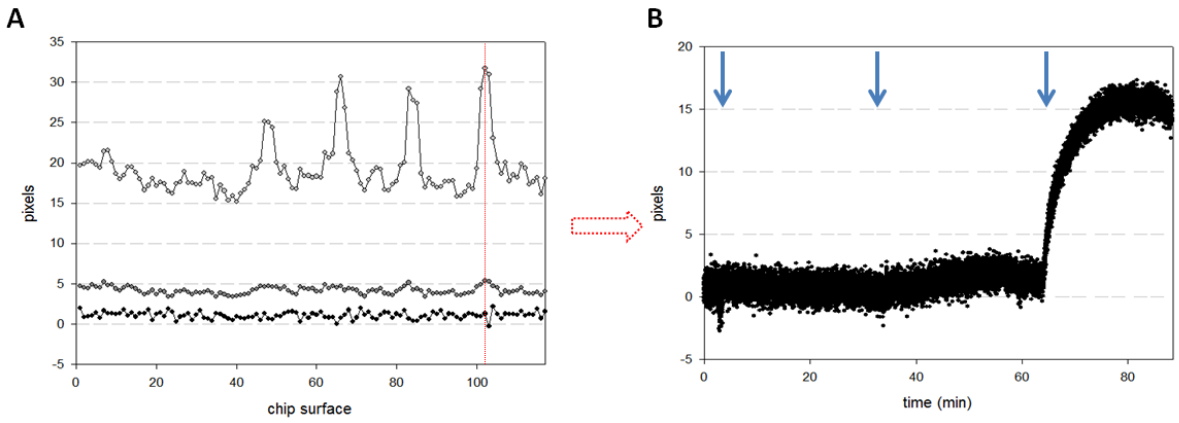

Figure 4-49. (A) Chip profile after the injection of anti-HER-2 antibody at 1:10000 (black dots), 1:1000 (dark grey dots) and 1: 100 (grey dots) dilution. The dashed red line corresponds to the position of the chip where the sensogram (B) was recorded. Blue arrows on the sensogram mark the injection time of the three analytes.

4.10.2 Binding of commercial polyclonal antibody to the immobilized HER-2

The same type of experiment was conducted with the commercial polyclonal antibody as analyte. Purified HER-2 from G1212/YRC102-6H-HER-2 was immobilized via His-tag chelation in six different channels of a chip and the chip profile of this immobilization can be observed in Figure 4-50. A signal at approximately 80 Pixels for the six positions can be observed.

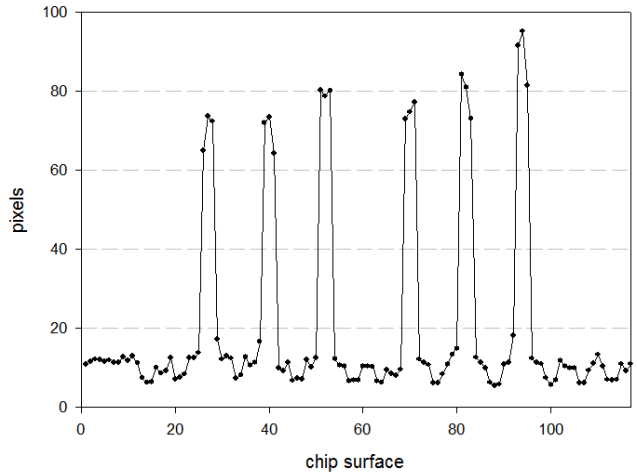

Figure 4-50. Chip profile after immobilization of HER-2 on four functionalized channels of the chip.

After that, two different concentrations (1 µg/ml and 3 µg/ml) of antibody were allowed to flow over the chip and the sensograms and chip profile were recorded. These diagrams are presented respectively in Figure 4-51.A and B. The sensogram of the position 92 shows a decrease of the SPR signal once the analyte is injected for both concentrations. This can be confirmed by the chip profile where negative signals can be observed at the positions were protein was immobilized. It is also to note that increasing the concentration of antibody makes the signal even more negative and that the nonfunctionnalized surfaces present a normal weak positive signal. This negative signal can be explained by the removal of the protein from the chip either due to other molecules in the antibody

solution or because of the position of the antibody epitope. Even though this antibody recognizes an amino acid sequence within the C-terminal intracellular part of HER-2, the protein secondary or tertiary structure could present this sequence next to the N-terminal sequence and then the binding of antibody can interfere with the chelation of the His-tag. Put all together, these results indicate that the commercial polyclonal antibody is not suited for this experiment as it removes the protein from the chip.

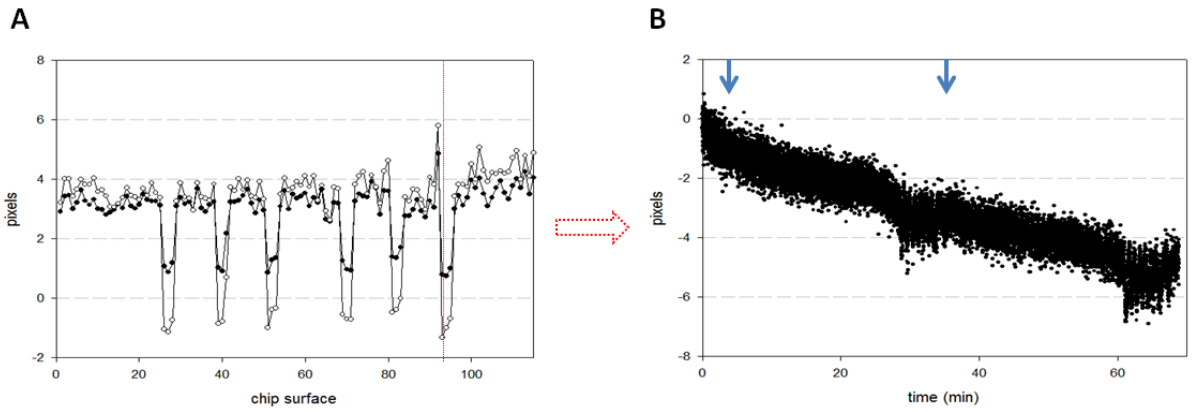

Figure 4-51. (A) Chip profile after the injection of anti-HER-2 antibody at 1 µg/ml (black dots) and 3µg/ml (white dots). The dashed red line corresponds to the position of the chip where the sensogram (B) was recorded. Blue arrows on the sensogram mark the injection time of the two analytes.

4.10.3 Binding of HER-2 to immobilized antibody

As the main strategy for HER-2 detection is the immobilization of antibody, three of them were tested in this experiment. For this, a chip was separated in two equal parts: one part was immobilized with the desired antibody and the other part with a control antibody to obtain a reference surface. The immobilization was performed by hydrophobic interaction on the gold surface and the three antibodies were: the serum from immunized rabbit, a commercial polyclonal antibody and a commercial monoclonal antibody. To ensure a real control, the reference surfaces were consisting in an antibody-containing rabbit serum, a commercial polyclonal antibody and a commercial monoclonal antibody at the same concentrations and directed against different proteins than HER-2. The results of this experiment are presented in Figure 4-52. Here, the three sensograms are showing the evolution of the SPR signal for the three immobilized antibodies after subtraction of the control surface. The monoclonal anti-HER-2 antibody is the only suited for immobilization on gold chip as only this treatment can cause a rise in the SPR signal once the HER-2 is injected.

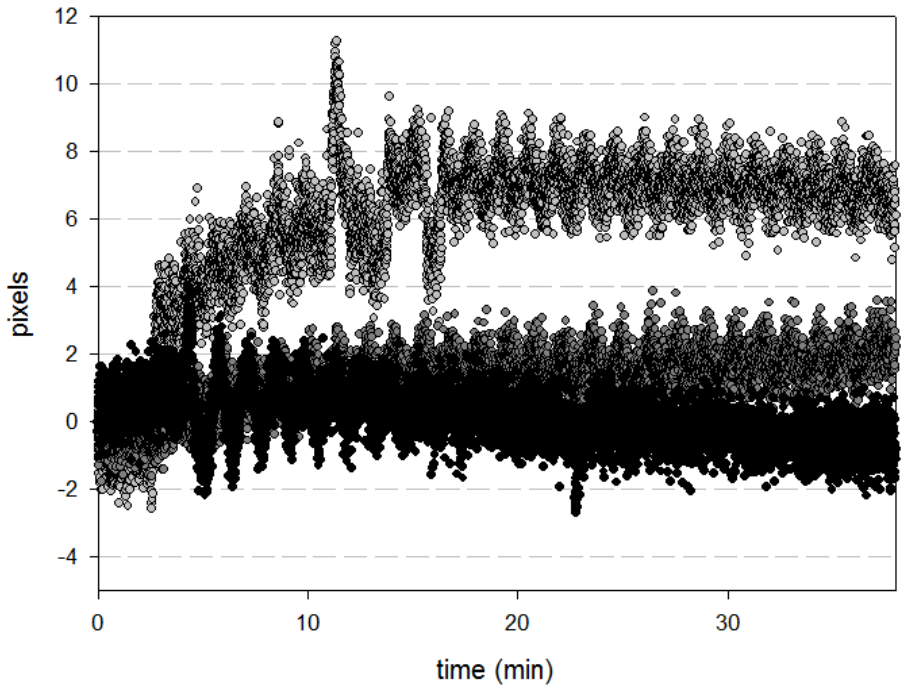

Figure 4-52. Sensograms after the injection of purified HER-2 on immobilized anti-HER-2 rich rabbit serum (black dots), commercial polyclonal antibody (dark grey dots) and monoclonal antibody (grey dots) after subtraction of the control surface.

4.10.4 Specificity of the interaction

To see if the interaction HER-2/antibody is specific, another experiment was performed. The commercial monoclonal antibody was immobilized on a chip by hydrophobic interaction at two different dilutions (1:100 and 1:10) together with a control surface consisting of blocked bare gold. The analyte consisted in a His-tag purification elution fraction of a *A. adeninivorans* G1212/YRC102 negative strain at a concentration of 5.5 µg/ml. After that, a second analyte, a His-tag purification elution fraction from G1212/YRC102-6H-HER-2 at a concentration of 5.5 µg/ml, was allowed to flow over the same chip. The sensograms of this experiment are presented in the Figure 4-53.A and B for the first and the second analyte. The sensograms after first analyte injection show no visible signal increase for both dilutions thus indicating a successful blocking of the chip. After the second analyte injection, a clear rise in the SPR signal can be observed for both immobilized antibodies with the less diluted giving the highest signal. The binding curve for both surfaces is following an exponential rise to the maximum shape typical for a 1:1 interaction. These results are confirmed by the Figure 4-53.C showing the signal value for the three surfaces after injection of both analytes (control analyte in purple and HER-2 in blue). Standard deviation calculations show significant differences between the signal for the control surface and both immobilized surfaces only in the case where the HER-2 containing analyte was used.

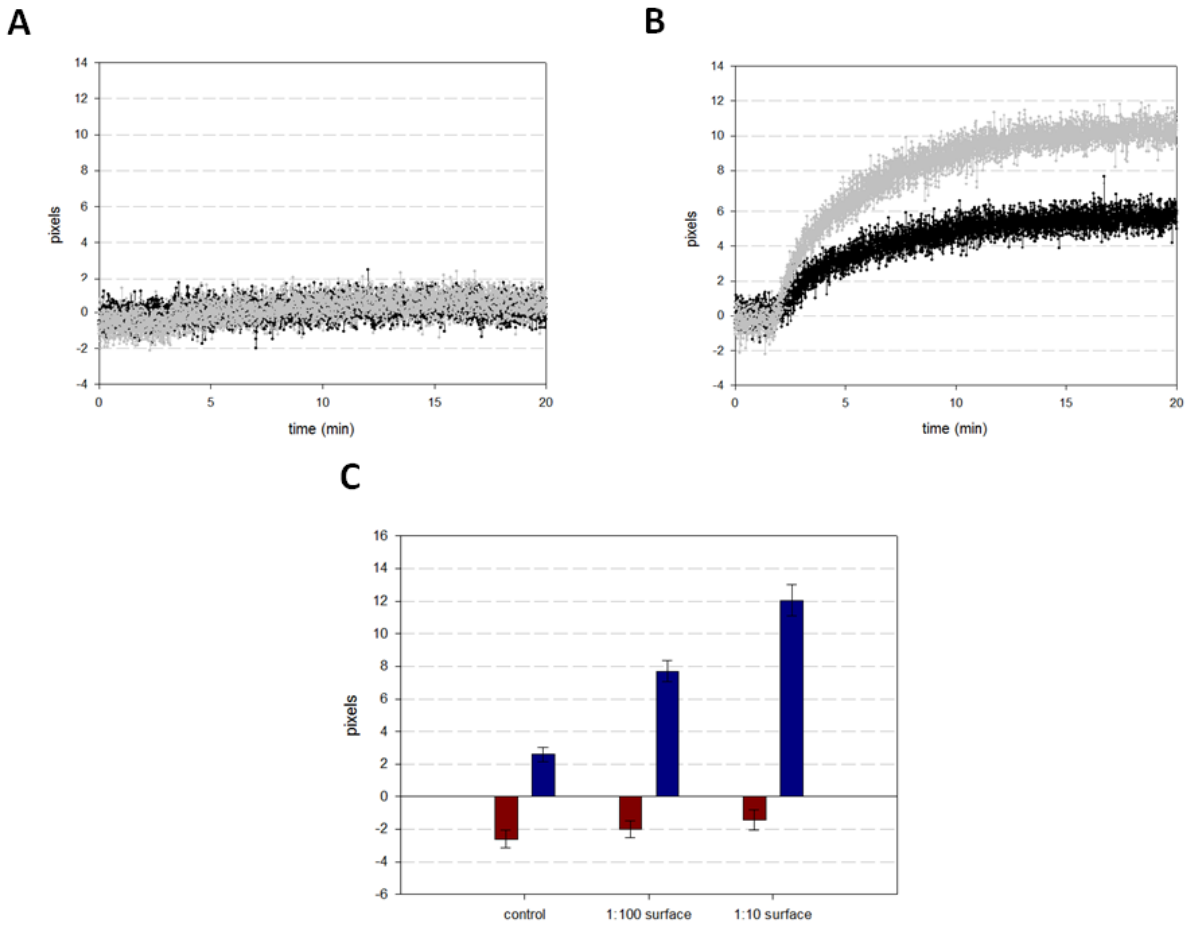

Figure 4-53. Sensograms of the binding of G1212/YRC102 elution fraction (A) and G1212/YRC102-6H-HER-2 elution fraction (B) to immobilized monoclonal anti-HER-2 antibody at 1:100 (black dots) and 1:10 (grey dots) dilutions.(C): SPR signal values for the different surfaces after injection of the negative control (red) and the purified HER-2 (blue). Errors bars represent the standard deviation for 15 positions of the chip.

4.10.5 Different strategies for antibody immobilization

Immobilization of antibody on gold surface can be performed via four main strategies by using linking agents or not. The hydrophobic interaction via sulfur-gold bond was already tested in the previous experiments and will act as reference in order to state if a new strategy is better or not. The three linking agents utilized for this experiments are protein G, protein A and dithiobis(sulfosuccinimidylpropionate) (DTSSP). Three chips were then separated in three parts by the help of hydrophobic barrier and the three surfaces were always prepared following the same scheme showed in Figure 4-54.

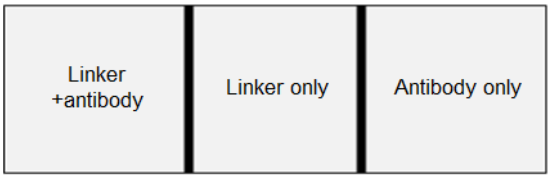

Figure 4-54. Partition of a SPR chip for immobilization strategies experiment

As all linker are different, different protocols were utilized for linker immobilization. Protein A and protein G were immobilized via hydrophobic interaction at a concentration of respectively 1 mg/ml and 0.1 mg/ml. DTSSP is the soluble form of the Lomant's reagent also called dithiobis(succinimidyl propionate) (DSP) which can make a gold-sulfur bond with the surface of the chip and possesses a functional group able to react with proteins primary amines to form amide bond. This cross linker was used at a concentration of 5 nM. For all linkers, the incubation was performed for 1 hour and was followed by a 3 h blocking step with concentrated BSA solution. The SPR signal values for at least 20 positions of each surface are presented in Figure 4-55. It is interesting to note that the signal obtained with linker immobilized surface was never superior to the one obtained with antibody alone. This indicates that none of the linker could improve the detection of HER-2. The particularly low values obtained in the case of protein G even when the antibody alone was immobilized can be explained by the fact that a another batch of affinity purified HER-2 was utilized for this experiment.

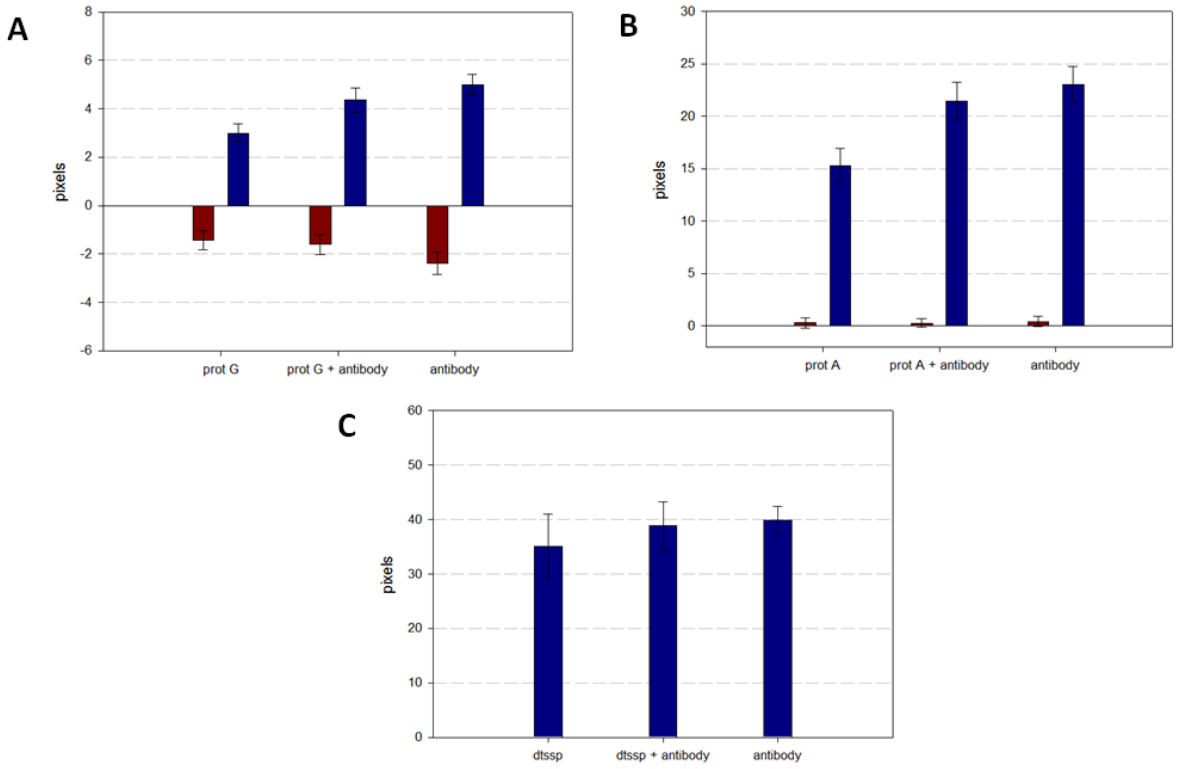

Figure 4-55. SPR signal after binding of negative control (red) and purified HER-2 (dark blue) on immobilized antibody with protein G strategy (A), protein A strategy (B) and DTSSP (C).

4.11 Protein extraction from paraffin-embedded breast tissue samples

4.11.1 Removal of paraffin and first extraction test

Even though protocols exist in order to handle paraffin-embedded tissues, most of the time they are followed by DNA extraction as it is one of the most utilized methods by pathologists. Adaptation for protein extraction was reported but stays very case dependent. In the case of the HER-2 protein, the particular length and the presence of a transmembrane domain are additional challenges. In order to extract this protein, several approaches were then tested but not all of them will be showed here as many of them failed. Two different protocols were used for the removal of paraffin from the tissue sample. One uses n-octane and methanol and the other protocol uses xylenes as major solvent. Both protocols are described in detail in the Material and Methods (section 3.11.2 and 3.11.3). Tissue samples were from two different breast tumors, one described as negative (0) and the other as positive (3+) for HER-2 overexpression by immunohistochemistry. All four samples were then submitted to the antigen retrieval (AR) technique by boiling the material at 100 °C for 20 minutes in a Tris-HCl based buffer at pH=7. After that, the samples were loaded on two SDS-PAA gels for either Coomassie staining or Western blot analysis. The results of breast cancer tissue sample protein extraction are visible in Figure 4-56 together with yeast cell extracts producing the recombinant HER-2 (G1212/YRC102-6H-HER-2) and producing no recombinant protein (G1212/YRC102) as positive and negative controls.

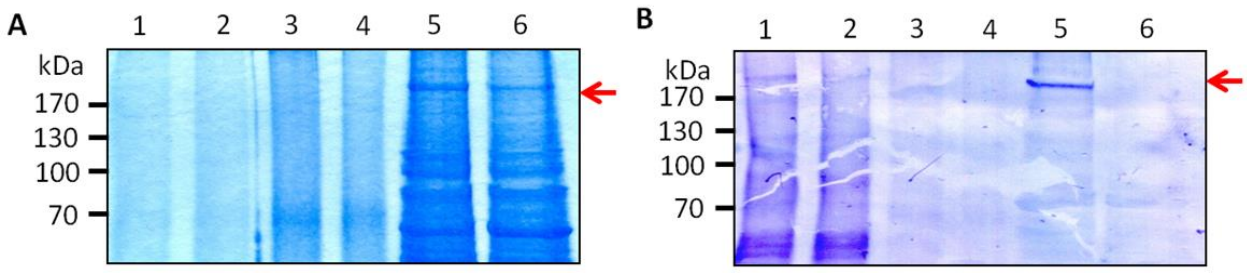

Figure 4-56. Coomassie staining (A) and Western blot analysis (B) of the protein extraction from breast cancer tissue sample after paraffin removal with n-octane (1 and 3) or xylene (2 and 4). 1 and 2: samples classified as 3+ by immunohistochemistry, 3 and 4: samples classified as 0 by immunohistochemistry.5: positive control, 6: negative control. The red arrow represents the position of the HER-2 protein. Total protein concentrations of the sample: 1=1,052 µg/ml, 2=820 µg/ml, 3=1,496 µg/ml, and 4=1,187µg/ml.

The Coomassie staining is showing smearing bands for the four samples and more bands for the controls from yeast extract. The two breast samples described as negative for HER-2 overexpression show higher band intensity than the two other, meaning that more proteins have been extracted from the tissue in this case. This result is confirmed by protein concentration determinations indicated in the label of the figure and which show higher protein concentrations for the extractions performed with the negative breast samples. In the Western blot, a band corresponding to the HER-2 protein can be observed for the positive control and this band is absent in the negative control. Additionally, bands at the same molecular mass can only be observed in both samples corresponding to the positive tissue. The whole lane shows also a background signal and additional

bands at lower molecular mass which are strong indicators for protein degradation. In comparison, both lanes corresponding to the negative sample show very faint reaction with the HER-2 specific antibody and no band can be observed. By looking more in detail, it can be seen that for both samples paraffin removal with octane led to higher protein concentrations and a stronger band intensity corresponding to the HER-2 in the Western blot. These results show that it is possible to detect the presence of the HER-2 after extraction from paraffin embedded tissue and that paraffin removal with n-octane shows the best results.

4.11.2 HER-2 overexpression determination for different samples

In order to see if Western blot can be used for distinguish between different HER-2 overexpression patterns, four tumor tissues were submitted to the same extraction protocol presented previously (with n-octane as paraffin removing solvent) and loaded on a SDS-PAA gel for Western blot analysis. As the most critical point in HER-2 overexpression determination is to differentiate between the cases 1+, 2+ and 3+, it was decided to process the samples 7, 10, 11 and 17 which have been determined respectively as positive, 1+, negative and positive by immunohistochemistry. Additionally, the same samples were submitted to two different anti-HER-2 antibodies for Western blot in order to compare their efficiency. The results and the Western blot analyses can be seen in Figure 4-57.

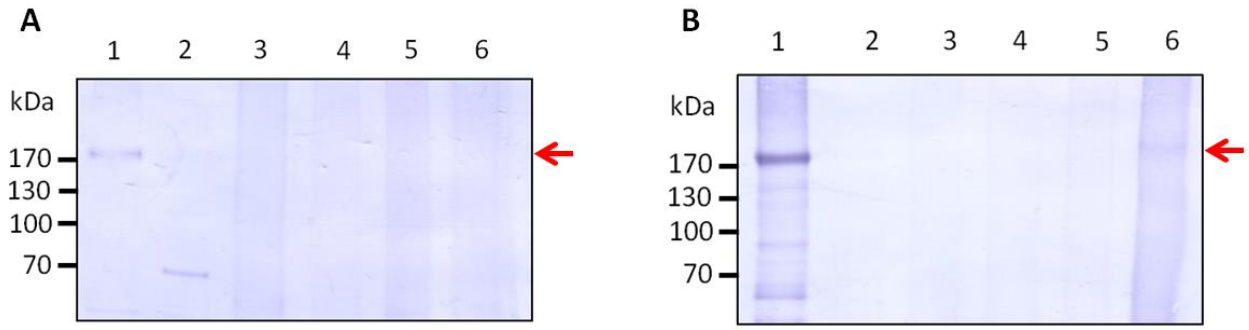

Figure 4-57. Western analysis of the breast cancer tissue sample protein extraction with anti-HER-2 rich rabbit serum (A) and commercial anti-HER-2 antibody (B) as detection antibody. The red arrow represents the position of the HER-2.1: positive control (G1212-YRC102-6H-HER-2), 2: negative control (G1212/YRC102), 3: sample n°11, 4: sample n°10, 5: sample n°7 and 6: sample n°17.

The Western blot using polyclonal anti-HER-2 antibody from rabbit serum is showing low intensity band corresponding to HER-2 in the positive control as well as one band in the negative control and background signal in almost all tissue samples. This indicates that this particular antibody is not particularly suited for this experiment. In the Western blot using commercial anti-HER-2 antibody as detection antibody, a band is present in the positive control and in the tissue sample n°17. For the three other samples, it is impossible to detect any visible difference between them as they all show very faint bands at 185 kDa. These results confirm that strong HER-2 overexpression in breast tissue can be detected by Western blot with the developed protocol but the technique is not sensitive enough to detect critical cases involving lower levels of receptors.

4.12 Direct comparison between ELISA and SPR for HER-2 detection

It was demonstrated in the precedent sections that both ELISA and SPR are suitable for the detection of recombinant HER-2 produced in yeast. Because the purity of elution fraction cannot be assessed with certitude and because each purification leads to high variability in elution fraction composition, it was decided to conduct an experiment in which a sufficient amount of HER-2 was produced and purified and then submitted to both detection methods. The recombinant protein was produced in *A. adeninivorans* (G1212/YRC102-6H-HER-2) and the purification via His-tag was performed without adding CHAPS. As negative control, an elution fraction of the negative *A. adeninivorans* strain (G1212/YRC102) was handled with exactly the same procedure.

- **Response curve via ELISA**

The obtained elution fractions were coated on micro-titter plate wells and ELISA was performed according to the optimized protocol described in the precedent sections. The signals are presented in Figure 4-58 with black and white dots representing respectively the purified HER-2 and the negative control. The first observation that can be made from these results is that the signals are in general relatively low in comparison to the signals obtained during ELISA optimization even though this experiment was performed with the optimized protocol. There is no clear explanation for this beside the fact that the purification was probably less efficient this time and led to a lower yield of HER-2 in comparison to the receptor obtained during ELISA optimization. Even though these signals are low, the very low standard deviation obtained for each concentration ensures enough sensitivity in order to exploit the results. It can be seen than the signal is rising only in the case where the HER-2 is immobilized and follow a sigmoidal shape materialized by the fit curve. The maximum signal is reached at a concentration of about 10 µg/ml and a linear part of the curve can be seen for concentrations between 0.01 and 10 µg/ml. The signal of the negative control stays always under 0.06 units and doesn't show a significant increase. Consistent with the accepted standards, the limit of quantification was calculated to be the mean value plus 10 times the standard deviation of the blank [225]. Then, a limit of quantification of 7.8 ng/ml was obtained.

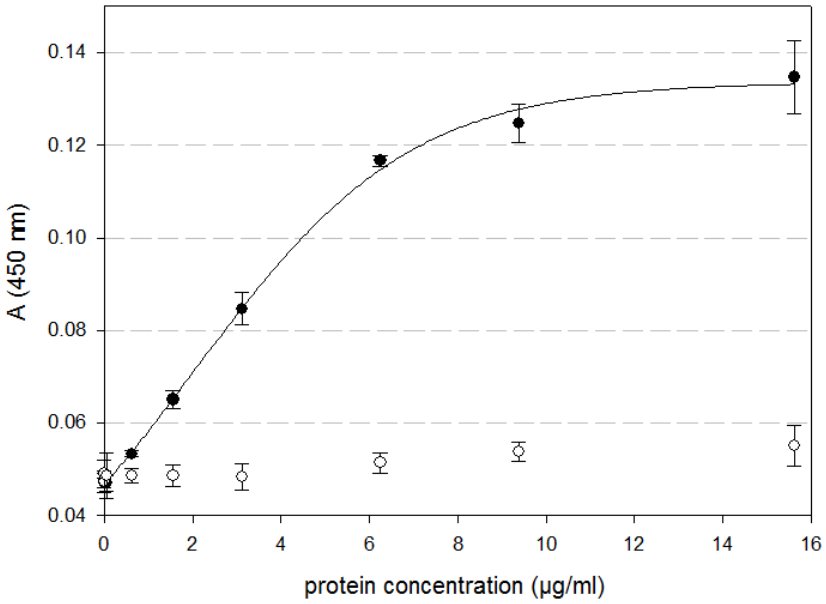

Figure 4-58. Absorbance at 450 nm for different concentration of immobilized HER-2 (black dots) and negative control (white dots). The fit curve following a sigmoidal shape was calculated by Sigmaplot. Error bars represent the standard deviation and all measurements were performed in triplicate.

- **Response curve by SPR**

The same type of experiment was performed with the already optimized SPR protocol. For this, several HER-2 concentrations were allowed to flow over SPR-chips immobilized with the same concentration of monoclonal antibody (1:10). The signal for each concentration was recorded and the signal of the control surface was subtracted in order to remove the effect of unspecific binding. In order to ensure that the signal obtained is not due to other proteins present in elution fraction, a negative control was applied to identically functionalized chips at exactly the same concentrations. The results of this experiment for both HER-2 containing analyte and the negative control are presented in Figure 4-59. No significant increase in the SPR signal can be detected when *A. adeninivorans* G1212/YRC-102 elution fraction is the analyte (Figure 4-59.A). Only at 50 µg/ml does the signal of the functionalized surface show a higher value than the control surface but the difference is small and doesn't exceed 2 pixels. However at 5 µg/ml, the binding of *A. adeninivorans* G1212/YRC102-6H-HER-2 elution fraction to the immobilized surface is significantly higher than the control surface signal (Figure 4-59.B). The negative values that can be seen are probably caused by a chip-dependent loss of blocking during the sample injection, leading to a smaller SPR signal at the end of the experiment because the analyte could not attach to the surface.

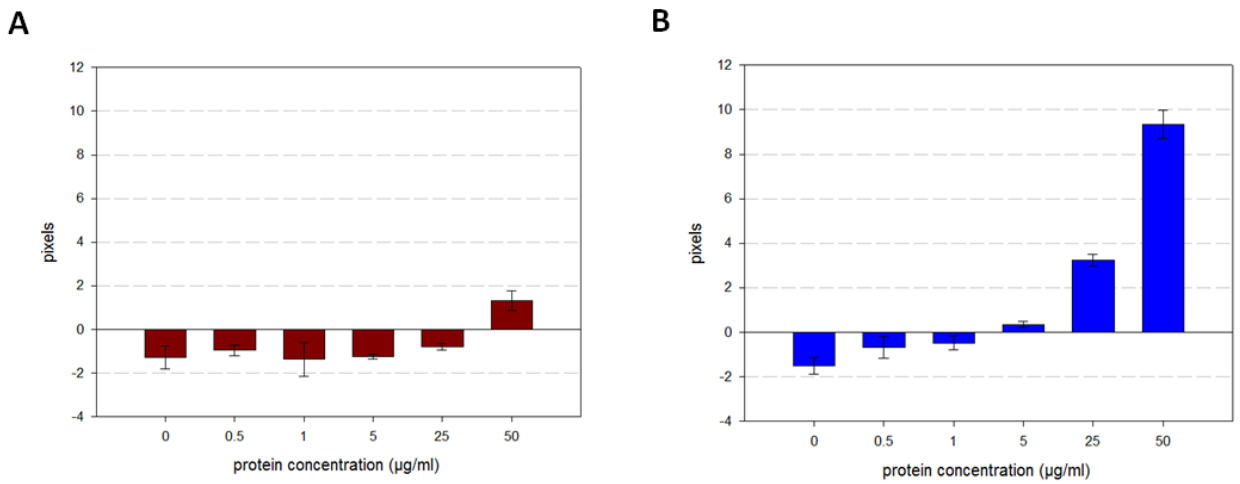

Figure 4-59. SPR signal value after injection of different concentrations of G1212/YRC102 elution fraction (A) and G1212/YRC102-6H-HER-2 elution fraction (B). All signal values were taken at the equilibrium. The error bars represent the standard deviation.

Even though the signal is clearly higher in the case of G1212-YRC-6H-HER-2 elution fraction, it should be noted that an unspecific binding occurs at 50 µg/mL for the control analyte thus meaning that the same may occur for the receptor containing analyte. To obtain a calibration curve which only relies on specific binding, the SPR signal values of the negative control were subtracted to the values of the HER-2 elution fraction and plotted in Figure 4-60. A clear dependence can be seen between the signal and the elution fraction concentration from 0.5 to 50 µg/ml following a linear shape. Using a same definition as for the precedent section, a limit of quantification of 760 ng/ml was calculated.

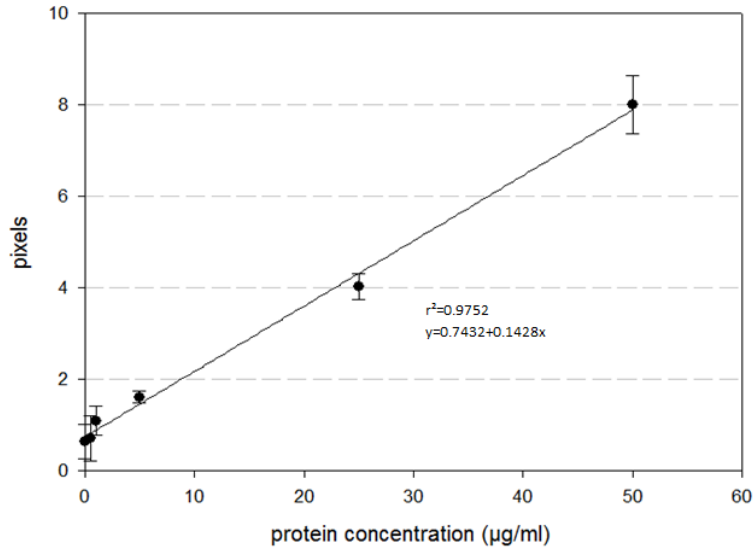

Figure 4-60. SPR signal value for different concentration of purified HER-2 after subtraction of the unspecific binding signal. The fit curve following a linear shape was calculated by Sigmaplot (parameters on the diagram).

4.13 First test of real samples by the SPR biosensor

Breast cancer sample were applied to antibody functionalized SPR-chips to see whether or not the developed biosensor is able to detect the presence of natural occurring HER-2. For this, two samples were processed according to the protocol in section 4.11.1. One, the sample n°3, is described as positive for HER-2 overexpression (3+) and the other, the sample n°2, didn't show any overexpression of this receptor by immunohistochemistry. After extraction, the total protein concentration was measured by Bio-Rad protein assay and then diluted to a final concentration for both sample of 0.5 mg/ml which is in the detectable range of the ELISA and the SPR detection method. The two tissue samples were then subjected to Western blot and the result of this analysis can be observed in Figure 4-61. There, a band corresponding to the HER-2 at 185 kDa can be observed in the positive control (recombinant protein from *A. adeninivorans* G1212/YRC102-6H-HER-2) and also in the sample n°3. The band is very faint und hardly distinguishable but it is due to the bad quality of the membrane. No band or smear can be observed where the sample n°2 was applied.

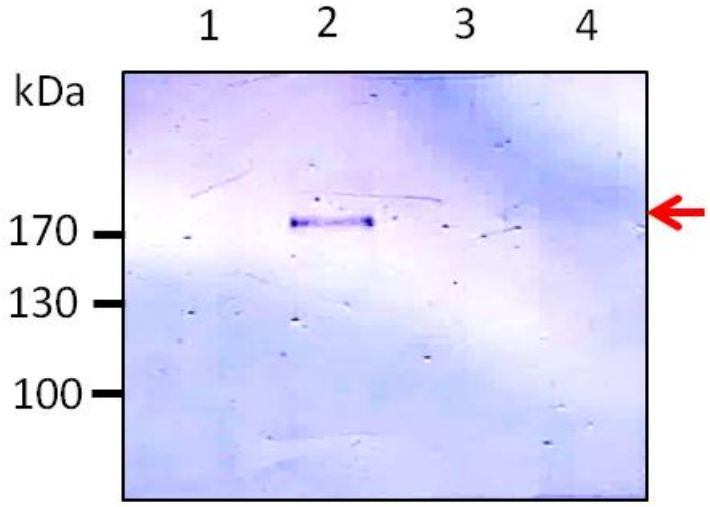

Figure 4-61. Western blot analysis of the extracted tissue samples. 1: negative control (G1212/YRC102), 2: positive control (G1212/YRC102-6H-HER-2), 3: sample n°2, 4: sample n°3. The red arrow represents the position of the HER-2 protein.

The extracted proteins were then submitted to both ELISA and SPR detection. In the ELISA, the absorbance signal of the two samples was measured and the results are presented in Figure 4-62. If there is a similar difference interval between the positive and negative control as in the precedent sections, no significant difference can be seen between the two samples.

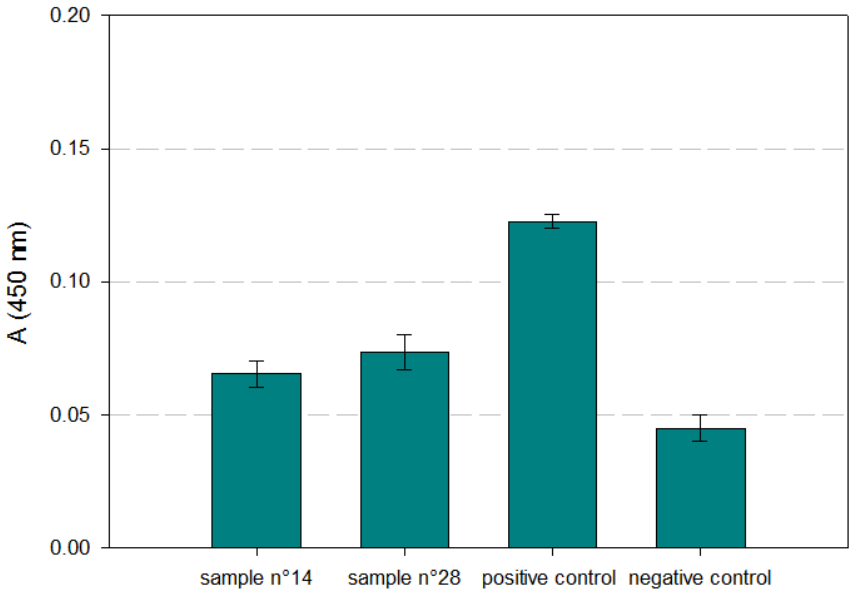

Figure 4-62. Absorbance at 450 nm for the two breast cancer tissue sample protein extracts, for the positive control (purified HER-2 from G1212/YRC102-6H-HER-2) and for the negative control (elution fraction from G1212/YRC102). Error bar represent the standard deviation and all measurements were performed in triplicate.

For SPR experiments, two separate chips were prepared by immobilizing an optimal concentration of monoclonal anti-HER-2 antibody and three increasing concentrations of breast cancer tissue protein extract were injected sequentially. Finally, a last analyte consisting in recombinant HER-2 produced in *A. adeninivorans* G1212/YRC102-6H-HER-2 was injected in order to compare the two chips. The sensograms resulting from these injections can be observed in Figure 4-63. There the blue dots represent the signal of the sample n°3 and the red dots represent the sample n°2. It can be seen that for a total protein concentration of 10 µg/ml, a clear rising signal can only be seen in the case of the sample n°3 which was described as positive for HER-2 overexpression by immunohistochemistry. The sample n°2 shows also a rise but is not reaching the same high values. At 50 µg/mL, both sample show a rise in the signal but the comportment of sample n°2 is non-conventional as it drops one minute after the injection. It is to note that every position of the surface of the chip followed this signal shape. At 500 µg/ml and for the positive control, no difference can be detected between the two samples which indicate that too high concentrations lead to high unspecific binding and that the both chips were identically functionalized. The sensograms obtained when the purified HER-2 from G1212/YRC102-6H-HER-2 was used as analyte (Figure 4-63.D) shows that both chips were identically functionalized as the signal for both chips are very similar.

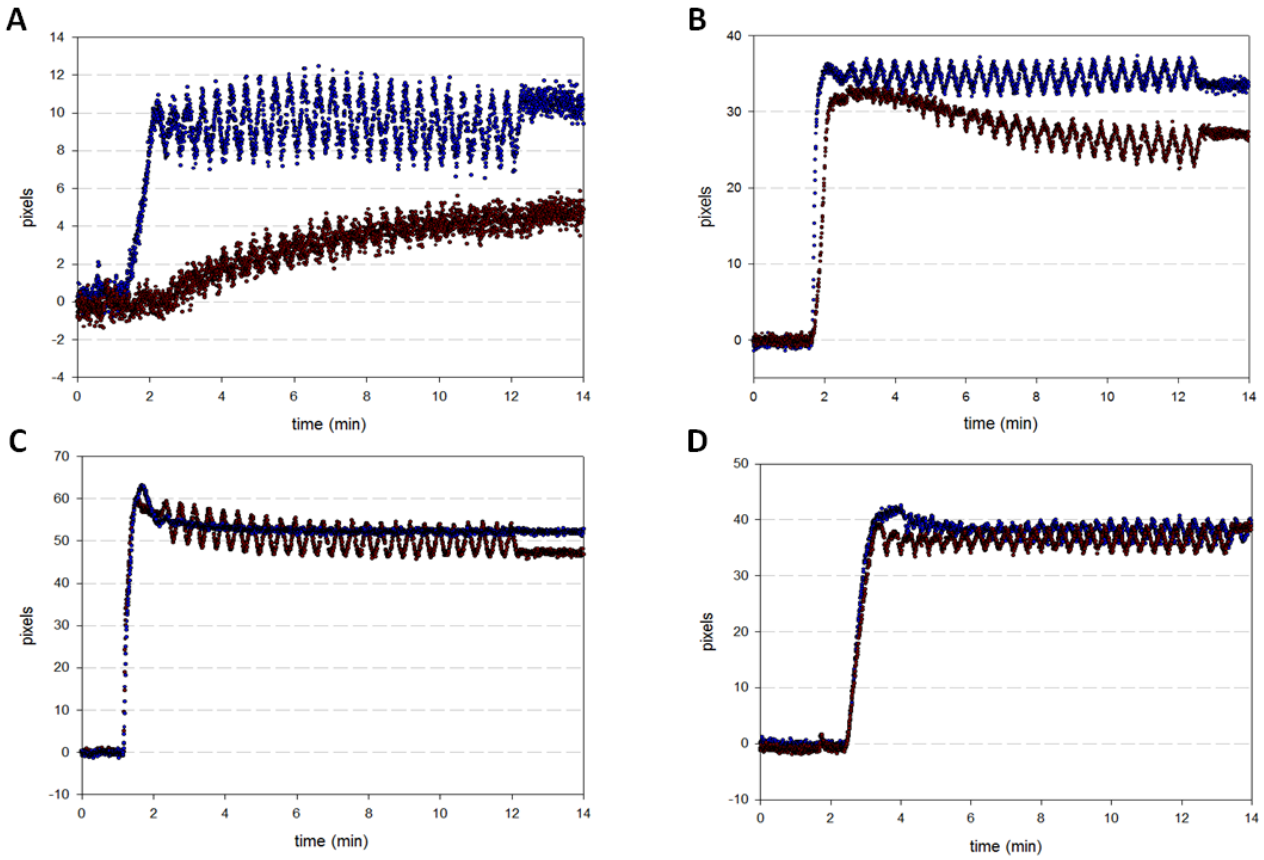

Figure 4-63. Sensograms of the binding on immobilized antibody of sample n°2 (red) and sample n°3 (blue) with concentrations of 10 µg/ml (A), 50 µg/ml (B), 500 µg/ml (C). (D): Binding of recombinant purified HER-2 to the same chips.

The results are summarized in the Figure 4-64 where at least 15 positions of each chip were selected to ensure statistically robustness. From this experiment, it can be stated that a difference in binding was observed between one sample showing high level of HER-2 protein and one sample showing low level of HER-2 protein when the total protein concentration stays in the range of 10 µg/ml.

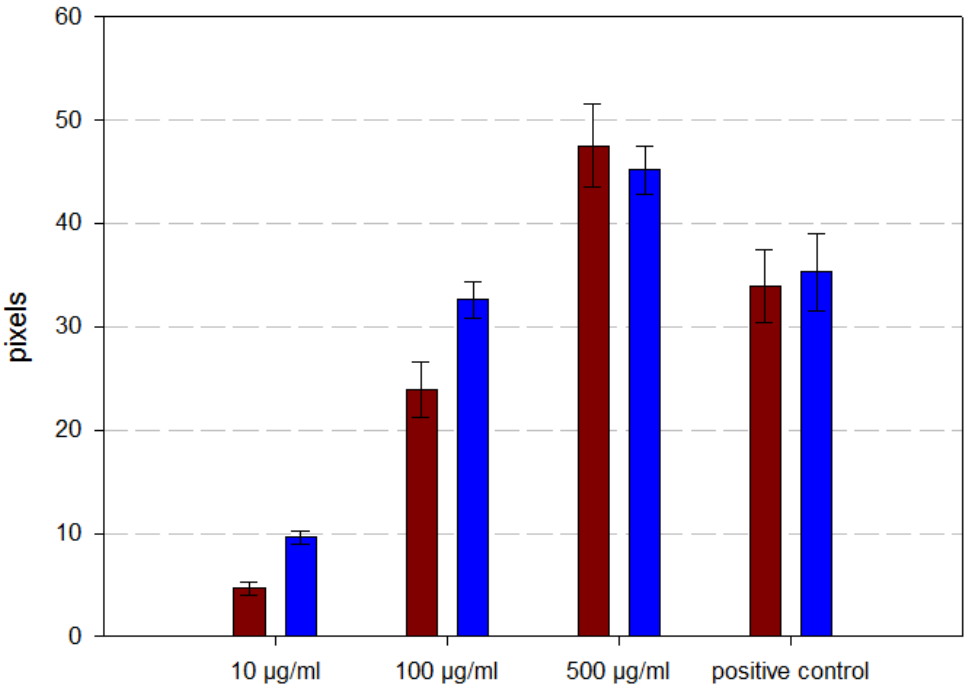

Figure 4-64. SPR signal values for the sample n°2 (red) and the sample n°3 (blue) when injected at three different concentrations (10µg/ml, 50 µg/ml and 500 µg/ml). Last two columns show the signal obtained after final injection of purified HER-2 from G1212/YRC102-6H-HER-2 to the chip treated with sample n°2 (red) and to the chip treated to the sample n°3 (blue). Error bars represent the standard deviation.

5 Discussion

5.1 Cloning and expression of *HER-2* and *hPR* genes in *A. adeninivorans*

The gene integration of the *hPR* and the *HER-2* genes in *A. adeninivorans* was performed by using the Xplor®2 expression platform. Based on one unique plasmid, Xplor2 allows the use of YIC (Yeast Integrative expression Cassettes) or YRC (Yeast rDNA integrative expression Cassettes) by alternative linearization of the plasmid by two different restriction enzymes. In this work, only results obtained via YRCs are presented even though transformation of *A. adeninivorans* yeast strain G1212 with the YICs variants was also successfully performed. No difference in transformation efficiency could be observed as for each transformation event, more than 100 transformants were obtained with YRCs and YICs. Unfortunately, it was materially impossible to use both YICs and YRCs transformants in the next steps as it would have doubled the time necessary to perform all experiments so it was decided to continue the work with the YRCs transformants only. In a previous study, Böer et al. [182] already compared the performance of YRCs and YICs for expression of heterologous gene with the final conclusion that YICs often present the best expression level but, due to variation between individual transformants, also advices to test 50 yeast colonies from each transformation event. After performing this test, it was interesting to note that in the case of the progesterone receptor and HER-2, transformation of G1212 by YRCs led most of the time to the strongest band intensity in Western blot analysis. In some cases (for transformation with YRC102-hPR, YRC102-hPR-6H and YRC102-HER-2-6H), no significant difference in band intensities between YRCs and YICs can be observed and therefore, in these particular cases, the YRCs were favored in order to have all transformants obtained by YRC transformation. The use of Western blot as only selection process could lead to misinterpretation as it is considered as a semi-quantitative method and as the color development can be dependent on many external factors. Unfortunately, it was at this particular moment the only rapid method for transformants screening available as the other thinkable detection method, namely ELISA, would have taken time to be established and become reliable. Moreover, the use of two different antibodies directed against the particular receptor (one commercial and one obtained by rabbit immunization) ensured a reasonable confidence as the chosen transformant was always exhibiting high band intensity in both treatments.

One major result that can be extracted from screening experiments in *A. adeninivorans* is that both proteins without His-tag showed low expression in comparison to the variants with His-tag at one side of the protein. In order to explain this result, it can be supposed that the presence of the His-tag could improve the production of the recombinant protein, increase the solubility of the receptor or decrease its degradation susceptibility. More experiments would be necessary in order to clarify this point. For example, the integration of less than six histidines could be performed and the protein expression of these transformants could be compared to the expression of the hexahistidine transformants. As the production of recombinant protein without His-tag was not crucial for the next steps of the work but only performed as a positive control, no further experiments were performed with the recombinant proteins without His-tag.

5.2 Cloning and expression of *HER-2* and *hPR* genes in *H. polymorpha*

For the production of recombinant protein in *H. polymorpha*, it was decided to use the already described pFPMT121 vector which has been used in several occasions [188, 196]. Being a methylotrophic yeast, *H. polymorpha* offers the possibility to use either the *MOX* or the *FMD* methanol-inducible promoters. In this work, the *FMD* promoter was favored as it is known to assure high expression level. In the case of HER-2, it is to note that lower intensity bands can be observed in the case of the transformation with pFPMT121-HER-2-6H in comparison to the transformation with pFPMT121-6H-HER-2. Additionally, thirty of the fifty tested transformants obtained by pFPMT121-HER-2-6H transformation were showing no band in Western blot analysis. As the production of recombinant protein is induced by the presence of methanol in the medium and because this production is time-dependent, an experiment was performed where culture samples were taken at regular time points and tested by Western blot but no increase in the protein production could be observed. The fact that this phenomenon was not observed in the case of *A. adeninivorans* transformants is also an indication that the cause of this low production of HER-2 by the pFPMT121-HER-2-6H transformants is to search in the *H. polymorpha* specific metabolism. The cause of low protein production can be searched at the gene expression level, the addressing level or related to the solubility or degradation of the protein in *H. polymorpha* but additional experiments will be necessary to determine it.

5.3 HER-2 localization and solubility

In human cells, the HER-2 protein is located in the cytoplasmic membrane where it can form heterodimers with other members of the EGFR family [117]. Such addressing to the membrane is a complicate mechanism implying the presence of a signal peptide which should be later removed, the possibility of post-translational events including disulfide-bond formation, acylation, prenylation, phosphorylation and certain types of O- and N-linked glycosylation as well as the presence in the membrane of certain types of lipids. Fortunately, yeast as an eukaryote is known to perform post-translational modification in a similar way than higher eukaryotes and even though some lipids like cholesterols are not synthetized by yeasts, it was shown that the predominant lipid in yeast, ergosterol, can mimic the effect of cholesterol [226] and ensures the stability of several membrane protein in yeasts. The localization of the HER-2 protein was performed only in *A. adeninivorans* as the production of this protein is under the strong constitutive *TEF1* promoter. This means that no specific attention should be given to the culture age in order to observe enough protein. In the case of *H. polymorpha*, the protein production is controlled by the inducible *FMD* promoter and is so very dependent on the culture age and medium composition. In order to perform localization experiments, samples at several time points would have been necessary, which would have be more time-consuming.

The first strategy envisaged in order to localize HER-2 in *A. adeninivorans* was transmission force microscopy of gold-labeled receptors. In this technique, antibodies directed against HER-2 are allowed to bind in fixed yeast samples and then, modified gold particles can bind to the IgG Fc region of these antibodies for visualization under microscope. This detection method is nowadays

well-established and has already been successfully utilized in the case of recombinant protein production in *A. adeninivorans* [227, 228]. Practically, a 1 ml volume of both *A. adeninivorans* G1212/YRC102-6H-HER-2 and G1212/YRC102 (negative control) were immobilized by high-pressure freezing and hybridization of three different antibodies raised against the HER-2 protein to the fixed material was performed. After addition of the gold particles, the presence of the receptor was determined with a Tecnai G^2 Sphera transmission electron microscope at 120 kV. Unfortunately, no strong difference between G1212/YRC102-6H-HER-2 and G1212/YRC102 strains could be observed as they both showed sparse gold labeling in the whole cells and no specific labeling at the cytoplasmic membrane. In some pictures, intense labeling could be seen at the membrane of some organelles in the G1212/YRC102-6H-HER-2 strain but it was restricted to a very low percentage of the cells.

It was then decided to use cell components ultracentrifugation in order to determine the position of the recombinant HER-2 in *A. adeninivorans*. As it can be observed in the corresponding results section, no HER-2 can be observed in the final supernatant and most of the intact protein is to find in the third pellet. This pellet which was formed after a centrifugation at 30,000 g consists generally in yeast of membrane vesicles and organelles other than mitochondrion and peroxisomes. As already mentioned, the absence of *A. adeninivorans* specific antibodies for cell components localization makes any more precise comments on the pellet composition impossible. These antibodies are only available for some yeast species like *S. cerevisiae* and showed unspecific binding in the case of *A. adeninivorans*. These results are sufficient to affirm that the recombinant HER-2 is located in the membrane even without the presence of some sterols like cholesterol. Moreover, these results can also potentially explain the observations made during transmission electron microscope analysis. It can be indeed considered that a membrane protein will be more affected or destroyed by the high pressure freezing process as a cytoplasmic protein. Some membrane proteins were already successfully detected by electron force microscopy but after a fixation step involving the preparation of plasma sheets [229, 230]. This specific tissue fixation should be tested in order to observe the HER-2 in yeast cells by transmission force microscopy.

As it was shown that the receptor HER-2 is located in the membrane fraction of the yeast *A. adeninivorans*, a solubilization strategy has been considered. Most of the purification strategies are indeed working with soluble proteins and purification will be obligatory in order to develop a functional and efficient biosensor. For this part, particular attention was given to the work of White et al. [221] who studied the solubility of hundreds of recombinant membrane proteins in yeast and found correlations between the expression level of proteins and some protein properties like size, number of transmembrane segments, GRAVY (GRand AVerage of hYdropathy) score, pI (isoelectric point) and the percentage of aromatic residues in the protein. Some of the major findings are that:

- ➔ a proteins with a molecular mass superior to 80 kDa showed often low expression than protein with lower molecular masses,
- ➔ a negative GRAVY score seems to positively affect the protein production,
- ➔ a pI under 8 seems to positively affect the protein production,
- ➔ a percentage of aromatic amino acids in the total protein inferior to 16 % leads to a higher protein production than proteins with more than 16 % of aromatic amino acids.

The HER-2 protein, with a theoretical molecular mass of 137.91 kDa, a GRAVY score of -0.247, a pI of 5.58 and a percentage of aromatic amino acids of 9.8% seems to be a good candidate for protein production in yeast except for its heavy molecular mass (all these values were calculated with ExPASy software in the UniProt database [231]).

It is known that the efficiency of a membrane-bound protein extraction is highly dependent on the particular detergent used, hence a screening procedure with a broad range of commonly used detergents. All of them are strict non-ionic detergents or zwitterionic detergents and have been used for membrane protein solubilization. The chemical formula of the eight tested detergents is indicated in the Table 5-1. Octylglucoside, Hecameg and decylmaltoside share similar hydrophilic segments with an oxygen-rich hexacyclic ring but have different chain lengths and hydrophobic regions. Triton X-100 and Nonidet-P40 have very similar chemical structure only differentiated by the length of the carbon chain. Digitonin have completely different structure than the other non-ionic detergent. The two last used detergents, CHAPS and LDAO, are zwitterionic detergents and were selected because they have been shown to be efficient for membrane protein solubilization. As it was often the case in previous works, solubilization with zwitterionic detergents in general and CHAPS in particular shows the best efficiency. On the opposite, most of the non-ionic detergents were unable to perform satisfying solubilization of this membrane protein except triton X-100 which was efficient but with strong protein degradation. These results show that, even though the charge of the detergent is an important parameter, the molecular composition of the detergent has also a great impact on the solubilization efficiency. Even though these results are in accordance with previous studies, they show the necessity to perform a detergent screening assay when considering the production of a membrane protein in yeast as detergents can have a great impact on protein solubilization.

Table 5-1. Chemical formula of the utilized detergents. All graphical representations are from the Chemspider database (www.chemspider.com/chemical structure) or from Sigma-Aldrich website for Dmal (www.sigmaaldrich.com/catalog/product/sigma/d7658).

Class	Detergent name	Chemical formula
non ionic	triton X-100	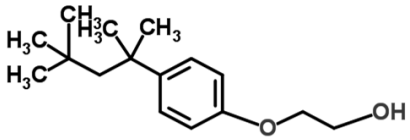
	Hecameg	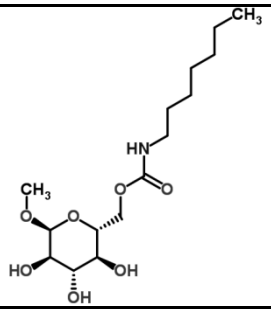

	Dmal	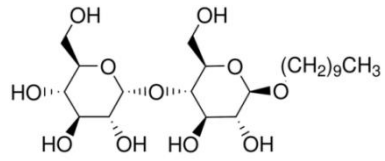
	OG	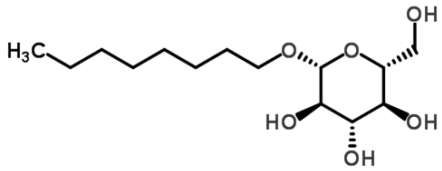
	digitonin	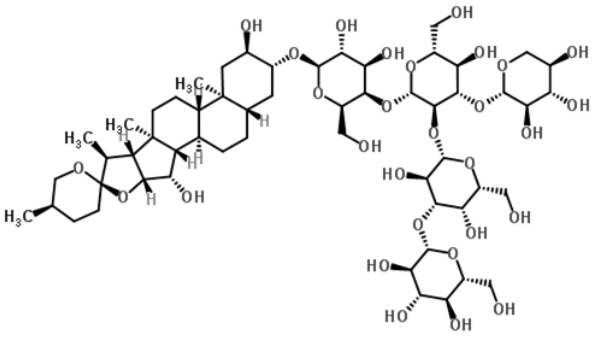
	NP-40	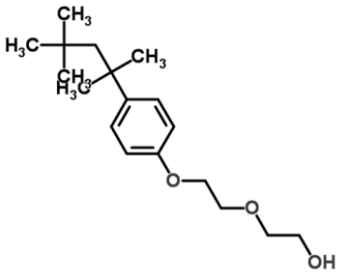
zwitterionic		
	CHAPS	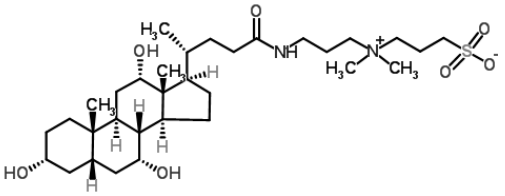
	LDAO	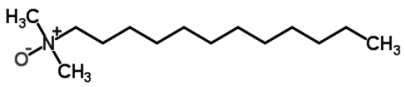

5.4 Batch cultivation experiments of transformed strains

Batch cultivation was performed in order to control and optimize the cultivation conditions and so produce the highest protein quantity possible for the next steps. For these experiments, the hypothesis was made that the position of the His-tag has a minimal influence on the growth behavior of the yeast. That's the reason why cultivation in batch reactor was only considered for the strains *A. adeninivorans* G1212/YRC102-6H-hPR, G1212/YRC-6H-HER-2, *H. polymorpha* RB11/pFPMT121-6H-hPR and RB11/pFPMT121-6H-HER-2.

In *A. adeninivorans* G1212, it is interesting to note that the specific growth rate is largely inferior when the strain was transformed to produce the HER-2 than when it was transformed to produce the progesterone receptor. One explanation could be that the production of the HER-2 requires more energy than the production of the progesterone receptor and this extra energy need will slow the yeast growth. Others indications about this phenomenon are given by the Western blot results. HER-2 production can be detected after 12 h culture together with all the other proteins which correspond to the beginning of the exponential growth phase. It is then constantly produced until the end of the culture. The comportment of the *A. adeninivorans* G1212/YRC102-6H-hPR strain is significantly different as the production of recombinant protein starts already after 3 h but only for one hour. The yeast strain will enter its exponential growth phase only after 5 h. This could mean that the yeast will first produce the recombinant protein and then digest it to use its amino acids for growth purposes instead of recombinant protein production. When the growth phase is over after approximately 10 h, the production of recombinant progesterone receptor starts again. Put all together, these results can be explain by two models of recombinant protein production for the two strains. In the case of G1212/YRC102-6H-hPR, the yeast will mainly use the available glucose substrate for growth and will then produce the recombinant protein when not enough substrate will be left in the medium. In the case of G1212/YRC102-6H-HER-2, the yeast will produce the recombinant protein continuously from the beginning of its growth phase thus using a part of the glucose substrate for non-growth purposes which will lead to a lower specific growth rate. In order to confirm these hypotheses, an interesting experiment could be to use an inducible promoter instead of the *TEF1* constitutive promoter. In a culture medium without the inducer, both yeast transformed with the *HER-2* gene and the *hPR* gene containing vector should show similar growth rate as no recombinant protein production should occur. In inducer containing medium, determination of the specific growth rate will indicate if the hypotheses are verified or not.

Concerning the experiments with *H. polymorpha* transformants, the two shifts in medium complicate the determination of growth behavior as the experiment last more than 160 h (more than six days). It is then not possible to take as many samples as necessary as it will reduce the culture volume dramatically at the end of the experiment. The diagrams presented in the results section are showing again that *H. polymorpha* RB11/pFPMT121-6H-HER-2 grow slowly than the RB11/pFPMT121-6H-hPR strain in YPD but reach then higher culture density after the first shift in minimal medium with glycerol. Both proteins are produced after the first shift and stay constantly produced until the end of the experiment. Apparition of degradation products is clearly visible and indicates that the shortest cultivation time possible will lead to the highest yield of preserved recombinant proteins. The fact that recombinant protein production starts in glycerol-based

medium whereas *FMD* promoter is a methanol induced promoter was already described in some publications for *H. polymorpha*. In many cases, derepression with glycerol seems to be more efficient than methanol induction [232, 233].
It is to note that for these cultivation experiments with *H. polymorpha*, two shifts were performed and YPD was utilized as first medium. This does not follow the recommendations of Suckow et al. [199] which rather consider the cultivation in a fed batch mode with glycerol and methanol and advice to avoid glucose. This is because glucose can be involved in Crabtree-effect which can lead to ethanol production and therefore growth hindrance of the yeast. The work of Suckow [198] also report maximum cell densities of 3-6 g/l and recombinant protein production after 20-30 h. During the experiments with *H. polymorpha* RB11/pFPMT121-6H-hPR and RB11/pFPMT121-6H-HER-2, if the recombinant protein production started after 25 h, higher cell densities could be obtained by rather using dextrose containing YPD during the first 24 h. This choice was made because cultivation tests in flasks showed that, in the present case, using YPD at the beginning of the cultivation allowed higher yield in recombinant protein production than by using glycerol during the whole cultivation. It would have been interesting to compare the cultivation with or without this first YPD cultivation step but it couldn't be realized during the time of this work.
These batch cultivations were from a great interest as they pointed some similarities between the productions of recombinant protein in two different yeast species as in both cases, yeast transformed to produce HER-2 showed a slower growth in comparison to the yeast transformed to produce the progesterone receptor. Differences between the two recombinant protein production platforms could also be observed as *A. adeninivorans* showed higher cell density and a more convenient cultivation procedure than *H. polymorpha*. The absence of medium shift - even though the experiment showed that *H. polymorpha* only need one medium shift instead of two- and the fact that cells can be harvested after less than 10 h in *A. adeninivorans* are indeed crucial advantages.

5.5 Purification of HER-2 and the progesterone receptor

Both the HER-2 and the progesterone receptor can be successfully produced in *A. adeninivorans* and *H. polymorpha* with His-tag either at the N or the C-terminus but a purification step is necessary in order to use them for biosensor development. Protein purification is a very wide field and more and more techniques were presented and optimized in the last decades [234]. Among all protein purification strategies, three main categories should be mentioned: the size exclusion purification, the separation based on charge and the affinity purification. Each of them has also several variants which broaden the possibilities of protein separation. It would have been impossible to test all of them for each particular protein produced in both yeast species, that's why the purifications in this work were performed by His-tag affinity [235], ion exchange [236] and MACRO-PREP ceramic hydroxyapatite [237]. It was decided to mainly focus on the His-tag affinity purification because His-tag integration on both ends of the receptors was successfully performed and because this method shows generally good purification efficiency without intensive experimental efforts [235]. Due to the routine use of this affinity chromatography, new upgrades of this technique have been developed thus increasing its performance. It consists in new resin chemistries (TED, NTA, IDA among others) or

in the use of alternative metals than nickel for protein chelation like cobalt. Ion exchange and MACRO-PREP ceramic hydroxyapatite can also be modified in order to optimize their efficiencies and even if some variants were tested, it would have been impossible to test each protocol for each produced protein.

- Progesterone receptor purification

In regards to the future applications of both developed biosensors, it was early considered that the His-tag position would be a major issue in the case of the progesterone receptor as it can have a great impact on the ligand binding capacities of the protein. The LBD being at the C-terminus of the receptor, integration of 6 histidine amino acids in this region could lead to an alternative tertiary structure and so impact the binding capacity of the protein. It was then decided to perform the purification of progesterone receptor with His-tag at the N and at the C terminus. As these both proteins have been successfully produced in *A. adeninivorans* and *H. polymorpha*, a total of four variants of the receptor were investigated for purification by affinity chromatography. The first conclusion that can be made from the affinity purification results is that for each variant, a band corresponding to the progesterone receptor can be observed in the elution fraction by Western blot thus indicating a purification effect. Moreover, a band in the Coomassie staining at the same molecular mass can be observed for all proteins except for the C-tagged receptor produced in *H. polymorpha*. For this particular variant, the weak recombinant production observed in the expression studies was confirmed as only a faint progesterone receptor band can be seen in the raw extract by Western blot. This weak expression led to a low concentration of total proteins in the elution fraction but also to a strong enrichment effect as the band in this fraction show a higher intensity than the band in raw extract.

Two other general conclusions from these experiments can also be made. First, the purity of the elution fraction cannot reach high value as many other proteins are co-eluted in the elution fraction together with the recombinant protein and secondly, the yield can be increased as an important proportion of the recombinant protein can be seen in the flow-through fractions or the wash fractions. This indicates a competition between the recombinant protein and the yeast own proteins for the chelation with nickel ions immobilized on the resin. Even though the presence of six consecutive histidines in the protein sequence has a very low probability to exist in native yeast proteins and should therefore procure a determining advantage for the recombinant receptor, its low expression level allows other proteins with a lower affinity but a higher expression level to occupy some of the binding sites of the column. In order to overcome this issue, some alternative strategies have been documented like the use of a deca-histidine tag [238], the increase of the resin volume or the use of an imidazole gradient in the elution process [239]. If the first alternative would have been interesting to test, it also would have required new cloning, transformation and screening of the transformants for receptor production and were therefore unrealizable as it would have taken additional time. The other alternatives also prove their efficiency in some cases but would not have led to a dramatic increase in elution fraction purity.

That is the reason why it was decided to perform a two-step purification in order to obtain an elution fraction containing the progesterone receptor with the highest purity possible. Generally, the first step of a multistep purification consists in a non-affinity chromatography which will result in very low purification degree but also in a maximum recombinant protein recovery. The first choice

was the weak anion exchanger DEAE as it was intensively utilized in many studies with success. Unfortunately for the present case, this technique was not successful as no recombinant protein could be detected in any of the elution fraction. The second choice for the first step of purification was then consisting of ceramic MACRO-PREP hydroxyapatite as this particular resin showed excellent results for different types of proteins [237, 240-244]. The fact that not only one type of binding but at least three interactions are occurring between the column surface and the proteins is a decisive advantage. Elution of the immobilized proteins with a phosphate gradient led to an expected low purity of the elution fraction as many proteins can be seen in each of the elution fraction. The recombinant progesterone receptor could be detected by Western blot in 5 to 6 fractions which were pooled together and concentrated for the next step of the purification. The Coomassie staining also shows that many other proteins are eluted before or after these elution fractions, thus leading to recombinant protein enrichment effect. After the subsequent affinity purification, a band in the Coomassie staining and in the Western blot analysis corresponding to the progesterone receptor could be detected. Additionally, no other strong bands can be seen in the Coomassie stained elution fraction, thus demonstrating the positive effect of two-step purification procedure. Improvement of the method can be achieved by increasing the stability of the protein as severe protein degradation could be observed in the Western blots performed during the experiment and increasing the culture volume.

- HER-2 purification

Concerning the recombinant HER-2 production, the most important parameter for the next analyses is the protein integrity as antibodies should be used in the developed biosensor to recognize both native and recombinant protein. With regards to this aspect, the position of the His-tag in the sequence is supposed to have a small impact. This explains why, by observing preliminary tests showing lower affinity purification efficiency for the C-tagged recombinant HER-2 than the N-tagged, it was decided to focus all purification experiments only on the N-tagged recombinant protein. It was not surprising to observe that the obtained purity degree in this case was lower than for the progesterone receptor as it is already known that high molecular mass and the presence of transmembrane domains are often decreasing the affinity purification efficiency. But it is also to note that each affinity purification variant was successful as a protein band corresponding to the HER-2 can be detected by Western blot when IDA, NTA and TED –based resins were used. If the purification of *A. adeninivorans* produced proteins and *H. polymorpha* produced proteins should be compared, a clear superiority of the first cited can be pointed as the Western blot describing the *H. polymorpha* proteins purification show weak signals in the elution fraction and large protein loss in the flow-through and wash fractions as well as no clear band in the Coomassie staining. In the case of *A. adeninivorans* produced proteins, a band in the Coomassie staining which correspond to the HER-2 can be detected in the cases of NTA and IDA together with other co-eluted proteins but not with TED resin where the elution fraction show very low total protein concentration. As for the progesterone receptor, two-steps purification strategy with the utilization of weak anion exchanger and ceramic MACRO-PREP hydroxyapatite were also tested but resulted in total protein loss after the application of protein lysate to the column. Even though separation of many proteins could be observed by Coomassie staining, no band corresponding to the receptor HER-2 could be observed in the Western blot of the elution fraction after DEAE anion exchange or ceramic hydroxyapatite

chromatography. Degradation products could be observed in some fractions, thus leading to the hypothesis that the membrane protein is not stable during the purification process. In order to solve this problem, other extraction buffers containing protective agents or different pH value were assayed but could not prevent the degradation of the receptor. Other strategies can be designed in order to perform a first purification before the affinity purification as for example size exclusion chromatography which will separate the proteins according to their molecular mass or cation exchanger ion chromatography. Unfortunately, these methods could not have been tested during the time of this work.

5.6 Progesterone receptor binding experiments

5.6.1 SPR assay for the determination of binding constants

As described in the Result section, the determination of the progesterone receptor/ligand binding constants is the results of some hypothesis and simplifications. These will now be examined in detail.

- The use of progesterone-BSA as ligand

The binding constants for a receptor/ligand interaction are always calculated towards the favorite ligand which is, in case of the progesterone receptor, the progesterone. Unfortunately, it is impossible to quantify the binding of free progesterone to the receptor without the help of a second ligand or without modifying the progesterone. That's why in this work, progesterone-BSA was used as the BSA part can be easily immobilized on the surface of the gold chip. But as one molecule BSA is conjugated with 5 to 10 molecules progesterone, it means that each molecule of progesterone-BSA can theoretically be involved in 1 to 10 interactions with the progesterone receptor. It becomes more complicated when the immobilization itself is considered. As no control is present during this step, the progesterone-BSA molecule can be immobilized in all possible positions and therefore the progesterone residues can be either free or unreachable for the receptor or a combination of both. Additionally, the ligand used in this study contained also 2-5 molecules FITC per molecule BSA. If this fluorescein conjugation has no interest for the present study, it should be also considered that its presence can interfere with the receptor/ligand binding. All these considerations can lead to the non-validity of the 1:1 interaction model chosen for the determination of binding constants.

- Absence of mass transport

To establish the binding model used in this study, it was also hypothesized that no mass transport was occurring. Mass transport is a phenomenon happening when a bulk solution containing the analyte (here the progesterone receptor) is injected in the chamber above the SPR chip. At the surface of the chip, the concentration of the analyte will not be immediately the same as in the rest of the solution because the analyte need to diffuse to the surface and this takes a certain time, dependent on a diffusion equation. This diffusion is highly dependent on the nature of the solution and of the nature of the chip surface [245]. This effect is mostly visible during the association or dissociation phases because the analyte concentration increase gradually in the chamber above the chip and if the diffusion time is very low, increasing of concentration will be limited by the diffusion time. This effect has been intensively studied in the case of the commercial SPR systems and recent

studies show that most of the SPR-experiments underestimate the effect of mass transport [246]. One of the most important factors increasing this effect is known to be the use of dextran matrix. Dextran matrix is a polymer surface immobilized on a gold chip which allows better immobilization of probe. When the user wants to use dextran matrix, it is advised to increase the flow rate of the experiment in order to decrease the mass transport effect. In the case of the present study, bare gold chip were used and ligand was immobilized without the help of any linker. This explains why the mass transport effect was neglected in this work.

- Rebinding of the ligand and dimerization

Rebinding of the ligand can occur and lead to non-validity of the 1:1 model. It is mainly visible when a high concentration of ligand is immobilized on the surface of the chip. This will be a particular high influence on the dissociation phase as the concentration of analyte should drop gradually to 0. If the receptor can rebind to the immobilized ligand, the shape of this dissociation phase will not follow the exponential decrease predicted by the model. As no parameter was determined by the use of the dissociation phase, the effect of rebinding was neglected in the case of the present experiment. Another point to consider is the fact that the progesterone receptor is known to dimerize upon binding with the progesterone. This will lead to the non-validity of the considered 1:1 interaction model as two progesterone receptor molecules will be binding to one molecule of progesterone. It is also known that this dimerization after binding to the steroid is only one part of a complex process and some other partners like heat shock protein are indispensable. As the progesterone receptor used in this experiment was purified, it is considered that no dimerization can occur as the other partners, and in particular the heat shock protein, are not present.

Even though these undesirable effects have been minimized, it is complicated to know if the model can still be used for this assay. To address this question, it was assumed that the progesterone receptor binding interaction is very similar to the estrogen receptor interaction. In the case of estrogen receptor, a similar SPR experiment was performed by Seifert et al. [247]. With a commercial SPR platform, they were able to calculate binding parameters for the interaction between a recombinant estrogen receptor α produced in yeast and an immobilized 17ß-estradiol-BSA ligand. This experiment is very similar to the experiment performed in this work because the estrogen receptor was also partially purified and because the ligand consisted in a BSA protein an which 5 to 10 moles of 17-β-estradiol were bound. Differences with the progesterone system are that the ligand was immobilized on gold surface with the help of a linker and that the experiments were performed with a Biacore instrument. They found a kd value of 1.05×10^{-5} s^{-1}, a ka value of 4.5 $M^{-1}s^{-1}$and a K_D value of 0.23 nM and compared these results with the available literature. As the values were similar, they stated that “the described biosensor set-up shows that the ER (estrogen receptor) binds 17ß-estradiol-BSA with high specificity and with similar binding characteristics known for free 17ß-estradiol. Therefore, 17ß-estradiol-BSA can be used as a coating conjugate for microwell plate receptor assay”. So, as no other SPR-experiments for determination of progesterone receptor binding parameters are available and as progesterone receptor and estrogen receptor have similar binding properties, it was assumed that the chosen model was suitable.

5.6.2 Comparison between the obtained binding constants values

Both ligand/receptor experiments performed in this work with the recombinant purified full-length progesterone receptor showed a clear binding signal thus indicating that the yeast-produced protein is active. In the developed ELRA as well as in the SPR format, the same approaches were utilized with immobilized progesterone-BSA ligand. Then, the binding of receptor to this ligand was quantified either label-free by SPR of with the help of an antibody in the case of ELRA. It gave a K_D value of 67.14 nM for SPR experiment and 6.28 nM for ELRA experiment. Both values are different, as expected for two completely different detection methods, but are also both low and thus showing a high affinity between the receptor and its ligand. The fact that ELRA show lower K_D is not surprising as this method is very close to the ELISA test which is known for its sensitivity. Unfortunately, if the ELRA test was also performed in the case of the estrogen receptor, no indications relating to the K_D can be found in the literature as it have been mainly used as a competition assay. It would have been interesting to see if the difference between SPR and ELRA value is in the same range in the case of the estrogen receptor. Concerning the kd and ka obtained by SPR experiment, they are in the range of normal constant values. More calculations would have been necessary to completely estimate how valuable these results are. For example, determination of kd and ka for different flow rates, temperature or buffer would have been of a great interest and would have allow to deepen the understanding of this receptor-ligand interaction. Unfortunately, the absence of an integrated algorithm in the software for parameter calculation, the establishment of the binding protocols and the manual immobilization of the chip made impossible these calculations during the time of this work.

The relatively low amount of biosensors designed to the determination of progesterone and the fact that most of the experiments are not using the full-length progesterone receptor are not allowing a direct comparison between the values obtained and the published literature. All available receptor/ligand binding data were obtained by radioimmunoassay experiments and the only biosensors for the detection of progesterone are not using the progesterone receptor as biological component. In a first description of radioassay using the complete human progesterone receptor extracted from tumoral tissue, the team of Pichon et al. [248] could determine a binding affinity towards progesterone of 3 nM in absence of glycerol and 1.1 nM in presence of glycerol. Later, Vonier et al. [11] extracted the progesterone receptor of American alligator (*Alligator mississippiensiens*) eggs and performed radioassay with the promegestone (R5020) as reference ligand. They found a binding affinity towards this ligand of 0.9 nM and this binding could be inhibited by the introduction of endosulfan, alachlor and kepone. In a study published in 2004, Scippo et al. [12] used the ligand binding domain of the human progesterone receptor produced in *E. coli* for radioassay and could find a IC50 value toward the progesterone of 50 nM.

As mentioned before, direct comparison between these values and the values obtained with the two developed assay is not possible but it should be noted that all values are in the same nanomolar range, thus indicating a relative concordance.

5.6.3 Competition assay

Even though receptor-saturation assay was successful, competition in binding with free ligand gave only a signal decrease in the ELRA when progesterone-BSA was the ligand. The use of free progesterone as well as progesterone-like compounds could not compete with the binding of the receptor to the immobilized ligand (data not shown). To explain these results, it should first be considered that such experiments are requiring strict experiment conditions concerning the concentration of the partners. It is generally advised to use concentrations below the K_D for the ligand and the receptor in order to observe a competition. As the maximal absorbance value obtained during the saturation assay was low (inferior to 0.5), using a ligand concentration below the K_D led to a maximal absorbance value for competition between 0.3 and 0.4, which is in the low range of measurable absorbance by the spectrophotometer. Another element in order to explain the failing competition assay can be the nature of the competitors. It is known that progesterone is a lipophilic substance with low solubility in aqueous phase as well as most of the progesterone derivatives. Only progesterone-BSA shows a higher solubility in water due to the chemical structure of this ligand. The solubility of some of the tested compounds can be observed in Table 5-2. It can then be inferred that the low hydrophilicity of the free progesterone will be a major hindrance to reach the binding site of the receptor. The table shows also a superior value for water solubility in the case of 17-ß-estradiol and this could explain why estrogen receptor based ELRA can perform competition assay.

Table 5-2. Solubility in water at 25 °C of some compounds with progesterone activity and of 17-ß estradiol. *As no value is available for progesterone-BSA, the value of the similar compound estradiol-BSA is indicated. All estimate solubilities were generated using the US Environmental Protection Agency's EPISuite™ which can be found at the following address: www.epa.gov/opptintr/exposure/pubs/episuite.

Compound	Estimated solubility in water at 25 °C(mg/l)
progesterone	5.003
mifepristone	0.049
medroxyprogesterone	22.22
progesterone-BSA	1020*
17-ß-estradiol	81.97

5.7 HER-2 detection experiments

5.7.1 ELISA

The results obtained demonstrate that the developed ELISA test can specifically detect the recombinant total HER-2. Even though special care has been taken to optimize the process, the relatively low absorbance values have to be noted. Different antibodies aimed to recognize the HER-2 are available but they have mostly not been tested for ELISA format as these antibodies are intended to be used for immunohistochemistry or *in situ* hybridizations. Moreover the fact that this study is the first to describe the production, solubilization and purification of the complete HER-2 has for disadvantage that no positive control is available. This have for consequence that the ELISA

test cannot be calibrated with a pure standard and therefore the concentration of HER-2 cannot be calculated precisely. There are commercial products on the market but it consists either in a chimeric product or a fragment of the receptor and would therefore not be equivalent to the recombinant full-length receptor.

The comparison between our assay and other ELISA tests available is difficult because other studies using ELISA kits are mainly detecting the soluble, short version of the HER-2 protein. For example two of those ELISA tests have limits of quantification of 0.34 ng/ml [163] and 0.123 ng/ml [168]. There are commercially available kits for the detection of the complete HER-2 but the values presented to date are only from the manufacturers and therefore should be viewed with caution as they were not published in a peer-reviewed journal. For example, the PathScan® Total HER2/ErbB2 Sandwich ELISA Kit from Cell Signaling Technology® does not give any value related to the limit of quantification but presents a curve showing a relationship between absorbance and protein concentration in a range from approximately 10 to 400 µg/ml. Another ELISA kit for total HER-2 detection, the Her2 (Total) Human ELISA kit from Life Technologies®, gives a sensitivity of 0.2 ng/ml but this parameter was calculated by adding two standard deviations to the mean OD of the zero. In this study, consistent with the accepted standards [225], he limit of quantification was calculated to be the mean value plus 10 times the standard deviation of the blank. With this method of calculation, a limit of quantification of 7.8 ng/ml was obtained.

Currently all the commercially available assays use the sandwich approach, which is known to give lower limits of quantification than the direct coating approach that was used in this work. In a sandwich approach, the antigen is not directly coated on the wells of the micro titter plate but captured by an antibody which is coated on the well. This allows more sensitivity as unspecific binding is dramatically avoided and as almost all antigen will be organized and in the same direction. One major drawback of the direct coating of protein that was used in this work is indeed the fact that no control over the immobilization of the HER-2 can be ensured. The amino acids involved in this hydrophobic interaction (valine, alanine, leucine, isoleucine, and phenylalanine) are distributed across the whole protein and this will lead to an uncontrolled binding and so probable epitope masking. The major drawback of the sandwich approach is the relative inflexibility of this technique. As no protocol for the produced recombinant protein was available and as not all antibodies are working in ELISA format, several detection antibodies were assayed during this work. Most of these antibodies are produced in rabbit or mouse and this had the consequence that anti-rabbit and anti-mouse carrying a peroxidase were used as secondary antibody. These secondary antibodies couldn't be used in a sandwich format as they would have bind directly to the coated detection antibody. The only possibility would have been to use three antibodies: one coated detection antibody directed against the HER-2 and produced in mouse for example, one primary antibody directed against the HER-2 protein (at a different epitope) produced in rabbit and one secondary antibody produced in goat directed against rabbit IgG. This would have been very restrictive. Another problem is the fact that most of the available antibodies are directed against epitopes of the HER-2 protein localized in the same region of the protein and they are often overlapping between them. This would have a strong negative effect in a sandwich assay. One solution to use this format would

be to find via direct ELISA two suitable antibodies directed against different epitopes of the HER-2 antibody and then to conjugate one of them with the horseradish peroxidase.

5.7.2 Recombinant HER-2 detection by SPR

With the experiment presented in the Results section, it could be stated that the recombinant HER-2 can be specifically detected via SPR experiments. Although the SPR limit of quantification of 760 ng/ml is significantly higher than the ELISA values obtained, some improvements of both the experiment and the SPR device let think that this value will decrease significantly. Every improvement in the purification process of the recombinant HER-2 will lead to a higher purity and then to a lower detection limit. It has been seen in the experiments of section 4.10.4 that, even low, an unspecific binding is still occurring for the binding to the antibody. A higher purity will also lead to higher SPR-signal values as more protein will have the possibility to bind to the antibody.

An improvement of the antibody immobilization is on progress too. It has been shown in section 4.10.5 that different linkers were assayed without success but only few experiment conditions have been tested. Gold-coating can be influenced by several factors like coating buffer composition, temperature, incubation time and these different parameters will be changed in new planned experiment.

One of the major improvements of the SPR-platform will be the routine use of a nanospotting device. In this work, all chip functionalization were performed either by the help of a 17-channels flow cell or by direct pipetting on the gold surface. The flow cell was abandoned for the later experiments as its stability was not good enough to ensure the performing of a high amount of experiments. After approximately five immobilizations, the flow cell needed to be sent for maintenance and the channels needed to be new shaped. It is because after a certain time, the PDMS material was not stable enough to ensure the isolation between the channels. This led to the outbreak of the probe from its channel and then the failure of the experiment. That's why direct immobilization with micropipette was used at a certain point of this work. It allowed the immobilization of probes to the chip in an easier way but unfortunately only to three surfaces. That means that only two surfaces could be immobilized with a probe as one should be the control surface and so many more chips than necessary have been used. It also complicated the exploitation of the experiments as comparisons were made between different chips instead of between different probes on one chip. Because of that, it was necessary to observe carefully all signals (and particularly the signal from the control surface) to affirm that all the chips used in one experiment were presenting the same characteristics. This led to the fact that many experiments were rejected, thus implying loosing time and material to perform repetition of these experiments. By using a nanospotter device with moisture and temperature control, more than hundred droplets of different probe solutions can be immobilized in one chip, thus removing the chip to chip effect and allowing the use of more controls and dilutions. As each droplet will have strictly the same volume, a better reproducibility of the results will also be expected.

5.7.3 Real samples measurement

In order to compare the abilities of both the ELISA and the SPR format to detect natural occurring receptor HER-2 in breast cancer tissue, a direct comparison was performed in section 4.13. It is to note that this test was performed even though none of these two detection systems were optimized for this specific experiment. All precedent optimization steps were performed in PBS buffers without taking into account that the breast cancer sample are in a totally different matrix. This could explain why no significant difference could be seen between positive and negative sample in ELISA format. The AR technique employed for extraction of proteins implies the use of high concentration of SDS and the co-extraction of protein which can disturb the test and those conditions should have been tested before utilizing this method with real samples. Moreover, the natural occurring HER-2 may react differently with immobilized antibodies as the recombinant produced receptor. It is also to note that only two samples were tested and more samples are necessary in order to draw definitive conclusions.

In the case of the SPR biosensor, exactly the same samples were utilized. Because the concentration of HER-2 at the surface of breast cell in normal state and in cancer state is not precisely known, it is impossible to set a goal detection limit which should be achieved. That's why three different concentrations of tissue sample were utilized in the section 4.13 in the case of the SPR experiment. The fact that a statistical difference can be observed between a negative and a positive sample for a concentration of 10 µg/ml indicates that the designed biosensor has the potential to detect over expression of the HER-2 in breast cancer tissue. This difference could not be observed for higher concentrations and that is probably due to the unspecific binding. The positive control injected at the end of the experiment is very important as it allows to compare directly the two chips. Due to the experimental design of the SPR platform, only one sample can be injected to the chip and this has for consequence that two different chips had to be used for two different samples. By reaching exactly the same value with recombinant HER-2 (the positive control), this result indicates that both chips possessed exactly the same binding capacities and therefore the results obtained with real samples can be trusted. Even though this first test was successful, more experiments with different real samples are necessary to confirm them. Moreover some elements have to be optimized or integrated in order to improve the detection system:

- Developers of the SPR platform are working on a new PDMS flow cell integrating two flow paths for the simultaneous injection of two samples on a same chip. This will offer the possibility to always insert a control solution in each experiment and therefore allow checking easily if the results are positive.
- The use of nanospotting device for immobilization of antibody will also have a positive impact for this experiment as exactly the same volume of antibody will be utilized and the use of positive control will then be not so important.
- Experiments performed with the recombinant HER-2 should also be performed in other conditions than the optimal ones. The optimal buffer, temperature, flow rate and incubation time were determined for the binding of recombinant receptor but it is possible that these conditions are not the best for HER-2 extracted from breast tissue. As the extraction was

only working in the buffer presented in section 4.11.1, SPR experiments with the recombinant receptor should be performed in a buffer which mimics this particular solution.

- The use of HER-2 extracted directly from fresh cancer lines can be a good compromise between recombinant receptor and proteins extracted from freshly frozen paraffin embedded tissue. These cell lines are easily available and they were all established in order to reflect all the naturally occurring molecular patterns of the breast cancer [249]. They are originating from human cells as the real samples so the presence of disturbing agents for SPR experiments specific for these cells would be detected and new strategies would be assayed in order to overcome these disturbances.

5.8 Perspectives

5.8.1 The progesterone receptor biosensor

In the actual state, the SPR-based progesterone receptor biosensor is not ready to be utilized for progesterone or progestin detection. The biological component - the progesterone receptor - was successfully produced in two different yeast species and can recognize its ligand progesterone as shown by both the ELRA and the SPR experiments. The next step of the biosensor development will be the realization of competition experiments where free ligand should be introduced in order to measure its concentration. For this step, new improvements of the SPR platform and better understanding of the recombinant receptor/ligand interaction will surely have a decisive impact in order to obtain a functional and reliable biosensor. In parallel, the fact that production of purified recombinant progesterone receptor in large quantities was performed allows to explore new assay strategies. Adding other tags than His-tag or modifications to the receptor could offer different immobilization strategies or allow improved assay stability. Among the biosensors developed in the previous years, production of the biological partner has always been one of the major issues. With *A. adeninivorans* or *H. polymorpha* as expression platform, it was possible to obtain large quantity of receptor in an active form. This will have a decisive advantage towards other developed biosensors. As already indicated in the introduction section, actual sensing methods are focused on the detection of specific compounds and cannot measure the total progesterone activity. This means that if a new compound is synthetized, analytic detection via LC-MS or GC-MS as well as biosensors using anti-progesterone antibodies will not have the possibility to determine if this compound presents a potential progesterone activity. This determination can only be performed by a biosensor possessing a progesterone receptor as biological partner.

5.8.2 The HER-2 biosensor

During this work, the biological partner of the HER-2 biosensor was successfully produced and purified. It could then be utilized for SPR experiments. After first optimizations, the ability of the SPR device to detect recombinant HER-2 protein was proven. Unfortunately, only one experiment with real samples could have been performed during the time of this study. Even though the results of one unique experiment should be taken with caution, they are showing very promising results. Towards actual detection methods, the SPR-based biosensor has the advantage to be quantitative

and is not relying on human observation. The biopsy tissue quantity used for this SPR assay was the same as the quantity used for IHC or FISH and the time of experiment comprising sample deparaffinization, proteins solubilization and injection in the SPR device doesn't exceed 6 hours. The SPR experiment alone only needs 30 min to be performed. To use this biosensor in a high throughput, two main improvements of the SPR platform remain to be achieved: the possibility to inject two samples simultaneously to the same chip and the possibility to reuse chips several times. This will ensure on one hand better reliability of the results and on the other hand lower the cost of the experiment.

6 References

1. Leblebicioglu, B., J. Connors and A. Mariotti, *Principles of endocrinology.* Periodontol 2000, 2013. **61**(1): p. 54-68.
2. Bolte, E., S. Coudert and Y. Lefebvre, *Steroid production from plasma cholesterol. II. In vivo conversion of plasma cholesterol to ovarian progesterone and adrenal C19 and C21 steroids in humans.* J Clin Endocrinol Metab, 1974. **38**(3): p. 394-400.
3. Nishida, S. and R.A. Jungmann, *Biosynthesis of steroids from (14C)cholesterol, (3H) progesterone and (3H)pregnenolone by human adrenal carcinoma tissue.* Clin Chim Acta, 1974. **52**(1): p. 97-103.
4. Bloch, G., E. Hazan and A. Rafaeli, *Circadian rhythms and endocrine functions in adult insects.* J Insect Physiol, 2013. **59**(1): p. 56-69.
5. LeBlanc, G.A., *Crustacean endocrine toxicology: a review.* Ecotoxicology, 2007. **16**(1): p. 61-81.
6. Huber, J.C. and J. Ott, *The dialectic role of progesterone.* Maturitas, 2009. **62**(4): p. 326-9.
7. Di Renzo, G.C., A. Mattei, M. Gojnic and S. Gerli, *Progesterone and pregnancy.* Curr Opin Obstet Gynecol, 2005. **17**(6): p. 598-600.
8. Wenner, M.M. and N.S. Stachenfeld, *Blood pressure and water regulation: understanding sex hormone effects within and between men and women.* J Physiol, 2012. **590**(Pt 23): p. 5949-61.
9. Schindler, A.E., C. Campagnoli, R. Druckmann, J. Huber, J.R. Pasqualini, K.W. Schweppe and J.H. Thijssen, *Classification and pharmacology of progestins.* Maturitas, 2003. **46 Suppl 1**: p. S7-S16.
10. Liu, Z.H., J.A. Ogejo, A. Pruden and K.F. Knowlton, *Occurrence, fate and removal of synthetic oral contraceptives (SOCs) in the natural environment: a review.* Sci Total Environ, 2011. **409**(24): p. 5149-61.
11. Vonier, P.M., D.A. Crain, J.A. McLachlan, L.J. Guillette, Jr. and S.F. Arnold, *Interaction of environmental chemicals with the estrogen and progesterone receptors from the oviduct of the American alligator.* Environ Health Perspect, 1996. **104**(12): p. 1318-22.
12. Scippo, M.L., C. Argiris, C. Van De Weerdt, M. Muller, P. Willemsen, J. Martial and G. Maghuin-Rogister, *Recombinant human estrogen, androgen and progesterone receptors for detection of potential endocrine disruptors.* Anal Bioanal Chem, 2004. **378**(3): p. 664-9.
13. Tolgyesi, A., Z. Verebey, V.K. Sharma, L. Kovacsics and J. Fekete, *Simultaneous determination of corticosteroids, androgens, and progesterone in river water by liquid chromatography-tandem mass spectrometry.* Chemosphere, 2010. **78**(8): p. 972-9.
14. Evans, R.M., *The steroid and thyroid hormone receptor superfamily.* Science, 1988. **240**(4854): p. 889-95.
15. Mangelsdorf, D.J., C. Thummel, M. Beato, P. Herrlich, G. Schutz, K. Umesono, B. Blumberg, P. Kastner, M. Mark, P. Chambon and R.M. Evans, *The nuclear receptor superfamily: the second decade.* Cell, 1995. **83**(6): p. 835-9.
16. Ota, T., Y. Suzuki, T. Nishikawa, T. Otsuki, T. Sugiyama, R. Irie, A. Wakamatsu, K. Hayashi, H. Sato, K. Nagai, K. Kimura, H. Makita, M. Sekine, M. Obayashi, T. Nishi, T. Shibahara, T. Tanaka, S. Ishii, J.-i. Yamamoto, K. Saito, Y. Kawai, Y. Isono, Y. Nakamura, K. Nagahari, K. Murakami, T. Yasuda, T. Iwayanagi, M. Wagatsuma, A. Shiratori, H. Sudo, T. Hosoiri, Y. Kaku, H. Kodaira, H. Kondo, M. Sugawara, M. Takahashi, K. Kanda, T. Yokoi, T. Furuya, E. Kikkawa, Y. Omura, K. Abe, K. Kamihara, N. Katsuta, K. Sato, M. Tanikawa, M. Yamazaki, K. Ninomiya, T. Ishibashi, H. Yamashita, K. Murakawa, K. Fujimori, H. Tanai, M. Kimata, M. Watanabe, S.

Hiraoka, Y. Chiba, S. Ishida, Y. Ono, S. Takiguchi, S. Watanabe, M. Yosida, T. Hotuta, J. Kusano, K. Kanehori, A. Takahashi-Fujii, H. Hara, T.-o. Tanase, Y. Nomura, S. Togiya, F. Komai, R. Hara, K. Takeuchi, M. Arita, N. Imose, K. Musashino, H. Yuuki, A. Oshima, N. Sasaki, S. Aotsuka, Y. Yoshikawa, H. Matsunawa, T. Ichihara, N. Shiohata, S. Sano, S. Moriya, H. Momiyama, N. Satoh, S. Takami, Y. Terashima, O. Suzuki, S. Nakagawa, A. Senoh, H. Mizoguchi, Y. Goto, F. Shimizu, H. Wakebe, H. Hishigaki, T. Watanabe, A. Sugiyama, M. Takemoto, B. Kawakami, M. Yamazaki, K. Watanabe, A. Kumagai, S. Itakura, Y. Fukuzumi, Y. Fujimori, M. Komiyama, H. Tashiro, A. Tanigami, T. Fujiwara, T. Ono, K. Yamada, Y. Fujii, K. Ozaki, M. Hirao, Y. Ohmori, A. Kawabata, T. Hikiji, N. Kobatake, H. Inagaki, Y. Ikema, S. Okamoto, R. Okitani, T. Kawakami, S. Noguchi, T. Itoh, K. Shigeta, T. Senba, K. Matsumura, Y. Nakajima, T. Mizuno, M. Morinaga, M. Sasaki, T. Togashi, M. Oyama, H. Hata, M. Watanabe, T. Komatsu, J. Mizushima-Sugano, T. Satoh, Y. Shirai, Y. Takahashi, K. Nakagawa, K. Okumura, T. Nagase, N. Nomura, H. Kikuchi, Y. Masuho, R. Yamashita, K. Nakai, T. Yada, Y. Nakamura, O. Ohara, T. Isogai and S. Sugano, *Complete sequencing and characterization of 21,243 full-length human cDNAs.* Nat Genet, 2004. **36**(1): p. 40-45.

17. Taylor, T.D., H. Noguchi, Y. Totoki, A. Toyoda, Y. Kuroki, K. Dewar, C. Lloyd, T. Itoh, T. Takeda, D.-W. Kim, X. She, K.F. Barlow, T. Bloom, E. Bruford, J.L. Chang, C.A. Cuomo, E. Eichler, M.G. FitzGerald, D.B. Jaffe, K. LaButti, R. Nicol, H.-S. Park, C. Seaman, C. Sougnez, X. Yang, A.R. Zimmer, M.C. Zody, B.W. Birren, C. Nusbaum, A. Fujiyama, M. Hattori, J. Rogers, E.S. Lander and Y. Sakaki, *Human chromosome 11 DNA sequence and analysis including novel gene identification.* Nature, 2006. **440**(7083): p. 497-500.
18. Conneely, O.M. and B.M. Jericevic, *Progesterone regulation of reproductive function through functionally distinct progesterone receptor isoforms.* Rev Endocr Metab Disord, 2002. **3**(3): p. 201-9.
19. Kastner, P., A. Krust, B. Turcotte, U. Stropp, L. Tora, H. Gronemeyer and P. Chambon, *Two distinct estrogen-regulated promoters generate transcripts encoding the two functionally different human progesterone receptor forms A and B.* EMBO J, 1990. **9**(5): p. 1603-14.
20. Li, X. and B.W. O'Malley, *Unfolding the action of progesterone receptors.* J Biol Chem, 2003. **278**(41): p. 39261-4.
21. Mulac-Jericevic, B., R.A. Mullinax, F.J. DeMayo, J.P. Lydon and O.M. Conneely, *Subgroup of reproductive functions of progesterone mediated by progesterone receptor-B isoform.* Science, 2000. **289**(5485): p. 1751-4.
22. Wen, D.X., Y.F. Xu, D.E. Mais, M.E. Goldman and D.P. McDonnell, *The A and B isoforms of the human progesterone receptor operate through distinct signaling pathways within target cells.* Mol Cell Biol, 1994. **14**(12): p. 8356-64.
23. Hirata, S., T. Shoda, J. Kato and K. Hoshi, *The novel isoform of the progesterone receptor cDNA in the human testis and detection of its mRNA in the human uterine endometrium.* Oncology, 2000. **59 Suppl 1**: p. 39-44.
24. Hirata, S., T. Shoda, J. Kato and K. Hoshi, *The novel exon, exon T, of the human progesterone receptor gene and the genomic organization of the gene.* J Steroid Biochem Mol Biol, 2002. **80**(3): p. 365-7.
25. Saner, K.J., B.H. Welter, F. Zhang, E. Hansen, B. Dupont, Y. Wei and T.M. Price, *Cloning and expression of a novel, truncated, progesterone receptor.* Mol Cell Endocrinol, 2003. **200**(1-2): p. 155-63.
26. Yamanaka, T., S. Hirata, T. Shoda and K. Hoshi, *Progesterone receptor mRNA variant containing novel exon insertions between exon 4 and exon 5 in human uterine endometrium.* Endocr J, 2002. **49**(4): p. 473-82.

27. Dai, Q., A.A. Shah, R.V. Garde, B.A. Yonish, L. Zhang, N.A. Medvitz, S.E. Miller, E.L. Hansen, C.N. Dunn and T.M. Price, *A truncated progesterone receptor (PR-M) localizes to the mitochondrion and controls cellular respiration.* Mol Endocrinol, 2013. **27**(5): p. 741-53.
28. Taylor, A.H., P.C. McParland, D.J. Taylor and S.C. Bell, *The progesterone receptor in human term amniochorion and placenta is isoform C.* Endocrinology, 2006. **147**(2): p. 687-93.
29. Condon, J.C., D.B. Hardy, K. Kovaric and C.R. Mendelson, *Up-regulation of the progesterone receptor (PR)-C isoform in laboring myometrium by activation of nuclear factor-kappaB may contribute to the onset of labor through inhibition of PR function.* Mol Endocrinol, 2006. **20**(4): p. 764-75.
30. Shyamala, G., X. Yang, G. Silberstein, M.H. Barcellos-Hoff and E. Dale, *Transgenic mice carrying an imbalance in the native ratio of A to B forms of progesterone receptor exhibit developmental abnormalities in mammary glands.* Proc Natl Acad Sci U S A, 1998. **95**(2): p. 696-701.
31. Cork, D.M., T.W. Lennard and A.J. Tyson-Capper, *Alternative splicing and the progesterone receptor in breast cancer.* Breast Cancer Res, 2008. **10**(3): p. 207.
32. Richer, J.K., B.M. Jacobsen, N.G. Manning, M.G. Abel, D.M. Wolf and K.B. Horwitz, *Differential gene regulation by the two progesterone receptor isoforms in human breast cancer cells.* J Biol Chem, 2002. **277**(7): p. 5209-18.
33. Cheung, J. and D.F. Smith, *Molecular chaperone interactions with steroid receptors: an update.* Mol Endocrinol, 2000. **14**(7): p. 939-46.
34. Tsai, M.J. and B.W. O'Malley, *Molecular mechanisms of action of steroid/thyroid receptor superfamily members.* Annu Rev Biochem, 1994. **63**: p. 451-86.
35. Tata, J.R., *Signalling through nuclear receptors.* Nat Rev Mol Cell Biol, 2002. **3**(9): p. 702-10.
36. Losel, R. and M. Wehling, *Nongenomic actions of steroid hormones.* Nat Rev Mol Cell Biol, 2003. **4**(1): p. 46-56.
37. Brian, J.V., C.A. Harris, M. Scholze, A. Kortenkamp, P. Booy, M. Lamoree, G. Pojana, N. Jonkers, A. Marcomini and J.P. Sumpter, *Evidence of estrogenic mixture effects on the reproductive performance of fish.* Environ Sci Technol, 2007. **41**(1): p. 337-44.
38. Jenkins, R.L., E.M. Wilson, R.A. Angus, W.M. Howell and M. Kirk, *Androstenedione and progesterone in the sediment of a river receiving paper mill effluent.* Toxicol Sci, 2003. **73**(1): p. 53-9.
39. Sumpter, J.P. and A.C. Johnson, *10th Anniversary Perspective: Reflections on endocrine disruption in the aquatic environment: from known knowns to unknown unknowns (and many things in between).* J Environ Monit, 2008. **10**(12): p. 1476-85.
40. Vulliet, E., L. Wiest, R. Baudot and M.F. Grenier-Loustalot, *Multi-residue analysis of steroids at sub-ng/L levels in surface and ground-waters using liquid chromatography coupled to tandem mass spectrometry.* J Chromatogr A, 2008. **1210**(1): p. 84-91.
41. Foster, W.G. and J. Agzarian, *Toward less confusing terminology in endocrine disruptor research.* J Toxicol Environ Health B Crit Rev, 2008. **11**(3-4): p. 152-61.
42. Soto, A.M., K.L. Chung and C. Sonnenschein, *The pesticides endosulfan, toxaphene, and dieldrin have estrogenic effects on human estrogen-sensitive cells.* Environ Health Perspect, 1994. **102**(4): p. 380-3.
43. Soto, A.M., C. Sonnenschein, K.L. Chung, M.F. Fernandez, N. Olea and F.O. Serrano, *The E-SCREEN assay as a tool to identify estrogens: an update on estrogenic environmental pollutants.* Environ Health Perspect, 1995. **103 Suppl 7**: p. 113-22.
44. White, R., S. Jobling, S.A. Hoare, J.P. Sumpter and M.G. Parker, *Environmentally persistent alkylphenolic compounds are estrogenic.* Endocrinology, 1994. **135**(1): p. 175-82.

45. Kelce, W.R., C.R. Stone, S.C. Laws, L.E. Gray, J.A. Kemppainen and E.M. Wilson, *Persistent DDT metabolite p,p'-DDE is a potent androgen receptor antagonist.* Nature, 1995. **375**(6532): p. 581-5.
46. Brambilla, G. and A. Martelli, *Are some progestins genotoxic liver carcinogens?* Mutat Res - Rev Mut Res, 2002. **512**(2–3): p. 155-163.
47. Besse, J.P. and J. Garric, *Progestagens for human use, exposure and hazard assessment for the aquatic environment.* Environ Pollut, 2009. **157**(12): p. 3485-94.
48. Pietsch, C., N. Neumann, T. Preuer and W. Kloas, *In vivo treatment with progestogens causes immunosuppression of carp Cyprinus carpio leucocytes by affecting nitric oxide production and arginase activity.* J Fish Biol, 2011. **79**(1): p. 53-69.
49. Paulos, P., T.J. Runnalls, G. Nallani, T. La Point, A.P. Scott, J.P. Sumpter and D.B. Huggett, *Reproductive responses in fathead minnow and Japanese medaka following exposure to a synthetic progestin, Norethindrone.* Aquat Toxicol, 2010. **99**(2): p. 256-62.
50. Zeilinger, J., T. Steger-Hartmann, E. Maser, S. Goller, R. Vonk and R. Lange, *Effects of synthetic gestagens on fish reproduction.* Environ Toxicol Chem, 2009. **28**(12): p. 2663-70.
51. Al-Odaini, N.A., M.P. Zakaria, M.I. Yaziz and S. Surif, *Multi-residue analytical method for human pharmaceuticals and synthetic hormones in river water and sewage effluents by solid-phase extraction and liquid chromatography-tandem mass spectrometry.* J Chromatogr, 2010. **1217**(44): p. 6791-6806.
52. Liu, S., G.G. Ying, J.L. Zhao, F. Chen, B. Yang, L.J. Zhou and H.J. Lai, *Trace analysis of 28 steroids in surface water, wastewater and sludge samples by rapid resolution liquid chromatography-electrospray ionization tandem mass spectrometry.* J Chromatogr, 2011. **1218**(10): p. 1367-1378.
53. Liu, X.J., J. Zhang, J. Yin, H.J. Duan, Y.N. Wu and B. Shao, *Analysis of hormone antagonists in clinical and municipal wastewater by isotopic dilution liquid chromatography tandem mass spectrometry.* Anal Bioanal Chem, 2010. **396**(8): p. 2977-2985.
54. Sun, L., W. Yong, X.G. Chu and J.M. Lin, *Simultaneous determination of 15 steroidal oral contraceptives in water using solid-phase disk extraction followed by high performance liquid chromatography-tandem mass spectrometry.* J Chromatogr, 2009. **1216**(28): p. 5416-5423.
55. Xu, Y.J., X.H. Tian, X.Z. Zhang, X.H. Gong, S.J. Zhang, H.H. Liu and L.M. Zhang, *Simultaneous Determination of Hormone Residues in Aquatic Products by UPLC-ESI-MS-MS.* Am Lab, 2010. **42**(7): p. 11-+.
56. Yu, Y.Y., Q.X. Huang, J.L. Cui, K. Zhang, C.M. Tang and X.Z. Peng, *Determination of pharmaceuticals, steroid hormones, and endocrine-disrupting personal care products in sewage sludge by ultra-high-performance liquid chromatography-tandem mass spectrometry.* Anal Bioanal Chem, 2011. **399**(2): p. 891-902.
57. Chimchirian, R.F., R.P. Suri and H. Fu, *Free synthetic and natural estrogen hormones in influent and effluent of three municipal wastewater treatment plants.* Water Environ Res, 2007. **79**(9): p. 969-74.
58. Velicu, M. and R. Suri, *Presence of steroid hormones and antibiotics in surface water of agricultural, suburban and mixed-use areas.* Environ Monit Assess, 2009. **154**(1-4): p. 349-359.
59. Pu, C., Y.F. Wu, H. Yang and A.P. Deng, *Trace analysis of contraceptive drug levonorgestrel in wastewater samples by a newly developed indirect competitive enzyme-linked immunosorbent assay (ELISA) coupled with solid phase extraction.* Anal Chim Acta, 2008. **628**(1): p. 73-79.

60. Qiao, Y.W., H. Yang, B. Wang, J. Song and A.P. Deng, *Preparation and characterization of an immunoaffinity chromatography column for the selective extraction of trace contraceptive drug levonorgestrel from water samples.* Talanta, 2009. **80**(1): p. 98-103.
61. Fayad, P.B., M. Prevost and S. Sauve, *Laser Diode Thermal Desorption/Atmospheric Pressure Chemical Ionization Tandem Mass Spectrometry Analysis of Selected Steroid Hormones in Wastewater: Method Optimization and Application.* Anal Chem, 2010. **82**(2): p. 639-645.
62. Viglino, L., K. Aboulfadl, M. Prevost and S. Sauve, *Analysis of natural and synthetic estrogenic endocrine disruptors in environmental waters using online preconcentration coupled with LC-APPI-MS/MS.* Talanta, 2008. **76**(5): p. 1088-1096.
63. Liu, Z.H., T. Hashimoto, Y. Okumura, Y. Kanjo and S. Mizutani, *Simultaneous Analysis of Natural Free Estrogens and Their Conjugates in Wastewater by GC-MS.* Clean-Soil Air Water, 2010. **38**(2): p. 181-188.
64. Seo, J., H.Y. Kim, B.C. Chung and J.K. Hong, *Simultaneous determination of anabolic steroids and synthetic hormones in meat by freezing-lipid filtration, solid-phase extraction and gas chromatography-mass spectrometry.* J Chromatogr, 2005. **1067**(1-2): p. 303-309.
65. Viglino, L., M. Prevost and S. Sauve, *High throughput analysis of solid-bound endocrine disruptors by LDTD-APCI-MS/MS.* J Environ Monit, 2011. **13**(3): p. 583-90.
66. Bezbaruah, A.N., Kalita, H., *Sensors and Biosensors for Endocrine Disrupting Chemicals: State-of-the-Art and Future Trends in Treatment of Micropollutants in Water and Wastewater*, J. Eds: Virkutyte, Varma, R.S., Hoag, G., Jegatheesan, V.,Editor. 2010, International Water Association: London, U.K. p. 93-128.
67. Charles, G.D., *In vitro models in endocrine disruptor screening.* ILAR J, 2004. **45**(4): p. 494-501.
68. Habauzit, D., J. Armengaud, B. Roig and J. Chopineau, *Determination of estrogen presence in water by SPR using estrogen receptor dimerization.* Anal Bioanal Chem, 2008. **390**(3): p. 873-83.
69. Miyashita, M., T. Shimada, H. Miyagawa and M. Akamatsu, *Surface plasmon resonance-based immunoassay for 17beta-estradiol and its application to the measurement of estrogen receptor-binding activity.* Anal Bioanal Chem, 2005. **381**(3): p. 667-73.
70. Claycomb, R.W. and M.J. Delwiche, *Biosensor for on-line measurement of bovine progesterone during milking.* Biosens Bioelectron, 1998. **13**(11): p. 1173-80.
71. Kreuzer, M.P., R. McCarthy, M. Pravda and G.G. Guilbault, *Development of electrochemical immunosensor for progesterone analysis in milk.* Anal Lett, 2004. **37**(5): p. 943-956.
72. Pemberton, R.M., J.P. Hart and T.T. Mottram, *An electrochemical immunosensor for milk progesterone using a continuous flow system.* Biosens Bioelectron, 2001. **16**(9-12): p. 715-23.
73. Gillis, E.H., J.P. Gosling, J.M. Sreenan and M. Kane, *Development and validation of a biosensor-based immunoassay for progesterone in bovine milk.* J Immunol Methods, 2002. **267**(2): p. 131-8.
74. Sananikone, K., M.J. Delwiche, R.H. BonDurant and C.J. Munro, *Quantitative lateral flow immunoassay for measuring progesterone in bovine milk.* Trans ASAE, 2004. **47**(4): p. 1357-1365.
75. Tschmelak, J., N. Kappel and G. Gauglitz, *TIRF-based biosensor for sensitive detection of progesterone in milk based on ultra-sensitive progesterone detection in water.* Anal Bioanal Chem, 2005. **382**(8): p. 1895-903.
76. Hahn, T., K. Tag, K. Riedel, S. Uhlig, K. Baronian, G. Gellissen and G. Kunze, *A novel estrogen sensor based on recombinant Arxula adeninivorans cells.* Biosens Bioelectron, 2006. **21**(11): p. 2078-85.

77. Kaiser, C., S. Uhlig, T. Gerlach, M. Korner, K. Simon, K. Kunath, K. Florschutz, K. Baronian and G. Kunze, *Evaluation and validation of a novel Arxula adeninivorans estrogen screen (nAES) assay and its application in analysis of wastewater, seawater, brackish water and urine.* Sci Total Environ, 2010. **408**(23): p. 6017-26.
78. Pillon, A., A.M. Boussioux, A. Escande, S. Ait-Aissa, E. Gomez, H. Fenet, M. Ruff, D. Moras, F. Vignon, M.J. Duchesne, C. Casellas, J.C. Nicolas and P. Balaguer, *Binding of estrogenic compounds to recombinant estrogen receptor-alpha: application to environmental analysis.* Environ Health Perspect, 2005. **113**(3): p. 278-84.
79. Srinivasan, G., J.F. Post and E.B. Thompson, *Optimal ligand binding by the recombinant human glucocorticoid receptor and assembly of the receptor complex with heat shock protein 90 correlate with high intracellular ATP levels in Spodoptera frugiperda cells.* J Steroid Biochem Mol Biol, 1997. **60**(1-2): p. 1-9.
80. Elliston, J.F., J.M. Beekman, S.Y. Tsai, B.W. O'Malley and M.J. Tsai, *Hormone activation of baculovirus expressed progesterone receptors.* J Biol Chem, 1992. **267**(8): p. 5193-8.
81. Melvin, V.S. and D.P. Edwards, *Expression and purification of recombinant human progesterone receptor in baculovirus and bacterial systems.* Methods Mol Biol, 2001. **176**: p. 39-54.
82. Williams, S.P. and P.B. Sigler, *Atomic structure of progesterone complexed with its receptor.* Nature, 1998. **393**(6683): p. 392-6.
83. Ferlay J, S.I., Ervik M, Dikshit R, Eser S, Mathers C, Rebelo M, Parkin DM, Forman D, Bray, F. *GLOBOCAN 2012 v1.0, Cancer Incidence and Mortality Worldwide: IARC CancerBase No. 11 [Internet].* 2013 20/07/2014]; Available from: http://globocan.iarc.fr.
84. Rakha, E.A., J.S. Reis-Filho, F. Baehner, D.J. Dabbs, T. Decker, V. Eusebi, S.B. Fox, S. Ichihara, J. Jacquemier, S.R. Lakhani, J. Palacios, A.L. Richardson, S.J. Schnitt, F.C. Schmitt, P.H. Tan, G.M. Tse, S. Badve and I.O. Ellis, *Breast cancer prognostic classification in the molecular era: the role of histological grade.* Breast Cancer Res, 2010. **12**(4): p. 207.
85. Cianfrocca, M. and L.J. Goldstein, *Prognostic and predictive factors in early-stage breast cancer.* Oncologist, 2004. **9**(6): p. 606-16.
86. Luparia, A., G. Mariscotti, M. Durando, S. Ciatto, D. Bosco, P.P. Campanino, I. Castellano, A. Sapino and G. Gandini, *Accuracy of tumour size assessment in the preoperative staging of breast cancer: comparison of digital mammography, tomosynthesis, ultrasound and MRI.* Radiol Med, 2013. **118**(7): p. 1119-36.
87. Galea, M.H., R.W. Blamey, C.E. Elston and I.O. Ellis, *The Nottingham Prognostic Index in primary breast cancer.* Breast Cancer Res Treat, 1992. **22**(3): p. 207-19.
88. Sundquist, M., S. Thorstenson, L. Brudin and B. Nordenskjold, *Applying the Nottingham Prognostic Index to a Swedish breast cancer population. South East Swedish Breast Cancer Study Group.* Breast Cancer Res Treat, 1999. **53**(1): p. 1-8.
89. Chin, K., S. DeVries, J. Fridlyand, P.T. Spellman, R. Roydasgupta, W.L. Kuo, A. Lapuk, R.M. Neve, Z. Qian, T. Ryder, F. Chen, H. Feiler, T. Tokuyasu, C. Kingsley, S. Dairkee, Z. Meng, K. Chew, D. Pinkel, A. Jain, B.M. Ljung, L. Esserman, D.G. Albertson, F.M. Waldman and J.W. Gray, *Genomic and transcriptional aberrations linked to breast cancer pathophysiologies.* Cancer Cell, 2006. **10**(6): p. 529-41.
90. Peppercorn, J., C.M. Perou and L.A. Carey, *Molecular subtypes in breast cancer evaluation and management: divide and conquer.* Cancer Invest, 2008. **26**(1): p. 1-10.
91. Sorlie, T., R. Tibshirani, J. Parker, T. Hastie, J.S. Marron, A. Nobel, S. Deng, H. Johnsen, R. Pesich, S. Geisler, J. Demeter, C.M. Perou, P.E. Lonning, P.O. Brown, A.L. Borresen-Dale and D. Botstein, *Repeated observation of breast tumor subtypes in independent gene expression data sets.* Proc Natl Acad Sci U S A, 2003. **100**(14): p. 8418-23.

92. Sotiriou, C., S.Y. Neo, L.M. McShane, E.L. Korn, P.M. Long, A. Jazaeri, P. Martiat, S.B. Fox, A.L. Harris and E.T. Liu, *Breast cancer classification and prognosis based on gene expression profiles from a population-based study.* Proc Natl Acad Sci U S A, 2003. **100**(18): p. 10393-8.
93. Elston, C.W. and I.O. Ellis, *Pathological prognostic factors in breast cancer. I. The value of histological grade in breast cancer: experience from a large study with long-term follow-up.* Histopathology, 1991. **19**(5): p. 403-10.
94. Frkovic-Grazio, S. and M. Bracko, *Long term prognostic value of Nottingham histological grade and its components in early (pT1N0M0) breast carcinoma.* J Clin Pathol, 2002. **55**(2): p. 88-92.
95. Rakha, E.A., M.E. El-Sayed, A.H. Lee, C.W. Elston, M.J. Grainge, Z. Hodi, R.W. Blamey and I.O. Ellis, *Prognostic significance of Nottingham histologic grade in invasive breast carcinoma.* J Clin Oncol, 2008. **26**(19): p. 3153-8.
96. *Guidelines for pathology reporting in breast disease, NHSBSP Publication No 58*. 2005, The Royal College of Pathologists: Sheffield.
97. Tavassoli FA, D.P., *World Health Organization classification of tumours*. 2003, IARC Press: Lyon. p. 19-23.
98. Hammond, M.E., D.F. Hayes, M. Dowsett, D.C. Allred, K.L. Hagerty, S. Badve, P.L. Fitzgibbons, G. Francis, N.S. Goldstein, M. Hayes, D.G. Hicks, S. Lester, R. Love, P.B. Mangu, L. McShane, K. Miller, C.K. Osborne, S. Paik, J. Perlmutter, A. Rhodes, H. Sasano, J.N. Schwartz, F.C. Sweep, S. Taube, E.E. Torlakovic, P. Valenstein, G. Viale, D. Visscher, T. Wheeler, R.B. Williams, J.L. Wittliff and A.C. Wolff, *American Society of Clinical Oncology/College Of American Pathologists guideline recommendations for immunohistochemical testing of estrogen and progesterone receptors in breast cancer.* J Clin Oncol, 2010. **28**(16): p. 2784-95.
99. Jordan, V.C. and B.W. O'Malley, *Selective estrogen-receptor modulators and antihormonal resistance in breast cancer.* J Clin Oncol, 2007. **25**(36): p. 5815-24.
100. Litton, J.K., B.K. Arun, P.H. Brown and G.N. Hortobagyi, *Aromatase inhibitors and breast cancer prevention.* Expert Opin Pharmacother, 2012. **13**(3): p. 325-31.
101. Chia, S., W. Gradishar, L. Mauriac, J. Bines, F. Amant, M. Federico, L. Fein, G. Romieu, A. Buzdar, J.F. Robertson, A. Brufsky, K. Possinger, P. Rennie, F. Sapunar, E. Lowe and M. Piccart, *Double-blind, randomized placebo controlled trial of fulvestrant compared with exemestane after prior nonsteroidal aromatase inhibitor therapy in postmenopausal women with hormone receptor-positive, advanced breast cancer: results from EFECT.* J Clin Oncol, 2008. **26**(10): p. 1664-70.
102. Spicer, D.V. and M.C. Pike, *Future possibilities in the prevention of breast cancer: luteinizing hormone-releasing hormone agonists.* Breast Cancer Res, 2000. **2**(4): p. 264-7.
103. Coussens, L., T.L. Yang-Feng, Y.C. Liao, E. Chen, A. Gray, J. McGrath, P.H. Seeburg, T.A. Libermann, J. Schlessinger and U. Francke, *Tyrosine kinase receptor with extensive homology to EGF receptor shares chromosomal location with neu oncogene.* Science, 1985. **230**(4730): p. 1132-9.
104. Semba, K., N. Kamata, K. Toyoshima and T. Yamamoto, *A v-erbB-related protooncogene, c-erbB-2, is distinct from the c-erbB-1/epidermal growth factor-receptor gene and is amplified in a human salivary gland adenocarcinoma.* Proc Natl Acad Sci U S A, 1985. **82**(19): p. 6497-501.
105. Shih, C., L.C. Padhy, M. Murray and R.A. Weinberg, *Transforming genes of carcinomas and neuroblastomas introduced into mouse fibroblasts.* Nature, 1981. **290**(5803): p. 261-4.
106. Schechter, A.L., M.C. Hung, L. Vaidyanathan, R.A. Weinberg, T.L. Yang-Feng, U. Francke, A. Ullrich and L. Coussens, *The neu gene: an erbB-homologous gene distinct from and unlinked to the gene encoding the EGF receptor.* Science, 1985. **229**(4717): p. 976-8.

107. Akiyama, T., C. Sudo, H. Ogawara, K. Toyoshima and T. Yamamoto, *The product of the human c-erbB-2 gene: a 185-kilodalton glycoprotein with tyrosine kinase activity.* Science, 1986. **232**(4758): p. 1644-6.
108. The UniProt Consortium. *Activities at the Universal Protein Resource (UniProt)*. 2014/01/01 Available from: http://www.uniprot.org/uniprot/P04626.
109. Shah, S. and B. Chen, *Testing for HER2 in Breast Cancer: A Continuing Evolution.* Patholog Res Int, 2011. DOI: 10.4061/2011/903202.
110. Yarden, Y. and M.X. Sliwkowski, *Untangling the ErbB signalling network.* Nat Rev Mol Cell Biol, 2001. **2**(2): p. 127-137.
111. Gschwind, A., O.M. Fischer and A. Ullrich, *Timeline - The discovery of receptor tyrosine kinases: targets for cancer therapy.* Nat Rev Cancer, 2004. **4**(5): p. 361-370.
112. Vandergeer, P., T. Hunter and R.A. Lindberg, *Receptor Protein-Tyrosine Kinases and Their Signal-Transduction Pathways.* Annu Rev Cell Biol, 1994. **10**: p. 251-337.
113. Ullrich, A. and J. Schlessinger, *Signal transduction by receptors with tyrosine kinase activity.* Cell, 1990. **61**(2): p. 203-12.
114. Barros, F.F., D.G. Powe, I.O. Ellis and A.R. Green, *Understanding the HER family in breast cancer: interaction with ligands, dimerization and treatments.* Histopathology, 2010. **56**(5): p. 560-72.
115. Hudis, C.A., *Trastuzumab--mechanism of action and use in clinical practice.* N Engl J Med, 2007. **357**(1): p. 39-51.
116. Olayioye, M.A., R.M. Neve, H.A. Lane and N.E. Hynes, *The ErbB signaling network: receptor heterodimerization in development and cancer.* EMBO J, 2000. **19**(13): p. 3159-67.
117. Dawson, J.P., M.B. Berger, C.C. Lin, J. Schlessinger, M.A. Lemmon and K.M. Ferguson, *Epidermal growth factor receptor dimerization and activation require ligand-induced conformational changes in the dimer interface.* Mol Cell Biol, 2005. **25**(17): p. 7734-42.
118. Graus-Porta, D., R.R. Beerli, J.M. Daly and N.E. Hynes, *ErbB-2, the preferred heterodimerization partner of all ErbB receptors, is a mediator of lateral signaling.* EMBO J, 1997. **16**(7): p. 1647-55.
119. Miaczynska, M., L. Pelkmans and M. Zerial, *Not just a sink: endosomes in control of signal transduction.* Curr Opin Cell Biol, 2004. **16**(4): p. 400-6.
120. Wells, A., *EGF receptor.* Int J Biochem Cell Biol, 1999. **31**(6): p. 637-43.
121. Hudziak, R.M., J. Schlessinger and A. Ullrich, *Increased expression of the putative growth factor receptor p185HER2 causes transformation and tumorigenesis of NIH 3T3 cells.* Proc Natl Acad Sci U S A, 1987. **84**(20): p. 7159-63.
122. Pierce, J.H., P. Arnstein, E. DiMarco, J. Artrip, M.H. Kraus, F. Lonardo, P.P. Di Fiore and S.A. Aaronson, *Oncogenic potential of erbB-2 in human mammary epithelial cells.* Oncogene, 1991. **6**(7): p. 1189-94.
123. Slamon, D.J., G.M. Clark, S.G. Wong, W.J. Levin, A. Ullrich and W.L. McGuire, *Human breast cancer: correlation of relapse and survival with amplification of the HER-2/neu oncogene.* Science, 1987. **235**(4785): p. 177-82.
124. Hoff, E.R., R.R. Tubbs, J.L. Myles and G.W. Procop, *HER2/neu amplification in breast cancer: stratification by tumor type and grade.* Am J Clin Pathol, 2002. **117**(6): p. 916-21.
125. Ross, J.S., E.A. Slodkowska, W.F. Symmans, L. Pusztai, P.M. Ravdin and G.N. Hortobagyi, *The HER-2 receptor and breast cancer: ten years of targeted anti-HER-2 therapy and personalized medicine.* Oncologist, 2009. **14**(4): p. 320-68.
126. Wolff, A.C., M.E. Hammond, D.G. Hicks, M. Dowsett, L.M. McShane, K.H. Allison, D.C. Allred, J.M. Bartlett, M. Bilous, P. Fitzgibbons, W. Hanna, R.B. Jenkins, P.B. Mangu, S. Paik, E.A. Perez, M.F. Press, P.A. Spears, G.H. Vance, G. Viale, D.F. Hayes, O. American Society of

Clinical and P. College of American, *Recommendations for human epidermal growth factor receptor 2 testing in breast cancer: American Society of Clinical Oncology/College of American Pathologists clinical practice guideline update.* J Clin Oncol, 2013. **31**(31): p. 3997-4013.

127. Baselga, J., D. Tripathy, J. Mendelsohn, S. Baughman, C.C. Benz, L. Dantis, N.T. Sklarin, A.D. Seidman, C.A. Hudis, J. Moore, P.P. Rosen, T. Twaddell, I.C. Henderson and L. Norton, *Phase II study of weekly intravenous recombinant humanized anti-p185HER2 monoclonal antibody in patients with HER2/neu-overexpressing metastatic breast cancer.* J Clin Oncol, 1996. **14**(3): p. 737-44.
128. Peintinger, F., A.U. Buzdar, H.M. Kuerer, J.A. Mejia, C. Hatzis, A.M. Gonzalez-Angulo, L. Pusztai, F.J. Esteva, S.S. Dawood, M.C. Green, G.N. Hortobagyi and W.F. Symmans, *Hormone receptor status and pathologic response of HER2-positive breast cancer treated with neoadjuvant chemotherapy and trastuzumab.* Ann Oncol, 2008. **19**(12): p. 2020-5.
129. Seidman, A., C. Hudis, M.K. Pierri, S. Shak, V. Paton, M. Ashby, M. Murphy, S.J. Stewart and D. Keefe, *Cardiac dysfunction in the trastuzumab clinical trials experience.* J Clin Oncol, 2002. **20**(5): p. 1215-21.
130. Ryan, Q., A. Ibrahim, M.H. Cohen, J. Johnson, C.W. Ko, R. Sridhara, R. Justice and R. Pazdur, *FDA drug approval summary: lapatinib in combination with capecitabine for previously treated metastatic breast cancer that overexpresses HER-2.* Oncologist, 2008. **13**(10): p. 1114-9.
131. Blackwell, K.L., H.J. Burstein, A.M. Storniolo, H. Rugo, G. Sledge, M. Koehler, C. Ellis, M. Casey, S. Vukelja, J. Bischoff, J. Baselga and J. O'Shaughnessy, *Randomized study of Lapatinib alone or in combination with trastuzumab in women with ErbB2-positive, trastuzumab-refractory metastatic breast cancer.* J Clin Oncol, 2010. **28**(7): p. 1124-30.
132. Nagy, P., A. Jenei, S. Damjanovich, T.M. Jovin and J. Szolosi, *Complexity of signal transduction mediated by ErbB2: clues to the potential of receptor-targeted cancer therapy.* Pathol Oncol Res, 1999. **5**(4): p. 255-71.
133. Difiore, P.P., O. Segatto, F. Lonardo, F. Fazioli, J.H. Pierce and S.A. Aaronson, *The Carboxy-Terminal Domains of Erbb-2 and Epidermal Growth-Factor Receptor Exert Different Regulatory Effects on Intrinsic Receptor Tyrosine Kinase Function and Transforming Activity.* Mol Cell Biol, 1990. **10**(6): p. 2749-2756.
134. Schuell, B., T. Gruenberger, W. Scheithauer, C. Zielinski and F. Wrba, *HER 2/neu protein expression in colorectal cancer.* BMC Cancer, 2006. **6**: p. 123.
135. Eltze, E., C. Wulfing, D. Von Struensee, H. Piechota, H. Buerger and L. Hertle, *Cox-2 and Her2/neu co-expression in invasive bladder cancer.* Int J Oncol, 2005. **26**(6): p. 1525-31.
136. McKenzie, S.J., K.A. DeSombre, B.S. Bast, D.R. Hollis, R.S. Whitaker, A. Berchuck, C.M. Boyer and R.C. Bast, Jr., *Serum levels of HER-2 neu (C-erbB-2) correlate with overexpression of p185neu in human ovarian cancer.* Cancer, 1993. **71**(12): p. 3942-6.
137. Hetzel, D.J., T.O. Wilson, G.L. Keeney, P.C. Roche, S.S. Cha and K.C. Podratz, *HER-2/neu expression: a major prognostic factor in endometrial cancer.* Gynecol Oncol, 1992. **47**(2): p. 179-85.
138. Hirashima, N., W. Takahashi, S. Yoshii, T. Yamane and A. Ooi, *Protein overexpression and gene amplification of c-erb B-2 in pulmonary carcinomas: a comparative immunohistochemical and fluorescence in situ hybridization study.* Mod Pathol, 2001. **14**(6): p. 556-62.
139. Mitra, A.B., V.V. Murty, M. Pratap, P. Sodhani and R.S. Chaganti, *ERBB2 (HER2/neu) oncogene is frequently amplified in squamous cell carcinoma of the uterine cervix.* Cancer Res, 1994. **54**(3): p. 637-9.

140. Beckhardt, R.N., N. Kiyokawa, L. Xi, T.J. Liu, M.C. Hung, A.K. el-Naggar, H.Z. Zhang and G.L. Clayman, *HER-2/neu oncogene characterization in head and neck squamous cell carcinoma.* Arch Otolaryngol Head Neck Surg, 1995. **121**(11): p. 1265-70.
141. Reichelt, U., P. Duesedau, M. Tsourlakis, A. Quaas, B.C. Link, P.G. Schurr, J.T. Kaifi, S.J. Gros, E.F. Yekebas, A. Marx, R. Simon, J.R. Izbicki and G. Sauter, *Frequent homogeneous HER-2 amplification in primary and metastatic adenocarcinoma of the esophagus.* Mod Pathol, 2007. **20**(1): p. 120-9.
142. Mrklic, I., A. Bendic, N. Kunac, J. Bezic, G. Forempoher, M.G. Durdov, I. Karaman, I.K. Prusac, V.P. Pisac, K. Vilovic and S. Tomic, *Her-2/neu assessment for gastric carcinoma: validation of scoring system.* Hepatogastroenterology, 2012. **59**(113): p. 300-3.
143. Harris, L., H. Fritsche, R. Mennel, L. Norton, P. Ravdin, S. Taube, M.R. Somerfield, D.F. Hayes, R.C. Bast, Jr. and O. American Society of Clinical, *American Society of Clinical Oncology 2007 update of recommendations for the use of tumor markers in breast cancer.* J Clin Oncol, 2007. **25**(33): p. 5287-312.
144. Jacobs, T.W., A.M. Gown, H. Yaziji, M.J. Barnes and S.J. Schnitt, *HER-2/neu protein expression in breast cancer evaluated by immunohistochemistry. A study of interlaboratory agreement.* Am J Clin Pathol, 2000. **113**(2): p. 251-8.
145. Keshgegian, A.A. and A. Cnaan, *erbB-2 oncoprotein expression in breast carcinoma. Poor prognosis associated with high degree of cytoplasmic positivity using CB-11 antibody.* Am J Clin Pathol, 1997. **108**(4): p. 456-63.
146. Wolff, A.C., M.E. Hammond, D.G. Hicks, M. Dowsett, L.M. McShane, K.H. Allison, D.C. Allred, J.M. Bartlett, M. Bilous, P. Fitzgibbons, W. Hanna, R.B. Jenkins, P.B. Mangu, S. Paik, E.A. Perez, M.F. Press, P.A. Spears, G.H. Vance, G. Viale and D.F. Hayes, *Recommendations for Human Epidermal Growth Factor Receptor 2 Testing in Breast Cancer: American Society of Clinical Oncology/College of American Pathologists Clinical Practice Guideline Update.* Arch Pathol Lab Med, 2013. DOI: 10.5858/arpa.2013-0953-SA.
147. Jacobs, T.W., A.M. Gown, H. Yaziji, M.J. Barnes and S.J. Schnitt, *Specificity of HercepTest in determining HER-2/neu status of breast cancers using the United States Food and Drug Administration-approved scoring system.* J Clin Oncol, 1999. **17**(7): p. 1983-7.
148. Powell, W.C., D.G. Hicks, N. Prescott, S.M. Tarr, S. Laniauskas, T. Williams, S. Short, J. Pettay, R.B. Nagle, D.J. Dabbs, K.M. Scott, R.W. Brown, T. Grogan, P.C. Roche and R.R. Tubbs, *A new rabbit monoclonal antibody (4B5) for the immunohistochemical (IHC) determination of the HER2 status in breast cancer: comparison with CB11, fluorescence in situ hybridization (FISH), and interlaboratory reproducibility.* Appl Immunohistochem Mol Morphol, 2007. **15**(1): p. 94-102.
149. Hoang, M.P., A.A. Sahin, N.G. Ordonez and N. Sneige, *HER-2/neu gene amplification compared with HER-2/neu protein overexpression and interobserver reproducibility in invasive breast carcinoma.* Am J Clin Pathol, 2000. **113**(6): p. 852-9.
150. Thomson, T.A., M.M. Hayes, J.J. Spinelli, E. Hilland, C. Sawrenko, D. Phillips, B. Dupuis and R.L. Parker, *HER-2/neu in breast cancer: interobserver variability and performance of immunohistochemistry with 4 antibodies compared with fluorescent in situ hybridization.* Mod Pathol, 2001. **14**(11): p. 1079-86.
151. Press, M.F., L. Bernstein, P.A. Thomas, L.F. Meisner, J.Y. Zhou, Y. Ma, G. Hung, R.A. Robinson, C. Harris, A. El-Naggar, D.J. Slamon, R.N. Phillips, J.S. Ross, S.R. Wolman and K.J. Flom, *HER-2/neu gene amplification characterized by fluorescence in situ hybridization: poor prognosis in node-negative breast carcinomas.* J Clin Oncol, 1997. **15**(8): p. 2894-904.

152. Hammock, L., M. Lewis, C. Phillips and C. Cohen, *Strong HER-2/neu protein overexpression by immunohistochemistry often does not predict oncogene amplification by fluorescence in situ hybridization.* Hum Pathol, 2003. **34**(10): p. 1043-7.
153. Mass, R.D., M.F. Press, S. Anderson, M.A. Cobleigh, C.L. Vogel, N. Dybdal, G. Leiberman and D.J. Slamon, *Evaluation of clinical outcomes according to HER2 detection by fluorescence in situ hybridization in women with metastatic breast cancer treated with trastuzumab.* Clin Breast Cancer, 2005. **6**(3): p. 240-6.
154. Rossi, E., A. Ubiali, M. Cadei, P. Balzarini, E. Valagussa, L. Lucini, F. Alpi, A. Galletti, L. Fontana, C. Tedoldi and P. Grigolato, *HER-2/neu in breast cancer: a comparative study between histology, immunohistochemistry, and molecular technique (FISH).* Appl Immunohistochem Mol Morphol, 2006. **14**(2): p. 127-31.
155. Varshney, D., Y.Y. Zhou, S.A. Geller and R. Alsabeh, *Determination of HER-2 status and chromosome 17 polysomy in breast carcinomas comparing HercepTest and PathVysion FISH assay.* Am J Clin Pathol, 2004. **121**(1): p. 70-7.
156. Bhargava, R., P. Lal and B. Chen, *Chromogenic in situ hybridization for the detection of HER-2/neu gene amplification in breast cancer with an emphasis on tumors with borderline and low-level amplification: does it measure up to fluorescence in situ hybridization?* Am J Clin Pathol, 2005. **123**(2): p. 237-43.
157. Gong, Y., W. Sweet, Y.J. Duh, L. Greenfield, Y. Fang, J. Zhao, E. Tarco, W.F. Symmans, J. Isola and N. Sneige, *Chromogenic in situ hybridization is a reliable method for detecting HER2 gene status in breast cancer: a multicenter study using conventional scoring criteria and the new ASCO/CAP recommendations.* Am J Clin Pathol, 2009. **131**(4): p. 490-7.
158. Dietel, M., I.O. Ellis, H. Hofler, H. Kreipe, H. Moch, A. Dankof, K. Kolble and G. Kristiansen, *Comparison of automated silver enhanced in situ hybridisation (SISH) and fluorescence ISH (FISH) for the validation of HER2 gene status in breast carcinoma according to the guidelines of the American Society of Clinical Oncology and the College of American Pathologists.* Virchows Arch, 2007. **451**(1): p. 19-25.
159. Papouchado, B.G., J. Myles, R.V. Lloyd, M. Stoler, A.M. Oliveira, E. Downs-Kelly, A. Morey, M. Bilous, R. Nagle, N. Prescott, L. Wang, L. Dragovich, A. McElhinny, C.F. Garcia, J. Ranger-Moore, H. Free, W. Powell, M. Loftus, J. Pettay, F. Gaire, C. Roberts, M. Dietel, P. Roche, T. Grogan and R. Tubbs, *Silver in situ hybridization (SISH) for determination of HER2 gene status in breast carcinoma: comparison with FISH and assessment of interobserver reproducibility.* Am J Surg Pathol, 2010. **34**(6): p. 767-76.
160. Nitta, H., B. Hauss-Wegrzyniak, M. Lehrkamp, A.E. Murillo, F. Gaire, M. Farrell, E. Walk, F. Penault-Llorca, M. Kurosumi, M. Dietel, L. Wang, M. Loftus, J. Pettay, R.R. Tubbs and T.M. Grogan, *Development of automated brightfield double in situ hybridization (BDISH) application for HER2 gene and chromosome 17 centromere (CEN 17) for breast carcinomas and an assay performance comparison to manual dual color HER2 fluorescence in situ hybridization (FISH).* Diagn Pathol, 2008. **3**: p. 41.
161. Barberis, M., C. Pellegrini, M. Cannone, C. Arizzi, G. Coggi and S. Bosari, *Quantitative PCR and HER2 testing in breast cancer: a technical and cost-effectiveness analysis.* Am J Clin Pathol, 2008. **129**(4): p. 563-70.
162. Du, X., X.Q. Li, L. Li, Y.Y. Xu and Y.M. Feng, *The detection of ESR1/PGR/ERBB2 mRNA levels by RT-QPCR: a better approach for subtyping breast cancer and predicting prognosis.* Breast Cancer Res Treat, 2013. **138**(1): p. 59-67.
163. Gauchez, A.S., N. Ravanel, D. Villemain, F.X. Brand, D. Pasquier, R. Payan and M. Mousseau, *Evaluation of a manual ELISA kit for determination of HER2/neu in serum of breast cancer patients.* Anticancer Res, 2008. **28**(5B): p. 3067-73.

164. Pupa, S.M., S. Menard, D. Morelli, B. Pozzi, G. De Palo and M.I. Colnaghi, *The extracellular domain of the c-erbB-2 oncoprotein is released from tumor cells by proteolytic cleavage.* Oncogene, 1993. **8**(11): p. 2917-23.
165. Carney, W.P., R. Neumann, A. Lipton, K. Leitzel, S. Ali and C.P. Price, *Potential clinical utility of serum HER-2/neu oncoprotein concentrations in patients with breast cancer.* Clin Chem, 2003. **49**(10): p. 1579-98.
166. Molina, M.A., J. Codony-Servat, J. Albanell, F. Rojo, J. Arribas and J. Baselga, *Trastuzumab (herceptin), a humanized anti-Her2 receptor monoclonal antibody, inhibits basal and activated Her2 ectodomain cleavage in breast cancer cells.* Cancer Res, 2001. **61**(12): p. 4744-9.
167. Tan, L.D., Y.Y. Xu, Y. Yu, X.Q. Li, Y. Chen and Y.M. Feng, *Serum HER2 level measured by dot blot: a valid and inexpensive assay for monitoring breast cancer progression.* PLoS One, 2011. **6**(4): p. e18764.
168. Loo, L., J.A. Capobianco, W. Wu, X. Gao, W.Y. Shih, W.H. Shih, K. Pourrezaei, M.K. Robinson and G.P. Adams, *Highly sensitive detection of HER2 extracellular domain in the serum of breast cancer patients by piezoelectric microcantilevers.* Anal Chem, 2011. **83**(9): p. 3392-7.
169. Martin, V.S., B.A. Sullivan, K. Walker, H. Hawk, B.P. Sullivan and L.J. Noe, *Surface plasmon resonance investigations of human epidermal growth factor receptor 2.* Appl Spectrosc, 2006. **60**(9): p. 994-1003.
170. Mattanovich, D., P. Branduardi, L. Dato, B. Gasser, M. Sauer and D. Porro, *Recombinant protein production in yeasts.* Methods Mol Biol, 2012. **824**: p. 329-58.
171. Ni, Y. and R. Chen, *Extracellular recombinant protein production from Escherichia coli.* Biotechnol Lett, 2009. **31**(11): p. 1661-70.
172. Pandhal, J., S.Y. Ow, J. Noirel and P.C. Wright, *Improving N-glycosylation efficiency in Escherichia coli using shotgun proteomics, metabolic network analysis, and selective reaction monitoring.* Biotechnol Bioeng, 2011. **108**(4): p. 902-12.
173. Middelhoven, W.J., I.M. de Jong and M. de Winter, *Arxula adeninivorans, a yeast assimilating many nitrogenous and aromatic compounds.* Antonie Van Leeuwenhoek, 1991. **59**(2): p. 129-37.
174. Minocha, N., P. Kaur, T. Satyanarayana and G. Kunze, *Acid phosphatase production by recombinant Arxula adeninivorans.* Appl Microbiol Biotechnol, 2007. **76**(2): p. 387-93.
175. Boer, E., F.S. Breuer, M. Weniger, S. Denter, M. Piontek and G. Kunze, *Large-scale production of tannase using the yeast Arxula adeninivorans.* Appl Microbiol Biotechnol, 2011. **92**(1): p. 105-14.
176. Boer, E., H.P. Mock, R. Bode, G. Gellissen and G. Kunze, *An extracellular lipase from the dimorphic yeast Arxula adeninivorans: molecular cloning of the ALIP1 gene and characterization of the purified recombinant enzyme.* Yeast, 2005. **22**(7): p. 523-35.
177. Jankowska, D.A., K. Faulwasser, A. Trautwein-Schult, A. Cordes, P. Hoferichter, C. Klein, R. Bode, K. Baronian and G. Kunze, *Arxula adeninivorans recombinant adenine deaminase and its application in the production of food with low purine content.* J Appl Microbiol, 2013. **115**(5): p. 1134-46.
178. Jankowska, D.A., A. Trautwein-Schult, A. Cordes, P. Hoferichter, C. Klein, R. Bode, K. Baronian and G. Kunze, *Arxula adeninivorans xanthine oxidoreductase and its application in the production of food with low purine content.* J Appl Microbiol, 2013. **115**(3): p. 796-807.
179. Trautwein-Schult, A., D. Jankowska, A. Cordes, P. Hoferichter, C. Klein, A. Matros, H.P. Mock, K. Baronian, R. Bode and G. Kunze, *Arxula adeninivorans recombinant urate oxidase and its application in the production of food with low uric acid content.* J Mol Microbiol Biotechnol, 2013. **23**(6): p. 418-30.

180. Boer, E., G. Steinborn, A. Matros, H.P. Mock, G. Gellissen and G. Kunze, *Production of interleukin-6 in Arxula adeninivorans, Hansenula polymorpha and Saccharomyces cerevisiae by applying the wide-range yeast vector (CoMed) system to simultaneous comparative assessment.* FEMS Yeast Res, 2007. **7**(7): p. 1181-7.
181. Wartmann, T., E. Boer, A.H. Pico, H. Sieber, O. Bartelsen, G. Gellissen and G. Kunze, *High-level production and secretion of recombinant proteins by the dimorphic yeast Arxula adeninivorans.* FEMS Yeast Res, 2002. **2**(3): p. 363-9.
182. Boer, E., M. Piontek and G. Kunze, *Xplor 2--an optimized transformation/expression system for recombinant protein production in the yeast Arxula adeninivorans.* Appl Microbiol Biotechnol, 2009. **84**(3): p. 583-94.
183. Giersberg, M., A. Degelmann, R. Bode, M. Piontek and G. Kunze, *Production of a thermostable alcohol dehydrogenase from Rhodococcus ruber in three different yeast species using the Xplor(R)2 transformation/expression platform.* J Ind Microbiol Biotechnol, 2012. **39**(9): p. 1385-96.
184. Steinborn, G., G. Gellissen and G. Kunze, *A novel vector element providing multicopy vector integration in Arxula adeninivorans.* FEMS Yeast Res, 2007. **7**(7): p. 1197-205.
185. Alvaro-Benito, M., M. Fernandez-Lobato, K. Baronian and G. Kunze, *Assessment of Schwanniomyces occidentalis as a host for protein production using the wide-range Xplor2 expression platform.* Appl Microbiol Biotechnol, 2013. **97**(10): p. 4443-56.
186. Klabunde, J., G. Kunze, G. Gellissen and C.P. Hollenberg, *Integration of heterologous genes in several yeast species using vectors containing a Hansenula polymorpha-derived rDNA-targeting element.* FEMS Yeast Res, 2003. **4**(2): p. 185-93.
187. Gellissen, G., *Heterologous protein production in methylotrophic yeasts.* Appl Microbiol Biotechnol, 2000. **54**(6): p. 741-50.
188. Gellissen, G., G. Kunze, C. Gaillardin, J.M. Cregg, E. Berardi, M. Veenhuis and I. van der Klei, *New yeast expression platforms based on methylotrophic Hansenula polymorpha and Pichia pastoris and on dimorphic Arxula adeninivorans and Yarrowia lipolytica - a comparison.* FEMS Yeast Res, 2005. **5**(11): p. 1079-96.
189. Roggenkamp, R., Z. Janowicz, B. Stanikowski and C.P. Hollenberg, *Biosynthesis and regulation of the peroxisomal methanol oxidase from the methylotrophic yeast Hansenula polymorpha.* Mol Gen Genet, 1984. **194**(3): p. 489-93.
190. Janowicz, Z.A., M.R. Eckart, C. Drewke, R.O. Roggenkamp, C.P. Hollenberg, J. Maat, A.M. Ledeboer, C. Visser and C.T. Verrips, *Cloning and Characterization of the Das Gene Encoding the Major Methanol Assimilatory Enzyme from the Methylotrophic Yeast Hansenula-Polymorpha.* Nucleic Acids Res, 1985. **13**(9): p. 3043-3062.
191. Ledeboer, A.M., L. Edens, J. Maat, C. Visser, J.W. Bos, C.T. Verrips, Z. Janowicz, M. Eckart, R. Roggenkamp and C.P. Hollenberg, *Molecular-Cloning and Characterization of a Gene Coding for Methanol Oxidase in Hansenula-Polymorpha.* Nucleic Acids Res, 1985. **13**(9): p. 3063-3082.
192. Gellissen, G., Z.A. Janowicz, U. Weydemann, K. Melber, A.W. Strasser and C.P. Hollenberg, *High-level expression of foreign genes in Hansenula polymorpha.* Biotechnol Adv, 1992. **10**(2): p. 179-89.
193. Janowicz, Z.A., K. Melber, A. Merckelbach, E. Jacobs, N. Harford, M. Comberbach and C.P. Hollenberg, *Simultaneous expression of the S and L surface antigens of hepatitis B, and formation of mixed particles in the methylotrophic yeast, Hansenula polymorpha.* Yeast, 1991. **7**(5): p. 431-43.
194. Roggenkamp, R., G. Reipen and C.P. Hollenberg, *Mediation, by Saccharomyces cerevisiae translocation signals, of beta-lactamase transport through the Escherichia coli inner*

membrane and sensitive method for detection of signal sequences. J Bacteriol, 1986. **168**(1): p. 467-9.
195. Weydemann, U., P. Keup, M. Piontek, A.W. Strasser, J. Schweden, G. Gellissen and Z.A. Janowicz, *High-level secretion of hirudin by Hansenula polymorpha--authentic processing of three different preprohirudins.* Appl Microbiol Biotechnol, 1995. **44**(3-4): p. 377-85.
196. Zurek, C., E. Kubis, P. Keup, D. Horlein, J. Beunink, J. Thommes, M.R. Kula, C.P. Hollenberg and G. Gellissen, *Production of two aprotinin variants in Hansenula polymorpha.* Process Biochem, 1996. **31**(7): p. 679-689.
197. Mayer, A.F., K. Hellmuth, H. Schlieker, R. Lopez-Ulibarri, S. Oertel, U. Dahlems, A.W. Strasser and A.P. van Loon, *An expression system matures: a highly efficient and cost-effective process for phytase production by recombinant strains of Hansenula polymorpha.* Biotechnol Bioeng, 1999. **63**(3): p. 373-81.
198. Khongto, B., K. Laoteng and A. Tongta, *Fermentation process development of recombinant Hansenula polymorpha for gamma-linolenic acid production.* J Microbiol Biotechnol, 2010. **20**(11): p. 1555-62.
199. Suckow, M. and G. Gellissen, *The Expression Platform Based on H. polymorpha Strain RB11 and Its Derivatives – History, Status and Perspectives*, in *Hansenula polymorpha*. 2005, Wiley-VCH Verlag GmbH & Co. KGaA. p. 105-123.
200. Wood, R.W., *XLII. On a remarkable case of uneven distribution of light in a diffraction grating spectrum.* Philos Mag, 1902. **4**(21): p. 396-402.
201. Kretschmann, E.R., H., *Radiative decay of non-radiative surface plasmons excited by light.* Z. Naturforsch, 1968. **23A**: p. 2135-2136.
202. Otto, A., *Excitation of surface plasma waves in silver by the method of frustrated total reflection.* Z. Physik., 1968. **216**: p. 398-410.
203. Rhodes, C., S. Franzen, J.P. Maria, M. Losego, D.N. Leonard, B. Laughlin, G. Duscher and S. Weibel, *Surface plasmon resonance in conducting metal oxides.* J Appl Phys, 2006. **100**(5).
204. Akimoto, T., S. Sasaki, K. Ikebukuro and I. Karube, *Effect of incident angle of light on sensitivity and detection limit for layers of antibody with surface plasmon resonance spectroscopy.* Biosens Bioelectron, 2000. **15**(7-8): p. 355-362.
205. Quinn, J.G., S. O'Neill, A. Doyle, C. McAtamney, D. Diamond, B.D. MacCraith and R. O'Kennedy, *Development and application of surface plasmon resonance-based biosensors for the detection of cell-ligand interactions.* Anal Biochem, 2000. **281**(2): p. 135-143.
206. Stenberg, E., B. Persson, H. Roos and C. Urbaniczky, *Quantitative-Determination of Surface Concentration of Protein with Surface-Plasmon Resonance Using Radiolabeled Proteins.* J Colloid Interface Sci, 1991. **143**(2): p. 513-526.
207. Florschutz, K., A. Schroter, S. Schmieder, W. Chen, P. Schweizer, F. Sonntag, N. Danz, K. Baronian and G. Kunze, *'Phytochip': on-chip detection of phytopathogenic RNA viruses by a new surface plasmon resonance platform.* J Virol Methods, 2013. **189**(1): p. 80-6.
208. Sonntag, F., S. Schmieder, N. Danz, M. Mertig, N. Schilling, U. Klotzbach and E. Beyer. *Novel lab-on-a-chip system for the label-free detection of DNA hybridization and protein-protein interaction by surface plasmon resonance (SPR)*. 2009. DOI: 10.1117/12.821467.
209. Homola, J., S.S. Yee and G. Gauglitz, *Surface plasmon resonance sensors: review.* Sens Actuators B: Chem, 1999. **54**(1-2): p. 3-15.
210. Liedberg, B., C. Nylander and I. Lundstrom, *Surface-Plasmon Resonance for Gas-Detection and Biosensing.* Sens Actuators, 1983. **4**(2): p. 299-304.
211. Regnault, V., J. Arvieux, L. Vallar and T. Lecompte, *Immunopurification of human beta(2)-glycoprotein I with a monoclonal antibody selected for its binding kinetics using surface plasmon resonance biosensor.* J Immunol Methods, 1998. **211**(1-2): p. 191-197.

212. Chapple, D.S., D.J. Mason, C.L. Joannou, E.W. Odell, V. Gant and R.W. Evans, *Structure-function relationship of antibacterial synthetic peptides homologous to a helical surface region on human lactoferrin against Escherichia coli serotype O111.* Infect Immun, 1998. **66**(6): p. 2434-2440.
213. Adamczyk, M., D.D. Johnson, P.G. Mattingly, J.A. Moore and Y. Pan, *Immunoassay reagents for thyroid testing. 3. Determination of the solution binding affinities of a T-4 monoclonal antibody Fab fragment for a library of thyroxine analogs using surface plasmon resonance.* Bioconj Chem, 1998. **9**(1): p. 23-32.
214. Bai, H., R. Wang, B. Hargis, H. Lu and Y. Li, *A SPR aptasensor for detection of avian influenza virus H5N1.* Sensors (Basel), 2012. **12**(9): p. 12506-18.
215. Choi, Y.H., G.Y. Lee, H. Ko, Y.W. Chang, M.J. Kang and J.C. Pyun, *Development of SPR biosensor for the detection of human hepatitis B virus using plasma-treated parylene-N film.* Biosens Bioelectron, 2014. **56**: p. 286-94.
216. Riedel, T., C. Rodriguez-Emmenegger, A. de los Santos Pereira, A. Bedajankova, P. Jinoch, P.M. Boltovets and E. Brynda, *Diagnosis of Epstein-Barr virus infection in clinical serum samples by an SPR biosensor assay.* Biosens Bioelectron, 2014. **55**: p. 278-84.
217. Bullock, W., *XL-1 Blue: a high efficiency plasmid transforming recA Escherichia coli strain with beta-galactosidase selection.* BioTechniques, 1987. **5**: p. 376-379.
218. Kleber-Janke, T. and W.-M. Becker, *Use of Modified BL21(DE3) Escherichia coli Cells for High-Level Expression of Recombinant Peanut Allergens Affected by Poor Codon Usage.* Protein Expr Purif, 2000. **19**(3): p. 419-424.
219. Hanahan, D., *Studies on transformation of Escherichia coli with plasmids.* J Mol Biol, 1983. **166**(4): p. 557-580.
220. Dohmen, R.J., A.W. Strasser, C.B. Honer and C.P. Hollenberg, *An efficient transformation procedure enabling long-term storage of competent cells of various yeast genera.* Yeast, 1991. **7**(7): p. 691-2.
221. White, M.A., K.M. Clark, E.J. Grayhack and M.E. Dumont, *Characteristics affecting expression and solubilization of yeast membrane proteins.* J Mol Biol, 2007. **365**(3): p. 621-36.
222. Shi, S.-R., C. Liu, B.M. Balgley, C. Lee and C.R. Taylor, *Protein Extraction from Formalin-fixed, Paraffin-embedded Tissue Sections: Quality Evaluation by Mass Spectrometry.* J Histochem Cytochem, 2006. **54**(6): p. 739-743.
223. Motulsky, H. and A.C.P.D.P.U. Melbourne, *Fitting Models to Biological Data Using Linear and Nonlinear Regression : A Practical Guide to Curve Fitting: A Practical Guide to Curve Fitting*. 2004: Oxford University Press, USA.
224. Krohn, K.A. and J.M. Link, *Interpreting enzyme and receptor kinetics: keeping it simple, but not too simple.* Nucl Med Biol, 2003. **30**(8): p. 819-26.
225. Currie, L.A., *Nomenclature in Evaluation of Analytical Methods Including Detection and Quantification Capabilities (Iupac Recommendations 1995).* Pure Appl Chem, 1995. **67**(10): p. 1699-1723.
226. Freigassner, M., H. Pichler and A. Glieder, *Tuning microbial hosts for membrane protein production.* Microb Cell Fact, 2009. **8**: p. 69.
227. Sedzielewska, K.A., E. Boer, C. Bellebna, T. Wartmann, R. Bode, M. Melzer, K. Baronian and G. Kunze, *Role of the AFRD1-encoded fumarate reductase in hypoxia and osmotolerance in Arxula adeninivorans.* FEMS Yeast Res, 2012. **12**(8): p. 924-937.
228. Wartmann, T., U.W. Stephan, I. Bube, E. Boer, M. Melzer, R. Manteuffel, R. Stoltenburg, L. Guengerich, G. Gellissen and G. Kunze, *Post-translational modifications of the AFET3 gene product - a component of the iron transport system in budding cells and mycelia of the yeast Arxula adeninivorans.* Yeast, 2002. **19**(10): p. 849-862.

229. Burns, A.R., J.M. Oliver, J.R. Pfeiffer and B.S. Wilson, *Visualizing clathrin-mediated IgE receptor internalization by electron and atomic force microscopy.* Methods Mol Biol, 2008. **440**: p. 235-45.
230. Ruspantini, I., M. Diociaiuti, R. Ippoliti, E. Lendaro, M.C. Gaudiano, M. Cianfriglia, P. Chistolini, G. Arancia and A. Molinari, *Immunogold localisation of P-glycoprotein in supported lipid bilayers by transmission electron microscopy and atomic force microscopy.* Histochem J, 2001. **33**(5): p. 305-9.
231. Gasteiger, E., E. Jung and A. Bairoch, *SWISS-PROT: connecting biomolecular knowledge via a protein database.* Curr Issues Mol Biol, 2001. **3**(3): p. 47-55.
232. Gellissen, G., *Hansenula polymorpha-biology and applications*. 2002, Weinheim: Wiley-VCH.
233. Hellwig S, S.C., Gellissen G, Büchs J, *Comparative fermentation. Production of recombinant proteins: novel microbial and eukaryotic expression systems*, G. G,Editor. 2005, Weinheim: Wiley-VCH. p. 287–317.
234. Graslund, S., P. Nordlund, J. Weigelt, B.M. Hallberg, J. Bray, O. Gileadi, S. Knapp, U. Oppermann, C. Arrowsmith, R. Hui, J. Ming, S. dhe-Paganon, H.W. Park, A. Savchenko, A. Yee, A. Edwards, R. Vincentelli, C. Cambillau, R. Kim, S.H. Kim, Z. Rao, Y. Shi, T.C. Terwilliger, C.Y. Kim, L.W. Hung, G.S. Waldo, Y. Peleg, S. Albeck, T. Unger, O. Dym, J. Prilusky, J.L. Sussman, R.C. Stevens, S.A. Lesley, I.A. Wilson, A. Joachimiak, F. Collart, I. Dementieva, M.I. Donnelly, W.H. Eschenfeldt, Y. Kim, L. Stols, R. Wu, M. Zhou, S.K. Burley, J.S. Emtage, J.M. Sauder, D. Thompson, K. Bain, J. Luz, T. Gheyi, F. Zhang, S. Atwell, S.C. Almo, J.B. Bonanno, A. Fiser, S. Swaminathan, F.W. Studier, M.R. Chance, A. Sali, T.B. Acton, R. Xiao, L. Zhao, L.C. Ma, J.F. Hunt, L. Tong, K. Cunningham, M. Inouye, S. Anderson, H. Janjua, R. Shastry, C.K. Ho, D. Wang, H. Wang, M. Jiang, G.T. Montelione, D.I. Stuart, R.J. Owens, S. Daenke, A. Schutz, U. Heinemann, S. Yokoyama, K. Bussow and K.C. Gunsalus, *Protein production and purification.* Nat Methods, 2008. **5**(2): p. 135-46.
235. Bornhorst, J.A. and J.J. Falke, *Purification of proteins using polyhistidine affinity tags.* Methods Enzymol, 2000. **326**: p. 245-54.
236. Wang, N.W., *Ion exchange in purification.* Bioprocess Technol, 1990. **9**: p. 359-400.
237. Gagnon, P., P. Ng, J. Zhen, J. He, C. Aberin and H. Mekosh, *BIOT 322-Practical issues in the industrial use of hydroxyapatite for purification of monoclonal antibodies.* Abstr Pap Am Chem S, 2006. **232**.
238. Nakagawa, T., K. Nishiuchi, J. Akaki, H. Iwata, R. Satou, F. Suzuki and Y. Nakamura, *Efficient production of recombinant human (pro)renin utilizing a decahistidine tag attached at the C-terminus.* Biosci Biotechnol Biochem, 2007. **71**(1): p. 256-60.
239. Bornhorst, B.J. and J.J. Falke, *Reprint of: Purification of Proteins Using Polyhistidine Affinity Tags.* Protein Expr Purif, 201110.1016/j.pep.2011.08.022.
240. Gagnon, P., *Monoclonal antibody purification with hydroxyapatite.* New Biotechnol, 2009. **25**(5): p. 287-293.
241. Gagnon, P., *Hydroxyapatite for Biomolecule Purification.* Genet Eng Biotechn N, 2010. **30**(7): p. 28-+.
242. Gorbunoff, M.J., *The Interaction of Proteins with Hydroxyapatite .2. Role of Acidic and Basic Groups.* Anal Biochem, 1984. **136**(2): p. 433-439.
243. Gorbunoff, M.J., *The Interaction of Proteins with Hydroxyapatite .1. Role of Protein Charge and Structure.* Anal Biochem, 1984. **136**(2): p. 425-432.
244. Gorbunoff, M.J. and S.N. Timasheff, *The Interaction of Proteins with Hydroxyapatite .3. Mechanism.* Anal Biochem, 1984. **136**(2): p. 440-445.
245. Gervais, T. and K.F. Jensen, *Mass transport and surface reactions in microfluidic systems.* Chem Eng Sci, 2006. **61**(4): p. 1102-1121.

246. Schuck, P. and A.P. Minton, *Analysis of Mass Transport-Limited Binding Kinetics in Evanescent Wave Biosensors.* Anal Biochem, 1996. **240**(2): p. 262-272.
247. Seifert, M., S. Haindl and B. Hock, *Development of an enzyme linked receptor assay (ELRA) for estrogens and xenoestrogens.* Anal Chim Acta, 1999. **386**(3): p. 191-199.
248. Pichon, M.F. and E. Milgrom, *Competitive protein binding assay of progesterone without chromatography.* Steroids, 1973. **21**(3): p. 335-46.
249. Holliday, D.L. and V. Speirs, *Choosing the right cell line for breast cancer research.* Breast Cancer Res, 2011. **13**(4): p. 215.

7 Declaration of originality

Hiermit erkläre ich, dass diese Arbeit bisher von mir weder an der Mathematisch-Naturwissenschaftlichen Fakultät der Ernst-Moritz-Arndt-Universität Greifswald noch einer anderen wissenschaftlichen Einrichtung zum Zwecke der Promotion eingereicht wurde.

Ferner erkläre ich, dass ich diese Arbeit selbstständig verfasst und keine anderen als die darin angegebenen Hilfsmittel und Hilfen benutzt und keine Textabschnitte eines Dritten ohne Kennzeichnung übernommen habe.

……

Alexandre Chamas